The influence of fold and fracture development on reservoir behavior of the Lisburne Group of northern Alaska

Fourth semi-annual report

For reporting period ending September 27, 2001

Principal investigator
Wesley K. Wallace

Co-principal investigators:
Catherine L. Hanks
Jerry Jensen[1]
Michael T. Whalen

Other contributors:
Paul K. Atkinson
Joseph Brinton
Thang Bui[1]
Margarete A. Jadamec
Alexandre V. Karpov[1]
Andrea P. Krumhardt
John C. Lorenz[2]
Michelle M. McGee
J. Ryan Shackleton

Report date: January, 2002

Department of Energy Award DE-AC26-98BC15102

Submitting organization:
Geophysical Institute
University of Alaska
Fairbanks, Alaska
99775-5780

[1]Department of Petroleum Engineering and Department of Geology and Geophysics, Texas A&M University, College Station, Texas 77843-3116
[2]Sandia National Laboratories, Albuquerque, New Mexico

Disclaimer

Abstract

The Carboniferous Lisburne Group is a major carbonate reservoir unit in northern Alaska. The Lisburne is detachment folded where it is exposed throughout the northeastern Brooks Range, but is relatively undeformed in areas of current production in the subsurface of the North Slope. The objectives of this study are to develop a better understanding of four major aspects of the Lisburne:

1. The geometry and kinematics of detachment folds and their truncation by thrust faults.
2. The influence of folding on fracture patterns.
3. The influence of deformation on fluid flow.
4. Lithostratigraphy and its influence on folding, faulting, fracturing, and reservoir characteristics.

The Lisburne in the main axis of the Brooks Range is characteristically deformed into imbricate thrust sheets with asymmetrical hangingwall anticlines and footwall synclines. In contrast, the Lisburne in the northeastern Brooks Range is characterized by symmetrical detachment folds. The focus of our 2000 field studies was at the boundary between these structural styles in the vicinity of Porcupine Lake, in the Arctic National Wildlife Refuge. The northern edge of thrust-truncated folds in Lisburne is marked by a local range front that likely represents an eastward continuation of the central Brooks Range front. This is bounded to the north by a gently dipping panel of Lisburne with local asymmetrical folds. The leading edge of the flat panel is thrust over Permian to Cretaceous rocks in a synclinal depression. These younger rocks overlie symmetrically detachment-folded Lisburne, as is extensively exposed to the north.

Six partial sections were measured in the Lisburne of the flat panel and local range front. The Lisburne here is about 700 m thick and is interpreted to consist primarily of the Wachsmuth and Alapah Limestones, with only a thin veneer of Wahoo Limestone. The Wachsmuth (200 m) is gradational between the underlying Missippian Kayak Shale and the overlying Mississippian Alapah, and increases in resistance upward. The Alapah consists of a lower resistant member (100 m) of alternating limestone and chert, a middle recessive member (100 m), and an upper resistant member (260 m) that is similar to Wahoo in the northeastern Brooks Range. The Wahoo is recessive and is thin (30 m) due either to non-deposition or erosion beneath the sub-Permian unconformity. The Lisburne of the area records two major episodes of transgression and shallowing-upward on a carbonate ramp. Thicknesses and facies vary along depositional strike.

Asymmetrical folds, mostly truncated by thrust faults, were studied in and south of the local range front. Fold geometry was documented by surveys of four thrust-truncated folds and two folds not visibly cut by thrusts. A portion of the local range front was mapped to document changes in fold geometry along strike in three dimensions. The folds typically display a long, non-folded gently to moderately dipping backlimbs and steep to overturned forelimbs, commonly including parasitic anticline-syncline pairs. Thrusts commonly cut through the anticlinal forelimb or the forward synclinal hinge. These folds probably originated as detachment folds based on their mechanical stratigraphy and the transition to detachment folds to the north. Their geometry indicates that they were asymmetrical prior to thrust truncation. This asymmetry may have favored accommodation of increasing shortening by thrust breakthrough rather than continued folding.

Fracture patterns were documented in the gently dipping panel of Lisburne and the asymmetrical folds within it. Four sets of steeply dipping extension fractures were identified, with strikes to the 1) N, 2) E, 3) N to NW, and 4) NE. The relative timing of these fracture sets is complex and unclear. En echelon sets of fractures are common, and display normal or strike-slip sense. Mesoscopic and penetrative structures are locally well developed, and indicate bed-parallel shear

within the flat panel and strain within folds. Three sets of normal faults are well developed in the area, and are unusual for the Brooks Range. One set is parallel to and another is transverse to the strike of the folds. A single major normal fault has an intermediate orientation. The normal faults cut across folds, but may have been active late during folding because fold geometry differs across faults and some folding apparently continued after normal faulting.

Folds in Lisburne carbonates reveal complex relations between folding and mesoscopic structures, including fractures. Different mesoscopic structures formed at different times during fold evolution. Orogen-normal extension fractures may form in relatively undeformed rocks ahead of the fold-and-thrust belt. A variety of mesoscopic structures accompany folding and reflect different mechanisms and conditions. Flexural slip and associated fractures are prevalent in the early evolution of the fold. Homogeneous fold flattening may supersede flexural slip as folds tighten and/or conditions favor ductile deformation, and earlier-formed fractures may be overprinted or destroyed by ductile strain. Extension fractures may again become important as brittle conditions return during unroofing, late during or after folding.

Wellbore trajectory and connectivity were analyzed for the two dominant sets of fractures in relatively undeformed Lisburne: a NNW-striking set and an ENE-striking set with smaller but more numerous fractures. The optimum wellbore trajectory bisects the two sets if fractures of both sets are assumed to cut across each other. However, if ENE fractures are assumed to terminate against the NNW fractures, the optimum trajectory is normal to the NNW set. Variability in the strike and dip of fractures has less effect than termination. Number vs. area of fractures connected to the wellbore may not correlate if one set terminates against the other. Sensitivity analysis indicates that a decrease in the largest fractures has the largest effects on conductance and connectivity. A significant decrease in transmissivity of the ENE fractures decreases conductance in both directions, but a significant decrease in transmissivity of the NNW fractures decreases conductance mainly in the NNW direction.

Table of contents

Part A: Introduction and geologic setting,
by Wesley K. Wallace
Definition of problem and objectives....A-1
Scope of this report....A-2
Geologic setting....A-3
Regional stratigraphy and its structural implications....A-3
Structural domains of the Porcupine Lake structural low....A-4
Questions about the Porcupine Lake structural low....A-5
Location of the field studies included in this report....A-6
References....A-6
Figures....A-8

Part B: Baseline stratigraphy of the Lisburne Group,
by Michelle M. McGee, Michael T. Whalen, and Andrea P. Krumhardt
Abstract....B-1
Objective....B-1
Methods....B-2
Observations and interpretations....B-2
Data analysis....B-4
XRD....B-4
Conodont biostratigraphy....B-4
Discussion/Conclusions....B-5
Research plan for project completion....B-5
Recommended approach for future similar research....B-6
References....B-7
Tables....B-8
Figures....B-13

Part C: Geometry and evolution of thrust-truncated detachment folds in the upper Marsh Fork area of the eastern Brooks Range fold-and-thrust belt, Alaska,
by Margarete A. Jadamec and Wesley K. Wallace
Abstract....C-1
Introduction....C-1
Geologic setting....C-2
Structural framework and location....C-2
Tectonic history....C-3

Regional stratigraphy..... C-3
Mechanical stratigraphy..... C-4
Methods..... C-5
Overview..... C-5
Survey data collection..... C-5
Mapping and survey results..... C-7
Overview of results..... C-7
Structural style along strike in the west UMF area..... C-8
Structural style across strike in the east UMF area..... C-8
Preliminary interpretations..... C-9
Questions raised..... C-10
Future work..... C-11
Acknowledgements..... C-11
References..... C-12
Figures..... C-15
Table..... C-27

Part D: The relationship between fracturing, asymmetric folding, and normal faulting in Lisburne Group carbonates: West Porcupine Lake valley, northeastern Brooks Range, Alaska,

by J.R. Shackleton, C.L. Hanks, and W.K. Wallace

Abstract..... D-1
Introduction..... D-2
Fractures and folds..... D-3
Mechanical stratigraphy and fracture development..... D-3
Geologic setting..... D-4
Lisburne Group stratigraphy..... D-5
Methodology..... D-5
Preliminary observations..... D-7
Mechanical stratigraphy of the Lisburne Group..... D-7
Map scale and mesoscopic scale structures..... D-8
Structure: fracturing..... D-9
Preliminary interpretations..... D-10
Structure: mechanism of folding..... D-10
Influence of mechanical stratigraphy on folds in the area..... D-10
Normal faulting..... D-10
Fracturing..... D-11
Future research..... D-12

References....D-13
Figures....D-16
Appendix: fracture data....D-32
Appendix A: Background fractures....D-33
Appendix B: Open folds....D-57
Appendix C: East camp syncline....D-75
Appendix D: West camp syncline: Lower transect....D-81
Appendix E: West camp syncline: Upper transect....D-102

Part E: Timing and character of mesoscopic structures in detachment folds and implications for fold development--An example from the northeastern Brooks Range, Alaska,

by C.L. Hanks, W.K. Wallace, J.C. Lorenz, P.K. Atkinson, J. Brinton, and J.R. Shackleton

Abstract....E-1
Introduction....E-1
Previous work....E-2
Detachment folds....E-2
Fold mechanisms: Flexural flow, flexural slip, and homogeneous flattening....E-3
Regional setting....E-3
Observations....E-4
Mesoscopic structures in non-folded Lisburne Group....E-4
Mesoscopic structures in detachment-folded Lisburne Group....E-5
Discussion....E-6
Implications of ductile vs. brittle structures for folding mechanism....E-6
Deformation conditions....E-7
Conclusions....E-7
References....E-9
Figures....E-12

Part F: Lisburne Group fracture distribution and flow modeling,

by A.V. Karpov, Thang Bui, J.L. Jensen, and C.L. Hanks

Abstract....F-1
Introduction....F-1
Fracture model....F-2
Wellbore modelling results....F-3
Wellbore modelling comments....F-4
Fracture system conductivity evaluation....F-5

Conductivity comments.....F-7
Conclusions.....F-7
Future work.....F-8
Acknowledgements.....F-8
References.....F-8

List of figures

Part A: Introduction and geologic setting

Figure 1. Map of western part of northeastern Brooks Range.....A-8
Figure 2. Generalized geologic map of the Porcupine Lake structural low.....A-9
Figure 3. Schematic cross section showing the major structural domains and features in western Porcupine Lake valley..... A-10

Part B: Baseline stratigraphy of the Lisburne Group

Figure 1.Map illustrating the location of measured stratigraphic sections..... B-13
Figure 2. Photomosaics of the Lisburne in Forks area and Marsh Fork area.....B-14
Figure 3. Cross section A-A'.....B-15
Figure 4. Simplified cross-section inllustrating the thicknesses of major lithologic units.....B-16
Figure 5. Stratigraphic section EF B-17

Part C: Geometry and evolution of thrust-truncated detachment folds in the upper Marsh Fork area of the eastern Brooks Range fold-and-thrust belt, Alaska

Figure 1. Schematic models of three thrust-related fold types.....C-15
Figure 2. Generalized tectonic map of the eastern and northeastern Brooks Range.....C-16
Figure 3. Cross section of the northeastern and eastern Brooks Range.....C-17
Figure 4. Stratigraphic columns for the North Slope parautochthon and Endicott Mountains allochthon.....C-18
Figure 5. Topographic map depicting the east, central, and west regions of the upper Marsh Fork field area.....C-19
Figure 6. Coordinate systems used in collection and processing of survey data.....C-20
Figure 7a. Schematic stratigraphic column of Lisburne Group and surrounding units.....C-21
Figure 7b. Outcrop character of Lisburne Group.....C-22
Figure 8. Interpretive bedrock geology map of west upper Marsh Fork area..... C-23
Figure 9. Interpretive bedrock geology map of east upper Marsh Fork area..... C-24
Figure 10. Preliminary cross section CC' in west upper Marsh Fork area.....C-25
Figure 11. Cross sectional plot of survey data from the east upper Marsh Fork area.....C-26

Part D: The relationship between fracturing, asymmetric folding, and normal faulting in Lisburne Group carbonates: West Porcupine Lake valley, northeastern Brooks Range, Alaska

Figure 1. Regional structure and tectonic map of the Brooks Range and North Slope....D-16
Figure 2. Fracture orientation with increasing strain and related to folds....D-17
Figure 3. Simplified models for detachment folds....D-18
Figure 4. Model for fault-propagation folding....D-19
Figure 5. Model for fault-bend folding....D-20
Figure 6. Lithostratigraphy and mechanical stratigraphy, northeastern Brooks Range....D-21
Figure 7. Geologic map of the western portion of the northeastern Brooks Range....D-22
Figure 8. Cross section through the northeastern Brooks Range....D-23
Figure 9. Generalized lithostratigraphy, Endicott, Lisburne, and Sadlerochit Groups....D-24
Figure 10. Photograph of the stratigraphy in west Porcupine Lake valley....D-25
Figure 11. Generalized mechanical stratigraphy of the Kayak Shale, Lisburne Group, and Sadlerochit Group in west Porcupine Lake valley....D-26
Figure 12. Geologic map of west Porcupine Lake valley....D-27
Figure 13. Cross section through west Porcupine Lake valley....D-28
Figure 14. View west of camp syncline with sample locations....D-29
Figure 15. View northeast of open anticline and syncline with sample locations....D-30
Figure 16. Preliminary interpretive sketch of selected fracture sets in camp syncline....D-31

Part E: Timing and character of mesoscopic structures in detachment folds and implications for fold development--An example from the northeastern Brooks Range, Alaska

Figure 1. Three types of fault-related folds....E-12
Figure 2a. Tectonic map of northern Alaska....E-13
Figure 2b. Tectonic map of the western part of the northeastern Brooks Range....E-14
Figure 2c. Regional balanced cross section across western part of the northeastern Brooks Range....E-15
Figure 3. Detachment fold models....E-16
Figure 4. Schematic stratigraphy of Triassic and older rocks

of the northeastern Brooks Range, emphasizing mechanical stratigraphy.....E-17
Figure 5. Non-folded but tilted Lisburne Group carbonates
display the simplest fracture pattern..... E-18
Figure 6. En echelon extension fractures suggest flexural slip
was an important mechanism during folding.....E-19
Figure 7. Sheared stylolites and crinoid columnals from a flat panel
suggest that layer-parallel shear preceded folding..... E-20
Figure 8. Penetrative strain and flattening resulted in
thickening in the hinge areas of detachment folds..... E-21
Figure 9. A well-developed set of conjugate fractures on a bedding surface.....E-22
Figure 10. Different folds may exhibit different types and
sequences of structures depending upon the depth at which deformation
occurred and the overall amount of shortening.....E-23
Figure 11. A fold-and-thrust belt generally grows at its leading edge.....E-24

Part F: Lisburne Group fracture distribution and flow modeling

Figure 1. Different cases simulated in FracMan software..... F-2
Figure 2. Fracture number contacted by the wellbore vs. matrix area
accessed, for the “base” case model.....F-3
Figure 3. FracMan working window showing orientations of
four 10-meter long wellbores used for the anisotropy analysis..... F-5
Figure 4. Conductance vs. flow direction for the “base” case and
six cases with variable relative transmissibility of the sets..... F-6
Figure 5. FracMan working window showing orientation of
two wellbores used for the sensitivity study..... F-6

List of tables

Part B: Baseline stratigraphy of the Lisburne Group

Table 1. Summary of outcrop and sample data collected in the northeastern Brooks Range during summer 2000.....B-8

Table 2. X-ray diffraction data.....B-9

Part C: Geometry and evolution of thrust-truncated detachment folds in the upper Marsh Fork area of the eastern Brooks Range fold-and-thrust belt, Alaska

Table 1. Summary of west and east upper Marsh Fork area anticline properties..... C-27

Introduction and geologic setting

by Wesley K. Wallace, Geophysical Institute and Department of Geology and Geophysics, University of Alaska, Fairbanks, Alaska 99775-5780

Definition of problem and objectives

Carbonate rocks of the Carboniferous Lisburne Group are found throughout a vast region of northern Alaska, including the subsurface of the North Slope and the northern Brooks Range. The Lisburne is a major hydrocarbon reservoir in the North Slope: It was the original target at Prudhoe Bay and is the currently producing reservoir in the Lisburne oil field. Folded and thrust-faulted Lisburne has been a past exploration target in the foothills of the Brooks Range, and will be increasingly important with growing interest in exploration for gas. It also is an important potential future target for oil and gas exploration in the coastal plain of the Arctic National Wildlife Refuge (1002 area). However, relatively little is known about the reservoir characteristics and behavior of the Lisburne and how they change as a result of deformation.

As in many carbonate reservoirs, most of the hydrocarbon production from the Lisburne Group is from naturally occurring fractures. Natural fractures play an essential role in production from the reservoir, but the geologic factors that control the origin, distribution, and character of these fractures are poorly understood. In the Lisburne oil field, less than 10% of the 2 billion barrels in place is recoverable at the present time. A clearer understanding of the nature and origin of these fractures has the potential to aid in the development of secondary and tertiary recovery programs for a reservoir that is large but difficult to produce.

Future targets for exploration in the Lisburne likely will be along the northern edge of the Brooks Range orogen, where the Lisburne has been modified by fold-and-thrust deformation. Such deformation has long been recognized both to enhance porosity and permeability, largely through the formation of fractures, and to reduce them by compression, as reflected by the formation of cleavage and stylolites. However, the ability to predict patterns of enhancement or reduction in porosity and permeability and how they vary within a particular fold trap remain quite limited. Recent rapid advances in the understanding of the geometry and kinematics of different types of folds that form in fold-and-thrust settings offer great potential to improve the systematic understanding of enhancement or reduction in porosity and permeability in fold traps, but these advances have only begun to be applied.

The Lisburne Group is a structurally competent unit that overlies an incompetent unit. Hence, the Lisburne undergoes a progressive evolution as shortening increases, from its undeformed state, to tightening detachment folds, to detachment folds that either continue to tighten or are truncated by thrust faults, depending on whether they are symmetrical or asymmetrical. How trap geometry and reservoir characteristics vary as this evolution progresses is not systematically understood, particularly with respect to differences in lithology and position within a fold. The basic objective of this study is to document and develop predictive models for structurally induced changes in reservoir geometry and characteristics at different stages in the evolution of detachment folds in the Lisburne Group.

Extensive exposures of the Lisburne Group in the northeastern Brooks Range fold-and-thrust belt offer the opportunity to develop a clearer understanding of the origin, distribution, and character of structurally induced enhancement and reduction of porosity and permeability in the Lisburne Group. The Lisburne Group is deformed into detachment folds that have evolved to different degrees, and thus provides a series of natural experiments in which to observe those structures and to develop models both for their formation and for the resulting patterns of enhancement and reduction of porosity and permeability. The results of these field-based observations and models

can then be used to develop quantitative models for characterization of Lisburne reservoirs and the fluid flow within them. Such models can be applied to a spectrum of traps from relatively undeformed to highly folded and thrust faulted.

This study of the Lisburne Group has the following major objectives:

•Establish 'baseline' reservoir characteristics in a relatively undeformed section and develop fracture and fluid flow models and a wellbore placement strategy in such reservoir.

•Document the evolution of trap-scale fold geometry with increasing shortening, with emphasis on changes in thickness across the fold and with respect to mechanical stratigraphy.

•Characterize the differences between folds that continue to shorten by tightening vs. those that are cut by thrust faults as shortening increases.

•Determine patterns in reservoir enhancement and destruction within a fold trap as a function of mechanical stratigraphy and of position within folds at different stages of evolution.

•Use observations of natural folds to constrain predictive models for the evolution of trap-scale fold geometry with increasing shortening and for the resulting modifications of reservoir characteristics.

•Use observations of natural folds and predictive fold models as a basis for fracture models for fluid flow and wellbore placement strategies in fold traps.

The results of this study will apply to current production in relatively undeformed Lisburne and to future exploration in deformed Lisburne. At least as important is the fact that the results will apply generally to carbonate reservoirs and to folded reservoirs, both of which are major producers and exploration targets worldwide.

Scope of this report

This report summarizes the results of this project's second season of field work, which was conducted during the summer of 2000. The report reflects progress to June, 2001. It presents examples of compiled data and interpretations based on field observations and preliminary analysis. Results of further data compilation, analysis, and interpretation will be presented in future reports. The report does not address studies begun during the project's first (1999) season of field work except for a discussion of mesoscopic structures and detachment fold development (Chapter E) and an update on fracture and flow modeling (Chapter F). Further results of these studies will be presented in future reports.

Participants in this report include six Master's students (P.K. Atkinson, J. Brinton, T. Bui, M.A. Jadamec, A.V. Karpov, and J.R. Shackleton), a Ph.D. student (M.M. McGee), a micropaleontological analyst (A.P. Krumhardt), three University of Alaska faculty (W.K. Wallace, C.L. Hanks, and M.T. Whalen), one Texas A & M faculty (J.L. Jensen), and a visiting scientist from Sandia National Laboratories (J.C. Lorenz).

The report consists of six chapters that each summarize a different aspect of the study and are written by different authors. These include:

•A. Introduction and geologic setting, by W.K. Wallace

•B. Baseline stratigraphy of the Lisburne Group, by M.M. McGee, M.T. Whalen, and A.P. Krumhardt

•C. Geometry and evolution of thrust-truncated detachment folds in the upper Marsh Fork area of the eastern Brooks Range fold-and-thrust belt, Alaska, by M.A. Jadamec and W.K. Wallace

•D. The relationship between fracturing, asymmetric folding, and normal faulting in Lisburne Group carbonates: West Porcupine Lake valley, by J.R. Shackleton, C.L. Hanks, and

W.K. Wallace

•E. Timing and character of mesoscopic structures in detachment folds and implications for fold development--An example from the northeastern Brooks Range, Alaska, by C.L. Hanks, W.K. Wallace, J.C. Lorenz, P.K. Atkinson, J. Brinton, and J.R. Shackleton

•F. Lisburne Group fracture distribution and flow modeling, by A.V. Karpov, T. Bui, J.L. Jensen, and C.L. Hanks

Geologic Setting

The Lisburne Group is the most abundant and widely distributed rock unit in the northern Brooks Range, where it forms the range front in most places and extends a significant distance southward into the range. This unit displays two distinct structural styles in different parts of the northern Brooks Range. Imbricately stacked thrust sheets characterize the Lisburne south of the range front in the western and central Brooks Range and south of the projection of the range front into the eastern Brooks Range. These thrust sheets commonly display asymmetrical hangingwall anticlines and footwall synclines, but only rare asymmetrical folds that have not been cut by thrust faults. In contrast, the northeastern Brooks Range is characterized by symmetrical detachment folds only rarely cut by thrust faults. The "Continental Divide thrust front" marks the boundary between these two structural styles (Figure A-1).

The focus of the first summer of field work for this study was on the Lisburne and its structures north of the Continental Divide thrust front, in the detachment-folded Lisburne of the northeastern Brooks Range. The second summer of field work addressed the asymmetrically folded and imbricated Lisburne south of the thrust front. This report presents results mainly from that second field season. The structural style south of the Continental Divide thrust front is exceptionally well exposed along the southern margin of an important structural low near Porcupine Lake (Figure A-1). This area was the geographic focus of most of the studies presented in this report.

Regional stratigraphy and its structural implications

Little published information is available on the stratigraphy in the Porcupine Lake area. Major differences in stratigraphy exist across the Continental Divide thrust front beneath the Mississippian Kayak Shale, but the differences are much less clear higher in the section. North of the thrust front, a complex of penetratively deformed and slightly metamorphosed pre-Middle Devonian sedimentary and subordinate volcanic rocks forms depositional basement and is unconformably overlain by a thin veneer of Mississippian Kekiktuk Conglomerate. To the south, a much expanded clastic succession exists downward from the stratigraphic position of the Kekiktuk Conglomerate and the underlying basement rocks are not exposed (e.g., Imm et al., 1993). This clastic succession probably is equivalent to the succession documented to the east-northeast by Anderson et al. (1994), where the Middle Devonian (and younger?) Ulungarat formation unconformably overlies basement and is in turn unconformably overlain by Mississippian Kekiktuk Conglomerate with a small angular discordance.

The Kekiktuk Conglomerate is conformably overlain by a succession that consists of the Mississippian Kayak Shale, carbonate rocks of the Mississippian and Pennsylvanian Lisburne Group, and shale and subordinate sandstone of the Permian and Lower Triassic Sadlerochit Group (or its equivalents). A similar succession is present on both sides of the Continental Divide thrust front. Preliminary work (detailed in chapter B of this report) indicates that the Lisburne south of the thrust front is thicker and represents deeper-water deposition than to the north.

The stratigraphic succession has a profound influence on the character of structures on both sides of the Continental Divide thrust front. Basement to the north forms thick fault-bend folded thrust sheets, whereas the clastic rocks at the base of the succession to the south are detached from basement and form thinner imbricate thrust sheets (Wallace, 1993). The Lisburne serves as a competent structural member bounded by structural detachments in the underlying and overlying incompetent shales on both sides of the thrust front, but forms thrust-truncated folds to the south and detachment folds to the north.

These are the stratigraphic units most relevant to this report. Other units that are locally preserved within the Porcupine Lake structural low are mentioned below.

Structural domains of the Porcupine Lake structural low

The Porcupine Lake structural low and a similar low at Bathtub Ridge to the east-northeast lie along structural strike with the range front of the central Brooks Range. They display similar structural characteristics to that range front and probably represent remnants of its eastern continuation. This range front originated as the leading edge of far-displaced allochthons in Late Jurassic to Early Cretaceous time (Moore et al., 1994a), but was structurally modified and attained the structural relief responsible for its present topographic expression in Paleocene time (O'Sullivan et al., 1997). In the eastern Brooks Range, the older range front became isolated within the range as the deformation front migrated northward to form the northeastern Brooks Range in Eocene and later time (Wallace and Hanks, 1990; Hanks et al., 1994; O'Sullivan, 1994). The Porcupine Lake and Bathtub Ridge structural lows locally preserve rocks and structures that have been uplifted and eroded elsewhere along the former range front.

A zone that consists of four distinct structural domains defines the boundary in structural styles between the central and northeastern Brooks Range across the Porcupine Lake structural low (Figures A-2 & A-3). The southernmost domain is a local range front that forms the southern edge of the lower topography of the structural low to the north. This range front is typical of the range front of the central Brooks Range, which lies along strike. It is marked by a distinct topographic front defined by folds at the leading edges of overlapping thrust sheets. This range front marks the northern edge of the structural style characteristic of the northern part of the main axis of the Brooks Range (Moore et al., 1994a; Wallace et al., 1997). South-dipping thrust sheets of Lisburne are bounded by décollements in the underlying Kayak Shale and overlying Sadlerochit Group. Asymmetrical hangingwall anticlines and footwall synclines commonly mark the leading and trailing edges of these thrust sheets. Local unbroken asymmetrical folds suggest that the hangingwall anticlines and footwall synclines formed by thrust-breakthrough of the steep limbs of asymmetrical folds.

The domain north of the local range front consists of an extensive, nearly flat-lying panel of Lisburne and Sadlerochit (Figures A-2 & A-3) that locally displays unbroken asymmetrical folds and is cut by two sets of normal faults, one parallel to and another transverse to regional structure. In the lowest part of the regional structural low, this panel is overlain by a klippe of Carboniferous to Cretaceous rocks that are probably equivalent to remnants of south-derived allochthons preserved along the central Brooks Range front and in the western Brooks Range. The leading edge of the flat-lying panel is locally exposed as a hangingwall anticline in Lisburne thrust over rocks of the Sadlerochit Group.

To the north of the flat panel, a synclinal depression centered near Porcupine Lake (Figures A-2 & A-3) preserves strata that have been eroded throughout most of the northeastern Brooks Range

except near its northern range front and at Bathtub Ridge. In addition to the Permian and Triassic Sadlerochit Group, these rocks include the Triassic Shublik Formation, the Jurassic and Lower Cretaceous Kingak Shale, the Lower Cretaceous Kongakut Formation, and the Lower Cretaceous Bathtub Graywacke. The youngest part of this succession includes probable equivalents of foreland basin deposits found in similar synclinal lows along strike to the west along the central Brooks Range front and to the east in Bathtub syncline. Local exposures of folded Lisburne within this synclinal depression suggest that it marks the southern extent of the symmetrical detachment folds characteristic of the northeastern Brooks Range.

A fourth domain is exposed only to the east (Figure A-2), where imbricated Lisburne and older rocks form a structural high that plunges westward beneath the Permian and younger rocks preserved in the synclinal depression. This structural high is bounded to the south by a thrust fault along the leading edge of the flat panel and to the north by a thrust fault that was itself folded when symmetrical detachment folds formed in the underlying Lisburne and Sadlerochit. The core of the structural high consists of imbricated coarse-grained siliciclastic rocks that are structurally bounded above and below by folded and imbricated Lisburne. The siliciclastic rocks lie beneath the sub-Lisburne décollement (in Kayak) and are probably equivalent to a parautochthonous Middle Devonian to Mississipian clastic wedge (Ulungarat and Kekiktuk Formations) that is exposed to the east.

Questions about the Porcupine Lake structural low

The structural characteristics of the Porcupine Lake structural low raise a number of unresolved questions that are relevant to this project. These questions are only briefly introduced here, but will be addressed in more detail in other parts of this report and in future research.

The most central of these questions is why structural style changes across the low from thrust-truncated asymmetrical folds to symmetrical detachment folds. Wallace (1993) suggested several possible controlling factors, including changes across the boundary in mechanical stratigraphy, dip of the basal detachment, amount of depositional and structural overburden, and/or amount of shortening. The role of each of these factors will be explored in future work, but field observations have already confirmed that differences in mechanical stratigraphy exist across the boundary. Specifically, the Lisburne south of the boundary is thicker and more competent than to the north, and the stratigraphic character and structural behavior of the underlying rocks changes across the boundary. These stratigraphic differences raise additional questions that may have bearing on interpretation of the factors controlling structural style.

The Endicott Mountains allochthon is interpreted to have been displaced a large distance northward over parautochthonous rocks of the North Slope and northeastern Brooks Range (Mull et al., 1987, 1989; Moore et al., 1994a & b). The Upper Devonian Hunt Fork Shale, Noatak Sandstone, and Kanayut Conglomerate are stratigraphic units found only in the allochthon. However, direct equivalents of the parautochthonous section are found in the overlying rocks of the allochthon, including the Kayak Shale, Lisburne Limestone, and Siksikpuk Formation, and distinction between the allochthon and parautochthon is difficult in this part of the section. The northern edge of the Endicott Mountains allochthon has generally been interpreted to lie a significant distance to the south of the Porcupine Lake structural low (e.g., Mull et al., 1989; Imm et al., 1993; Moore et al., 1994b). However, two observations suggest the possibility that the leading edge of the Endicott Mountains allochthon might extend northward to the northern edge of the flat panel. First, the northern edge of the flat panel is locally seen to be a thrust fault whose displacement is indeterminate. Second, the stratigraphy of the Lisburne and Sadlerochit-equivalent rocks of the flat

panel and the local range front differ somewhat from those of the known parautochthon to the north. Detailed stratigraphic study is required to determine whether or not these rocks belong to the allochthon. The location of the northern edge of the Endicott Mountains allochthon could have a bearing on the change from thrust-truncated to untruncated folds in the Lisburne, although this change in structural style does not coincide with the allochthon boundary farther west (Wallace et al., 1997).

A similar question involves the stratigraphic affinity of the sub-Kayak clastic rocks in the structural high east of the Porcupine Lake structural low. Based on their location and character, these rocks most likely are equivalent to the parautochthonous Middle Devonian to Mississipian Ulungarat and Kekiktuk Formations. However, the possibility must also be considered that they are equivalents of the Kanayut Conglomerate of the Endicott Mountains allochthon. The identity of these rocks has major implications for structural interpretation, but requires detailed stratigraphic study to resolve.

Two other questions involve structural characteristics of the Porcupine Lake structural low that are apparently absent from the central Brooks Range front. First, why does the flat panel exist, and why are the folds within it not generally truncated by thrust faults? Second, why are two different sets of normal faults so prominently developed within the flat panel? The answers to these questions are obviously relevant to our studies of fold and fracture evolution within the flat panel.

Location of the field studies included in this report

The focus of the 2000 field season was on the stratigraphy, folding, thrust truncation, and fracturing of Lisburne that has been asymmetrically folded. Consequently, the field observations summarized in chapters B, C, and D of this report are from the local range front and flat panel domains of the Porcupine Lake area (Figures A-2 & A-3). Lisburne stratigraphy appears to be the same in the two domains and is described in Chapter B. Chapter C describes thrust-truncated asymmetrical folds along the local range front south of the central part of the Porcupine Lake structural low. Chapter D describes the structure of the western part of the flat panel, including asymmetrical folds, normal faults, and associated fractures.

References

Anderson, A.V., Wallace, W.K., and Mull, C.G., 1994, Depositional record of a major tectonic transition in northern Alaska: Middle Devonian to Mississippian rift-basin margin deposits, upper Kongakut River region, eastern Brooks Range, Alaska, in Thurston, D., and Fujita, K., eds., 1992 Proceedings International Conference on Arctic Margins, U.S. Minerals Management Service Outer Continental Shelf Study 94-0040, p. 71-76.

Hanks, C.L., Wallace, W.K., and O'Sullivan, P., 1994, The Cenozoic structural evolution of the northeastern Brooks Range, Alaska, in Thurston, D., and Fujita, K., eds., 1992 Proceedings International Conference on Arctic Margins, U.S. Minerals Management Service Outer Continental Shelf Study 94-0040, p. 263-268.

Imm, T.A., Dillon, J.T., and Bakke, A.A., 1993, Generalized geologic map of the Arctic National Wildlife Refuge, northeastern Brooks Range, Alaska: Alaska Division of Geological and Geophysical Surveys Special Report 42, scale 1:500,000, 1 sheet.

Moore, T.E., Wallace, W.K., Bird, K.J., Karl, S.M., Mull, C.G., and Dillon, J.T., 1994a, Chapter 3: Geology of northern Alaska, in Plafker, G., and Berg, H.C., eds., The geology of Alaska: The Geology of North America, Geological Society of America, Boulder, Colorado, v. G1, p. 49-140.

Moore, T.E., Wallace, W.K., Mull, C.G., Karl, S.M., and Bird, K.J., 1994b, Generalized geologic

map and sections for northern Alaska, in Plafker, G., and Berg, H.C., eds., The geology of Alaska: The Geology of North America, Geological Society of America, Boulder, Colorado, v. G1, p. Plate 6.

Mull, C.G., Roeder, D.H., Tailleur, I.L., Pessel, G.H., Grantz, A., and May, S.D., 1987, Geologic sections and maps across Brooks Range and Arctic Slope to Beaufort Sea: Geological Society of America Map and Chart Series MC-28S, scale 1:500,000, 1 sheet.

Mull, C.G., Adams, K.E., and J.T. Dillon, J.T., 1989, Stratigraphy and structure of the Doonerak fenster and Endicott Mountains allochthon, central Brooks Range, in Mull, C.G., and Adams, K.E., eds., Dalton Highway, Yukon River to Prudhoe Bay, Alaska, Bedrock geology of the eastern Koyukuk basin, central Brooks Range, and east central Arctic Slope: Alaska Division of Geological and Geophysical Surveys Guidebook 7, v. 2, p. 203-217.

O'Sullivan, P.B., 1994, Timing of Tertiary episodes of cooling in response to uplift and erosion, northeastern Brooks Range, Alaska, in Thurston, D., and Fujita, K., eds., 1992 Proceedings International Conference on Arctic Margins, U.S. Minerals Management Service Outer Continental Shelf Study 94-0040, p. 269-274.

O'Sullivan, P.B., Murphy, J.M., and Blythe, A.E., 1997, Late Mesozoic and Cenozoic thermotectonic evolution of the central Brooks Range and adjacent North Slope foreland basin, Alaska: Including fission track results from the Trans-Alaska Crustal Transect (TACT): Journal of Geophysical Research, v. 102, no. B9, p. 20,821-20,845.

Wallace, W.K., 1993, Detachment folds and a passive-roof duplex: Examples from the northeastern Brooks Range, Alaska, in Solie, D.N., and Tannian, F., eds., Short Notes on Alaskan Geology 1993: Alaska Division of Geological and Geophysical Surveys Geologic Report 113, p. 81-99.

Wallace, W.K., and Hanks, C.L., 1990, Structural provinces of the northeastern Brooks Range, Arctic National Wildlife Refuge, Alaska: American Association of Petroleum Geologists Bulletin, v. 74, no. 7, p. 1100-1118.

Wallace, W.K., Moore, T.E., and Plafker, G., 1997, Multistory duplexes with forward dipping roofs, north central Brooks Range, Alaska: Journal of Geophysical Research, v. 102, no. B9, p. 20,773-20,796.

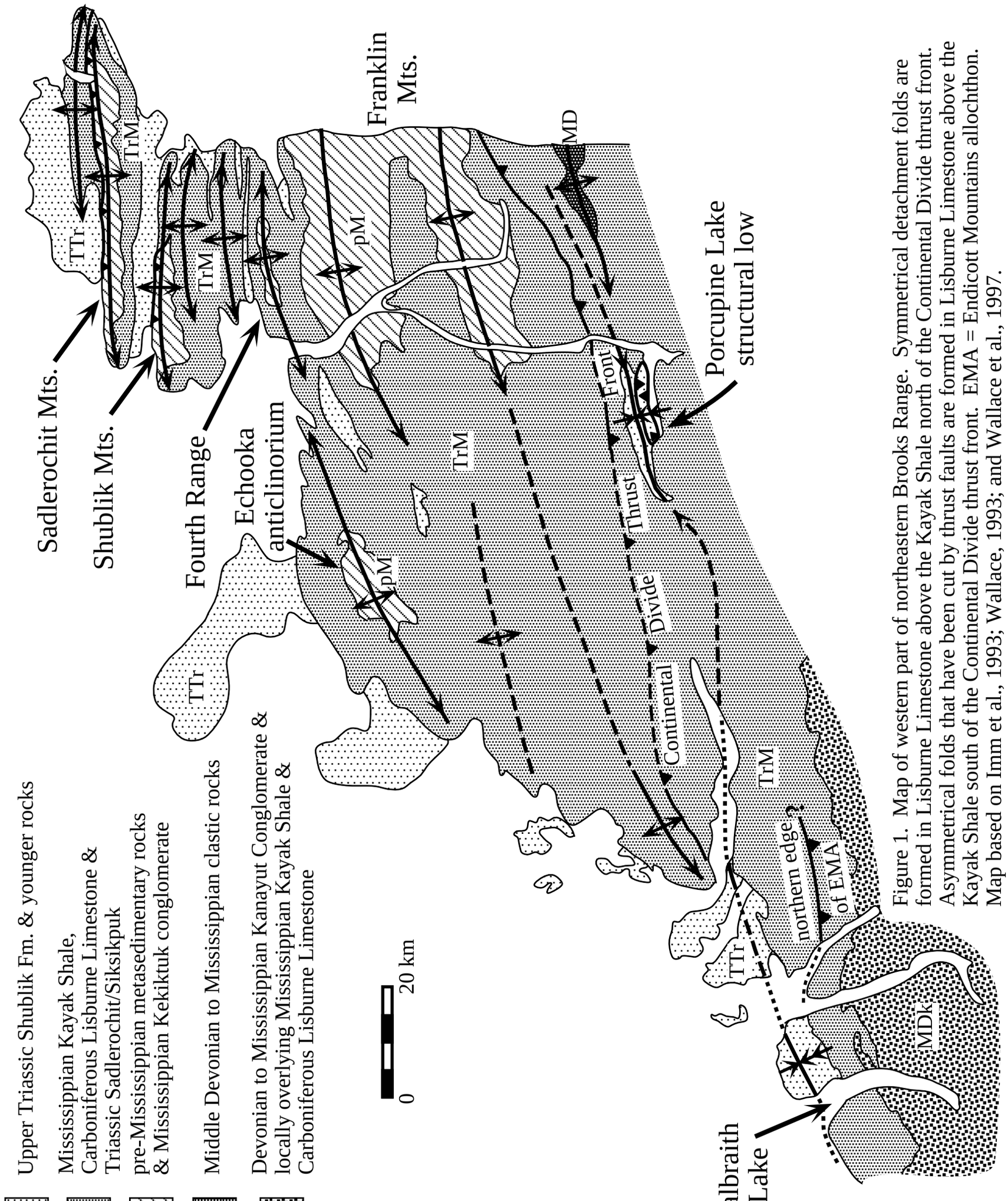

Figure 1. Map of western part of northeastern Brooks Range. Symmetrical detachment folds are formed in Lisburne Limestone above the Kayak Shale north of the Continental Divide thrust front. Asymmetrical folds that have been cut by thrust faults are formed in Lisburne Limestone above the Kayak Shale south of the Continental Divide thrust front. EMA = Endicott Mountains allochthon. Map based on Imm et al., 1993; and Wallace et al., 1997.

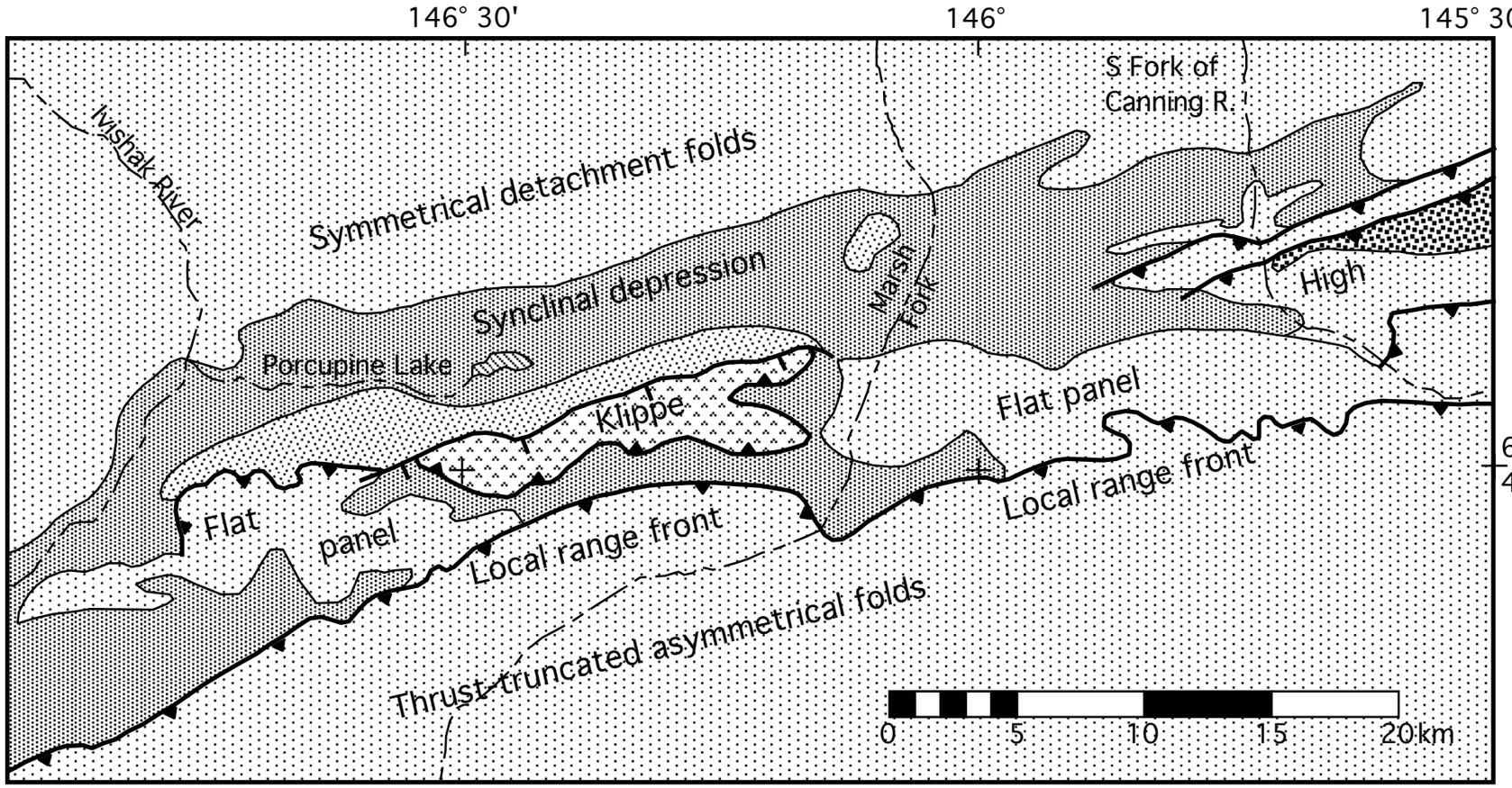

Devonian to Mississippian conglomerate, sandstone, and shale (Ulungarat & Kekiktuk Fms., Kayak Shale)

Carboniferous limestone (Lisburne Group)

Permian to Triassic shale and sandstone (Sadlerochit Group and local Shublik Fm.)

Jurassic and Lower Cretaceous shale and sandstone (Kingak Sh., Kongakut Fm., Bathtub Graywacke)

Mt. Annette allochthon, Mississippian to Lower Cretaceous

Figure 2. Generalized geologic map of the Porcupine Lake structural low showing the main structural domains and related structural features.

DE-AC26-98BC15102

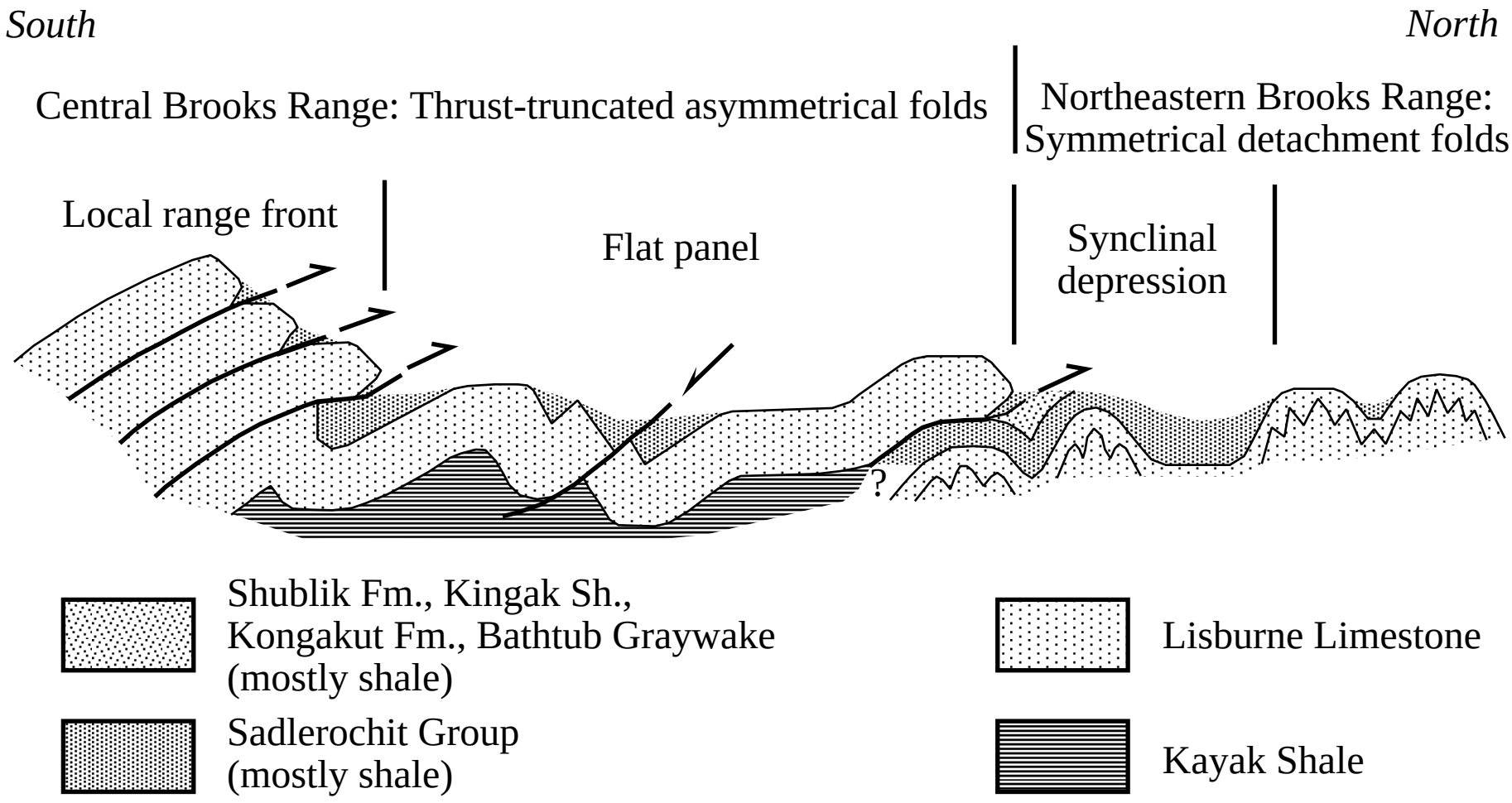

Figure 3. Schematic cross section showing the major structural domains and features in western Porcupine Lake valley. The structural high that exposes Devonian to Mississippian clastic rocks to the east is not shown here.

DE-AC26-98BC15102

Baseline stratigraphy of the Lisburne Group

by Michelle M. McGee, Michael T. Whalen, and Andrea P. Krumhardt Geophysical Institute and Department of Geology and Geophysics, University of Alaska, Fairbanks, Alaska 99775-5780

Abstract

Further progress has been made on establishing the baseline stratigraphy of the Lisburne Group in the northeastern Brooks Range. This report concentrates on analysis of field data collected in the Porcupine Lake area, Philip Smith Mountains. Six partial sections in the Wachsmuth and Alapah Limestone were the focus of the 2000 field season. Subsequent laboratory analysis of samples collected during the field season and synthesis of lab and field data represent the progress completed since our last report.

The Wachsmuth Limestone is poorly exposed in the field area and appears to be gradational with the underlying Kayak Shale and overlying lower Alapah Limestone. The lower Alapah is resistant and displays dark (chert) and light (limestone) banding. The middle Alapah is recessive and the upper Alapah is resistant and lithologically similar to the Wahoo Limestone in the north. Cycles in the Alapah, overall, shallow up from mudstones or wackestones to packstones, grainstones, or rudstones. Several parasequences were identified in the upper middle Alapah and upper Alapah. These packages are based on weathering profiles and may have an impact on the mechanical stratigraphy. A very thin package of Wahoo Limestone overlain by the Sadlerochit group was identified in the field area. The thin Wahoo Limestone may be due to non-deposition but is more likely the result of subsequent erosion associated with unconformity development.

Laboratory analyses consisted of collection of x-ray diffraction, thin section petrography, and initial processing off conodont samples collected in the field. Thin sections were stained with Alizarin Red-S to help differentiate calcite from dolomite and identify samples to be subjected to x-ray diffraction analysis. X-ray diffraction was performed on 132 samples from 3 stratigraphic sections and has provided data on the mineralogic content. Peak area analysis was also performed on 56 samples where dolomite was present to quantitatively determine the relative percentages of calcite and dolomite in each sample. Twenty-five samples processed for conodonts and have yielded biostratigraphic and relative age data.

The data collected will be used to identify depositional cycles and parasequences and provide criteria for correlations between different outcrops and between Prudhoe Bay and rocks exposed in outcrop. To this end a stratigraphic cross section for the Porcupine Lake field area was constructed and for the final phase of the project these sections will be correlated with sections further north and with subsurface core and well logs. Subsurface and surface data will delineate package geometries, lateral changes of lithology and reservoir characteristics, and paleogeography across the broad carbonate platform. Seismic scale cross sections will eventually be constructed that will aid in sequence stratigraphic interpretations and delineation of major reservoir units.

Objective

The goals of this phase of the research project are to establish a “baseline” for Lisburne reservoir characteristics in relatively undeformed rocks using surface and subsurface data. The goals of this portion of the project are being met through a multi-phase approach to stratigraphic data collection to insure the development of a comprehensive database for establishing the stratigraphic baseline. The multi-phase approach includes collection of high-resolution lithostratigraphic data, petrographic, mineralogic, and X-ray diffraction data, and outcrop spectral gamma ray profiles and

comparable subsurface geophysical logs. Progress on the baseline stratigraphic study of the Lisburne Group includes acquisition of outcrop lithologic data from distal portions of the field area in the Philip Smith Mountains, collection of petrographic and x-ray diffraction data, and construction of a stratigraphic cross section.

Methods

During the summer of 2000, high-resolution lithostratigraphic data were collected from six partial sections in the south Porcupine Lake area, Philip Smith Mountains (Figure 1) by Michelle McGee and Michael Whalen with assistance from Andrea Krumhardt, Sue Morgan and Rachael Pachter. Measured sections include Forks Canyon (FC), Forks Wahoo (FW), East Fork (EF), East Fork 2 (EF2), Marsh Fork (MF), and Marsh Fork 2 (MF2)(Table 1). Sections were measured at meter intervals using a jacob staff and fist sized hand samples were collected every meter or at smaller intervals. One four to five kilogram conodont sample was collected every ten to twenty meters. Detailed sedimentologic data collected included descriptions of depositional fabrics, sedimentary structures, bed thickness, lithologic contrasts, paleontologic content, porosity types and amounts, chert content, fracture type and location, and ichnofabric and identification of dolomitized intervals, Outcrop gamma ray data was not collected this field season because no complete stratigraphic sections were identified.

All hand samples collected (964) have been cut and 210 samples have been thin sectioned and stained for calcite (Alizarin Red S). X-ray diffraction has been completed on 139 samples and peak area analysis was performed on 56 samples found to contain both calcite and dolomite (Fig. 5). Petrographic analysis will be completed on 210 samples and will be used to determine reservoir properties, such as primary and secondary porosity. Point counting will quantitatively identify skeletal and other sedimentary grains, matrix, pores, cements, and compaction features. Cathodoluminescent analysis will help further delineate diagenesis.

Twenty-five conodont samples have been processed, conodonts have been identified and samples placed within a zonal framework. Conodonts will be used in biostratigraphy and correlation of spatially separated stratigraphic sections and will aid in the identification of the Mississippian-Pennsylvanian boundary.

Data analysis will include identification of depositional cycles and parasequences, construction of cross-sections, and correlations between Prudhoe Bay cores and outcrop. Depositional cycles and unconformities will be used to classify units that are genetically similar. Cross-sections will be used to identify vertical variations in lithology and changes in reservoir properties. Correlations between subsurface and surface will delineate package geometries, lateral changes of lithology and reservoir characteristics, and paleogeography across the broad carbonate platform.

Observations And Interpretations

The Lisburne is approximately 700 meters thick in the south Porcupine Lake field area. The Lisburne in the field area can be subdivided into the Wachsmuth, Alapah and Wahoo limestones (Brosgé and others, 1962). We have informally divided the Alapah Limestone into lower, middle, and upper units based on lithofacies and weathering profiles (Figure 2). Only a thin interval of the lowermost Wahoo Limestone crops out in the field area and the top of this unit appears to represent the pre-Upper Permian unconformity (Armstrong and Mamet, 1975; Hubbard and others, 1987; Jameson, 1994; Watts and others, 1995). Erosion associated with this unconformity removed most of the Wahoo Formation which is overlain by the Kavik Shale member of the Sadlerochit Group. The rocks in the field area subsequently experienced thrust faulting followed by normal faulting (Fig. 2).

The Wachsmuth is approximately 200 m thick and recessive weathering at the base and becomes more resistant with increasing chert content (Figs. 2, 3, 4). The Wachsmuth displays a cyclic alternation of dark and light banding resulting from alternating gray wackestone and dark gray to black chert (Fig. 2). Alternating layers are relatively equal in thickness. The Wachsmuth changes laterally between the Forks and Marsh Fork field areas. In the Forks area, (sections FC, FW, EF and EF2), the Wachsmuth contains cycles that are coarser grained and less cherty. Cycles begin with greenish, calcareous shale that coarsens upward into crinoid-bryozoan-coral grainstone to rudstone and coral framestone. Basal shales drape over coral heads that form the top of the subjacent cycles. Progressively coarsening upward cycles indicate a progradational facies stacking pattern. In the Marsh Fork area (sections MF and MF2), the Wachsmuth is finer grained and cherty. Overall, the Wachsmuth is interpreted to have been deposited in a deep ramp environment below fair weather wave base.

The lower Alapah overlies the Wachsmuth is approximately 100 m thick and relatively resistant in the Marsh Fork and the Forks area (Figs. 2, 3, 4). The lower Alapah also displays significant lateral variations between the Forks and Marsh Fork areas. In the Forks area, the lower Alapah cycles coarsen-up from shaley bases to crinoid grainstones is generally coarser-grained and contains less chert than in the Marsh Fork area. The base of the lower Alapah in the Marsh Fork area displays a dark and light banding but this differs from that observed in the Wachsmuth. Dark layers observed in the lower Alapah consist of shaley or argillaceous wackestones with nodular or bedded chert overlain by thicker light colored crinoid-bryozoan wackestone with large sub-horizontal, silicified burrows. These Marsh Fork facies are overlain by meter-thick crinoid rudstones with reworked coral fragments. The cherty wackestones are interpreted to have been deposited below fair weather wave base in a moderately deep ramp environment that shallow upward into shoal environments represented by crinoid rudstones.

The middle Alapah is 100 meters thick, cyclic, has a recessive weathering profile, and is darker colored than the lower and upper unit (Figs. 2, 3, 4). Cycles in the Forks area are 0.25 m thick, recessive, and coarsen-up from a shaley base to crinoid wackestone, packstone, and rarely grainstone or rudstone. Cycles are thicker and coarser grained in the Marsh Fork area. Calcite replaced evaporites observed in section EF2 at the middle-upper Alapah contact and the cycle stacking patterns are interpreted to indicate shallowing upward from deep ramp to shallow subtidal environments.

The 260 m thick upper Alapah is relatively resistant, light in color, cyclic, and grainier than the middle interval (Figs. 2, 3, 4). Cycles are a few meters to tens of meters thick. They coarsen upward from crinoid-bryozoan wackestone to crinoid-bryozoan packstone to grainstone. The cycles become muddier and bryozoan and chert abundance increases upward. The upper Alapah was not described in the Marsh Fork area. The stratal stacking pattern and fauna from the Forks area indicate a change from open to restricted lagoonal environments on a shallow ramp.

The lower Wahoo is recessive and is unconformably overlain by the Kavik Shale member of the Sadlerochit Group. The unit is approximately 30 m thick and has not been described because it is very recessive and rubbly. The recessive nature of the unit makes it easy to identify in the field. The pre-Upper Permian unconformity that separates the Wahoo from the overlying Kavik Shale was either the result of simple erosion subsequent to a Permian drop in relative sea level or due to Permian uplift and related erosion (Watts and others, 1995).

The Lisburne Group in the Porcupine Lake Valley, Philip Smith Mountains records an initiation of deep-water carbonate ramp sedimentation atop the underlying Kayak Shale. Two major episodes of transgression and shallowing upward indicate significant relative changes in sea-level. Lateral facies changes within the units suggest that the Forks area was depositionally shallower than the marsh Fork area.

Data Analysis

XRD

X-Ray diffraction has been completed on 139 samples. Table 2 summarizes sample results. Section EF has the most complete data and will be the only one discussed in this report. XRD data from additional sections will be analyzed and discussed in the sixth semi-annual report.

Seventy nine samples from Section EF were analyzed by XRD to assess their carbonate mineralogy. Peak area analysis provided quantitative relative percentages of calcite and dolomite. Seventy samples from the Wachsmuth and 9 from the lower Alapah were analyzed. Samples from the lower Alapah were mostly calcite. However, one sample (98 m) contained less than 50% calcite (similar to samples from 48 and 78 m). The Wachsmuth contains six dolomitic intervals where calcite is below 75% (Figure 5). When these intervals are compared, 52 to 63 m and 78 to 90 m have similar thicknesses between the major dolomitic intervals giving the calcite percentages in section EF a cyclical quality (Figure 6). Interval 52 to 63 has slightly lower relative calcite percentages than 78 to 90. This apparent cyclicity will be scrutinized further when additional XRD data becomes available. The cyclicity of the dolomitic intervals could have implications for correlating within the field study areas and between study areas to the north and potentially Prudhoe Bay.

Conodont Biostratigraphy

Twenty five samples from the Porcupine Lake area have been processed, picked, and identified for conodonts. Samples were crushed to approximately 1 cm in diameter and then placed in a 5% acetic acid bath. The samples were routinely washed through nested Tyler no. 20 and 140 screens to remove mud and concentrate the insoluble residue. Many samples produced an oily sheen on the water surface during processing. The conodont elements were separated from the residue using sodium polytungstate set at a specific gravity of 2.85. The conodont elements were hand picked and identified by Andrea Krumhardt.

Conodont recovery from the samples was generally poor; the most abundant sample only yielded 30 elements per kilogram. Elements are commonly abraded and broken and have a sugary texture indicating exposure to caustic hydrothermal fluids. In addition, dolomite crystals are often stuck to the surface of the elements making positive identification difficult. Preliminary analysis of the color alteration indices (CAI) ranged from 4.5 to 6 with the values of 6 most likely hydrothermally induced.

Preliminary age determinations for samples range from the Middle to Late Mississippian. Intermediate samples not yet processed may refine the Series designation. Series assignments for the samples processed to date are as follows.

East Fork (EF section)
0-44: upper Osagean to Chesterian, but probably late Merimecian to Chesterian based on overlying samples.
44-89m: late Merimecian to Chesterian

East Fork 2 (EF2)

0-270.25m : late Merimecian to Chesterian

Forks Canyon (FC)
1-132m: upper Osagean to Chesterian, but probably late Merimecian to Chesterian based on proximity to East Fork sections.

Forks Wahoo (FW)
12-20m: late Merimecian to Chesterian
20-90m: Chesterian
90-178m: middle Chesterian
178: upper Chesterian

Discussion/Conclusions

Further progress has been made on establishing the base-line stratigraphy of the Lisburne Group. Six partial sections were described in detail from the Porcupine Lake area, Philip Smith Mountains during the summer of 2000. The Lisburne Group in the Porcupine Lake Valley, Philip Smith Mountains records an initiation of deep-water carbonate ramp sedimentation atop the underlying Kayak Shale. Lithofacies analysis indicate that the Wachsmuth and lower portion of the lower Alapah were deposited in a deep ramp environment below fair weather wave base. Facies of the upper part of the lower Alapah indicate shallowing into shoal environments. Facies stacking patterns in the middle Alapah are interpreted to indicate transgression followed by shallowing upward from deep ramp to shallow subtidal environments as evidenced by calcite replaced evaporites near the middle-upper Alapah boundary. The fauna and stratal stacking pattern in the upper Alapah indicate continued shoaling and deposition in open followed by restricted lagoonal environments on a shallow ramp. Comparison of the facies stacking patterns and conodont biostratigraphy of these sections with those further north in the Fourth Range, Shublik Mts., and Sadlerochit Mts. Confirms a progressive northward onlap on the Lisburne Group.

XRD analysis has identified several cyclic dolomite intervals in the Wachsmuth of section EF. Further XRD analysis is needed to document patterns of dolomitization in the Alapah Limestone and determine if cyclic dolomitized intervals are restricted to section EF and the Wachsmuth Limestone

Research Plan For Project Completion

Fieldwork during 2000 and subsequent lab analyses have permitted identification of priorities for research during the next field season. The ultimate goal of this portion of the project is to develop a stratigraphic baseline along a proximal-to-distal transect. This necessitates visiting the best-exposed outcrop sections to refine the stratigraphic data base. One priority is to revisit the well-exposed section at "Mosquito Bee Creek" in the Fourth Range to help document small-scale stratigraphic cycles and to collect gamma ray data. This section is exposed in the creek drainage and will provide some of the most continuous exposure of the Alapah in a mid-ramp paleogeographic setting (Gruzlovic, 1991). Other well-exposed sections in the Philip Smith Mountains in the north and south Porcupine Lake areas will also be examined to provide detailed stratigraphic data from the distal portion of the field area.

The boundary between parautochthonous rocks of the northeastern Brooks Range and the Endicott Mountains allochthon appears to be between the north and south Porcupine Lake areas. These areas display markedly different structural styles. Documentation of the sedimentology and stratigraphy of the north Porcupine Lake area

during summer 2002 will be crucial to unraveling the paleogeography and controls on deformation of the Lisburne Carbonate ramp. Analysis of subsurface core and log data is also an integral part of this study. At least two entire cores of the Lisburne Group from Prudhoe Bay will be logged in detail. Cores targeted for analysis include: L2-06, L4-15, and possibly L5-13. Core L2-06 is on loan from Philips Petroleum and additional work on that core will be completed by May 2002.

Field and most subsurface stratigraphic data has been drafted as stratigraphic sections and important mechanical and sequence stratigraphic subdivisions have been identified. Detailed petrographic analysis will help refine the high-resolution lithostratigraphy and aid in identification of sedimentary cycles or parasequences that might influence reservoir characteristics. Identification of different phases of diagenesis will also lend insight into variations in reservoir characteristics. Petrographic analysis will be used to identify microscopic variations in lithofacies important to determining reservoir properties. X-ray diffraction will be conducted on additional samples to quantify the percentage of calcite and dolomite in lithologic samples collected from outcrop and core. These data, along with quantitative porosity and fracture-related data, will allow us to gauge the importance of differing patterns of dolomitization on reservoir development.

Seismic-scale outcrop and subsurface analysis will permit the identification of large-scale (tens to hundreds of meters) lithologic variations that might influence reservoir characteristics. Because the Lisburne represents a broad carbonate ramp (Gruzlovic, 1991; Watts and others, 1995), lateral facies variations may not be apparent in single outcrops or cores. Analysis of facies variations along a transect from paleogeographically proximal cores in the subsurface at Prudhoe Bay to more distal outcrop localities in the northeastern Brooks Range will help identify lithologic trends that produce lateral reservoir heterogeneities. Seismic-scale analyses in conjunction with high-resolution lithostratigraphy will also aid in the identification of larger-scale depositional sequences, the boundaries of which may be related to subaerial exposure surfaces or other stratal discontinuities with reservoir or mechanical significance.

Recommended Approach For Future Similar Research

The Lisburne Group presents significant challenges to obtaining high-resolution stratigraphic data in outcrop. The lateral extent (along both strike and dip) of the Lisburne ramp necessitates correlation of spatially distant sections. Outcrop gamma ray profiles of well-exposed sections also appear to be a useful correlation tool although nearly continuous exposure is necessary for this tool to be used effectively. Large-scale weathering patterns that define outcrop exposure are related to the overall mechanical stratigraphy (Figures 2, 3, 4). A fruitful approach to determining overall mechanical stratigraphy involves relating sections measured in the field to outcrop photos or photomosaics. Relating the weathering patterns to lithology will permit further evaluation of the lithologic controls on mechanical stratigraphy. Application of these methods to future studies in the Brooks Range and correlation of outcrop exposures with the subsurface will enhance our understanding of the geologic history of Arctic Alaska and improve our ability to predict the reservoir potential of folded and fractured carbonates.

References

Armstrong, A. K., and Mamet, B. L., 1975, Carboniferous biostratigraphy, northeastern Brooks Range, Arctic Alaska: U. S. Geological Survey Professional Paper 884, 29 p.

Brosgé, W. P., Dutro, J. T., Mangus, M. D., and Reiser, H. N., 1962, Paleozoic sequence in eastern Brooks Range, Alaska: American Association of Petroleum Geologists Bulletin, v. 46, p. 2174-2198.

Gruzlovic, P. D., 1991, Stratigraphic evolution and lateral facies changes across a carbonate ramp and their effect on parasequences of the Carboniferous Lisburne Group [M. S. thesis]: University of Alaska, 201 p.

Hubbard, R.J., Edrich, S.P., and Rattey, P.R., 1987, Geologic evolution and hydrocarbon habitat of the "Arctic Alaska microplate," *in* Talleur, I.L., and Weimer, P., eds., Alaskan North Slope Geology: Bakersfield, California, SEPM Pacific Section, v. 1, p. 797-830.

Jameson, J., 1994, Models of porosity formation and their impact on reservoir description, Lisburne Field Prudhoe Bay, Alaska, American Association of Petroleum Geologists Bulletin, v. 78, p. 1651-1678.

Watts, K. F., Harris, A. G., Carlson, R. C., Eckstein, M. K. Gruzlovic, P. D., Imm, T. A., Krumhardt, A. P., Lasota, D. K., Morgan, S. K., Dumoulin, J. A., Enos, P., Goldstein, R. H., and Mamet, B. L., 1995, Analysis of reservoir heterogeneities due to shallowing-upward cycles in carbonate rocks of the Pennsylvanian Wahoo Limestone of northeastern Alaska: United States Department of Energy, final Report for 1989-1992 (DOE/BC/14471-19), Bartlesville, CA Project Office, 433 p.

Table 1

Section	Section Measured	Thickness/ Stratigraphic Interval	# Lithologic Samples	Analyzed XRD Samples	# Conodont Samples	# Thin Sections
FC	Summer 2000	135 m, lower, middle, and upper Alapah	94	0	5	0
FW	Summer 2000	178 m, upper Alapah; lower Wahoo; Sadlerochit Group	108	0	8	0
EF	Summer 2000	105 m, Wachsmuth and lower Alapah	79	79	5	0
EF2	Summer 2000	320 m, Wachsmuth; lower, middle and upper Alapah; lower Wahoo; Sadlerochit Group	221	56	12	0
MF	Summer 2000	383 m, Wachsmuth; lower and middle Alapah	295	4	11	0
MF2	Summer 2000	228 m, Wachsmuth and lower Alapah	164	0	7	10
TOTALS:		1538 m total; 465 m Wachsmuth; 363 m lower Alapah; 234 m middle Alapah; 415 m upper Alapah; 61 m lower Wahoo	964	139	48	10

Table 1. Summary of outcrop and sample data collected in the northeastern Brooks Range during summer 2000.

Table 2

Sample #	Mineralogy C=Calcite D=Dolomite Q=Quartz	Calcite Peak Area	Dolomite Peak Area	Relative % Calcite	Relative % Dolomite
EF-0	C, D	54	20	73.0	27.0
EF-1	C				
EF-2	C, D	62	7	89.9	10.1
EF-3	C				
EF-32	C, D	45	20	69.2	30.8
EF-33	C				
EF-34	C				
EF-35	C				
EF-36	C				
EF-37	C				
EF-38	C				
EF-39	C				
EF-40	C, D	34	18	65.4	34.6
EF-41	C, D	33	19	63.5	36.5
EF-42	C, D	49	4	92.5	7.5
EF-43	C				
EF-43.3	C				
EF-44	C, D	42	2	95.5	4.5
EF-45	C	Too little dolomite to calculate area			
EF-46	C				
EF-47	C, D				
EF-48	C, D	38	46	45.2	54.8
EF-49	C				
EF-50	C, D	47	11	81.0	19.0
EF-51	C				
EF-52	C, D	44	26	62.9	37.1
EF-53	C, D	52	2	96.3	3.7
EF-54	C, D	39	10	79.6	20.4
EF-55	C				
EF-56	C, D	51	3	94.4	5.6
EF-56.3	C, D	47	16	74.6	25.4
EF-57	C, D	45	12	78.9	21.1
EF-58	C, D	46	7	86.8	13.2
EF-59	C, D	38	13	74.5	25.5
EF-60	C				
EF-62	C				
EF-63	C, D	33	14	70.2	29.8
EF-64	C, D	48	22	68.6	31.4
EF-65	C, D	47	9	83.9	16.1

EF-66	C, D	54	3	94.7	5.3
EF-67	C, D	61	2	96.8	3.2
EF-68	C, D	58	1	98.3	1.7
EF-69	C				
EF-70	C, D	59	6	90.8	9.2
EF-71	C,D	59	7	89.4	10.6
EF-72	C				
EF-73	C				
EF-73.8	C, D	52	22	70.3	29.7
EF-74	C, D	49	6	89.1	10.9
EF-75	C, D	47	8	85.5	14.5
EF-76	C, D	53	6	89.8	10.2
EF-77	C				
EF-78	C, D	34	21	61.8	38.2
EF-79	C				
EF-81	C				
EF-82	C, D	62	6	91.2	8.8
EF-83	C, D	53	4	93.0	7.0
EF-84	C				
EF-85	C				
EF-86	C, D	65	3	95.6	4.4
EF-87	C				
EF-88	C				
EF-89	C, D	58	1	98.3	1.7
EF-90	Q, C, D	46	11	80.7	19.3
EF-90.5	C				
EF-91	C, Q, D	Too little dolomite to caculate area			
EF-92	Q, C				
EF-93	C				
EF-94	C				
EF-95	C				
EF-96	C				
EF-96.3	C				
EF-96.3L	C				
EF-97	C				
EF-98	D, C	28	32	46.7	53.3
EF-99	C, D	60	13	82.2	17.8
EF-100	C				
EF-101	C				
EF-102	C				
EF-103	C				
EF-104	C, D, Q				
EF-105	C, D	52	8	86.7	13.3
EF2-19	Q, C, D	37	6	86.0	14.0
EF2-20	C				

EF2-54	C				
EF2-55	C				
EF2-68	C				
EF2-69	C				
EF2-70	C, D	64	1	98.5	1.5
EF2-71	C				
EF2-75	C				
EF2_76	C, D	51	5	91.1	8.9
EF2-134	C				
EF2-135	C				
EF2-136	C, D	36	11	76.6	23.4
EF2-137	D, C, Q	13	38	25.5	74.5
EF2-145	C				
EF2-146	C, Q, D	69	1	98.6	1.4
EF2-147	C, D	77	18	81.1	18.9
EF2-165	C				
EF2-166	C				
EF2-167	C, D, Q	53	20	72.6	27.4
EF2-172	C				
EF2-173	C				
EF2-173.5	C, D	45	32	58.4	41.6
EF2-175	C				
EF2-176	C, D	34	29	54.0	46.0
EF2-189	C, D	37	25	59.7	40.3
EF2-190	C, D	52	2	96.3	3.7
EF2-191	C, D	Too little dolomite to caculate area			
EF2-192	C				
EF2-193	C				
EF2-199	C				
EF2-200	C, D, Q	54	2	96.4	3.6
EF2-213.5	D, C	13	69	15.9	84.1
EF2-214	C				
EF2-215	C, D, Q	47	26	64.4	35.6
EF2-216	C				
EF2-218	C				
EF2-219	C, Q				
EF2-220	C, Q				
EF2-221	C				
EF2-222	C				
EF2-223	C, D	40	22	64.5	35.5
EF2-269.5	D, C	13	85	13.3	86.7
EF2-278	C				
EF2-279	Q, C				
EF2-280	C, Q, D	60	6	90.9	9.1
EF2-285	C				

EF2-286	C				
EF2-287	C				
EF2-288	Q, C				
EF2-289	C, Q				
EF2-290	C, Q				
EF2-291	Q, C				
EF2-292	Q, C				
EF2-296	C				
EF2-297	C, Q				
EF2-298	C				
MF-143.5	Shale				
MFB-165	C				
MFB-166	C				
MFB-167	C				

Table 2. X-ray diffraction data. Table illustrates the mineralogy of each sample, measured area of calcite and dolomite peaks, and relative percentages of calcite and dolomite based on peak area.

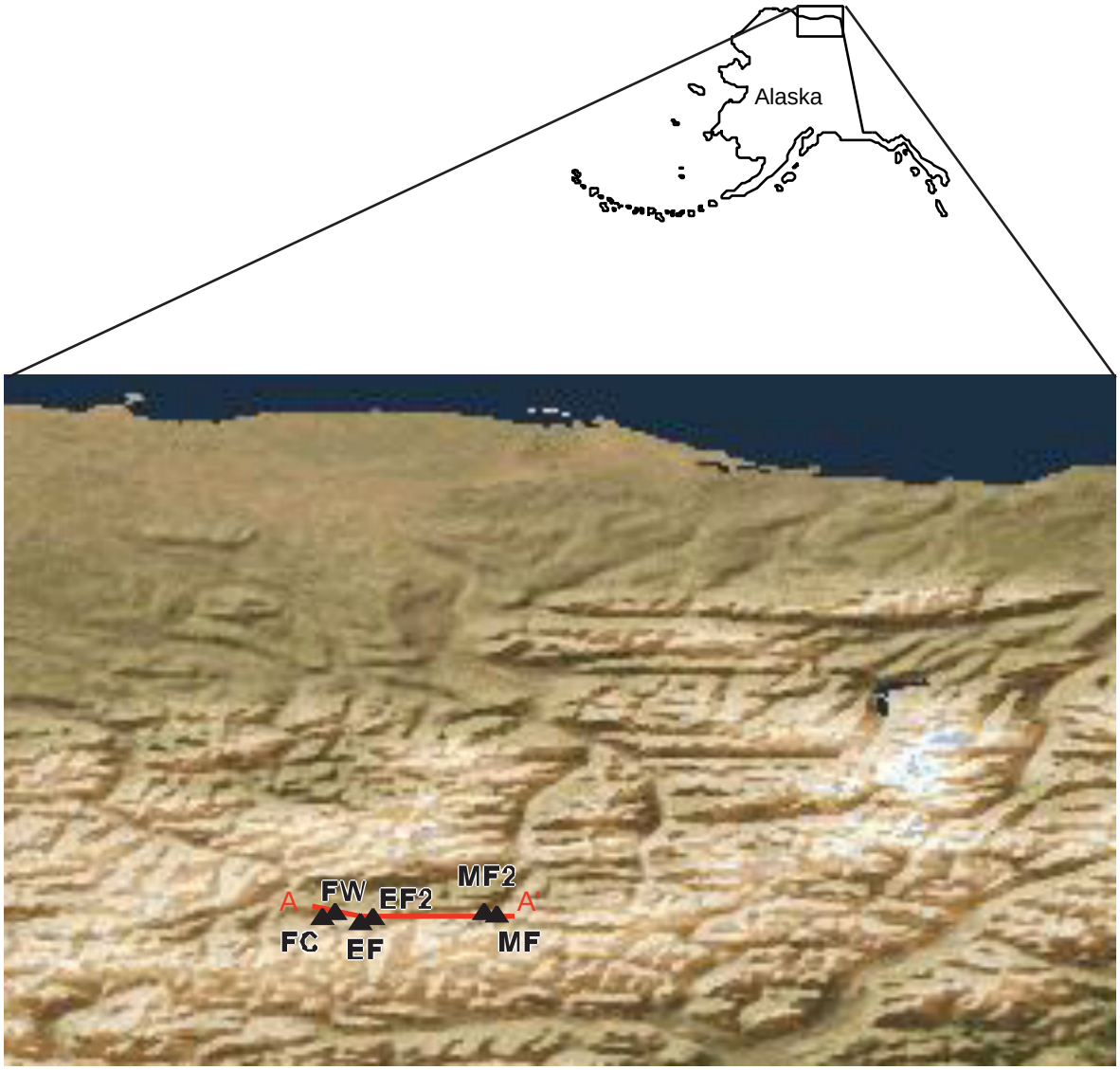

Figure 1. Map illustrating the location of measured stratigraphic sections in the south Porcpine Lake Valley area and the location of cross section A-A' illustrated in Fig. 3.

Figure 2. Photomosaics of the Lisburne in Forks area (A) and Marsh Fork area (B). Each Lisburne unit has distinct large-scale weathering characteristics that are similar throughout the field areas. The Wachsmuth is color banded and resistant. The L. Alapah is slightly lighter colored that the Wachsmuth and resistant. In contrast, the M. Alapah is the darkest unit and most recessive. The U. Alapah is the lightest colored and resistant. It typically forms cliffs above the recessive M. Alapah. The L. Wahoo is recessive and present as a thin veneer on top of the U. Alapah.

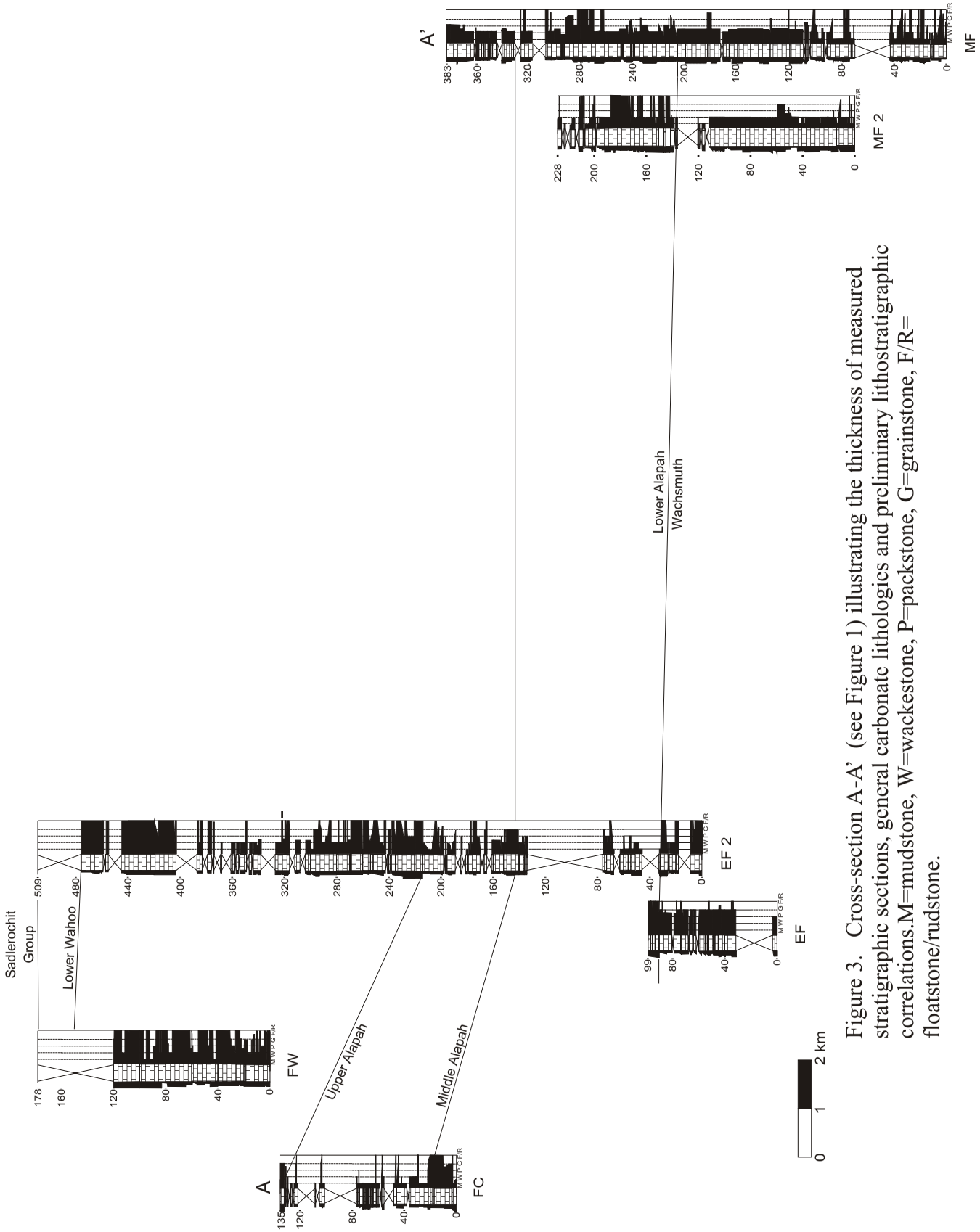

Figure 3. Cross-section A-A' (see Figure 1) illustrating the thickness of measured stratigraphic sections, general carbonate lithologies and preliminary lithostratigraphic correlations.M=mudstone, W=wackestone, P=packstone, G=grainstone, F/R= floatstone/rudstone.

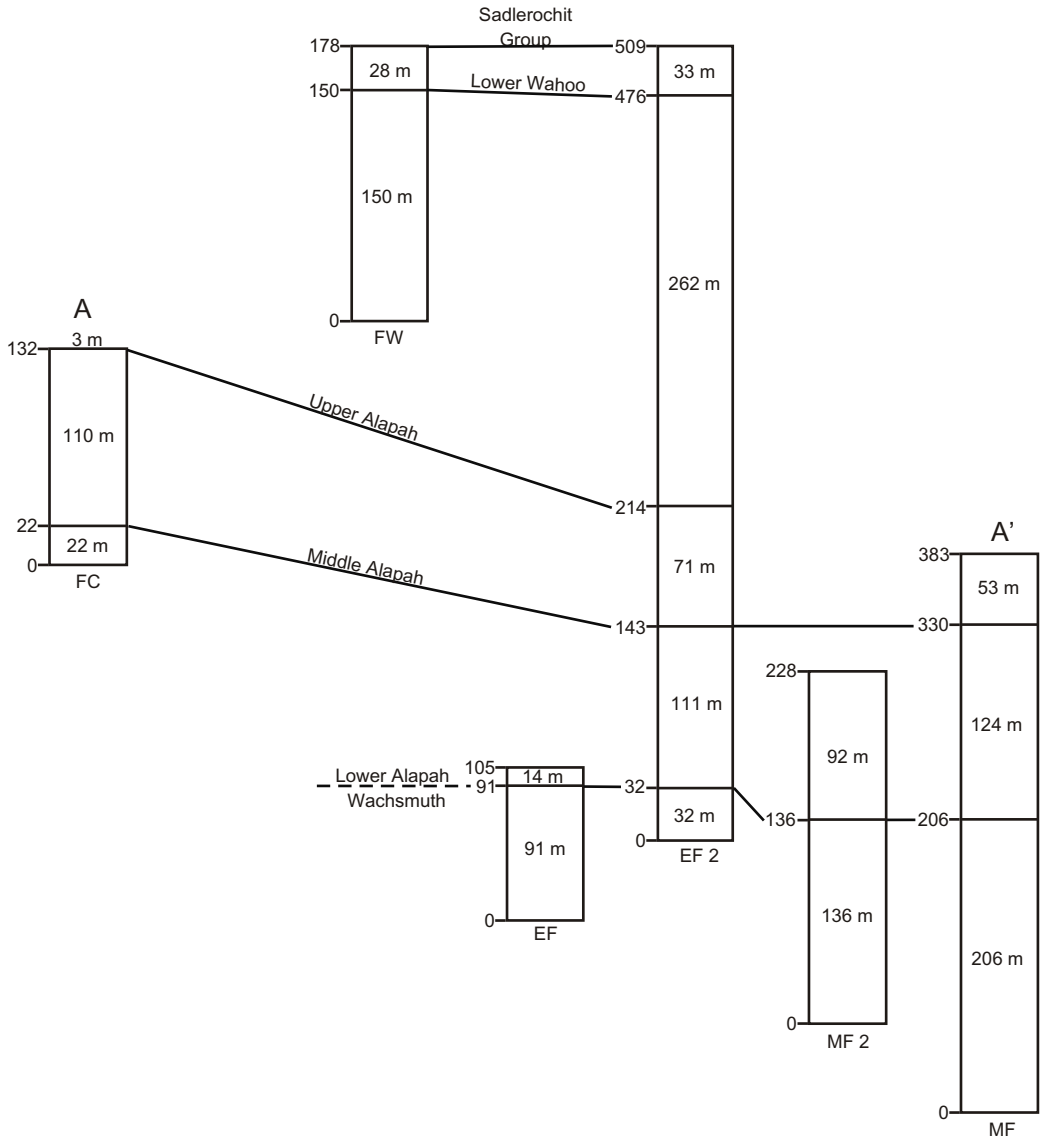

Figure 4. Simplified cross-section illustrating the thicknesses of major lithologic units in the field area.. Horizontal dimension is not to scale.

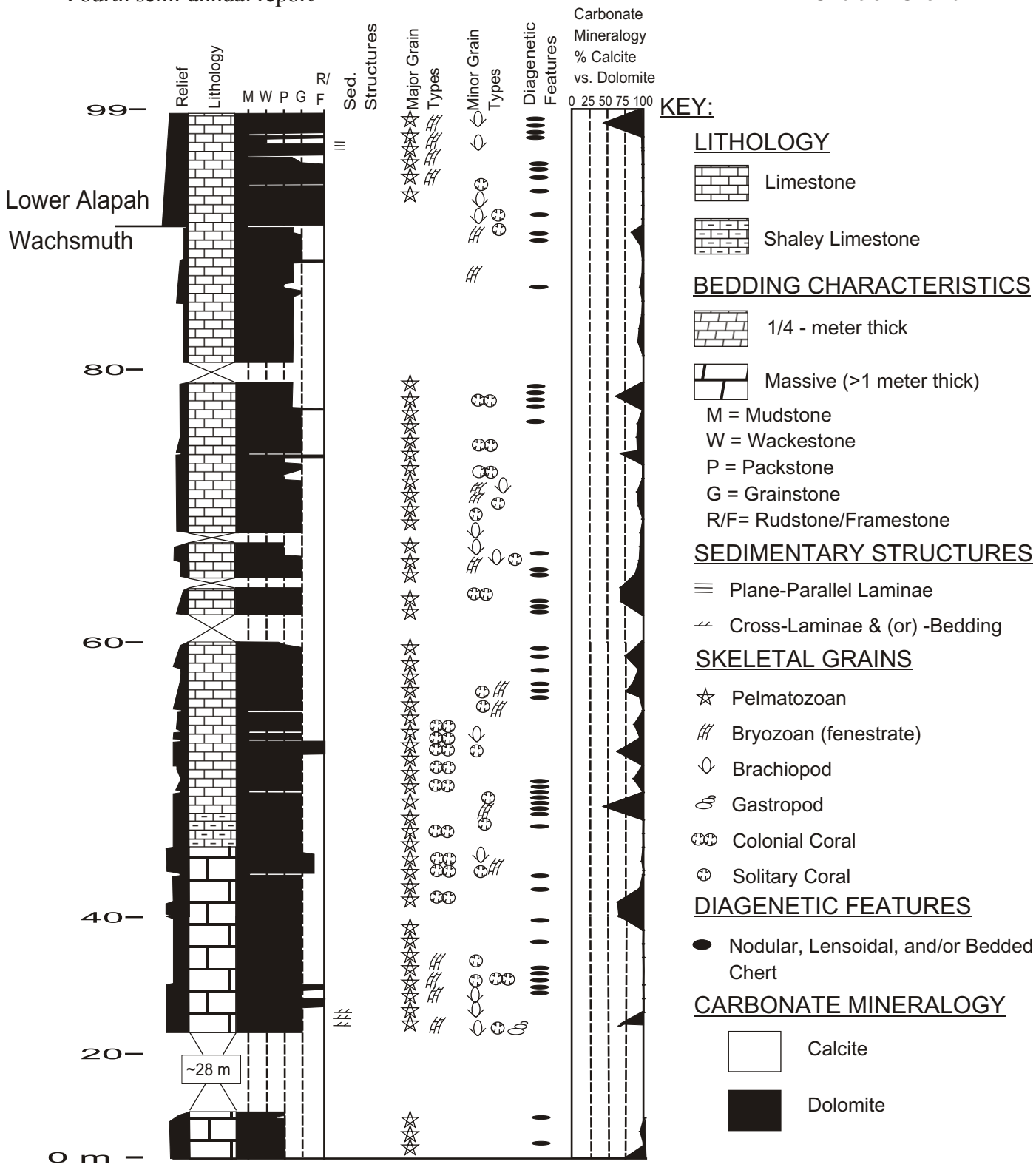

Figure 5. Stratigraphic section EF illustrating carbonate lithologies, grain types, diagenetic features, and relative percent calcite vs. dolomite from peak area analysis of XRD data.Note the dolomitic intervals from 40 to 63 m, 63 to 90 m, and 90 to 99 m. Dolomite appears to occur cyclically within this portion of the stratigraphic section. Further XRD analysis will be necessary to explore the implications of this cyclic pattern.

Geometry and Evolution of Thrust-truncated Detachment Folds in the Upper Marsh Fork Area of the Eastern Brooks Range Fold-and-thrust Belt, Alaska

By Margarete A. Jadamec and Wesley K. Wallace, Geophysical Institute and Department of Geology and Geophysics, University of Alaska, Fairbanks, AK 99775, ftmaj@uaf.edu

Abstract

In the Brooks Range of northeastern Alaska, the Carboniferous Lisburne Group carbonates and underlying Mississippian Kayak Shale are separated into two structural domains by the east-trending Continental Divide thrust front. North of the thrust front, the northeastern Brooks Range is characterized by symmetric, upright, east-northeast-trending detachment folds formed by buckling of the Lisburne Group above a decollement in the Kayak Shale. South of the thrust front, folds in the Lisburne Group typically are asymmetric, east-northeast-trending, and cut by thrust faults. Field research in the upper Marsh Fork (UMF) area of the Canning River in the southern domain suggests that the folds evolved by thrust-breakthrough of asymmetric detachment folds rather than as fault-propagation folds, as is commonly assumed for strongly asymmetric thrust-related folds.

Novel surveying methods were utilized to collect quantitative data on fold geometry that potentially record several stages in the evolution of thrust-truncated folds. Thrust faults appear preferentially to truncate the folds within the anticline forelimb and/or adjacent syncline hinge. This is indicated by the prevalence of truncated, steeply dipping, anticline forelimbs in contrast to the planar, gently to moderately dipping, relatively undeformed anticline backlimbs. Furthermore, parasitic folds and thrust faults in the anticline forelimb region suggest that the accumulation of strain is typically greater in the anticline forelimb than in the backlimb, thus rendering the anticline forelimb prone to thrust-truncation. The structural geometry of the truncated anticlines resembles a superimposed fault-bend-fold geometry. This may be formed by translation of the truncated fold over the footwall ramp to upper footwall flat or by folding of the thrust above an underlying horse. A better understanding of the geometry and evolution of thrust-truncated detachment folds in the UMF area may be applicable to the interpretation of Lisburne Group structures located in the subsurface beneath the foothills north of the central Brooks Range.

The structural style of the Lisburne Group in the UMF area is the same as that displayed by the Lisburne Group throughout the Endicott Mountains allochthon. This and the presence of deep-water facies in the Lisburne in the UMF area suggest the possibility that the Continental Divide thrust front in this area may correspond with the leading edge of the Endicott Mountains allochthon.

1. Introduction

Three general categories of thrust-related folds are common in foreland fold-and-thrust belts: detachment folds, fault-propagation folds, and fault-bend folds (figure 1). Various authors have proposed geometric models that explain fold geometry and predict the kinematic evolution of

each fold type (Suppe, 1983; Jamison, 1987; Mitra, 1990; Suppe and Medwedeff, 1990; Homza and Wallace, 1995, 1997; Poblet and McClay, 1996). For example in the Suppe (1983) model, a fault-bend fold occurs during thrust faulting as the hanging wall is displaced over a bend in the footwall ramp and onto the upper footwall flat. In this model, area, bed length, and layer thickness are conserved and deformation occurs by layer-parallel slip. In the fault-propagation fold models, the fold forms in the hanging wall to accommodate slip from the underlying propagating ramp tip (Suppe and Medwedeff, 1990; Mitra, 1990). A detachment fold forms as a relatively weak unit detaches and thickens above a basal decollement. Most models assume that a relatively competent unit deforms above the weak detachment unit and displays parallel fold geometry (Jamison, 1987; Wallace, 1993; Homza and Wallace, 1995, 1997; Poblet and McClay, 1996). Unlike fault-bend and fault-propagation folds, a detachment fold lacks a fault ramp.

A natural outgrowth of the construction of geometric and kinematic models for the development of thrust-related folds is the attempt to model and explain the truncation of these folds by late-stage thrust faults. One of the earliest documented analyses of fold truncation by a late-stage thrust fault is the Willis break-thrust model (1893). More recently, numerous authors have explored the geometry and kinematics of the truncation and subsequent displacement of thrust-related folds, but their interpretations vary widely (Jamison, 1987; Mitra, 1990; Suppe and Medwedeff, 1990; Fischer et al., 1992; McNaught and Mitra, 1993; Morley, 1994; Thorbjornsen and Dunne, 1997; Wallace and Homza, in press). Moreover, the process of fold truncation is often overlooked in the interpretation of natural thrust-related folds.

Numerous examples of truncated and nontruncated folds in the eastern Brooks Range provide a natural laboratory to document the geometry of these structures and explore models for their evolution. Quantitative data on the geometry of near-profile exposures of kilometer-scale truncated and nontruncated folds were collected using a novel surveying method. In addition, the geometry of folds that display two potentially separate stages in the evolution of thrust-truncation was documented.

The geometric analyses of the map-scale folds and thrust sheets in the upper Marsh Fork (UMF) area of the eastern Brooks Range leads us to suggest that asymmetric detachment folds evolved into thrust-truncated folds in order to accommodate increased shortening. This hypothesis includes three major assumptions: (1) the folds formed by detachment folding, (2) the folds were asymmetric prior to thrust truncation, and (3) breakthrough of the detachment folds occurred as a distinct stage after initial fold formation.

2. Geologic Setting

2.A Structural Framework and Location

Helicopter-supported research was conducted in the Philip Smith Mountains along the upper Marsh Fork of the Canning River where both faulted and nonfaulted folds in the Pennsylvanian to Mississippian Lisburne Group carbonates are exposed (figure 2). The rugged Philip Smith Mountains are located in the eastern Brooks Range, which is considered to be the northern extension of the Rocky Mountain fold-and-thrust belt.

The Continental Divide thrust front separates the eastern Brooks Range, to the south, from the northeastern Brooks Range, to the north, and delineates a major structural boundary between the two regions (figures 2 & 3). South of the thrust front, in the UMF area, folds in the Lisburne Group typically are asymmetric, east-northeast-trending, and cut by thrust faults. A similar structural style has been documented in the Endicott Mountains allochthon to the southwest where, in the Galbraith Lake area, asymmetric, thrust-truncated detachment folds occur in two structural levels (Wallace et al., 1997; Maclean, 2001). The upper structural level contains thrust-truncated detachment folds in the Lisburne Group carbonates and the lower structural level exhibits the same deformation style but in the Kanayut Conglomerate (Wallace et al., 1997).

North of the Continental Divide thrust front in the northeastern Brooks Range, the Lisburne Group carbonates display symmetric, upright, east-northeast-trending, nonfaulted detachment folds (Homza and Wallace, 1995, 1997). In the northeastern Brooks Range, the detachment folds formed by buckling of the Lisburne Group carbonates above a decollement in the underlying Mississippian Kayak Shale (Wallace 1993; Homza and Wallace, 1995, 1997). Kilometer-scale fault-bend folds composed of the sub-Middle Devonian basement and Lower Mississippian Kekiktuk Conglomerate underlie the detachment folds in the overlying Lisburne Group (Wallace and Hanks, 1990).

2.B Tectonic history

Multiple deformation events have shaped northern Alaska since pre-Middle Devonian time (Moore et al., 1994). Geochronologic and structural data suggest that deformation, metamorphism, and igneous activity affected lower Paleozoic and Proterozoic rocks during one or more orogenic events in northern Alaska in pre-Middle Devonian time. The formation of rift basins, with possibly associated magmatic activity, characterized Arctic Alaska in the Middle to Late Devonian (Moore et al., 1994). During the Mississippian through Jurassic, the tectonic setting was that of deposition and erosion on a south-facing passive continental margin. In particular, the Mississippian Kayak Shale, Carboniferous Lisburne Group, and Permian to Triassic Sadlerochit Group were deposited (Lepain, 1993; Watts 1995; Crowder, 1990). The main axis of the Brooks Range formed during the Middle Jurassic to Early Cretaceous and was marked by the emplacement of a series of allochthons that were thrust northward, in present day coordinates (Moore et al., 1994). The lowest and most extensive of these allochthons is the Endicott Mountains allochthon, which overlies the North Slope autochthon and parautochthon to the north. During the Brooks Range orogeny, the total structural shortening along the southern margin of Arctic Alaska is estimated at 200-500 km (Plafker and Berg, 1994). During the Paleocene, renewed contraction led to uplift of the main axis of the Brooks Range and formation of the range front to the north. From the Eocene to the present, continued contraction resulted in the formation of the prominent salient that is the northeastern Brooks Range.

2.C Regional Stratigraphy

The regional stratigraphy of both the Endicott Mountains allochthon and the North Slope parautochthon will be described here, because the affinity of UMF area rocks to either stratigraphic sequence is uncertain (figure 4). Both the Endicott Mountains allochthon and the North Slope parautochthon contain the two units, the Lisburne Group and underlying Kayak Shale, whose deformation is the focus of this paper. However, the structural style of the Lisburne Group in the Endicott Mountains allochthon and northeastern Brooks Range is

dramatically different. Differences between the rock units of the Endicott Mountains allochthon and North Slope parautochthon may have influenced the distinct deformation styles of the Lisburne Group carbonates in each region.

The Endicott Mountains allochthon marks the range front along much of the northern central Brooks Range and lies along structural trend of the Carboniferous rocks in the UMF area. In ascending stratigraphic order, the Endicott Mountains allochthon is composed of the Upper Devonian to Lower Mississippian Endicott Group which grades into the Carboniferous Lisburne Group which is in turn unconformably overlain by the Permain to Triassic Etivluk Group (Wallace et al., 1997). Various dominantly clastic formations of Jurassic to Lower Cretaceous age overlie the Etivluk Group. From oldest to youngest, the 4.5 km thick Endicott Group is composed of the Hunt Fork Shale, Noatak Sandstone, Kanayut Conglomerate, and Kayak Shale. The approximately 1 km thick Lisburne Group is composed of three formations from oldest to youngest: the Wachsmuth Limestone, the Alapah Limestone, and the Wahoo Limestone. The approximately 200 m thick Etivluk Group is composed of the Siksikpuk Formation and overlying Otuk Formation.

North of both the UMF area and the Continental Divide thrust front, the parautochthonous rocks of the northeastern Brooks Range constitute the North Slope parautochthon. In the northeastern Brooks Range, the North Slope parautochthon has been separated into three general stratigraphic sequences from oldest to youngest: the Pre-Cambrian to Devonian sequence, the Mississippian to Lower Cretaceous Ellesmerian sequence, and the Lower Cretaceous and younger Brookian sequence (Wallace and Hanks, 1990). The emphasis here will be placed on the first two stratigraphic sequences. The pre-Middle Devonian sequence is composed of a lithologically heterogeneous assemblage of weakly metamorphosed sedimentary and volcanic rocks and Devonian granitic batholiths. An angular unconformity separates the pre-Middle Devonian sequence from the overlying Ellesmerian sequence. The Ellesmerian sequence is composed, in ascending order, of the Lower Mississippian Endicott Group, the Mississippian to Pennsylvanian Lisburne Group, the Permian to Triassic Sadlerochit Group, and various dominantly clastic formations of Triassic to Lower Cretaceous age. The Endicott Group is approximately 700 m thick and composed of two members: the Kekiktuk Conglomerate and overlying Kayak Shale. The Kayak Shale was deposited in a marginal marine setting and thickens to the south (Lepain, 1993). Conformably overlying the Endicott Group, the approximately 1 km thick Lisburne Group is composed of the Alapah Limestone and Wahoo Limestone. The Lisburne Group was deposited on an extensive south-facing carbonate platform (Watts, 1995). A disconformity separates the overlying Sadlerochit Group from the Lisburne Group. The approximately 700 m thick Sadlerochit Group is composed of deltaic and shallow marine clastic rocks of the distinctive orange-brown Echooka Formation and the overlying Ivishak Formation (Crowder, 1990). It is important to point out the contrast in stratigraphic thickness of the Endicott Group in the Endicott Mountains allochthon and North Slope parautochton, 4500 m versus 700 m respectively. The Endicott Group is not exposed in the UMF area.

2.D Mechanical Stratigraphy

The Lisburne Group and bounding strata will be described here in the context of mechanical stratigraphy, that is the description of stratigraphy in terms of the structural and mechanical behavior of the rock units rather than in terms of the depositional history. Recent workers have

reemphasized that the stratigraphic character of rock units influences their deformation style (Woodward and Rutherford, 1989; Wallace, 1993; Erickson, 1996; Fischer and Jackson, 1999). Moreover, field evidence suggests that the thickness, relative proportions, lateral extent, and distribution of rock types significantly affect their mechanical response to deformation (Woodward and Rutherford, 1989; Chester et al., 1991; Pfiffner, 1993; Wallace, 1993; Fischer and Jackson, 1999). Assuming that the intensive variables, e.g., temperature, confining pressure, fluid pressure, and strain rate, are the same, the mechanical stratigraphy will strongly influence the character and relative importance of folding, faulting, and penetrative strain. Both in the Endicott Mountains allochthon and the northeastern Brooks Range, the mechanical stratigraphy of the Lisburne Group and surrounding rock units is that of a relatively competent layer of limestone sandwiched between two significantly less competent intervals of shale and subordinate fine-grained sandstone (figure 4). The underlying incompetent unit is the Kayak Shale and the overlying incompetent units are the Siksikpuk and Echooka Formations, respectively. A detailed description of both the litho-stratigraphy and mechanical stratigraphy within the Lisburne Group will be presented in the results section of this report.

3. Methods

3.A Overview

The rugged topography of the eastern Brooks Range lent itself perfectly to two distinct methods of field analysis: traditional field mapping at 1:25,000 scale and surveying the geometry of individual map-scale folds. The objective of the field mapping was to define three-dimensional changes in structural geometry along strike. The mapping was supplemented by measuring the orientations of faults, fold limbs, and various mesostructures, constructing detailed sketches of outcrops, interpreting field photographs, and collecting conodont samples and oriented hand samples. The objective of the plane surveys was to document exceptional cross-strike exposures of individual structures. Precise surveying data will serve to quantitatively test the assumptions and predictions of published fold models.

The UMF field area is subdivided into the west, central, and east areas (figure 5). The west UMF area was mapped in detail at the 1:25,000 scale. Five map-scale folds were surveyed in the east UMF area with less emphasis placed on field mapping. Mapping in the central UMF area and surveying the fold geometry in the west UMF area was the focus of the 2001 field season.

3.B Survey data collection

Six plane surveys were conducted in the UMF area of the Canning River in the eastern Brooks Range. Of these six surveys, five were conducted in the UMF east area and one was conducted in the UMF west area. Results for four of the five surveys conducted in the UMF east area are included in this report. A plane survey means that the reference plane over which you are suveying, i.e., the earth's surface, can be approximated as a plane as opposed to an arcuate surface. In other words, in a plane survey, the plumb line is vertical, parallel at each point in the survey, and perpendicular to a local horizontal plane at each point in the survey. It is important to point out, then, the degree to which the earth's surface can be approximated as planar. At 1.6 km from the point of tangency, a horizontal plane deviates from an averaged ellipsoidal earth by approximately 20 cm (Wolf and Brinker, 1994). For folds 1, 2, and 3 the survey station was less

than 1.6 km from each surveyed point which leads to a maximum deviation of approximately 20 cm from a planar earth. For fold 5, the survey station was a maximum of 3.2 km from the farthest surveyed point, and thus the deviation of this survey from a plane is up to approximately 40 cm.

To begin the survey, a reference line was established and oriented with a Brunton compass. The reference line, marked by a series of 1 m tall wooden stakes, was oriented parallel to true north for all surveyed folds except for fold 5. The survey station was the origin of the coordinate system that contains the 3D distribution of the surveyed points. A surveyed point is a specific location on a feature, where a feature is defined as an outcrop of a marker horizon, bedding contact, fault surface, or fold hinge. Once a point on a feature was located, the azimuth angle, zenith angle, and linear distance were measured for that point (figure 6). The azimuth angle, ϕ, measured in a horizontal plane, is the angular distance from the reference line to a surveyed point. The zenith angle, θ, measured in a vertical plane, is the angular distance from the vertical zenith to a surveyed point. The linear distance, r, is the shortest distance in space from the survey station to the surveyed point. A minimum of three unique points defines a plane, and thus, at least three points were collected for each planar segment of the features surveyed. Depending on the nature of the feature, between 3 and 25 points were measured. Between 26 and 50 features were surveyed for each of the six plane surveys conducted in the UMF area. As a measure of the quality control, the coordinates of the same point on the reference were recorded before and after each feature was surveyed.

A Wild T16 scale-reading theodolite mounted on a standard aluminum surveyer's tripod was used to measure the angular distances, ϕ and θ. In the T16 model, the circle graduation interval is 1^{o}, and each degree is divided into 60 1' intervals. The angular location of each point surveyed can be estimated to the nearest tenth of a minute, or six seconds. At 1.6 km, the arc length subtended by 6'' is approximately 0.5 m. Because the T16 theodolite lacks any electonic components, the instrument is useful for remote fieldwork involving a small number of survey stations and where a power source is unavailable.

A pair of Rockwell Viper laser range finder binoculars was used to measure the linear distance, r. The binoculars were mounted on a tripod and placed adjacent to the T-16 theodolite. The Viper laser range finder contains a class 1 laser and an internal magnetic compass. The internal compass was not used for data measurements. The instrument indirectly calculates linear distance through the transmission of a laser beam that reflects off a surface and back to the laser range finder. A hand held prism is not needed for laser reflection. The maximum displayed resolution of the Viper laser range finder is approximately 30 cm. At a distance of between 50 – 2000 m the accuracy is approximately $\pm$ 2 m. The accuracy of the range finder depends on the reflective properties of the rock, size of the target, angle of the rock-laser interface, atmospheric conditions, local vibrations, and to a lesser degree, lighting conditions.

Both a handheld GPS unit and topographic maps were used to identify the position of the survey station for each of the six folds surveyed. As a result, the origin of the 3D-coordinate system and all surveyed points can be located in the geographic reference system of choice. A UTM system was chosen for the display of these data.

4. Mapping and Survey Results

4.A Overview of results

Based on field observations in this study, the Lisburne Group in the UMF area is informally divided into an upper and lower part (figure 7). The upper and lower parts can be recognized easily in the field on the basis of their color and weathering pattern. The lower part is in turn divided into three subunits, in ascending order: a lower dark-gray cliff- to slope-forming unit, a middle light-gray cliff-forming unit, and an upper dark-gray slope-forming unit. The lower dark-gray unit contains dark- to light-gray interlayered chert and medium- to fine-grained limestone. About 20 m of light-gray limestone is exposed locally at the base of this unit and may be structurally emplaced. The middle light-gray unit forms a cliff in outcrop and is composed of massive to interlayered chert, crinoid and bryozoan wackestone to rudstone and, to a lesser extent, dark-gray, fine-grained limestone. The upper dark-gray unit displays a recessive weathering pattern, is composed of dark-gray crinoid- and brachiopod-bearing packstone, wackestone, floatstone, and mudstone, and contains lesser light-gray chert and medium- to coarse-grained limestone. The subordinate light-gray beds are asymmetrically folded and faulted locally (figure 7b). The three subunits of the lower part have been generally correlated with the Wachsmuth, Lower Alapah, and Middle Alapah (McGee and Whalen, this report). The base of the Lisburne Group and, therefore, the underlying Lisburne Group-Kayak Shale contact is not exposed.

The upper part of the Lisburne in the UMF area forms a prominent cliff in outcrop, is composed of a light-gray, massive, crinoid and brachiopod packstone, grainstone, and rudstone, and contains subordinate interlayered and nodular chert. The chert nodules range from 10 cm to 0.5 m in diameter. Slickenlines in this relatively competent upper part show evidence of interlayer slip. The upper part has been correlated with the Upper Alapah and Lower Wahoo (?) (McGee et al., this report). A disconformity separated the Lisburne Group from the overlying Permian to Triassic Echooka or Etivluk Formations. This overlying unit contains two members: a lower orange-brown shale to fine-grained sandstone, and an upper dark brown shale to sandstone. The total thickness of the Lisburne Group in the UMF area is approximately 525 m, although the UMF contains several thrust sheets across some of which the Lisburne varies in thickness on the order of about 100 m.

The structural style in the UMF area is defined by a series of map-scale hangingwall anticlines imbricately stacked via southeast dipping thrust faults. The hangingwall anticlines are composed of the competent Lisburne Group that is bounded between two incompetent detachment units, the underlying Kayak Shale and overlying Sadlerochit Group (?). The Kayak Shale is not exposed in the UMF area. However, the Kayak Shale crops out in the cores of the detachment folded Lisburne Group to the north and in the cores of thrust-truncated asymmetric folds in the Lisburne Group elsewhere along strike and to the south (e.g., Maclean, 2001; Wallace, 1993; Homza and Wallace, 1995, 1997; Wallace et al., 1997).

Maps of the east and west field areas are shown in figures 8 & 9. The fieldwork in the west UMF consisted primarily of traditional field mapping. Here, data on fold and fault attitude were

collected from four river drainages that are spaced roughly 1.6 km apart and oriented transverse to the structural trend. These data will later allow the changes in fold and fault geometry along strike to be displayed in multiple cross sections. The map-scale structures in the east UMF area were documented primarily by the surveying method described above, with less emphasis placed on field mapping.

4.B Structural style along strike in the west UMF area

Figure 8 depicts the key structures observed along the range front in the west UMF area, in particular a north-vergent anticline in the Lisburne Limestone that can be traced along strike for approximately 8 km. This anticline displays a south-dipping axial plane, a long planar south-dipping backlimb, and a parasitically folded forelimb that contains a syncline-anticline pair. Table 1 outlines the geometric properties of this frontal anticline.

A map-scale hangingwall anticline structurally overlies the planar backlimb of the frontal anticline (figures 8 & 10). This hangingwall anticline is the southern of the two main folds in section CC'. The axial plane of the hangingwall anticline dips gently to moderately to the south. The gently folded relatively long backlimb dips gently to the north and moderately to the south. The overturned forelimb dips steeply to the south and is cut by a thrust fault that separates the hangingwall anticline from the frontal anticline. The thrust fault dips approximately 30^{o} to the southeast. In the footwall, the thrust fault consistently parallels bedding in the structurally underlying Sadlerochit Group. The geometric properties of the hangingwall anticline are summarized in Table 1. At least three steeply southwest (?) dipping transverse faults, spaced approximately 1.6 km apart along the trend of the folds, appear to cut the both the frontal and hangingwall anticlines and the intervening thrust fault. The transverse faults exhibit apparent southwest side down normal displacement. Rubbly outcrop and lack of markers made these faults difficult to trace into the Lisburne Group away from the thrust fault.

Along strike in the west UMF area, the map-scale folds and faults change shape notably. This could be due to out-of-plane motion, change in amount of shortening along strike, or change in the manner that the same amount shortening is accommodated along strike.

4.C Structural style across strike in the east UMF area

Five map-scale folds were surveyed in the east UMF area (figures 9 & 11). Here, the folds are separated into two categories on the basis of their structural character. In the northern region of the east UMF area, anticlines 4 & 5 display a structural style that resembles and may be a continuation along strike of the hangingwall anticline in the west UMF area. In the southern part of the east UMF area, the structural character of the anticlines in the Lisburne Group differs and will be described later.

In the northern east UMF area, fold 5 is characterized by a south-dipping axial plane, a steeply south-dipping overturned forelimb that is cut by at least two thrust faults, and a gently north-dipping backlimb (figures 9 & 11, Table 1). Much of the backlimb has been eroded. Nonetheless, both limbs of the anticline are planar, with the exception of the sigmoidal drag folds located adjacent to the thrust faults that cut the anticline forelimb.

Fold 4, in the northern east UMF area, is characterized by a south-dipping axial plane, a long planar southeast-dipping backlimb, and a north- to overturned south-dipping forelimb that is cut by a thrust fault. The hinge area of fold 4 contains a prominent calcite (?) vein several meters wide that is sub-parallel to the axial trace. Other smaller veins are sub-parallel to the axial surface throughout the hinge area. The thrust fault is exposed across the entire width of the exposed anticline, lies along a hangingwall flat in the anticline backlimb, and forms a hangingwall ramp forward of the anticline hinge. In the footwall, the fault parallels bedding in the Sadlerochit Group. An open anticline in the footwall has been superimposed on both the thrust fault and the overlying overturned anticline.

In the southern east UMF area, an anticline-syncline-fault/syncline system, respectively composed of folds 1, 2, and 3, differs in structural character from the folds in the northern east UMF area and the west UMF area (figures 9 & 11). Fold 1 is a nearly upright anticline containing an axial-plane that dips very steeply to the south. The anticline backlimb dips moderately to the south and is strongly parasitically folded rather than planar (figure 11, Table 1). Fold 2 is an open syncline adjacent to and north of fold 1. Fold 2 is significantly less tight than the syncline forward of the frontal anticline in the west UMF area. The fold 2 syncline displays very little parasitic folding. Fold 3 consists of an asymmetric anticline-syncline pair in the Lisburne Group with at least four thrust splays in the core of the anticline. The upper hinge area of the anticline is eroded. Most of the splays dip steeply and are associated with very small asymmetric parasitic folds. The lowest and northernmost splay flattens into bedding in the forelimb of the syncline, and the adjacent, higher splay appears to tip out in the hinge of the syncline. The presence of a fault tip in the syncline suggests that fault-propagation folding may have played a role in the formation of this fold.

5. Preliminary Interpretations

The overall structural style in the UMF area of the eastern Brooks Range is defined by a series of map-scale hangingwall anticlines imbricately stacked via south-dipping thrusts. More specifically, the thrust sheets strike east-northeast and dip gently to moderately towards the south-southeast. Each thrust sheet typically contains a map-scale, truncated anticline at its leading edge and consists of the Lisburne Group and the stratigraphically overlying Sadlerochit or Etivluk Group. The east-northeast trending hangingwall anticlines typically possess a parasitically folded, overturned, truncated forelimb, a planar, upright, relatively long backlimb, and a gently to moderately south-dipping axial surface. This deformation pattern indicates that folds in the Lisburne Group are preferentially truncated between the anticline hinge and forward syncline hinge. The exception to this structural style is fold 1 that is an upright fold and displays a parasitically folded backlimb. Within the west and central UMF areas, steeply dipping faults that are transverse to the northeast-trending structural grain cut the hangingwall anticlines, footwall anticlines and synclines (?), and intervening thrust sheets. The transverse faults may be normal faults related to extension oriented perpendicular to the maximum shortening direction. Alternatively, the transverse faults may be tear faults resulting from differential amounts and modes of shortening along strike.

Three lines of evidence suggest that, in the UMF area, the folds in the Lisburne Group formed as detachment folds. First, the mechanical stratigraphy in the UMF area favors detachment folding in the Lisburne Group. Here, the Lisburne Group is a relatively competent unit sandwiched between two incompetent units, the underlying Kayak Shale and overlying Sadlerochit or Etivluk Group. Second, detachment style folding was the dominant mechanism of deformation in the same units to the north, in the northeastern Brooks Range (Homza and Wallace, 1995, 1997). Third, folds that are not cut by thrusts, and so may be remnant detachment folds, are present in the study area, to the west, and along strike of structural trend of the UMF area (Wallace et al., 1997).

The folds in the Lisburne Group carbonates in the UMF area appear to be asymmetric; in other words, the folds contain unequal limb lengths. The total limb lengths cannot be determined unequivocally, because the forelimbs have been truncated and trailing cutoffs are not exposed within the area. Nonetheless, the contrast of long, planar, anticline backlimbs with the asymmetric fold pairs present in several anticline forelimbs indicates that the folds were separated by long non-folded panels and were probably asymmetrical prior to their truncation by thrust faults. This is in contrast to the detachment folds in the Lisburne Group of the northeastern Brooks Range that are symmetric, upright, and lack separation by non-folded panels (Wallace, 1993; Homza and Wallace, 1997). These folds in the northeastern Brooks Range are rarely cut by thrust faults and accommodate a wide range of shortening, by what appears to be a combination of flexural-slip folding and fold flattening (Atkinson, 2001; Wallace, 2001). Therefore, within the UMF area, the correlation of fold asymmetry and thrust truncation suggests the possibility that, as shortening increases, fold asymmetry favors thrust truncation.

In a regional context, the stratigraphic affinity of the Lisburne Group in the UMF area is uncertain. Presently, it is unknown whether the Lisburne Group in the UMF area is part of the leading edge of the Endicott Mountains allochthon or the North Slope parautochthon and, thus, is allochthonous or parautochthonous. Preliminary stratigraphic interpretations suggest that the Lisburne Group in the UMF area may represent a deeper-water facies than that of the northeastern Brooks Range. A deeper-water facies in the Lisburne Group is consistent with, but does not necessitate, an interpretation that the UMF area Lisburne Group is part of a far-traveled thrust sheet. In addition, the lowermost formation in the Lisburne Group of the UMF resembles the Wachsmuth Formation of the Lisburne Group in the Endicott Mountains allochthon. Insufficient work has been done on the shale/minor sandstone unit directly overlying the Lisburne Group of the UMF area to determine whether this overlying unit is more appropriately assigned to the Sadlerochit Group of the North Slope parautochthon or the Etivluk Group of the Endicott Mountains allochthon. Previous mapping has identified the northern boundary of the Endicott Mountains allochthon only approximately, and this boundary was primarily based on the northern limit of the Kanayut Conglomerate. West of the UMF area, the Endicott Mountains allochthon appears to lie along strike with the structural trend of the Lisburne Group in the UMF area. The structural style of the Lisburne Group in the UMF area resembles that of the Lisburne Group of the Endicott Mountains allochthon, although this style is also locally present within the southern edge of the North Slope parautochon.

6. Questions Raised

This research identifies three key questions that will be explored as the research continues: (1) Did the folds in the Lisburne Group originate as detachment folds or fault-propagation folds, (2) If the folds formed as detachment folds, what was their character, and (3) How were the folds truncated by thrust faults? If the folds originated as detachment folds before truncation, three geometric and kinematic questions are important. First, were the detachment folds originally asymmetrical or did they evolve from symmetrical to asymmetrical folds? This question is important, because fold asymmetry may be a critical factor favoring late-stage truncation of detachment folds. Second, did the folds form as buckle or kink folds? The sense of fold asymmetry has been shown to differ on the basis of whether a fold formed by the buckle or kink mechanisms (Reches and Johnson, 1976; Anthony and Wickham, 1978). Third, did the fold hinges remain fixed or did they migrate? Kinematic models for detachment folds have been proposed with either migrating or fixed fold hinges. Whether or not the fold hinges migrate has direct implications for kinematic models that describe the thrust-truncation of folds. An additional question is why the structural style of the Lisburne Group differs on either side of the Continental Divide thrust front. One hypothesis to explore further is whether the asymmetry of the folds in the Lisburne Group south of the Continental Divide thrust front caused them to deform by thrust-truncation rather than by fold flattening, as in the symmetrical folds of the northeastern Brooks Range.

6. Future Work

The overall goal of this project is to assess the influence of fold asymmetry, mechanical stratigraphy, and fold locking angle on thrust truncation of detachment folds. Immediate goals for this research are the completion of cross sections AA', BB', DD', EE', addition of the field map for the central UMF area, and completion of the displays of survey data for folds 4 and 6. These will serve as a basis to integrate serial cross sections in the west UMF area into one or more block diagrams and to partially restore the cross sections. Preliminary results were presented at the Geological Society of America annual conference in November 2001, and final results will be presented at the American Association of Petroleum Geologists Pacific section meeting in Anchorage, May 2002.

7. Acknowledgements

Special thanks to Jeff Crocker - the tireless field assistant, Paul Atkinson, Andy Krumbhardt, Michelle McGee, Mike Whalen, John Craven, Larry King, Kris Meisling and Samantha Smith. Thanks to Bill Witte for technical support and Ray Ecke for skilled flying. Department of Energy Contract #DE-AC26-98BC15102 primarily funded this research. The following scholarships, awarded to M. Jadamec, also supported this research: ARCO Alaska/ Phillips Petroleum Inc. Research Grant, UAF Graduate School Thesis Completion Fellowship, Women's Auxiliarly to the American Institute of Mining, Metallurgical, and Petroleum Engineers Inc. Scholarship, Jessie O'Brian Macintosh Scholarship, UAF Geophysical Institute/IARC Travel Grant, UAF Graduate School Travel Grant, and a travel grant from the UAF College of Science, Engineering, and Mathematics.

8. References

Anthony, M., and Wickham, J., 1978, Finite-element simulation of asymmetric folding: Tectonophysics, v. 47, p. 1-14.

Atkinson, P.K., 2001, A geometric analysis of detachment folds in the Lisburne Limestone, Arctic National Wildlife Refuge, Alaska: in Wallace, W.K., ed., The influence of fold and fracture development on reservoir behavior of the Lisburne Group of northern Alaska: Department of Energy, Fossil Energy, National Petroleum Technology Office, Tulsa, Oklahoma, Second semi-annual report for work performed under contract no. DE-AC26-98BC15102.

Chester, J.S., Logan, J.M., and Spang, J.H., 1991, Influence of layering and boundary conditions on fault-bend and fault-propagation folding: GAS Bulletin, vol. 103, p. 1059-1072.

Crowder, R.K., 1990, Permian and Triassic sedimentation in the northeastern Brooks Range, Alaska: Depostion of the Sadlerochit Group: The American Association of Petroleum Geologists Bulletin, v. 74, no. 9, p. 1351-1370.

Erickson, S. G., 1996, Influence of mechanical stratigraphy on folding vs faulting: Journal of Structural Geology, vol. 18, no. 4, p. 443-450.

Fischer, M.P. and Jackson, P.B., 1999, Stratigraphic controls on deformation patterns in fault-related folds: a detachment fold example from the Sierra Madre Oriental, northeast Mexico: Journal of Structural Geology, vol. 21, p. 613-633.

Fischer, M.P., Woodward, N.B., and Mitchell, M.M., 1992, The kinematics of break-thrust folds: Journal of Structural Geology, v.14, p. 451-560.

Homza, T.X., and Wallace, W.K., 1995, Geometric and kinematic models for detachment folds with fixed and variable detachment depths: Journal of Structural Geology, v. 17, no. 4, p. 475-588.

Homza, T.X., and Wallace, W.K., 1997, Detachment folds with fixed hinges and variable detachment depth, northeastern Brooks Range, Alaska: Journal of Structural Geology, v. 19, nos. 3-4 (special issue on fault-related folding), p. 337-354.

Jamison, W.R., 1987, Geometric analysis of fold development in overthrust terranes: Journal of Structural Geology, v. 9, p. 207-219.

Lepain, D.L., 1993, Transgressive sedimentation in rift-flank region: Deposition of the Endicott Group (Early Carboniferous), northeastern Brooks Range, Alaska: University of Alaska, Ph.D Thesis, 325 p.

Maclean, E. A., 2001, Structural geology and evolution of a duplex Southwest of Galbraith Lake, north central Brooks Range, Alaska: Geological Society of America, Abstracts with Programs, v. 33, n. 6, p. A-150.

McGee, M., Whalen, M., and Krumhardt, A. P., 2002, Baseline stratigraphy of the Lisburne Group: in Wallace, W.K., ed., The influence of fold and fracture development on reservoir behavior of the Lisburne Group of northern Alaska: Department of Energy, Fossil Energy, National Petroleum Technology Office, Tulsa, Oklahoma, Fourth semi-annual report for work performed under contract no. DE-AC26-98BC15102.

McNaught, M. A., and Mitra, G., 1993, A kinematic model for the origin of footwall synclines: Journal of Structural geology, v. 15, n. 6, p. 805-808.

Mitra, S., 1990, Fault-propagation folds: geometry, kinematic evolution, and hydrocarbon traps: American Association of Petroleum Geologists Bulletin, v. 74, p. 921-945.

Moore, T.E., Wallace, W.K., Bird, K.J., Karl, S. M., Mull, C.G., Dillon, J.T., 1994, Geology of northern Alaska: in Plafker, G., and Bird, K.J., eds., The Geology of North America Volume G-1, The Geology of Alaska: The Geological Society of America, p. 49-140.

Morely, C.K., 1994, Fold-generated imbricates: examples from the Caledonides of Southern Norway: Journal of Structural Geology, v. 16, n. 5, p. 619-631.

Pfiffner, O.A., 1993, The structure of the Helvetic nappes and its relation to the mechanical stratigraphy: Journal of Structural Geology, v. 15, nos. 3-5, p. 511-521.

Plafker, G., and Berg, H.C., 1994, Overview of the geology and tectonic evolution of Alaska: in Plafker, G., and Berg, H.C., eds., The Geology of North America Volume G-1, The Geology of Alaska: The Geological Society of America, p. 989-1021.

Poblet, J., and McClay, K., 1996, Geometry and kinematics of single-layer detachment folds: American Association of Petroleum Geologists Bulletin, v. 80, p. 1085-1109.

Reches, Z., and Johnson, A.M., 1976, A theory of concentric, kink, and sinusoidal folding and of monoclinal flexuring of compressible, elastic multilayers: Tectonophysics, v. 35, p. 295-334.

Suppe, J., 1983, Geometry and kinematics of fault-bend folding: American Journal of Science, v. 283, p. 684-721.

Suppe, J., and Medwedeff, D.A., 1990, Geometry and kinematics of fault-propagation folding: Ecolgae Geologicae Helvetiae, v. 83, p. 409-454.

Thorbjornsen, K.L., and Dunne, W.M., 1997, Origin of a thrust-related fold: Geometric vs. kinematic tests: Journal of Structural Geology, v. 19, nos. 3-4 (special issue on

fault-related folding), p. 303-319.

Wallace, W.K., 1993, Detachment fold and a passive-roof duplex: Examples from the northeastern Brooks Range, Alaska, in Solie, D.N., and Tannian, F., eds., Short Notes on Alaskan Geology 1993: Alaska Division of Geological and Geophysical Surveys Geologic Report 113, p. 81-99.

Wallace, W.K., 2001, Detachment folds and their truncation by thrust faults: in Wallace, W.K., ed., The influence of fold and fracture development on reservoir behavior of the Lisburne Group of northern Alaska: Department of Energy, Fossil Energy, National Petroleum Technology Office, Tulsa, Oklahoma, Second semi-annual report for work performed under contract no. DE-AC26-98BC15102.

Wallace, W.K., and Hanks, C.L., 1990, Structural provinces of the northeastern Brooks Range, Arctic National Wildlife Refuge, Alaska: American Association of Petroleum Geologists Bulletin, v. 74, no. 7, p. 1100-1118.

Wallace, W.K. and Homza, T., In press, Detachment folds vs. fault propagation folds, and their truncation by thrust faults: in McClay, K.R., editor, Thrust tectonics and Petroleum Systems: American Association of Petroleum Geologists memoir.

Wallace, W.K., Moore, T.E., Plafker, G., 1997, Multistory duplexes with forward dipping roofs, north central Brooks Range, Alaska: Journal of Geophysical Research, v. 102, no. B9 (special section on the USGS Trans-Alaska Crustal Transect), p. 20,773-20,796.

Watts, K.F., Harris, A.G., Carlson, R.C., Eckstein, M.K., Gruslovic, P.D., Imm, T.A., Krumhardt, A.P., Lasota, D.K., Morgan, S.K., Dumoulin, J.A., Enos, P., Goldstein, R.H., and Mamet, B.L., 1995, Analysis of reservoir heterogeneities due to shallowing upward cycles in carbonate ricks of the Pennsylvanian Wahoo Limestone of northeastern Alaska: United States Department of Energy, Final Report for 1989-1992 (DOE/BC/14471-19), Bartlesville Project Office, 433 p.

Willis, B., 1893, Mechanics of Appalachian structure: U.S. Geological Survey Annual Report, 13, part 2, p. 217-281.

Wolf, P.R., and Brinker, R.C., 1994, Elementary Surveying: HarperCollins College Publishers, 760 p.

Woodward, N.B., and Rutherford, E. Jr., 1989, Structural lithic units in external orogenic zones: Tectonophysics, 158, p. 247-267.

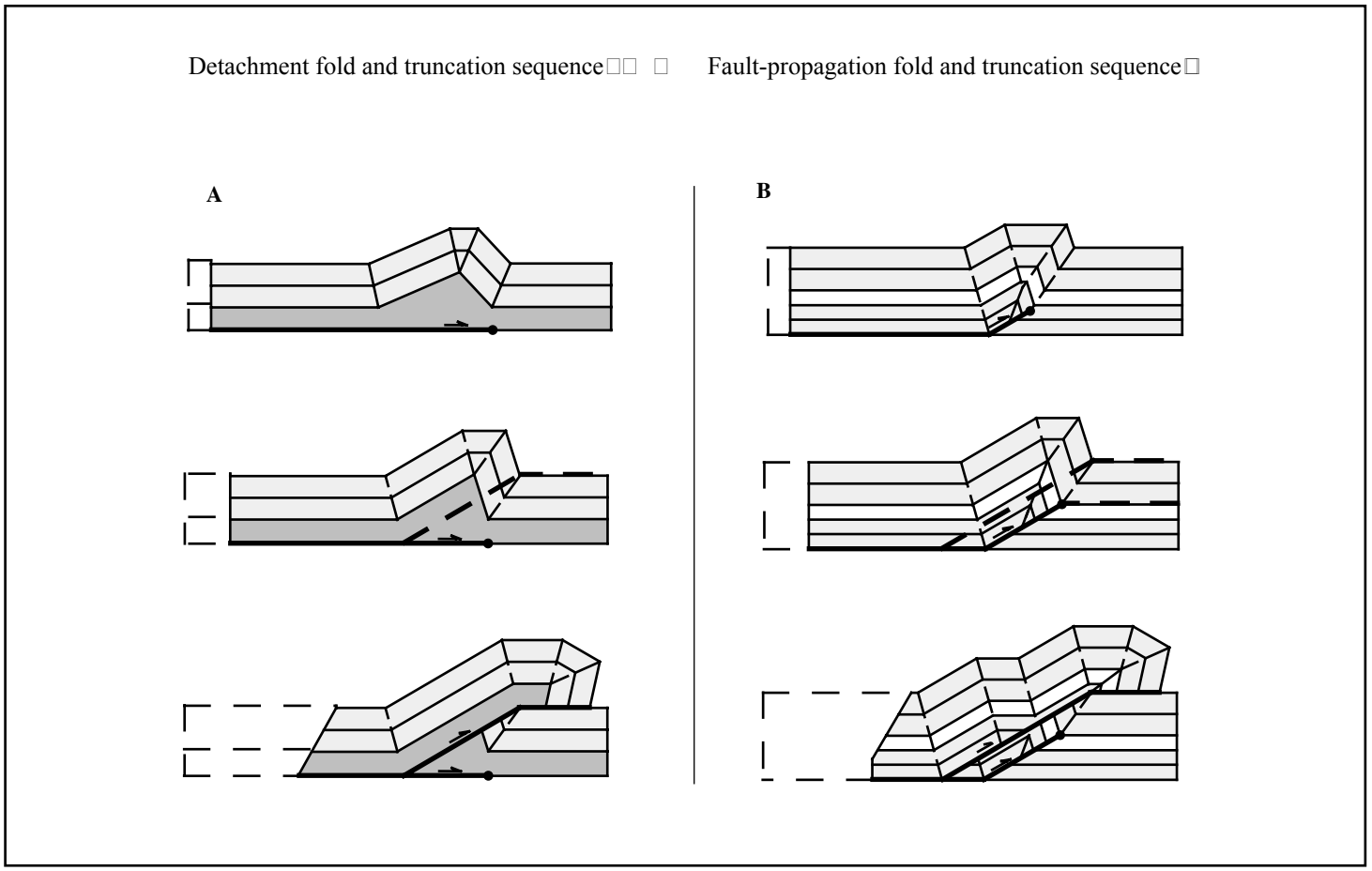

Figure 1. Schematic models of two thrust-related fold types common in foreland fold-and-thrust belts. Upper row illustrates fold geometry for (A) detachment fold and (B) fault-propagation fold. The vertical sequence in the column to the left depicts a model for the eventual truncation of a detachment fold. The column on the right shows that for a truncated fault-propagation fold. Models assume parallel folding and the conservation of both line length and area. Parallel folding and conservation of line length do not apply in the incompetent unit (dark gray) in the core of the detachment fold (A). Modified from Wallace and Homza, in press.

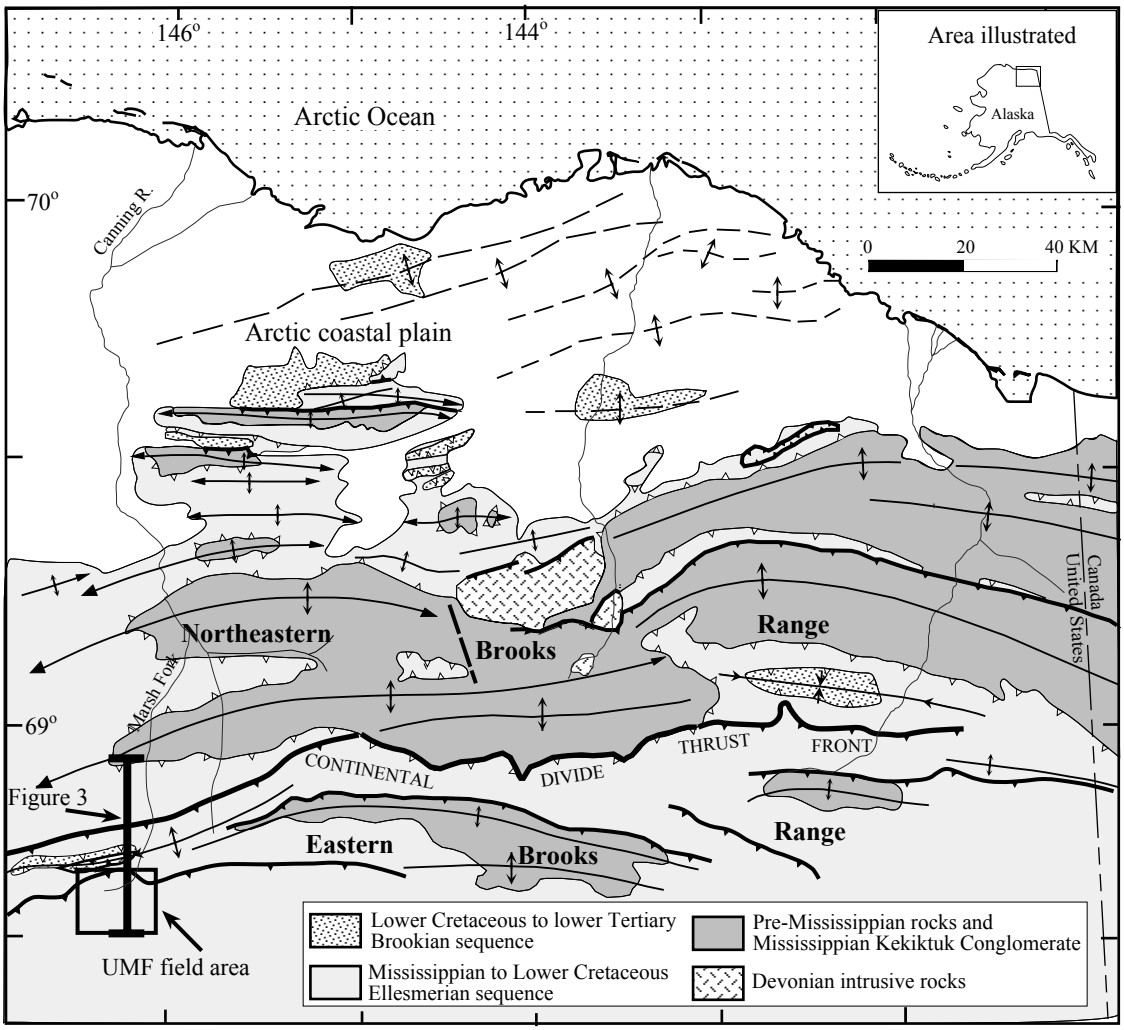

Figure 2. Generalized tectonic map of the eastern and northeastern Brooks Range, Alaska (modified from Wallace and Homza, in press). Here, the two regions are separated by the Continental Divide thrust front. The upper Marsh Fork (UMF) field area and line of section for Figure 3 are indicated by the box outline and solid bar in the southwestern corner of the map, respectively.

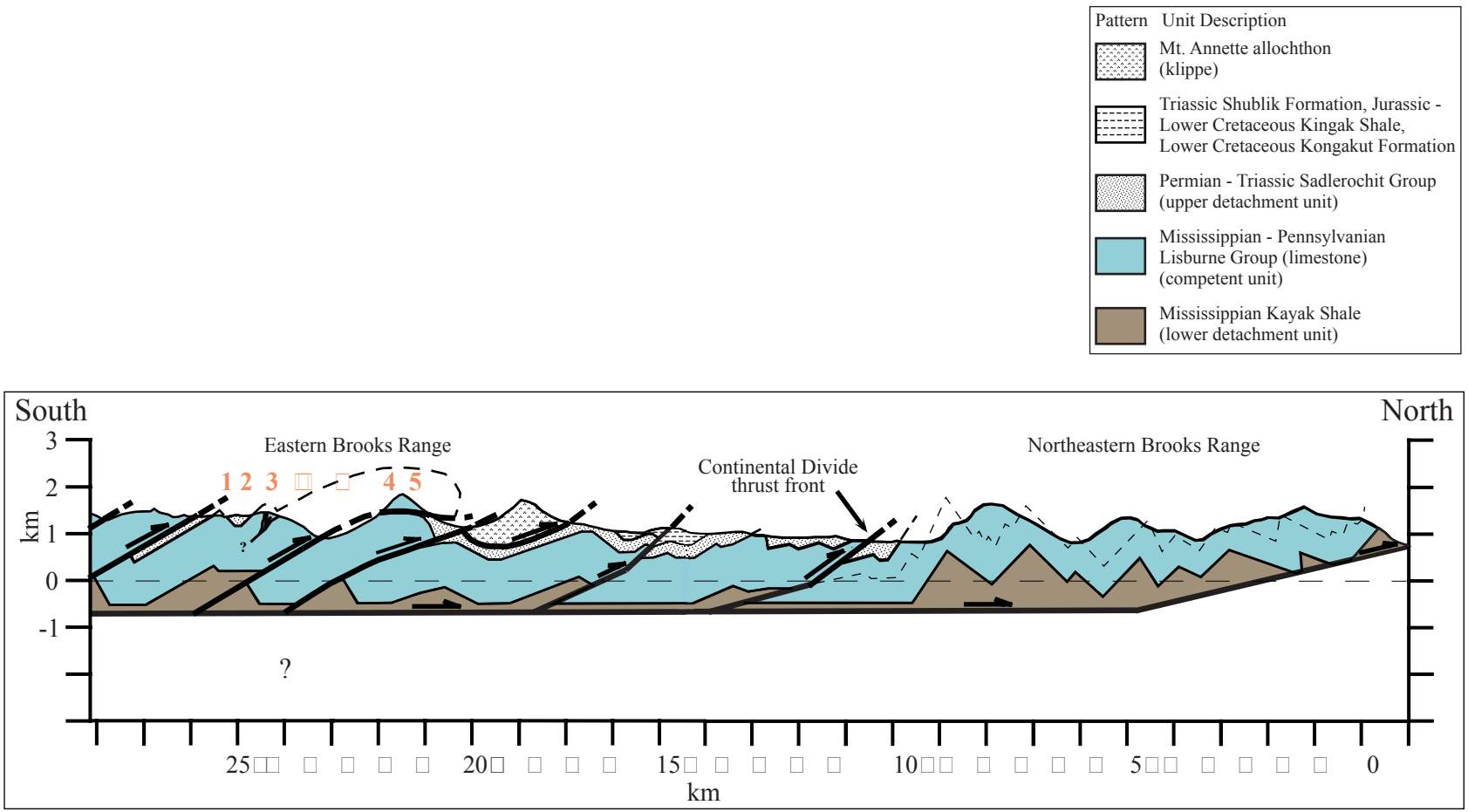

Figure 3. Cross section of the northeastern and eastern Brooks Range that illustrates the change in deformation style of the Carboniferous units from symmetric and upright detachment folds to the north to asymmetric and thrust-truncated detachment (?) folds to the south. Here, the Continental Divide thrust front separates the two regions. Numbers 1 through 5 indicate five surveyed folds in the upper Marsh Fork east field area. The location of fold 5 is projected into the line of section from the east. Location of cross section is shown in Figure 2. Modified from Wallace and Homza, in press.

DE-AC26-98BC15102

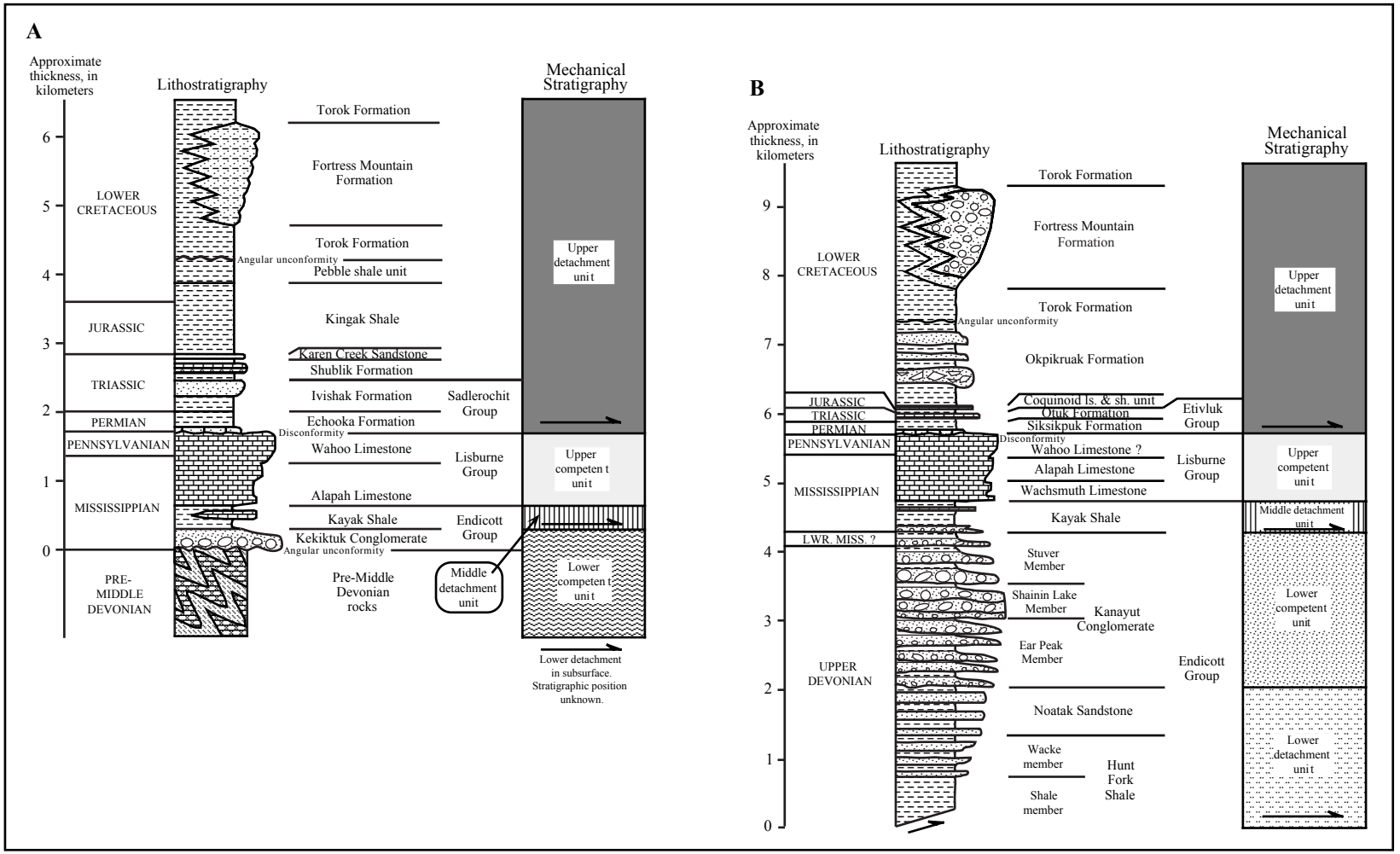

Figure 4. Stratigraphic columns for the (A) North Slope parautochthon and (B) Endicott Mountains allochthon. The Endicott Mountains allochthon contains a thick sequence of Upper Devonian clastic rocks beneath the Kayak Shale that is absent in the North Slope parautochthon. Mechanical stratigraphic units are identified and illustrate the general deformation response of the rock units to shortening. Modified from Wallace et al., 1997.

Figure 5. Topographic map depicting the east, central, and west regions of the upper Marsh Fork (UMF) field area located along the upper Marsh Fork of the Canning River (base from USGS Arctic quadrangle, Alaska 1:250,000 topographic series). Numbers 1-6 indicate the locations of the six map-scale folds surveyed. The east, central, and west areas were mapped at the 1:25,000 scale.

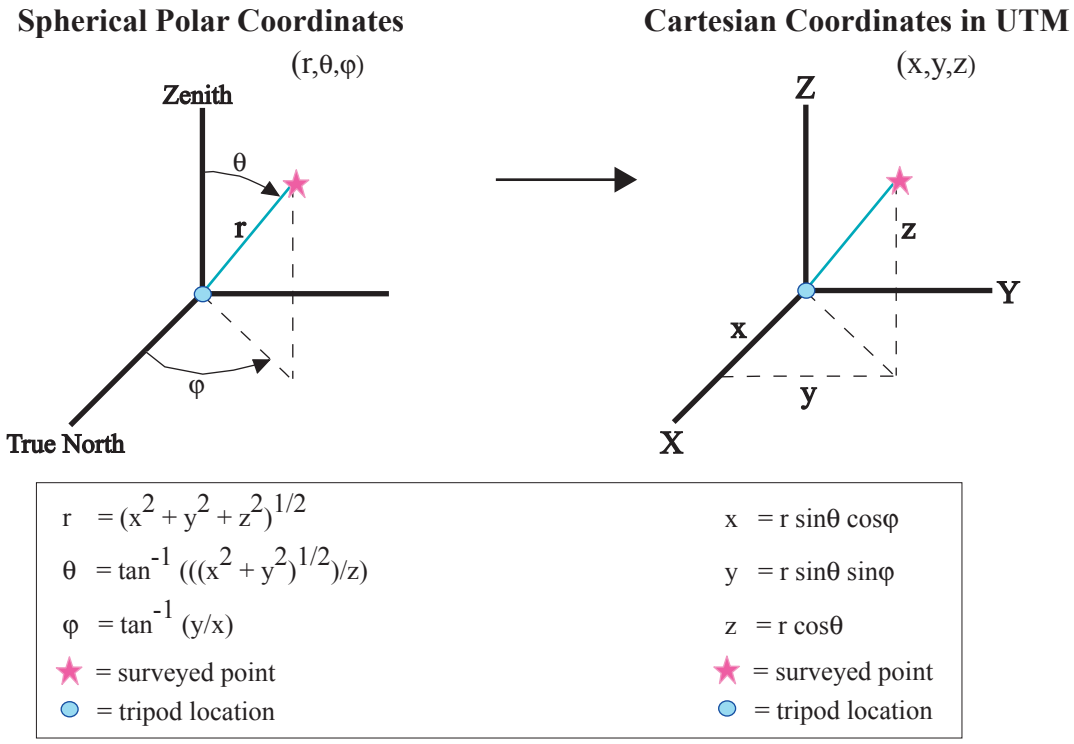

Figure 6. Illustration showing the coordinate systems used in collection and processing of survey data. The data were collected in a spherical polar coordinate system. Rockworks99 software converted the spherical data to a cartesian data set and plotted the data on a UTM grid. GPS locations were taken at the tripod location and thus enabled the data to be referenced to the UTM system. Theta (θ) is the angle from vertical to a surveyed point. Psi (ϕ) is the horizontal angle from true north to the surveyed point. r is the distance from the origin to the surveyed point.

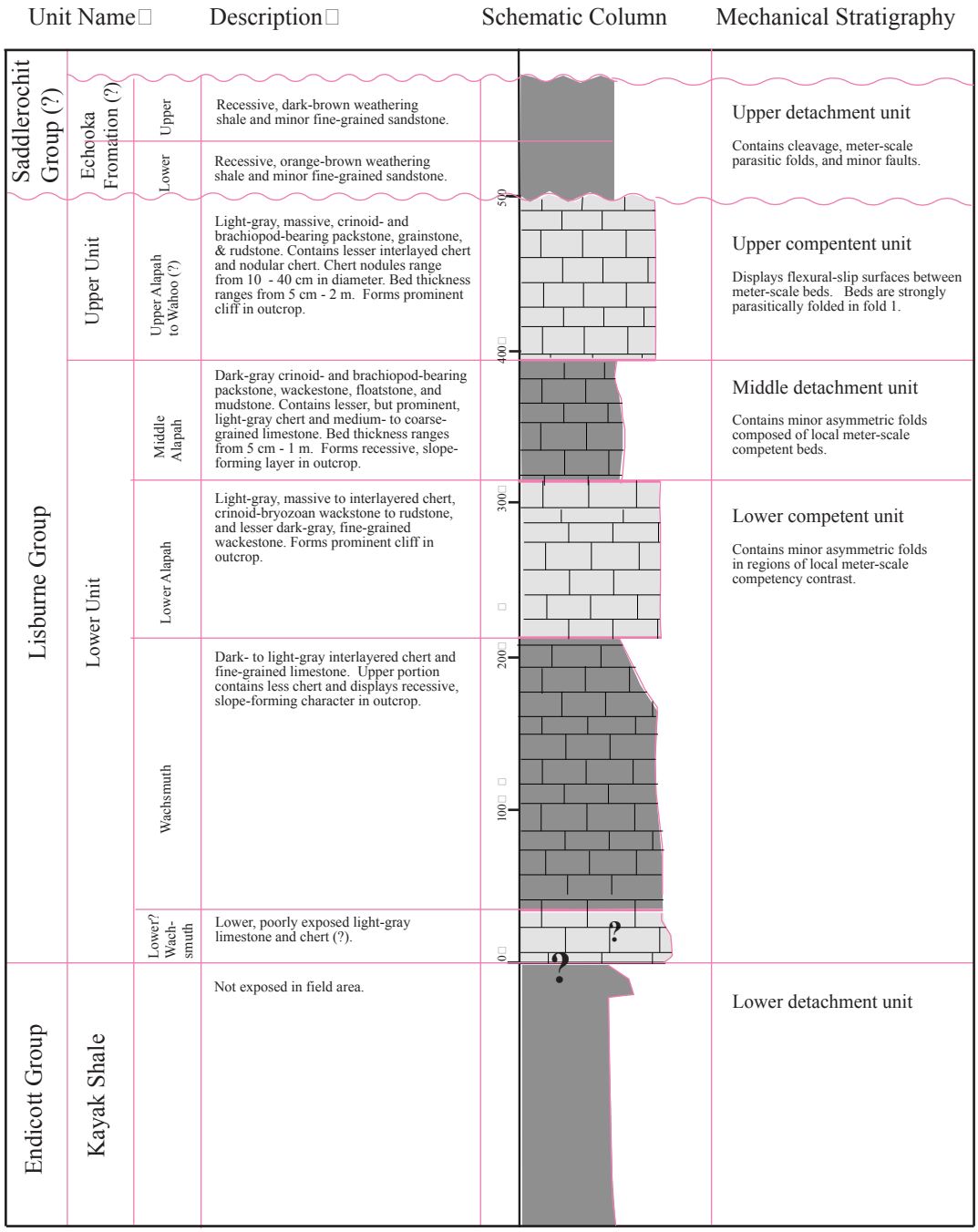

Figure 7a. Schematic sratigraphic column of Lisburne Group and surrounding units. Column is based on field observations in the upper Marsh Fork area of the Canning River. Unit thicknesses are approximate values determined from field observations by the authors and stratigraphic data collected in the upper Marsh Fork area by Michelle McGee (McGee personal communication; McGee et al., this report). Total Lisburne Group thickness in the southern east UMF area is approximately 525 m. Scale bar represents Lisburne Group thickness in meters. The Kayak Shale thickness is schematic and the contact between Lower Lisburne and Kayak Shale is not exposed.

Figure 7b. Outcrop character of Lisburne Group in southern UMF east area. The upper Lisburne Group unit increases in thickness in west UMF area anticlines and decreases in thickness in the northern east UMF area anticlines. The thickness increase of the upper Lisburne Group unit may be due to less erosion of the Wahoo Limestone in the west UMF area.

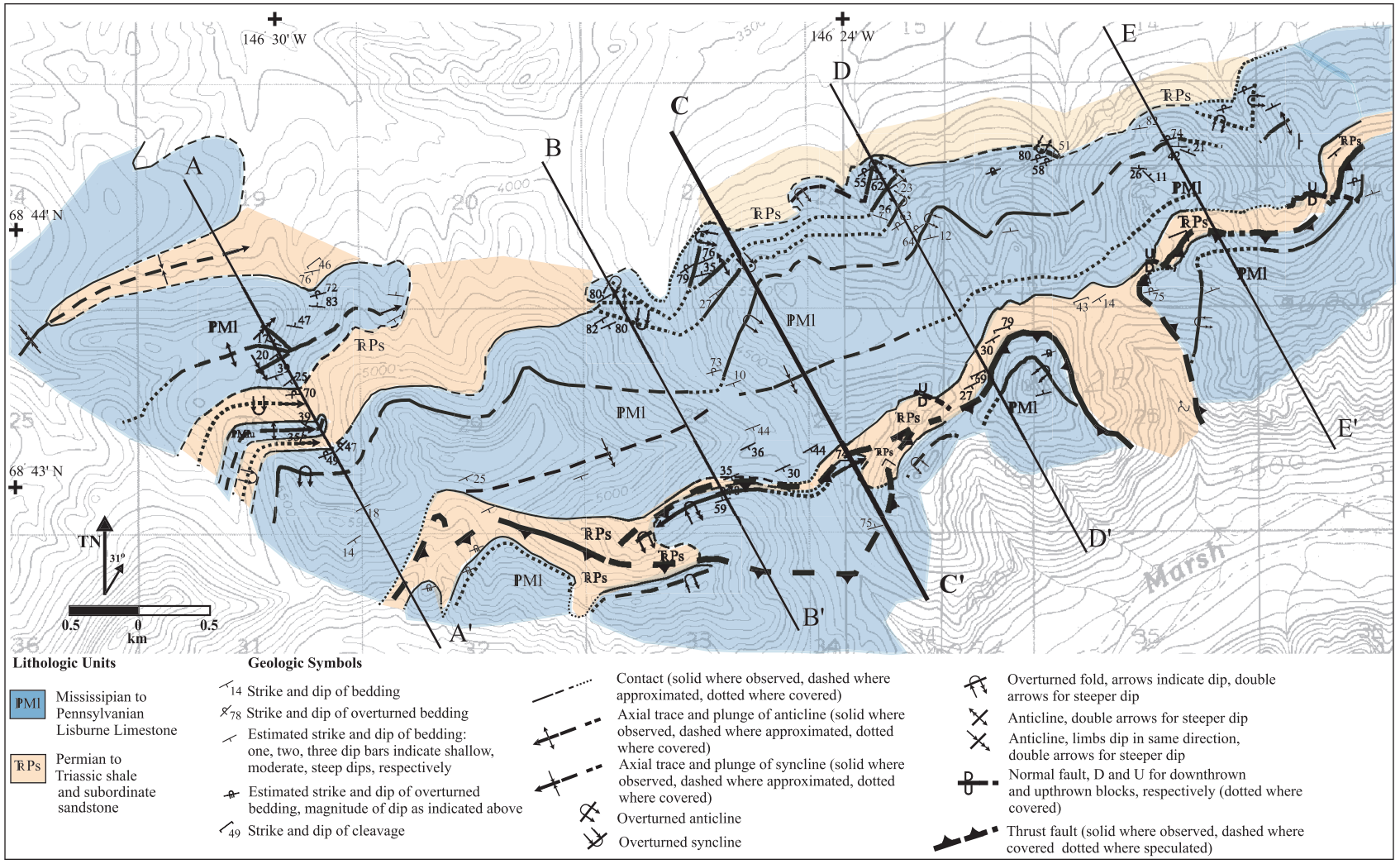

Figure 8. Interpretive bedrock geology map of west UMF area and location of cross section CC' (figure 10). The overall structural style is defined by a series of map-scale hangingwall anticlines imbricately stacked via southeast dipping thrust faults. Two detachment units, the underlying Kayak Shale and overlying Sadlerochit Group, sandwich the Lisburne Group (limestone). Sections AA', BB', DD', and EE' are not shown in this report.

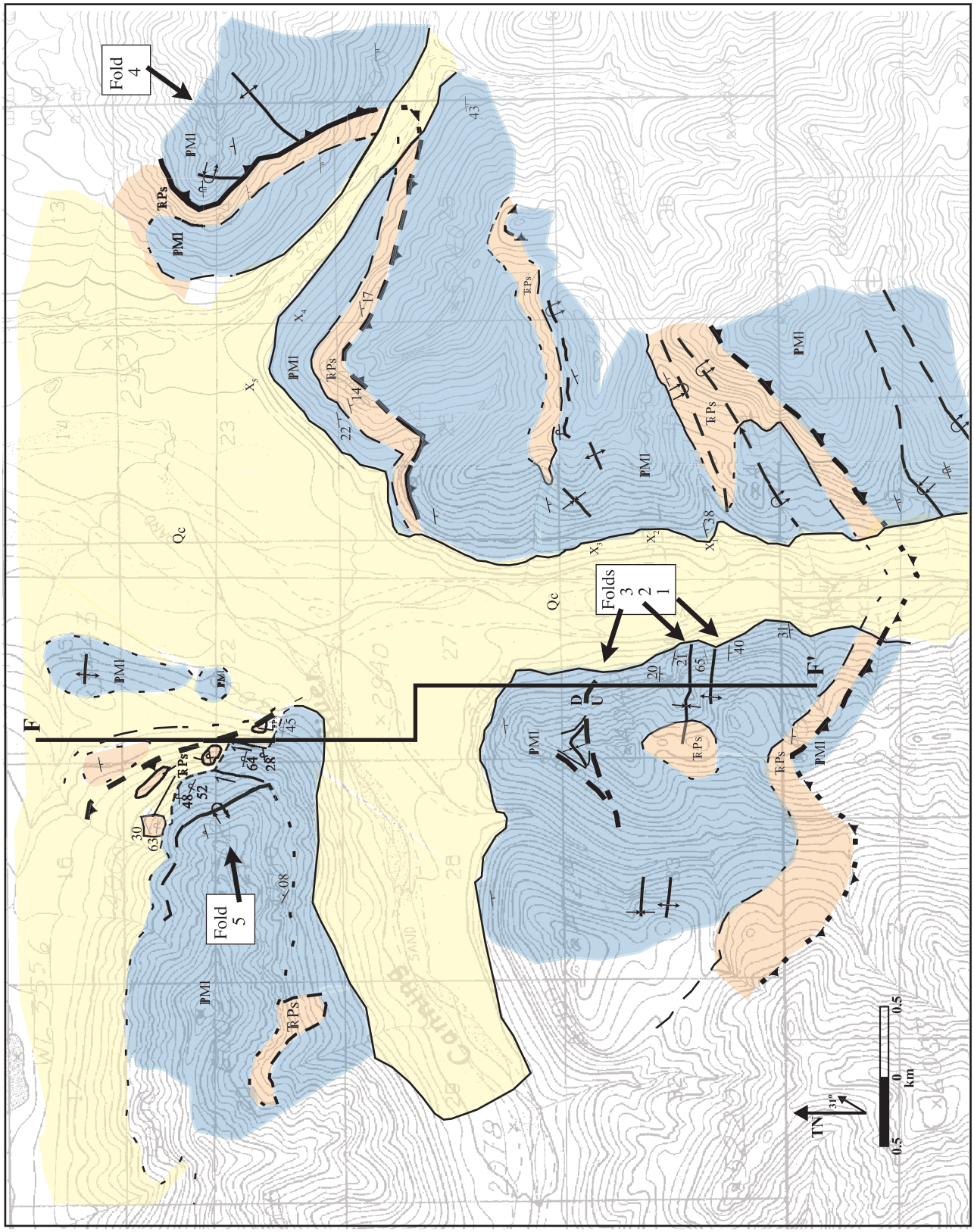

Figure 9. Interpretive bedrock geology map of east UMF field area and location of cross section FF' (figure 11). See figure 8 for legend. Heavy solid arrows point to five surveyed folds. X_1-X_5 are approximate locations of survey stations.

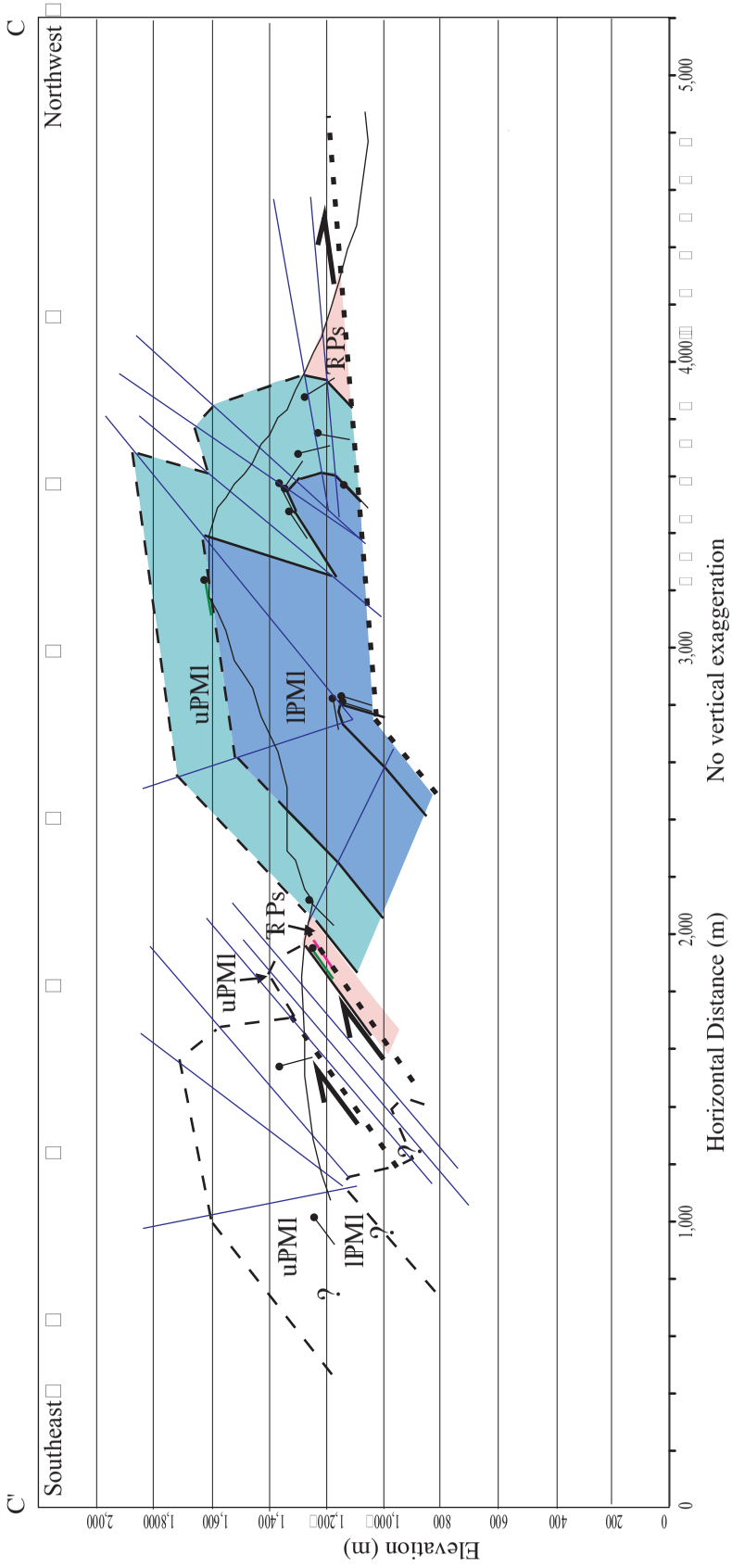

Figure 10. Preliminary cross section CC' in west UMF area. Location of section is show in figure 8. This section is located to the west of the section shown in figure 11.

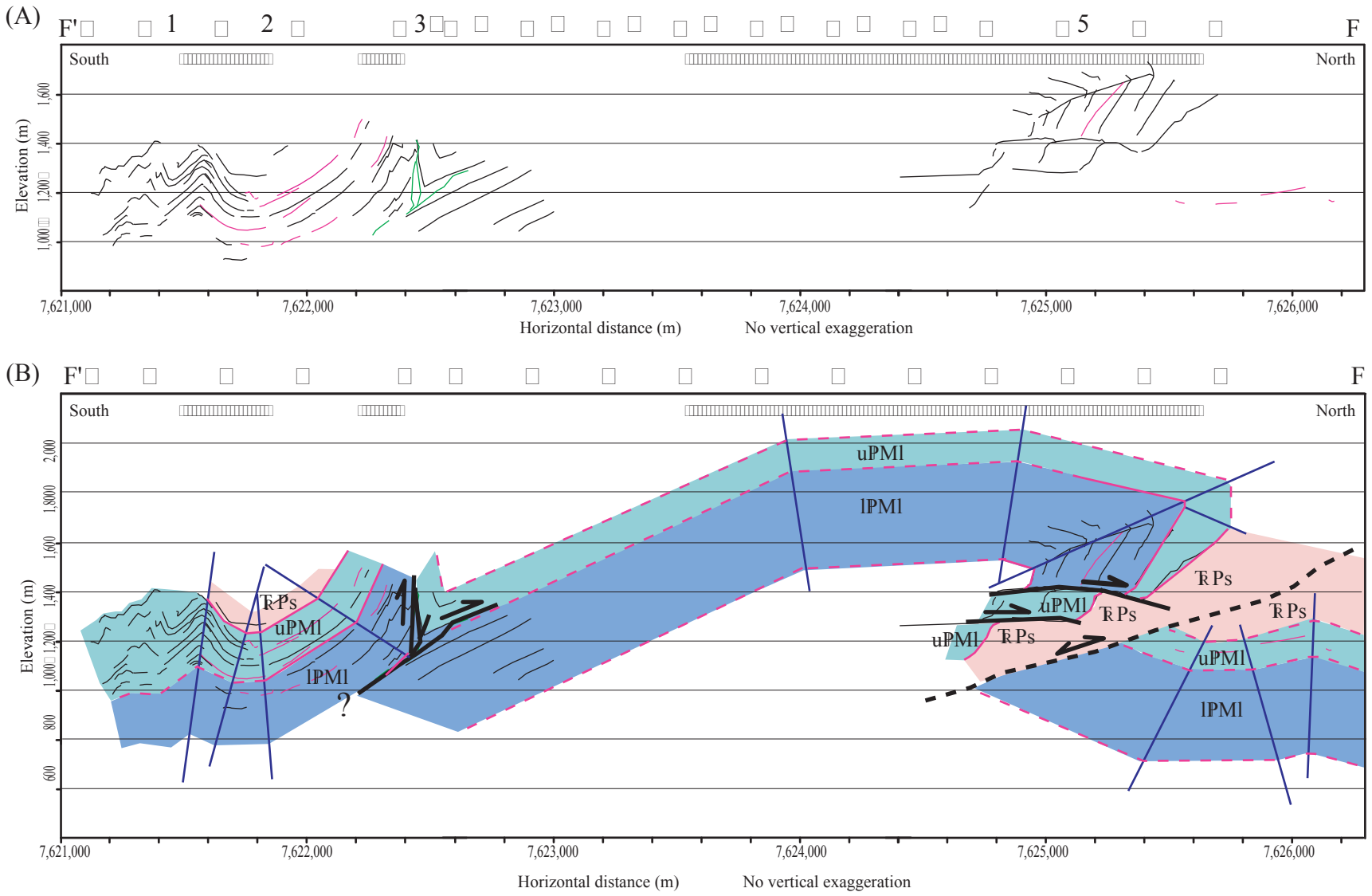

Figure 11. Cross sectional plot of survey data from the east UMF field area. (A) Thin lines in the upper figure are connected survey points. Numbers 1,2,3, & 5 indicate the structures surveyed. (B) Preliminary interpretation of the survey data. See figure 9 for section location.

Fold name	Approximate interlimb angle (°)	Axial plane dip (°)	Forelimb dip (°)	Minimum forelimb length (m)	Forelimb character	Backlimb dip (°)	Minimum backlimb length (m)	Backlimb character	Distinctive properties
Frontal fold AA'	40	35 S	49 SE overturned	~ 110	planar; folds to the north may be parasitic to forelimb	20 SE	~ 710	planar	plunges NE ~ 15°
Frontal fold CC'	37	39 SE	71 SE overturned	~ 260	parasitic syncline-anticline pair	35 SE	~ 750	planar	round hinge
Frontal fold DD'	40	10 S	60 S overturned	~ 375	parasitic syncline-anticline pair	12 N	~ 475	planar	fault within forelimb-folds, round hinge
Frontal fold EE'	40	40 S	74 SE overturned	~ 300	parasitic syncline-anticline pair	25 NE	~ 375	planar	round hinge
Frontal fold east of EE'	150	80 S	~ 45 N to overturned	~ 330	planar to gently curved	~ 20 S	~ 300	planar; cut by normal fault	NE plunge, round hinge
HW fold EE'	60	30 S	75 S overturned	~ 90	planar; cut by thrust fault	~ 30 N	~ 580	planar	angular hinge
HW fold east of EE'	80	10 S	~ 20 S overturned	~ 180	planar; cut by thrust fault	~ 30 N	~ 375	planar	angular hinge
Fold 5 FF'	100	20 S	~ 60 S overturned	~ 270	planar; cut by faults	~ 50 N	~ 300	planar	box fold, angular hinge
Fold 4 east of FF'	95 multiple axial surfaces	25 S	~ 80 NNW to overturned ~ 60 S	~ 120	planar; cut by thrust fault	~ 45 SE	~ 975	planar; minor parasitic folds	calcite (?) veins in hinge area crosscut bedding
Fold 1 FF'	76 widens to ~120 downward	80 S	65 NW	~ 105	gently curved; syncline-fault	43 S	~ 490	numerous parasitic folds	folded backlimb chevron fold, angular hinge

Table 1. Summary of west and east UMF area anticline properties. Letters AA', CC', DD', EE', and FF' denote section lines on figures 8 & 9. HW refers to southern hangingwall anticline in west UMF area. Limb lengths are rough estimates.

The relationship between fracturing, asymmetric folding, and normal faulting in Lisburne Group carbonates: West Porcupine Lake Valley, northeastern Brooks Range, Alaska

J.R. Shackleton, C.L. Hanks, and W.K. Wallace

Abstract

The area of Porcupine Lake Valley in the northeastern Brooks Range (NEBR) is at a major structural transition between symmetric detachment folds that are characteristic of the NEBR proper, and asymmetric thrust truncated folds resembling those along the main axis of the Brooks Range. Lisburne Group carbonates in the western end of Porcupine Lake Valley are locally folded into strongly asymmetric NE striking and plunging (detachment?) folds characterized by short, steep to overturned forelimbs, and long (up to 1 km) gently dipping backlimbs. Only one thrust fault was documented in the NW end of the field area that places a long, relatively flat panel of Lisburne Group carbonates above the Sadlerochit Group. NE and NW striking normal faults with relatively small displacements cut folds in West Porcupine Lake Valley.

Four major sets of extension fractures were documented in West Porcupine Lake valley, the majority of which dip steeply between 60º-90º in both directions: 1) a N-S striking set; 2) an E-W striking set; 3) a N-S to NW striking set; and 4) a NE striking set. While the relative timing of each of these fracture sets is unclear, some generalities can be made. The NW set appears to be younger than the N-S and E-W sets. E-W fractures terminate against N-S fractures at most sample locations. However, the opposite relationship was documented elsewhere in the field area, possibly suggesting multiple generations of N-S and E-W fracturing. All three fracture sets were found in en echelon sets of extension fractures, which indicate a component of shear during formation. Shear sense on these sets was commonly normal or strike slip, suggesting that many fractures are related to normal faulting in the area. The N-S and NW striking fractures were often found in 3-5 meter wide swarms of en echelon fractures, each swarm spaced approximately 10-20 meters apart. NE striking fractures were well developed in the lower portions of one of the major synclines in the area, although the timing of these fractures is unclear. Other major mesoscopic-scale structures indicate some period of penetrative semi-ductile deformation, including dissolution cleavage, deformed crinoid stems, sheared stylolites, and elongated and transposed chert nodules.

Normal faulting in West Porcupine Lake Valley is atypical for the NEBR, and may have influenced fracture character and distribution. Cross cutting relationships suggest that NE striking faults occurred after thrusting, whereas folds truncated by hinge sub-parallel normal faults suggest that normal faulting may have occurred during folding, or may have significantly modified fold geometries after a previous phase of compressional deformation. Changes in fold geometry were observed across NW striking normal faults, suggesting that either the normal faulting modified fold geometries, or that these faults originated as transverse structures and developed a normal sense of shear during or after folding.

The goal of this project is to understand the relationship between fracturing, faulting and folding in West Porcupine Lake Valley. Some important questions to be addressed are: did folds in the field area form as detachment folds or fault propagation folds, and how does each of these fold models influence fracturing? Conversely, can we use fracture distribution to understand the kinematics of fold formation? Another important question is how normal faulting has affected fracturing and folding in the area, and whether or not fractures related to folding can be distinguished from those related to faulting. In order to answer these previous questions, it will be important to understand how lithology and bed thickness affect fracturing, since changes in these two variables affect fracture spacing within the stratigraphy.

Future work includes: 1) completion of data compilation and production of mechanical stratigraphic sections; 2) construction of balanced, restored cross-sections; 3) statistical analysis of fracture data in order to understand the relationship between fracture density, folding, bed thickness, and lithology; 4) integration of fracture data into a three-dimensional fold model in order to understand the relationship between fracturing and folding; and 5) detailed statistical and geometric analysis to distinguish between fractures and fracture sets related to faulting vs. folding.

Introduction

Fractures in flat lying rocks in advance of fold and thrust belts have been studied by numerous authors (eg. Hanks et al., 1997, Lorenz et al, 1991, Hancock and Engelder, 1989, Narr and Suppe, 1991, Ladeira and Price, 1981). However, few models exist for the distribution and/or character of fracturing and strain indicators in folded rocks of specific fold geometries (Hennings et al., 2000, Homza and Wallace, 1997, Stearns and Friedman, 1969, Stearns, 1968). Understanding the distribution and character of fractures in folds is important for hydrocarbon exploration because fractures may enhance certain reservoir characteristics such as porosity and permeability in certain regions of folds such as the hinges or near bed surfaces. Since there are a variety of fold geometries found in the natural world, it is important to understand the relationship between fracturing and folding for each type of fold.

This report summarizes the preliminary field results of research on Lisburne group carbonates located at a major structural transition between symmetric detachment folds that are characteristic of the northeastern Brooks Range (NEBR) proper, and asymmetric thrust truncated folds resembling those along the main axis of the Brooks Range (figure 1). The field area is structurally bounded to the NW by a large displacement thrust fault that places Lisburne Group carbonates above Sadlerochit Group siltstones and sandstones, and to the SW by range front thrusts that stack Lisburne carbonates to form duplexes in the Phillip Smith Mountains. The study area in West Porcupine Lake Valley consists of NE striking and plunging asymmetrically folded Lisburne Group carbonates with short, steep to overturned forelimbs and long backlimbs. NE and NW striking normal faults with relatively small displacements cut folds in West Porcupine Lake Valley. The relatively subdued topography in the area provides easy access to outcrops, making the study area an excellent location for close examination of fracturing in

asymmetric folds. The purpose of this research is to understand the relationship between fracturing, normal faulting and asymmetric folding in Lisburne Group carbonates in order to develop a predictive model for fracture density and distribution in asymmetric folds in the northeastern Brooks Range.

Fractures and Folds

Models for fracturing in flat-lying and folded rocks are derived from a few important experimental and field observations. A summary of one set of early rock deformation experiments is shown in figure 2A (Griggs and Handin, 1960). Stage 1 shows that at low differential stresses, mode I (extensional) fractures develop parallel to σ_1. Lorenz et al. (1991) used the results of this laboratory experiment to explain regional extension fractures in front of an advancing mountain belt. According to this model, high pore pressures and low differential stresses created by far field compression of an advancing mountain belt create regional extension fractures perpendicular to the strike of the advancing mountain belt.
Figure 2A (stages 2-4) shows that with increasing differential stresses, shear fractures develop at an oblique orientation (usually between 30° and 60° relative to σ_1. This experimental observation is applicable in models of fracturing in folds, such as that of Stearns and Friedman (1969) (figure 2B). Most models for fracturing in folds are based on Stearns and Friedman's (1969) model, which is not only very generalized, but does not take into account fold geometry or kinematics. Since Stearns and Friedman (1969) published their model, different fold types have been recognized, necessitating further studies of fractures in various fold types. The major types of fault related folds are detachment folds (figure 3)(Jamison, 1987, Poblet and McClay, 1996, Homza and Wallace, 1997), fault propagation folds (figure 4)(Suppe and Medwedeff, 1990, Mitra, 1990), and fault-bend folds (figure 5)(Suppe, 1983). Very little detailed work has been done on fracture distributions within each type of fault related fold. Homza and Wallace (1997) showed that fractures and other strain indicators tend to be localized in the hinge regions of upright detachment folds in the Franklin Mountains, but little work has been published on fracture distributions in other types of folds. In general, it has been hypothesized that fixed hinge folding tends to localize fractures in the hinge regions (Homza and Wallace, 1997). Migrating hinge folding has been hypothesized to produce uniform fracture distributions throughout the hinges and limbs, since the limbs of a fold must pass through the hinges (Homza and Wallace, 1997). These distributions of fracture density in a fold can be strongly influenced by the kinematics of folding. Conversely, the distribution of fractures may yield clues to the kinematic history of fold formation.

Mechanical Stratigraphy and Fracture Development

The term “mechanical stratigraphy” or “mechanical layering” has been used to describe the way in which a given package of lithologically heterogeneous rocks responds to deformation (Erickson, 1996, Narr and Suppe, 1991.) A description of mechanical stratigraphy usually takes into account 1) the rheology of each lithologic unit and how rheology changes during deformation, 2) the relative thicknesses and nature of interfaces between rock layers, 3) boundary conditions on the stratigraphic section, and 4) the scale

of the deformed layers (Ramsay & Huber, 1987). Fracturing is one particular mechanical or rheological response of the stratigraphy to deformation. Understanding the mechanical stratigraphy of a package of rocks is important for studies of fracture density since laboratory experiments as well as field research have shown that there is a general relationship between fracture spacing, lithology, and bed thickness. In its simplest form, that relationship states that higher densities of fractures tend to be found in finer grained lithologies and/or in thinner beds (Hanks, et al, 1997, Narr and Suppe, 1991, Hancock and Engelder, 1989, Ladeira and Price, 1981). Therefore, in order to study the distribution of fracture density throughout a given fold, one must have an understanding of both the mechanical stratigraphy and the distribution of fracturing within that stratigraphy.

Geologic Setting

The Brooks Range is the northernmost part of the Rocky Mountain fold-and-thrust belt. The majority of shortening in the fold-and-thrust belt occurred in Late Jurassic to Early Cretaceous time when a wide, south-facing late Paleozoic to early Mesozoic passive continental margin collapsed in response to the collision of an intra-oceanic arc (Mayfield and others, 1988; Moore and others, 1994). The Colville basin formed in advance of, and was filled with sediment shed from, the growing fold-and-thrust belt (Mull, 1985; Bird and Molenaar, 1992). Shortly after the main phase of compressional collapse of the continental margin, rifting led to the eventual formation of the Canada basin to the north (present geographic coordinates) in Early Cretaceous time (Grantz and May, 1983; Moore and others, 1994). Post-collisional contraction in the Brooks Range increases eastward along strike and has resulted in progradation of fold-and-thrust deformation northward toward, and locally across, the Barrow arch and the Cretaceous rifted margin (figure 1, Grantz and others, 1990).

The stratigraphy of the northeastern Brooks Range consists of three major depositional sequences (figure 6). The Franklinian basement sequence is Proterozoic to middle-Devonian in age and consists of weakly metamorphosed sedimentary and volcanic rocks that were eroded prior to deposition of the Ellsmerian sequence. The Ellsmerian sequence is a Mississippian to Lower Cretaceous sequence of marine clastics, carbonates, and shales deposited on a south facing passive continental margin. The uppermost sequence in the northeastern Brooks Range is the Brookian sequence, a Cretaceous to Cenozoic sequence which consists of sediments derived from the early forming Brooks Range to the south (Wallace and Hanks, 1990). The structural style of the main axis of the Brooks Range is characterized by north vergent, thrust-truncated asymmetric folds, duplexes and allochthons that were shortened by hundreds of kilometers during the Middle Jurassic to Early Cretaceous (Wallace and Hanks, 1990). The northeastern Brooks Range, however, is characterized by a passive roof duplex that has been shortened by less than 100 kilometers (Wallace and Hanks, 1990).

This research focuses on folds within the Carboniferous Lisburne Carbonate Group of the Ellsmerian sequence in the Phillip Smith Mountains near an important structural transition between the Franklin Mountains and the Phillip Smith Mountains. The

structural style of the Franklin Mountains Domain is characteristic of the structural style of the northeastern Brooks Range, consisting of upright detachment folded Lisburne Limestone and younger rocks that developed above the roof of a passive roof duplex cored by sub-Mississippian basement horses (figures 7 & 8) (Wallace and Hanks, 1990). The Phillip Smith Mountains Domain lies directly south of the Franklin Mountains Domain and the continental divide thrust front. The Phillip Smith Mountains domain has a structural style more characteristic of the main axis of the Brooks Range, and consists of asymmetric, north vergent, thrust-truncated folds that have been interpreted as thrust-truncated detachment folds (Wallace, 1993).

Lisburne Group Stratigraphy

The stratigraphy of the Lisburne Group has been well studied both in the subsurface on the north slope of Alaska and in the front ranges of the northeastern Brooks Range (Watts, et al., 1995, Krumhardt, et al., 1996). An unconformity truncates the uppermost Lisburne Group, which is overlain by the Sadlerochit Group, a clastic unit of variable composition ranging from quartz sandstone to shales and siltstones (figure 9). Previous studies have grouped the Lisburne into two separate units: the Wahoo Limestone, which is a cliff forming unit consisting primarily of grainstones and packstones, and the Alapah Limestone, which is generally more recessive and consists of a variety of carbonate lithologies. The lower contact of the Lisburne Group with the Kayak shale is often gradational and sometimes contains a discontinuous layer of sandy limestone (figure 9).

Methodology

This project was broken down into five major tasks:

1) Construct a 1:25,000 scale map of the chosen field area in order to document the fold geometries and sequence of deformation that may have affected fracture development. This includes detailed photographic documentation and sketches of fold geometries in order to produce balanced cross-sections of the field area, as well as to locate fracture sample locations relative to hinges and limbs of each fold.
2) Characterization of fracture patterns within a relatively undeformed section of Lisburne Group carbonates in order to understand the “background” fracture patterns and the relationship between fracturing, lithology and bed thickness. Since the chosen field area contained asymmetric folds with long, flat backlimbs, these backlimbs could be used to examine a relatively undeformed section of Lisburne.
3) Characterization of the fractures in a variety of folds with various interlimb angles in order to understand the relationship between fracturing and folding. Due to exposure limitations in the field area, a single stratigraphic horizon was sampled in detail throughout a fold. This method normalizes the effects of bed thickness and lithology on fracturing, and is aimed at understanding the relationship between fracturing and folding for a single bed.
4) Qualitatively define the mechanical stratigraphy of the Lisburne Group carbonates in the area.

5) Characterization of fracturing within the entire mechanical stratigraphic section in order to compare fracture patterns in folded and relatively unfolded Lisburne group carbonates. Synclines tended to be better exposed in the area, and were therefore preferentially sampled.

Measurement and description of fractures followed three major strategies: detailed fracture sampling, generalized characterization of fracturing, and surveys of fractures within the stratigraphic section. Each of these methods is described below.

1) Detailed fracture sampling. This method of sampling was employed both along a single stratigraphic horizon (as described in #3 above) and for selected representative lithologies in the mechanical sections (as described in #4 above). The following information was collected about the outcrop itself:
    a. location (on map, within the stratigraphy, and on a photograph of each fold)
    b. type of outcrop (pavement or cross-section)
    c. collection of oriented samples of representative lithologies for thin section identification of lithology and/or strain analysis
    d. photograph/sketch of relevant aspects of the outcrop
    e. lithology
    f. bed thickness
    g. nature of contacts between layers
    h. major diagenetic features (presence/shape of cherts, dolomitization, etc.)
    i. orientation/characteristics of strain indicators

    After the characteristics of the outcrop were examined, characteristics of each fracture set were recorded. A measuring tape was placed along each fracture set and the orientation of the measuring tape was recorded in order to determine the true spacing of each fracture. Where it was possible, the measuring tape was placed orthogonal to the fracture set to record the true spacing directly. The following information was recorded at each fracture:
    a. orientation of fractures
    b. spacing between fractures
    c. aperture (size of the opening of the fracture)
    d. fill (any mineral fillings of the aperture such as calcite)
    e. height perpendicular to bedding
    f. width parallel to bedding
    g. terminations (how the fracture interacts with bed surfaces or other fractures)
    h. mode (type of fracture: extensional or shear) where observable

    Where possible, 25 fractures in each set were measured in order to obtain statistically significant sample at outcrop. In addition, any en echelon sets were noted along with their direction of shear. Conjugate sets were noted when observed. Other features that were often recorded were timing relationships

between fractures, slickenlines and slickensides, dissolution cleavages, strained fossils, folded veins, and sheared stylolites.

2) Generalized fracture sampling. This method was very similar to the detailed method of sampling in that all of the aspects of the outcrop were recorded, but the detailed characteristics of each fracture set (spacing, aperture, fill, etc.) were not measured. Instead, the orientations of the major fracture sets were recorded, as well as any additional features such as slickenlines and slickensides, dissolution cleavages, strained fossils, etc. were recorded.

3) Surveys of fracture characteristics in the stratigraphic section in order to determine the mechanical behavior of the stratigraphic section. This method was often employed where UAF Department of Geology stratigraphers (Mike Whalen, Michelle McGee, and Andy Krumhardt) had measured stratigraphic section. Lithology and other stratigraphic information were sampled (by the UAF stratigraphers or myself and field assistant) at a given interval (usually 1 meter.) In order to understand how fracture density changed throughout the section, the orientations of major fracture sets were measured, in addition to a rough estimate of their spacing. This estimate was obtained by counting the number of fractures in a 0.5 meter interval. These data were generally collected every meter or every 0.5 meter within the stratigraphic section. Approximate bed thicknesses and presence/absence of diagenetic features or strain indicators were also noted.

Preliminary Observations

Mechanical Stratigraphy of the Lisburne Group:

The general stratigraphy of the Lisburne is somewhat different from that previously studied in the Franklin Mountains and front ranges of the northeastern Brooks Range. Since work on the stratigraphic section is still in progress and the temporal boundaries within the stratigraphy are still being explored, the more traditional divisions of "Wahoo" and "Alapah" limestone will not be used. The generalized lithostratigraphy can be divided into mechanical packages as shown in figure 10. The mechanical behavior of each unit is shown in figure 11.

A. Upper Lisburne

This unit is approximately 500 meters thick (McGee, this volume) consisting primarily of massively bedded, light gray colored grainstones and packstones. The upper Lisburne tends to be the most structurally competent unit in the section, and defines the map scale fold geometry in the area.

B. Lower Lisburne

The overall thickness of the lower Lisburne is approximately 400-500 meters. This unit can be divided into three major mechanical packages as follows.

1. Lower Lisburne, upper portion

This unit is composed primarily of recessively weathering, relatively thinly bedded, dark colored floatstones and shales that tend to behave slightly less competently than the upper Lisburne. Little bed parallel shear was observed within this unit in the northwestern end of the field area, but minor parasitic

folding and/or bed parallel shear within this unit was observed in folds in the southwestern end of the field area (E and W fork box folds).

2. Lower Lisburne, middle portion

Composed primarily of massively bedded floatstone units that behave mechanically like the upper Lisburne. Bed parallel slip and duplexing were documented within this unit in the flat panel in the northwest end of the field area.

3. Lower Lisburne, lower portion

A dark colored, recessive unit that appears similar in outcrop to the upper portion of the lower Lisburne. This unit is also less competent than the Upper Lisburne or the middle portion of the Lower Lisburne. Bed parallel shear along bed contacts, duplexing, parasitic folding, and well developed dissolution cleavage were observed in the flat panel in the northwest end of the field area near the thrust. The contact between the lower portion of the lower Lisburne and the Kayak shale below appears to be gradational.

Map Scale and Mesoscopic Scale Structures:

The general structure of West Porcupine Lake Valley is characterized by strongly asymmetric, NE striking, NE plunging folds that involve Sadlerochit siltstones, Lisburne Group carbonates, and probably Kayak Shale. These are map scale (300-1000 m high in outcrop) folds with interlimb angles between approximately 130° and 30°. Some of the folds in the southeast side of the field area are overturned (figures 12 & 13). One major fold in the field area (East Fork Box Fold on figures 12 & 13) deviates from the geometry of the majority of other folds in the field area. This particular fold lies in the southeastern end of the field area and, while still asymmetrical, is characterized by a box fold geometry. The geometry of this fold changes dramatically along strike, both in the general fold shape, and in the location of normal faults in the fold. Detailed geometric analysis of this fold may reveal important information about timing relationships that can be compared to fracture timing relationships in order to understand the tectonic history of the area.

In the northwest end of the field area, a major thrust fault places Lisburne Group carbonates on top of siltstones, shales and sandstones of the Sadlerochit Group. This is the only major thrust fault that was found in the field area.

Mesoscopic scale structures in the field area suggest a predominance of "top-to-northwest" oriented layer parallel shear in West Porcupine Lake Valley, especially in the northwestern end of the field area in the relatively flat panel of Lisburne carbonates near the thrust. Numerous en echelon fractures and veins, shear planes along bed surfaces, as well as bed scale duplex structures indicate that top to north oriented layer parallel shear occurred during the structural history of the area. These north vergent structures were found throughout the field area, in both the flat backlimbs of folds and more tightly folded rocks to the southeast.

Three major sets of normal faults were documented in the area: Set 1) a NE striking, predominantly SE dipping set; Set 2) a NW striking, SW dipping set; and Set 3) an E striking; S dipping fault (figures 12 & 13). Normal faults of Set 1 were sub-parallel to

the regional strike, and appeared to be concentrated both in the relatively gently folded flat panel in the northwestern end of the field area and near the hinges of some of the major anticlines in the area. Set 2 was sub-perpendicular to the regional strike and was best exposed in the southeast end of the field area, although many of these faults likely continue to the northwest. Changes in fold geometry were documented across this set of normal faults. Set 3 is actually only composed of one normal fault, but is included as a major "set" because of its anomalous orientation, large displacement and lateral extent. This fault is oriented obliquely to the regional strike and has arguably the largest displacement of any of the faults in the area, with a down-to-the-south sense of displacement.

Structure: Fracturing:

A. General Character

Four major sets of extension fractures were documented in West Porcupine Lake valley, the majority of which dip steeply between 60º-90º in both directions: 1) a N-S striking set; 2) an E-W striking set; 3) a N-S to NW striking set; and 4) a NE striking set. While the relative timing of each of these fracture sets is unclear, some generalities can be made. The NW set appears to be younger than the N-S and E-W sets. E-W fractures terminate against N-S fractures at most sample locations. However, the opposite relationship was documented elsewhere in the field area, possibly suggesting multiple generations of N-S and E-W fracturing. All three fracture sets were found in en echelon sets of extension fractures, which indicate a component of shear during formation. Shear sense on these sets was commonly normal or strike slip, suggesting that many fractures are related to normal faulting in the area. The N-S and NW striking fractures were often found in 3-5 meter wide swarms of en echelon fractures, each swarm spaced approximately 10-20 meters apart. NE striking fractures were well developed in the lower portions of one of the major synclines in the area (Camp Syncline, figures 12&13), although the timing of these fractures is unclear. Other major mesoscopic-scale structures indicate some period of penetrative semi-ductile deformation, including dissolution cleavage, deformed crinoid stems, sheared stylolites, and elongated and transposed chert nodules.

B. Distribution within the stratigraphy

General surveys of fracture distribution in a relatively complete stratigraphic section were conducted in three areas; A) in the upper Lisburne and part of the lower Lisburne in a long, relatively flat backlimb in the northwestern end of the field area (see figures 12, 13), B) in the upper Lisburne in the backlimb of "Camp Syncline" (figure 14), C) and in the upper Lisburne in the backlimb of "Open Syncline" (figures 12,13,15). Detailed sampling of representative lithologies in each stratigraphic section was also conducted. In general, finer grained lithologies such as dark colored wackestones tended to have higher fracture densities than light gray colored packstones and grainstones. Higher fracture densities seemed to be found in thinner beds, although further analysis of fracturing within the stratigraphic sections may help quantify this relationship. The lower Lisburne seemed to have higher fracture densities than the upper Lisburne, although many wackestones in the upper Lisburne were highly fractured.

C. Distribution of fracturing within folds

The upper Lisburne of three major folds was sampled in detail at: 1) "Camp Syncline", where two stratigraphic horizons were sampled (figures 12,13,14), 2) "Open Anticline", and 3) "Open Syncline" (figures 12,13,15). The lower Lisburne was not exposed in any of these folds and was therefore not sampled. Within Camp Syncline, the "Upper Camp Syncline" sample locations (UCS1-1 through UCS-7 on figure 14) tended to have higher fracture densities than the "Lower Camp Syncline" (F3-F12 on figure 14). No obvious change in fracture density was observed between limbs and hinges, although further analysis may elucidate more subtle trends in fracture distribution.

Preliminary Interpretations

Structure: mechanism of folding:

Since the mechanism by which the folds in West Porcupine Lake Valley formed has important implications for fracture distribution and character within the folds, it is important to understand their kinematic history. No definitive evidence was found as to whether the West Porcupine Lake Valley folds are detachment folds or fault propagation folds, but current research (Jadamec, this volume) may help to answer this question. Future construction of balanced cross sections of the field area may also provide constraints on the kinematic history of these folds.

Influence of mechanical stratigraphy on folds in the area:

Preliminary observations indicate that the mechanical stratigraphy of the Lisburne in West Porcupine Lake Valley is different from the Lisburne in the front ranges. In the Franklin Mountains and front ranges, the lower Lisburne (Alapah) tends to behave as a relatively weak unit, often containing numerous parasitic folds that thicken the unit, commonly in the cores of detachment folds. In West Porcupine Lake Valley, very few parasitic folds were seen in the lower Lisburne. This suggests that either a change in the mechanical stratigraphy prevented this type of thickening, or another factor (such as an increased tectonic overburden?) prevented parasitic folding from occurring. Although the relationship is unclear, the absence of thickening in the Alapah may favor asymmetric detachment folding.

Alternatively, the mechanical stratigraphy described above may have favored the propagation of a fault ramp, leading to fault propagation folding. In the study area the middle portion of the lower Lisburne was observed to be more competent than the upper or lower portions of the lower Lisburne. This mechanically rigid layer buttressing the lower Lisburne might favor the propagation of a ramp, leading to fault propagation folding. Fault propagation folding would also explain the fold asymmetry in the area since the leading models on fault propagation folding (Suppe and Medwedeff, 1990, Mitra, 1990) require asymmetric folds due to the geometry of the ramp. Further detailed geometric analysis and cross section balancing may aid in understanding the effect of the change in mechanical stratigraphy on fold kinematics.

Normal Faulting:

Preliminary results suggest that at least one stage of normal faulting post-dated, or was possibly concurrent with folding and/or thrusting. This is suggested by a cross cutting relationship between the major thrust fault and one of the NE striking, SE dipping normal faults in the northwestern end of the field area. Another possible line of evidence for folding concurrent with normal faulting lies in one fold in the southeast side of the field area ("East Fork Box Fold"). This fold has two different hinges separated by a normal fault. The geometry of this particular fold may suggest concurrent folding and normal faulting. Future analysis will address this question.

While the timing of each set of normal faults relative to the other is somewhat unclear at this point, many of the NW oriented normal faults (of set 2) appear to be the sites of major changes in fold geometry along strike. This suggests that these faults may have originated as accommodation structures that formed concurrent with folding and/or thrusting, and were activated as normal faults during or after folding had occurred.

The numerous normal faults found in the Porcupine Lake structural low are atypical for the Brooks Range and may be related to the origin of the structural low. Several hypotheses were developed over the course of the summer to explain the presence of both the Porcupine Lake structural low itself and the normal faults associated with it. These included some combination of the following: 1) extension above the trailing edge of the basement thrust sheets that form the major structures of the northeastern Brooks Range; 2) extension of the Mississippian and younger rocks over the buried edge of a rifted Devonian continental margin; 3) normal faulting in the west associated with inversion of an isolated Devonian basin in the east; and 4) segmentation of the thrust front by transverse normal faults due to a combination of a complex basement topography and lateral variations in the amount and distribution of shortening.

Fracturing:

Preliminary observations of fracturing in the field area suggest a complicated history of fracturing related to pre-folding processes, folding processes and normal faulting. Numerous fractures were documented that strike both sub-parallel (NE striking) and sub-perpendicular (NW striking) to regional trends, which are sub-parallel and perpendicular to the orientations of normal faults in the area. Models and field observations for fracturing in advance of a developing fold and thrust belt, (Hanks, et al, 1997, Lorenz, et al, 1997, Lorenz et al, 1991, Hancock and Engelder, 1989), as well as models for fractures related to folding (Stearns, 1968, Stearns and Friedman, 1969) commonly have two major fracture orientations that strike parallel and perpendicular to regional trends. The N-S, and E-W striking trends seem to fit the model for fracturing in advance of a developing fold and thrust belt. Since many of these fractures exhibit a sense of shear, very often with a strike slip component, they don't fit particularly well with the models described above. In addition, many N-S striking fractures were found in en echelon sets with a given sense of shear, which can be compared to senses of shear on normal faults in the area. This is one method of distinguishing which sets of fractures are related to normal faulting vs. folding. However, since normal faulting in the area may have produced an "overprint" of fractures in the field area, any analysis of the distribution of fracturing in folds will be ambiguous. Since fractures with similar orientation may be

produced by multiple mechanisms through time, further statistical and three-dimensional analysis will be conducted to attempt to distinguish each generation of fracturing.

Future research:

Future research will include the following:

1) Completion of data compilation.
2) Production of mechanical stratigraphic sections with integrated fracture data.
3) Construction of balanced, restored cross-sections. Balanced and restored cross sections will help constrain the relevant structural history in the area, as well as accurately place fracture sample locations.
4) Statistical and three-dimensional analysis of fracture data. The relationship between fracture density, folding, bed thickness, and lithology is important when developing a predictive model for fracture density within a folded stratigraphic section. Statistical analysis will focus on fracture spacing as a measure of fracture density and the distribution of fracture density throughout a given fold. This analysis will enable comparison of relatively unfolded sample locations to open folds and tight folds in order to understanding the kinematic history of fracturing and folding. In addition, statistical analysis and restoration techniques may aid in distinguishing between fractures related to folding and normal faulting.
4) Integration of fracture data into a three-dimensional fold model. Since folds and fractures are three-dimensional structures, the third dimension is critical to understanding the relationship between fracturing and folding, highlighting areas of higher fracture density, and understanding the kinematic history of folding and fracturing.

References

Bird, K.J., and Mollenaar, C.M., 1992, The North Slope foreland basin, *in* Macqueen, R.W., and Leckie, D.A., eds., Foreland basins and foldbelts: American Association of Petroleum Geologists Memoir 55, p. 363-393.

Chester, J.S., Logan, J.M, Spang, J.H., 1991, Influence of layering and boundary conditions on fault-bend and fault-propagation folding: Geological Society of America Bulletin, v. 103, p. 1059-1072.

Erickson, S.G., 1996, Influence of mechanical stratigraphy on folding vs. faulting: Journal of Structural Geology, v. 18, no. 4, p. 443-450.

Fischer, M.W., and Coward, M.P., 1982, Strains and folds within thrust sheets: an analysis of the Heliam sheet, Northwest Scotland: Tectonophysics v. 88, p. 291-312.

Grantz, A., and May, S.D., 1983, Rifting history and structural development of the continental margin of north Alaska, in Watkins, J.S., and Drake, C.L., eds., Studies in continental margin geology: AAPG Memoir 34, p. 77-100.

Grantz, A., May, S.D., and Hart, P.E., 1990, Geology of the Arctic continental margin of Alaska, in Grantz, A., Johnson, L., and Sweeney, J.F., eds., The Arctic Ocean region: Boulder Colorado, GSA, The Geology of North America, v.L,. p. 257-288.

Hancock, P.L., and Engelder, T., 1989, Neotectonic Joints: Geological Society of America Bulletin, v. 101, p. 1197-1028.

Hanks, C.L., Lorenz, J.C., Teufel, L.W., and Krumhardt, A.P., 1997, Lithologic and Structural Controls on Natural Fracture Distribution and Behavior within the Lisburne Group, Northeastern Brooks Range and North Slope Subsurface, Alaska: American Association of Petroleum Geologists Bulletin, v. 81, no. 10, p. 1700-1720.

Hennings, Peter H., Olson, Jon E., and Thompson, Laird B., 2000, Combining Outcrop Data and Three-Dimensional Structural Models to Characterize Fractured Reserviors: An Example from Wyoming. AAPG Bulletin v. 84, no. 6, p. 830-849.

Homza, T.X., and Wallace, W.K., 1997, Detachment folds with fixed hinges and variable detachment depth, northeastern Brooks Range, Alaska: Journal of Structural Geology, v. 19, nos. 3-4, p. 337-354.

Jamison, W.R., 1987, Geometric analysis of fold development in overthrust terranes: Journal of Structural Geology, v. 9, p. 207-219.

Krumhardt, A.P., Harris, A.H., and Watts, K.F., 1996, Lithostratigraphy, Microlithofacies, and Condodont Biostratigraphy and Biofacies of the Wahoo Limestone (Carboniferous), Eastern Sadlerochit Mountains, Northeast Brooks Range, Alaska: U.S. Geological Survey Professional Paper 1568, 70 p.

Ladeira, F.L., and Price, N.J., 1981, Relationship between fracture spacing and bed thickness: Journal of Structural Geology, v. 3, p.179-183.

Lorenz, J.C., Farrell, H.E., Hanks, C.L., Rizer, W.C., and Sonnenfield, M.D., 1997, The Characteristics of Natural Fractures in Carbonate Strata: *in* Palaz, I., and Markfurt, K, eds., Carbonate Seismology: Society of Exploration Geophysics Publication, p. 179-201.

Lorenz, J.C., Teufel, L.W., and Warpinski, N.R., 1991, Regional Fractures I: A Mechanism for the Formation of Regional Fractures at Depth on Flatlying Reservoirs: American Association of Petroleum Geologists Bulletin, v. 75, no. 11, p. 1714-1737.

Mayfield, C.F., Tailleur, I.L., and Ellersieck, I., 1988, Stratigraphy, structure, and palinspatic synthesis of the western Brooks Range, northwest Alaska: *in* Gryc, G. ed., Geology and Exploration of the National Petroleum Reserve in Alaska, 1974 to 1982: U.S. Geological Survey Professional Paper 1399, p.143-186.

McClay, Ken, 1987, The mapping of geological structures, Geological Society of London handbook series, Open Univ. Press, Milton Keynes, United Kingdom, Halsted Press, New York, NY, United States, 161 p.

Moore, T.E., Wallace, W.K., Bird, K.J., Karl, S.M., Mull, C.G., and Dillon, J.T., 1994, Geology of northern Alaska, *in* Tailleur, I.L., and Weimer, P., eds., Alaskan North Slope geology: Pacific Section, SEPM and Alaska Geological Society, Book 50, p. 513-528.

Mull, C.G., 1985, Cretaceous tectonics, depositional cycles, and the Nanushuk Group, Brooks Range and Arctic Slope, Alaska, *in* Huffman, A.C., Jr., ed., Geology of the Nanushuk Group and related rocks, North Slope, Alaska: U.S. Geological Survey Bulletin 1614, p. 7-36.

Narr, W., and Suppe, J., 1991, Joint spacing in sedimentary rocks: Journal of Structural Geology, v. 13, no. 9, p. 1037-1048.

Mitra, S., 1990, Fault propagation folds: geometry, kinematic evolution, and hydrocarbon traps: American Association of Petroleum Geologists Bulletin, v. 74, p. 921-945.

Poblet, J., and McClay, K., 1996, Geometry and kinematics of single-layer detachment folds: American Association of Petroleum Geologists Bulletin, v. 80, p. 1085-1109.

Ramsay, J.G., and Huber, M.I., 1987, Techniques of Modern Structural Geology, Volume 2: Folds and Fractures, Session 20: Fold Mechanics 2: Multilayers, p. 405-444, Academic Press Inc, San Diego CA.

Stearns, D.W., 1968, Certain aspects of fracture in naturally deformed rocks *in* Riecker, R.E., ed., NSF Advanced Science Seminar in Rock Mechanics: Bedford, Massachusetts, Air Force Cambridge Research Lab. Special Report, p. 97-118.

Stearns, D.W., and Friedman, M., 1969, Reservoirs in Fractured Rock *in* Stratigraphic oil and gas fields: Classification, exploration methods, and case histories: American Association of Petroleum Geologists Memoir 16, p. 82-106.

Suppe, J., 1983, Geometry and kinematics of fault-bend folding: American Journal of Science, v. 283, p. 684-721.

Suppe, J., and Medwedeff, D.A., 1990, Geometry and kinematics of fault-propagation folding: Ecolgae Geologicae Helvetiae, v. 83, p. 409-454.

Wallace, W.K., 1993, Detachment fold and a passive roof duplex: Examples from the northeastern Brooks Range, Alaska *in* Solie, D.N., and Tannian, F., eds., Short Notes on Alaskan Geology 1993: Alaska Division of Geological and Geophysical Surveys Geologic Report 113, p. 81-99.

Wallace, W.K., and Hanks, C.L., 1990, Structural Provinces of the northeastern Brooks Range, Arctic National Wildlife Refuge, Alaska: American Association of Petroleum Geologists Bulletin, v. 74, no. 7, p. 1100-1118.

Watts, K.F., Harris, A.G., Carlson, R.C., Eckstein, M.K., Gruslovic, P.D., Imm, T.A., Krumhardt, A.P., Lasota, D.K., Morgan, S.K., Dumoulin, J.A., Enos, P., Goldstein, R.H., and Mamet, B.L., 1995, Analysis of reservoir heterogeneities due to shallowing upward cycles in carbonate rocks of the Pennsylvanian Wahoo Limestone of northeastern Alaska: United States Department of Energy, Final Report for 1989-1992 (DOE/BC/14471-19), Bartlesville Project Office, 433 p.

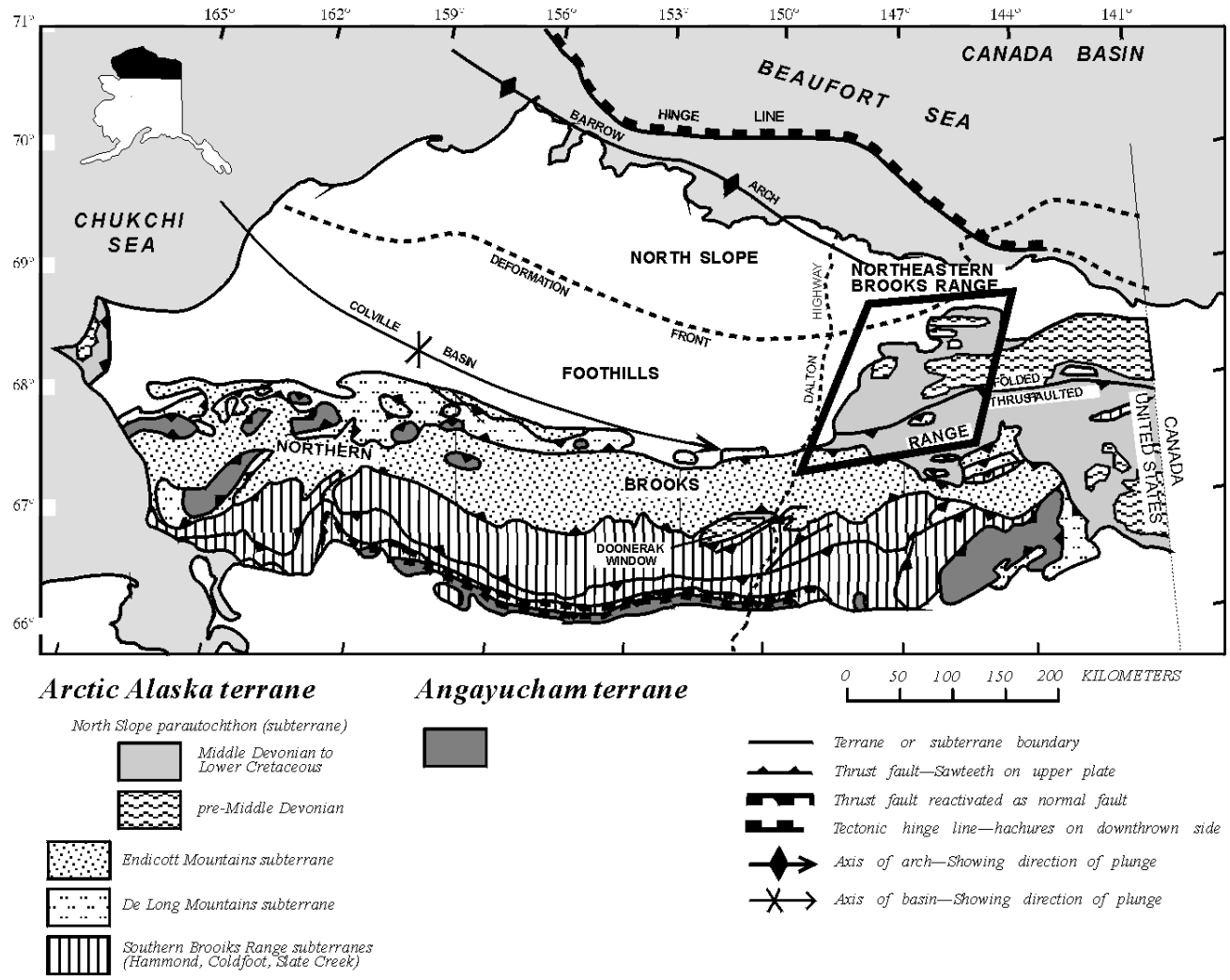

Figure 1: Regional Structure and tectonic map of the Brooks Range and North Slope of Alaska. Outline area is illustrated in more detail in figure 7. (modified from Wallace and others, 1997).

A

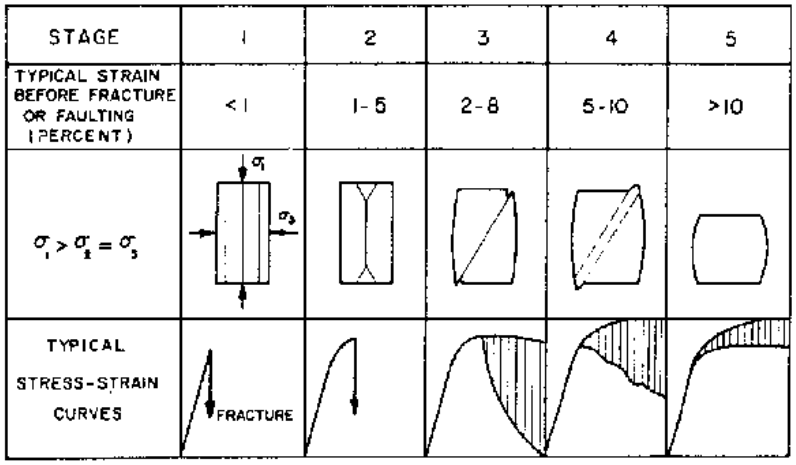

B

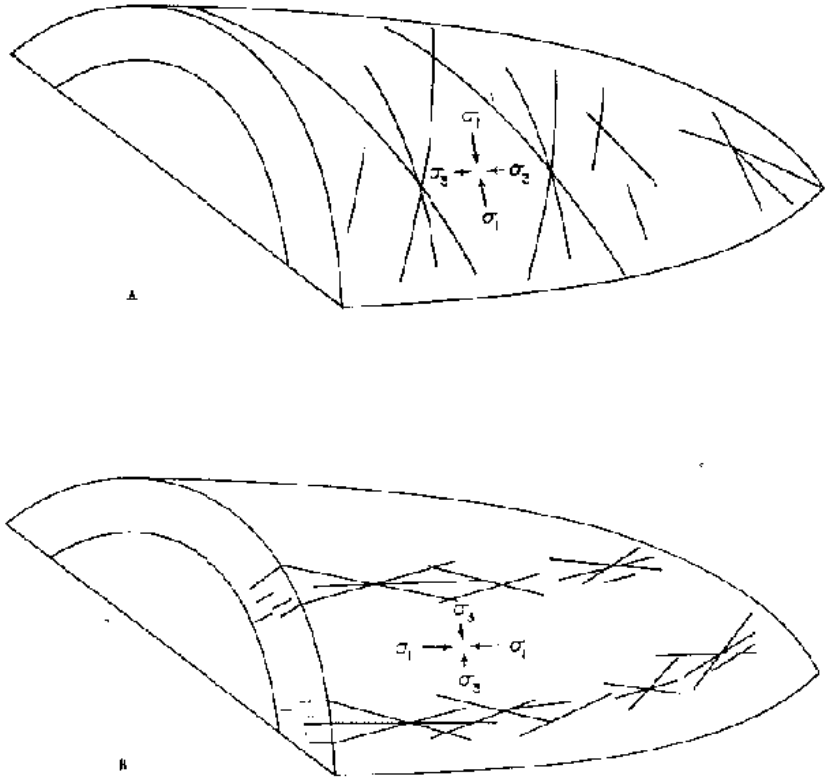

Figure 2: Part A: Diagram showing fracture orientation with increasing strain (from: Griggs and Handin, 1960), Part B: Stearns and Friedman's (1969) model for fractures related to folds. Note the different orientations of fractures with respect to σ_1, σ_2, and σ_3.

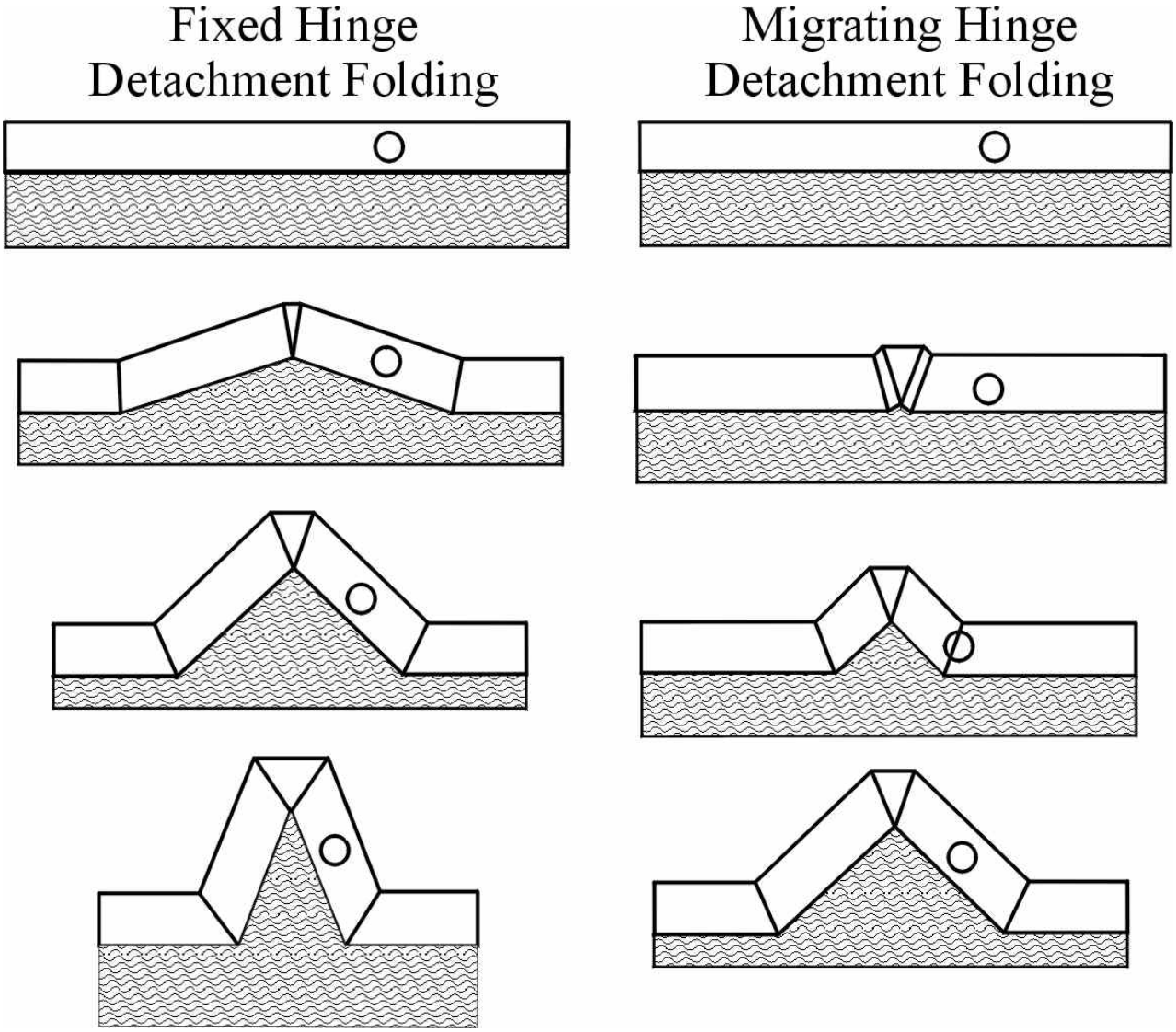

Figure 3: Simplified models for detachment folds. Detachment unit is stippled. Fixed hinge folding requires that the limbs rotate with respect to relatively fixed hinges. Migrating hinge folding requires that the hinges migrate through the upper unit (circle shows a single point in the competent unit). Note that the detachment volume must migrate to fill the core of the fold in both cases. (Modified from: Homza and Wallace, 1995)

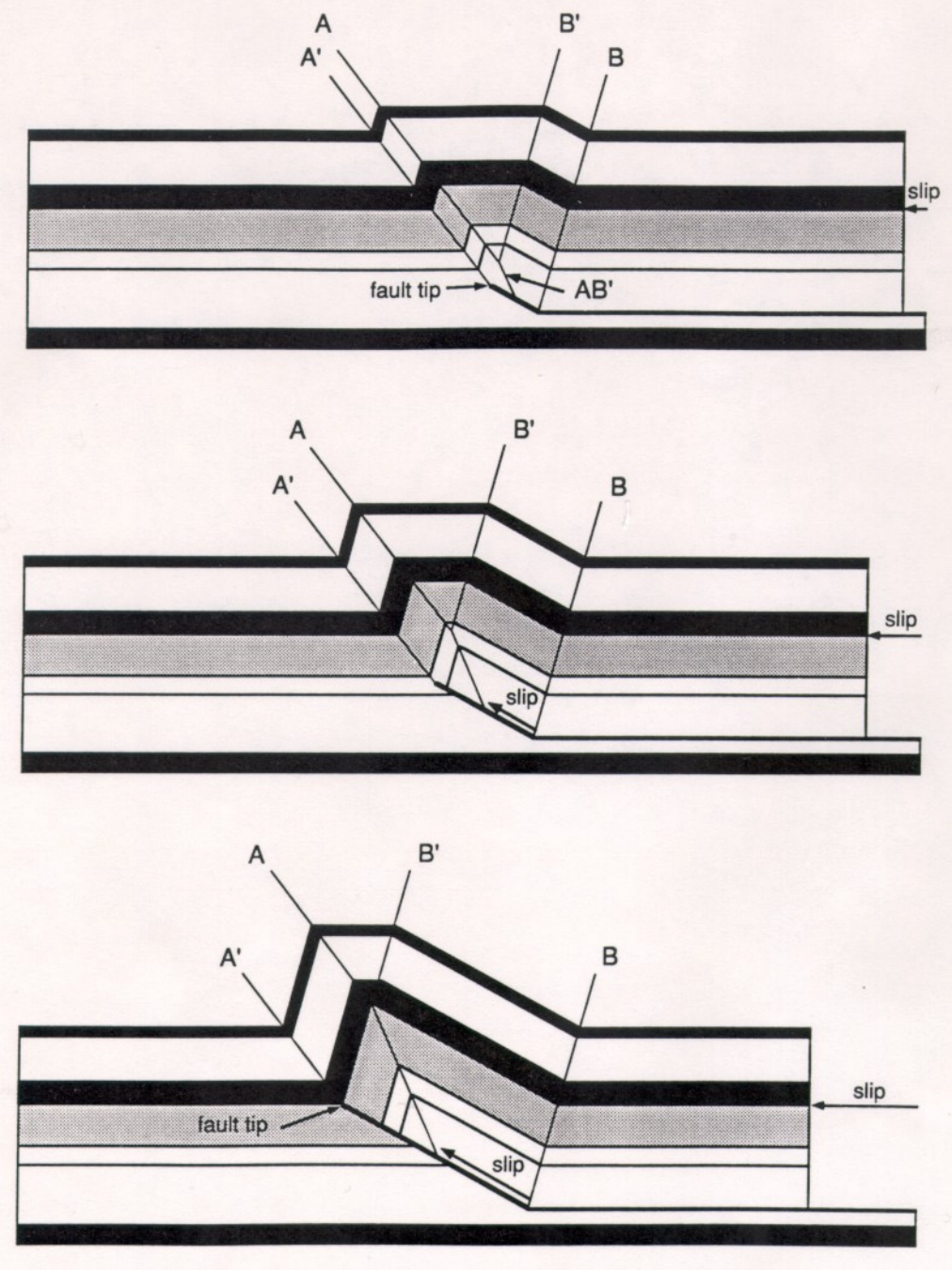

Figure 4: Suppe and Medwedeff's (1990) model for fault propagation folding.

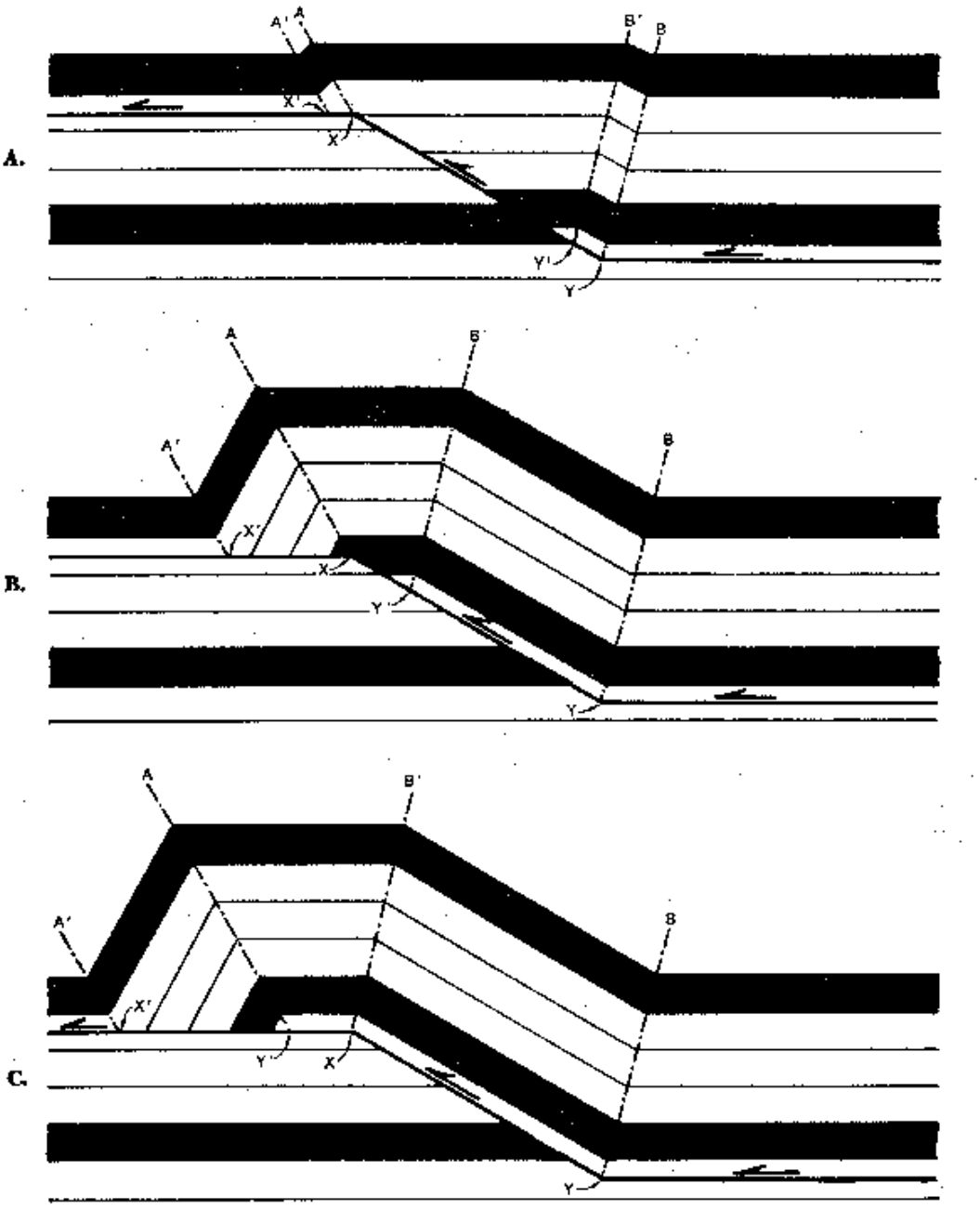

Figure 5: Model for fault bend folding (from Suppe, 1983).

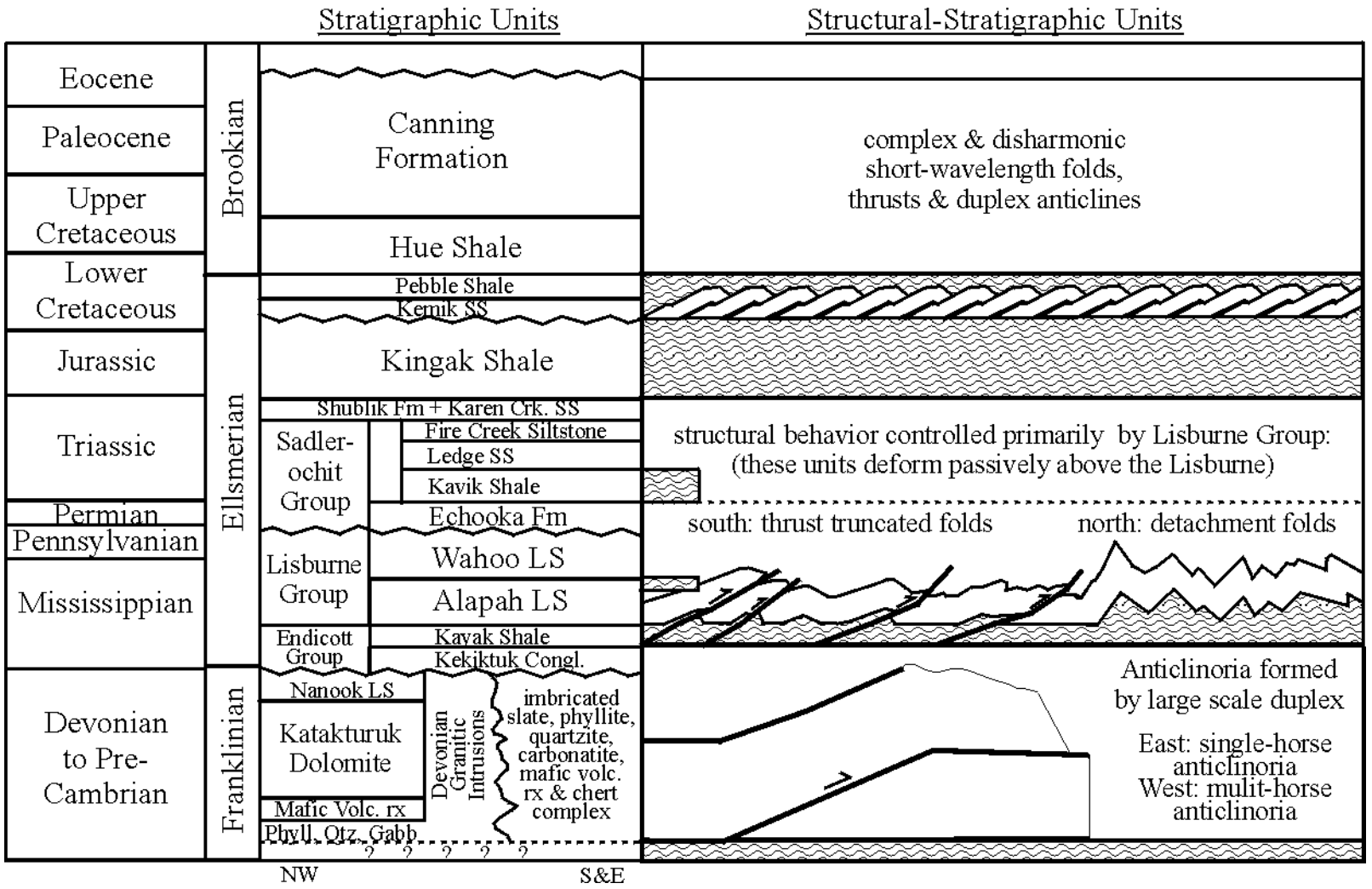

Figure 6: Lithostratigraphy and mechanical stratigraphy of the northeastern Brooks Range. Detachment units are stippled (modified from Wallace and Hanks 1990, and Wallace, 1993)

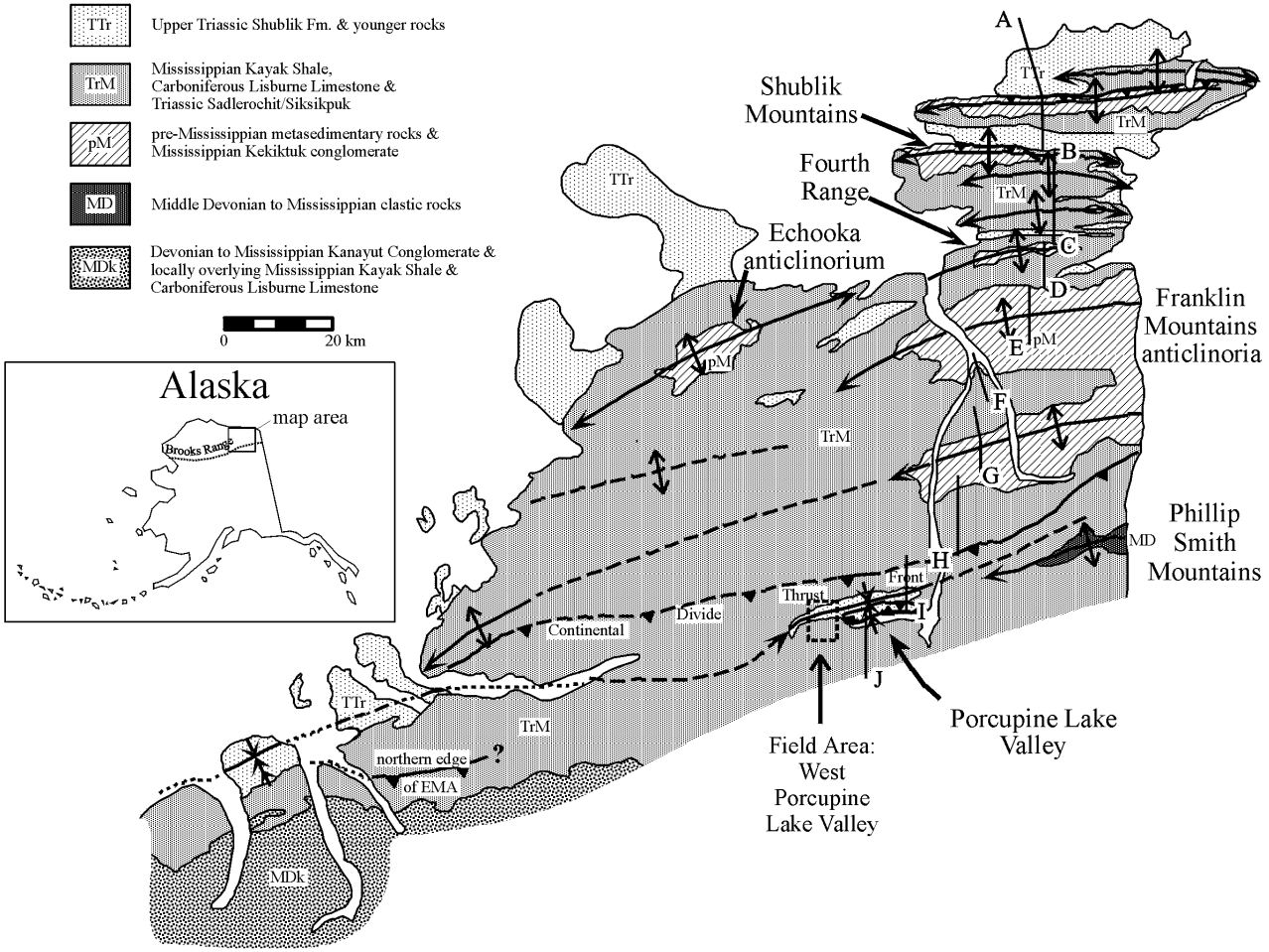

Figure 7: The geologic map of the western portion of the northeastern Brooks Range. Section lines F through J correspond with the cross section in figure 8.

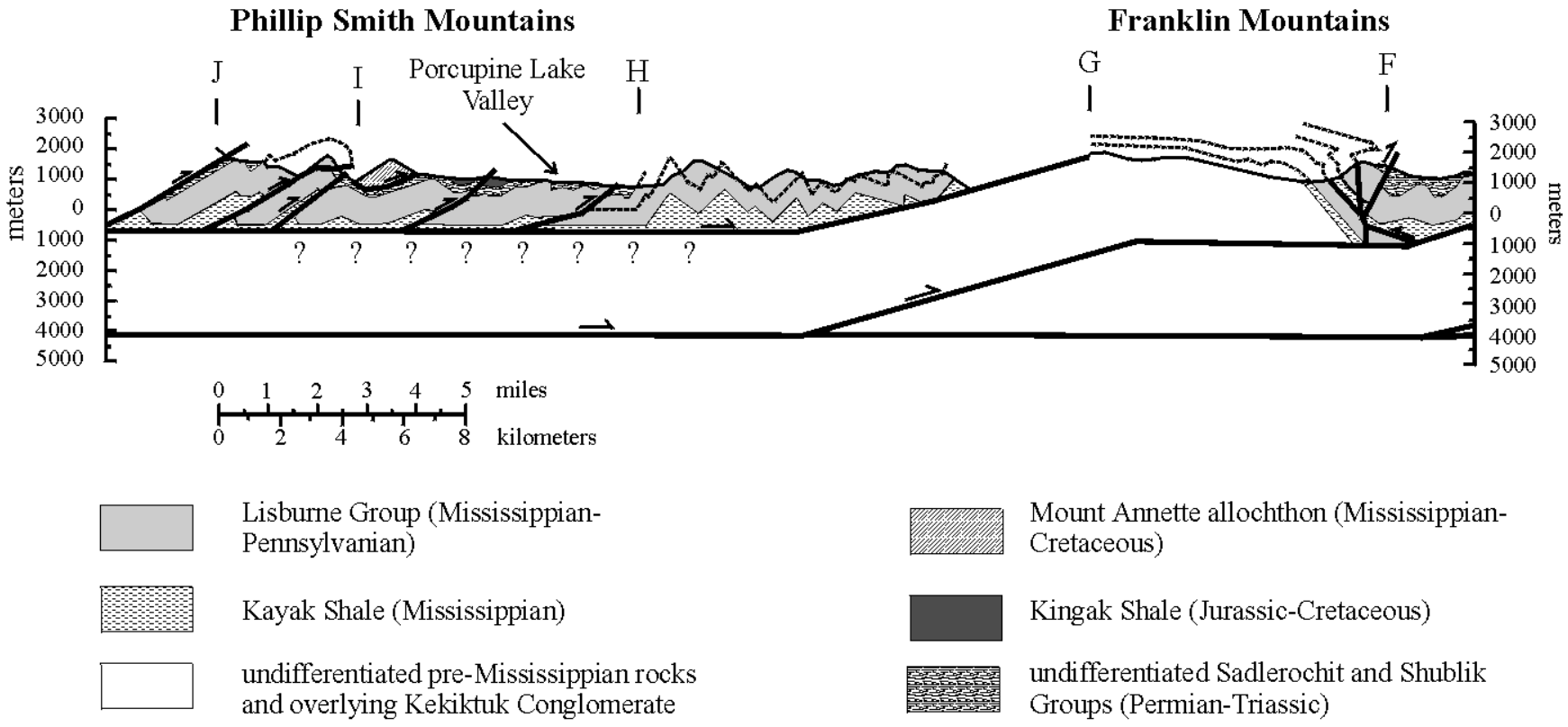

Figure 8: Cross section through the northeastern Brooks Range. See figure 7 for section line locations (letters F-J on cross section correspond to letters on figure 7). Note the difference in structural behavior of the Lisburne group between the Porcupine Lake area and the southernmost Franklin Mountains (north of the "H" section boundary). Modified from: Wallace, 1993.

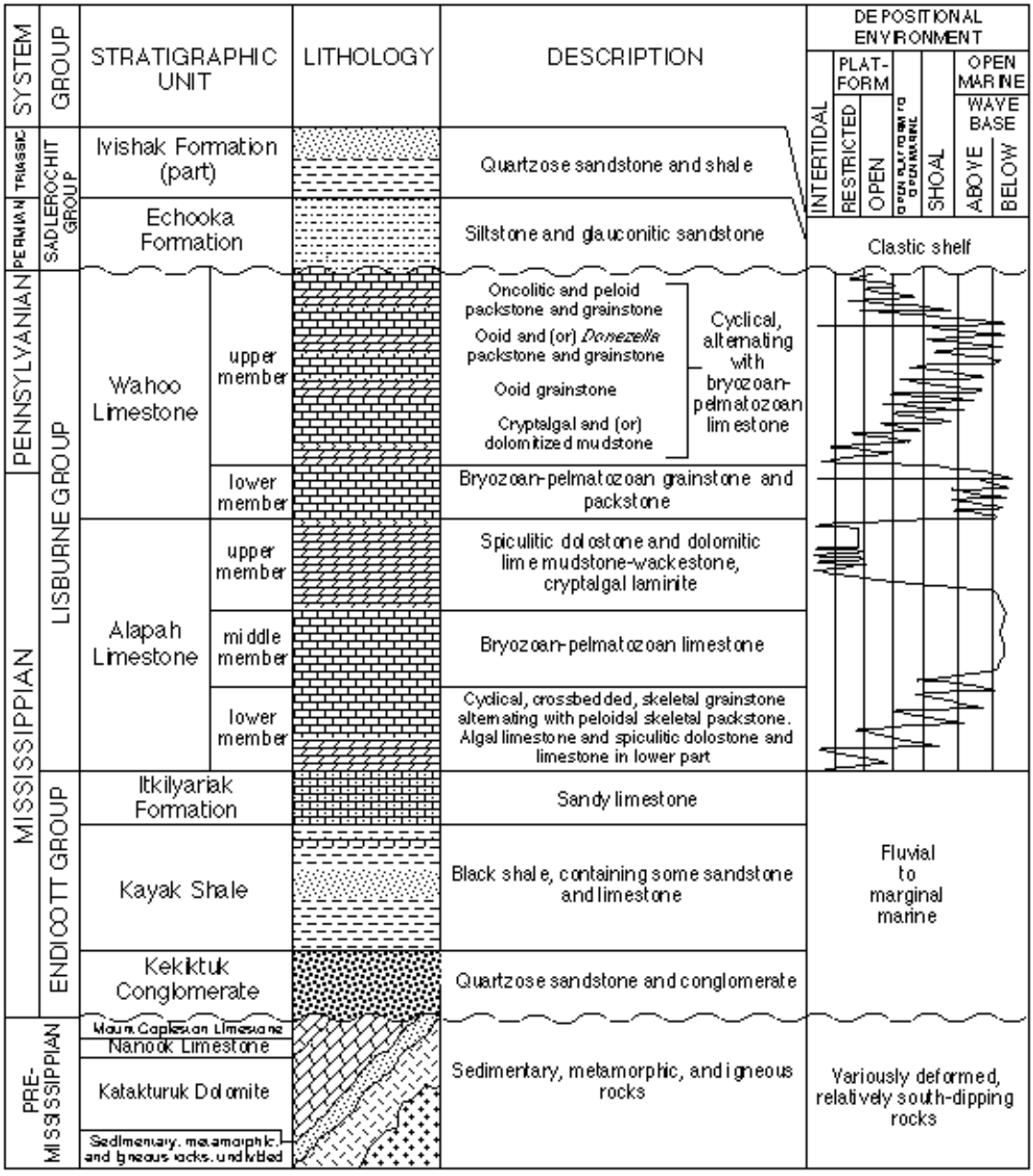

Figure 9: Generalized lithostratigraphy of the Endicott, Lisburne, and Sadlerochit groups in the northeastern Brooks Range.
(From: Krumhardt et al., 1996)

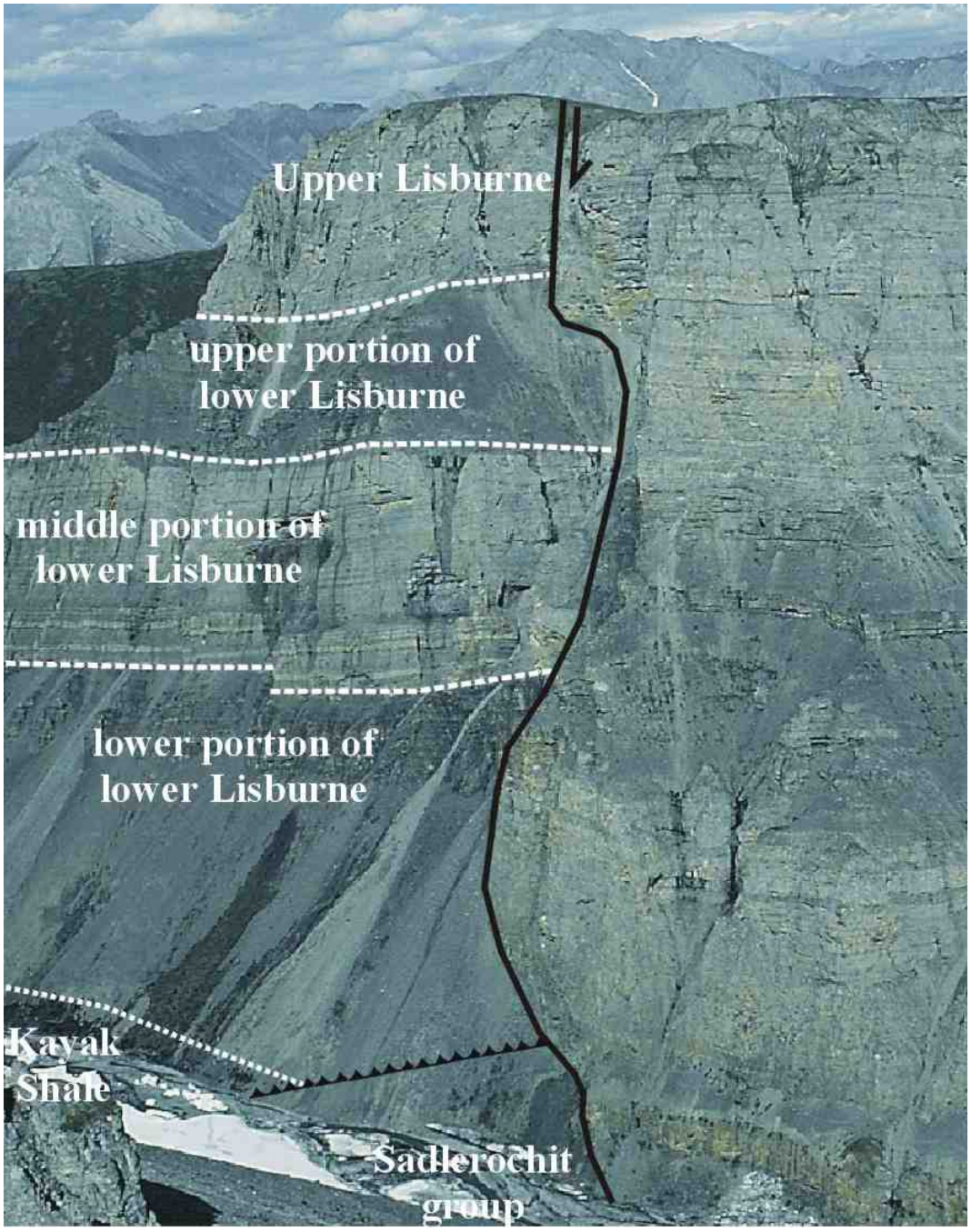

Figure 10: Photograph of the stratigraphy in West Porcupine Lake Valley. View is toward the northeast at the northwestern most Lisburne in the field area. The full thickness of the upper Lisburne is not shown here. Partial sections of the upper Lisburne are shown either side of the normal fault. The upper and lower portions of the lower Lisburne tended to be both recessive in their weathering patterns and mechanically weaker than the upper Lisburne or the middle portion of the lower Lisburne. Note the thrust, which places Lisburne and Kayak Shale above the Sadlerochit group.

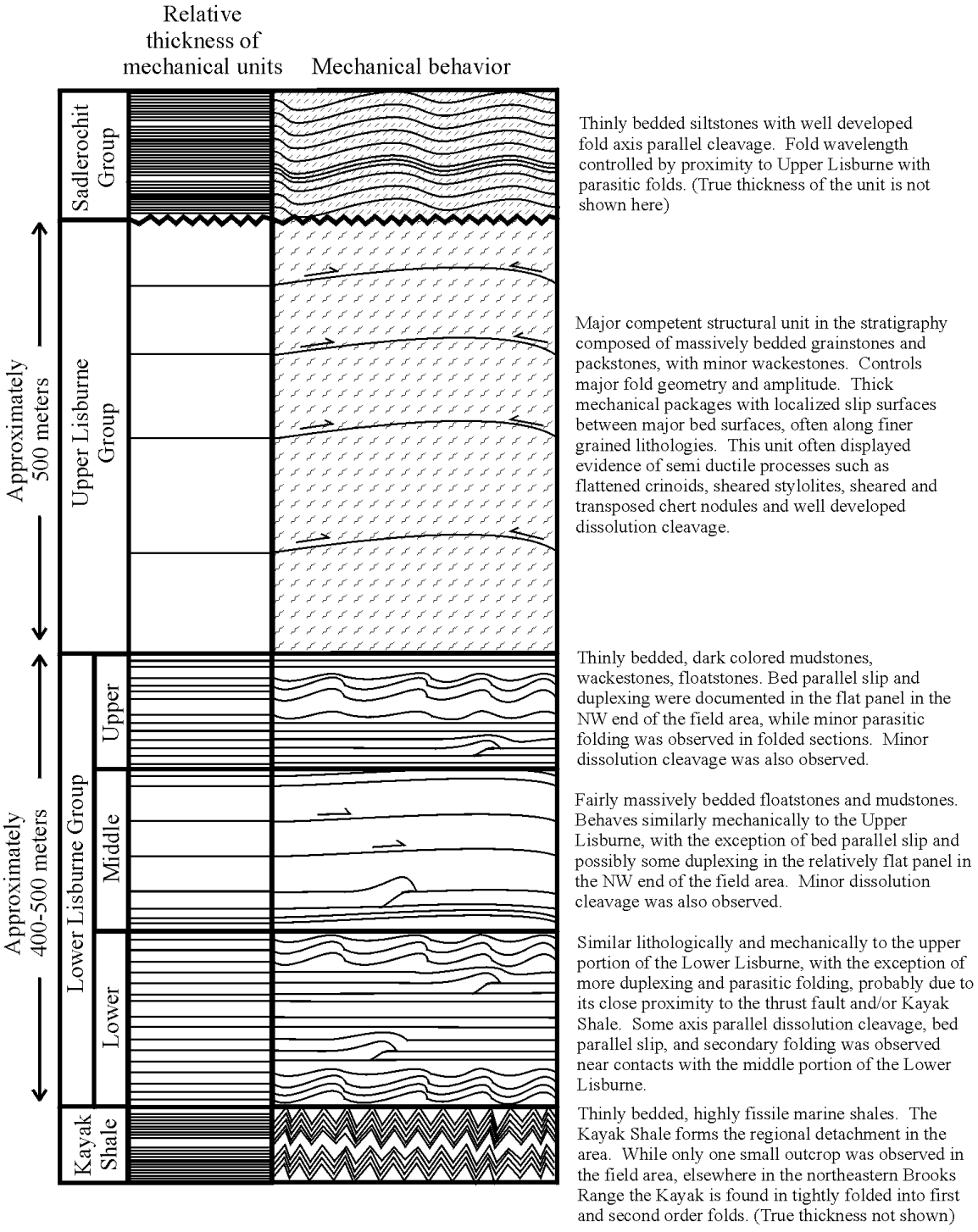

Figure 11: Generalized Mechanical Stratigraphy of the Kayak Shale, Lisburne Group, and Sadlerochit Group in West Porcupine Lake Valley. Thicknesses of units are approximate. The full thickness of Sadlerochit Group and Kayak Shale are not shown.

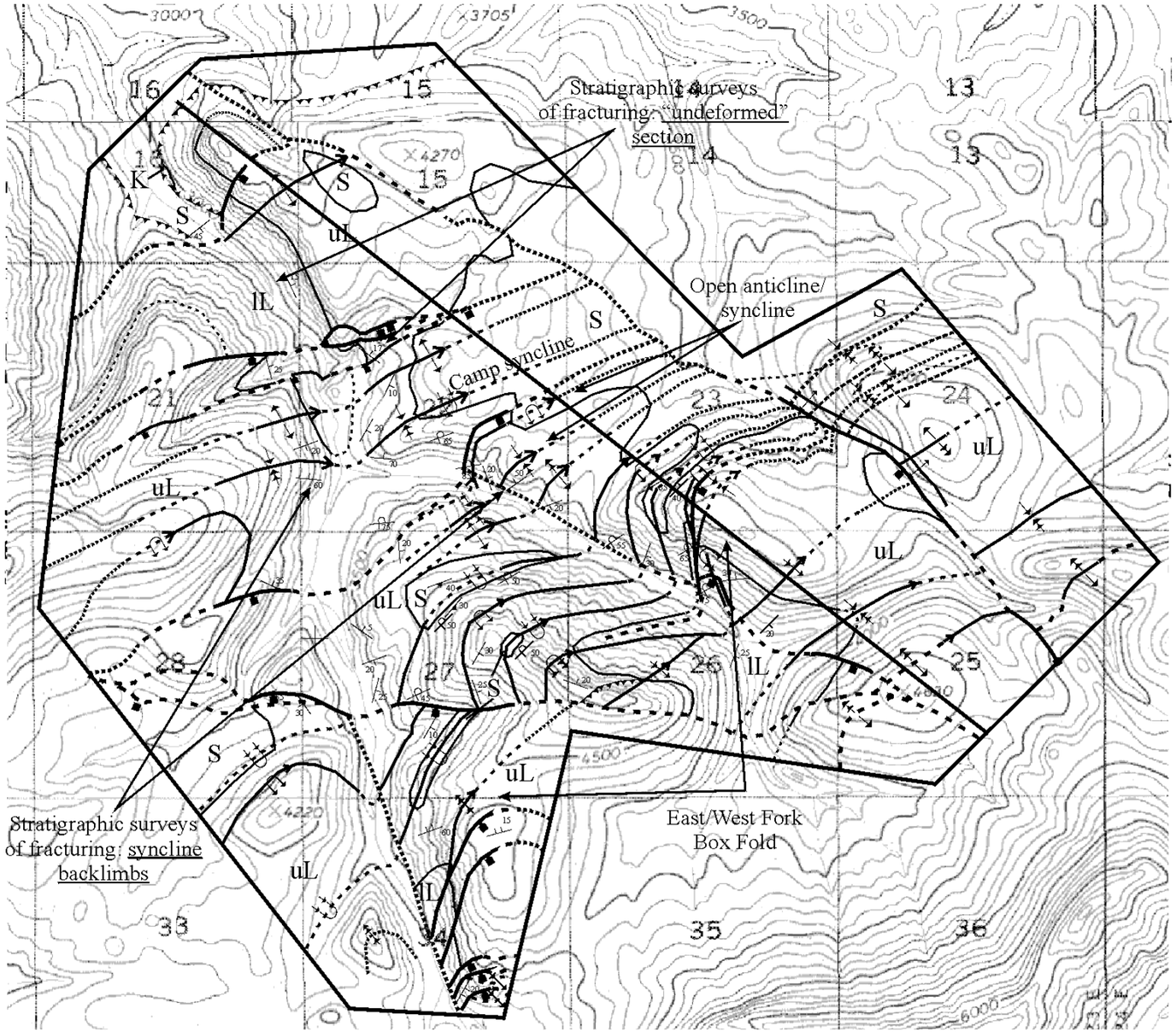

Legend

Contacts, faults, and fold axes are solid where precisely located, dashed where approximate, dotted where inferred (see below).

Faults

Thrust fault

other faults

(ball on down dropped block)

Folds: general geometry map symbol

- symmetric anticline
- asymmetric anticline
- asymmetric/tilted anticline
- overturned anticline
- overturned/tilted anticline
- monocline
- symmetric syncline
- asymmetric syncline
- overturned syncline
- -arrows indicate direction of plunge

Contacts and Symbols

Sadlerochit: **S**
Upper Lisburne: **uL**
Lower Lisburne: **lL**
Kayak Shale: **K**

solid dashed dotted

Strike and Dip Symbols dip 0-90 horizontal vertical

- measured bedding
- measured overturned bedding
- estimated bedding
- estimated overturned bedding (dips away from curve)
- measured cleavage

Figure 12: Geologic map of West Porcupine Lake Valley. Township and range grid boxes are 1 mile square. Line of section corresponds with the cross section in figure 13

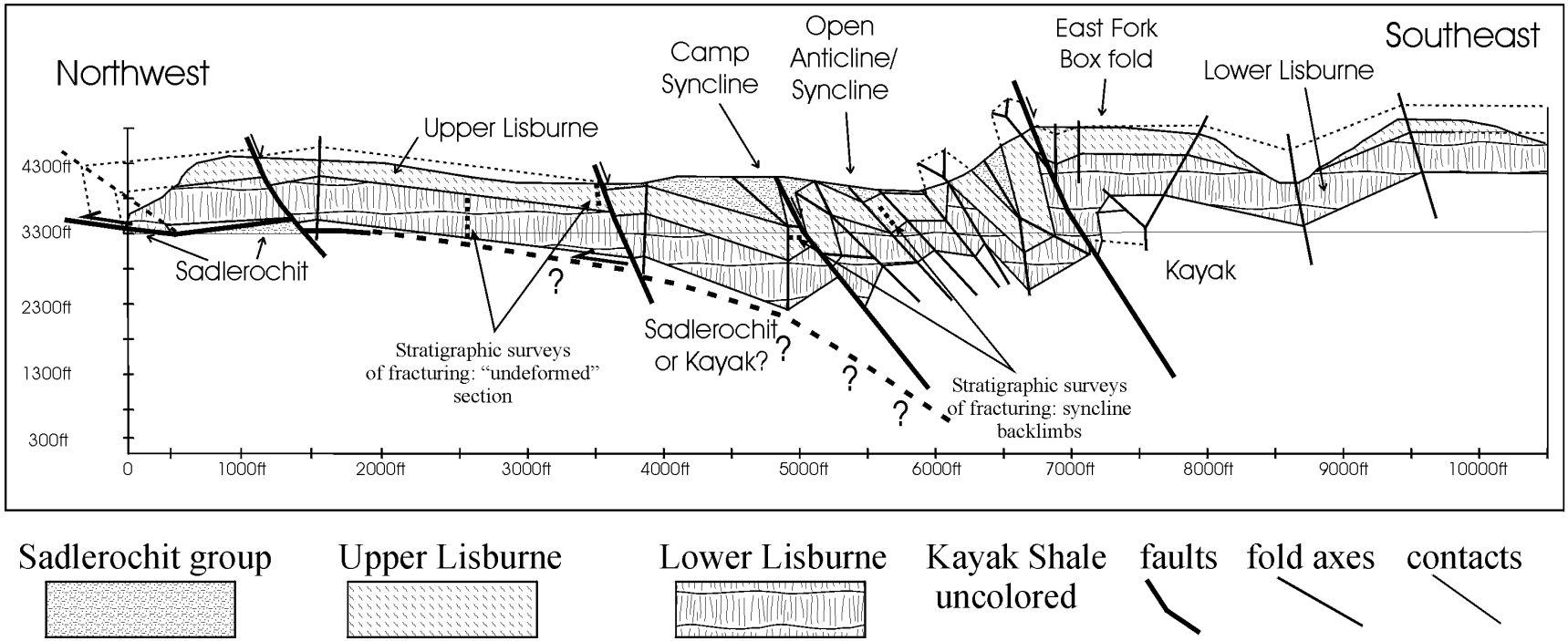

Figure 13: Unbalanced cross section through West Porcupine Lake Valley. Section line shown on figure 12. Photographs of Camp Syncline, Open Anticline, and Open Syncline are shown in following figures

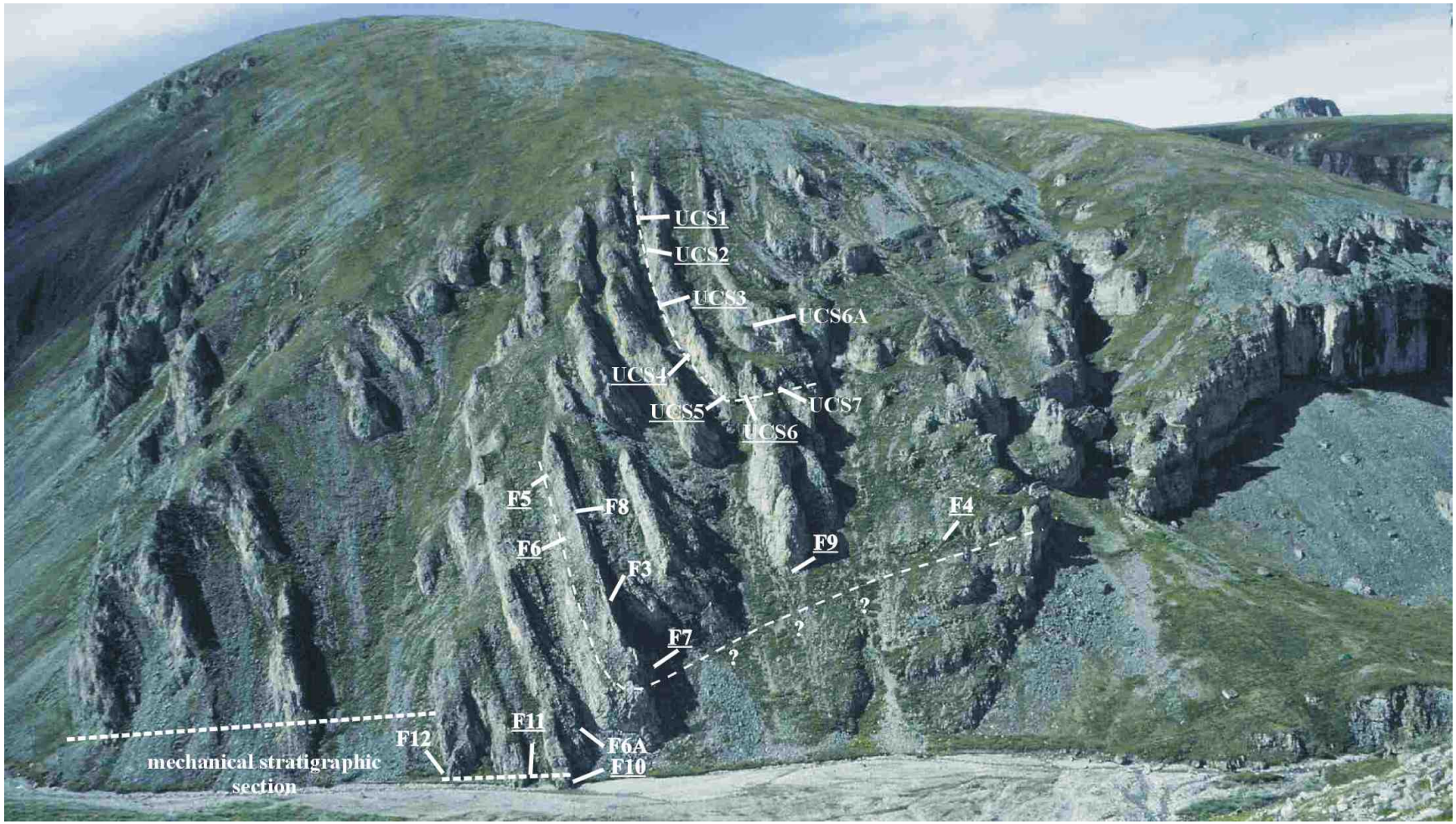

Figure 14: West view of Camp Syncline with sample locations. Underlined sample locations designate detailed fracture sampling method, non-underlined sample locations designate generalized fracture sampling method, and dotted line indicates the location of stratigraphic survey.

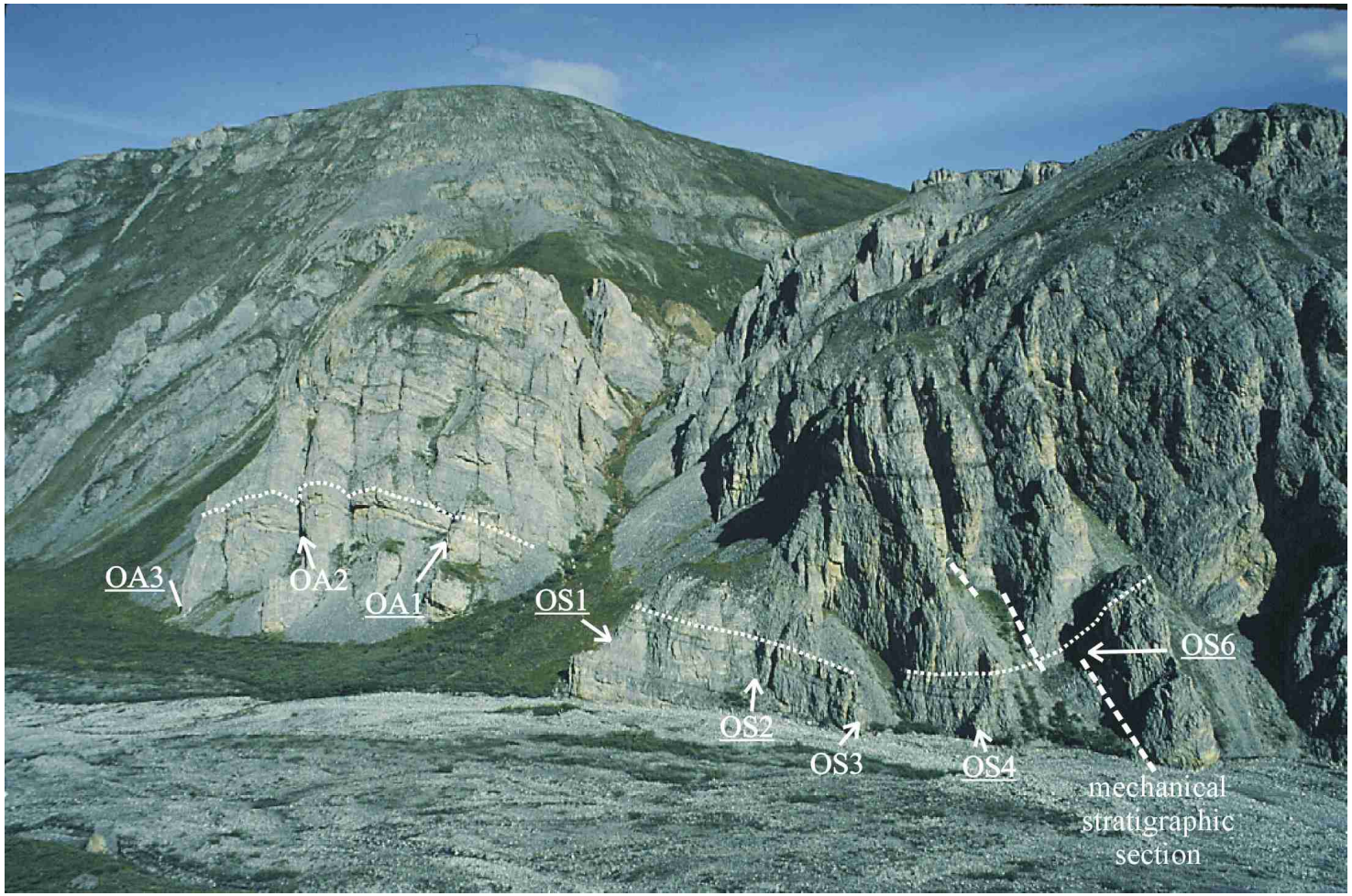

Figure 15: Northeast view (strike sub-perpendicular) of open anticline and syncline with sample locations. Underlined sample locations designate detailed fracture sampling method, non-underlined sample locations designate generalized fracture sampling method, and dotted line indicates the location of stratigraphic survey.

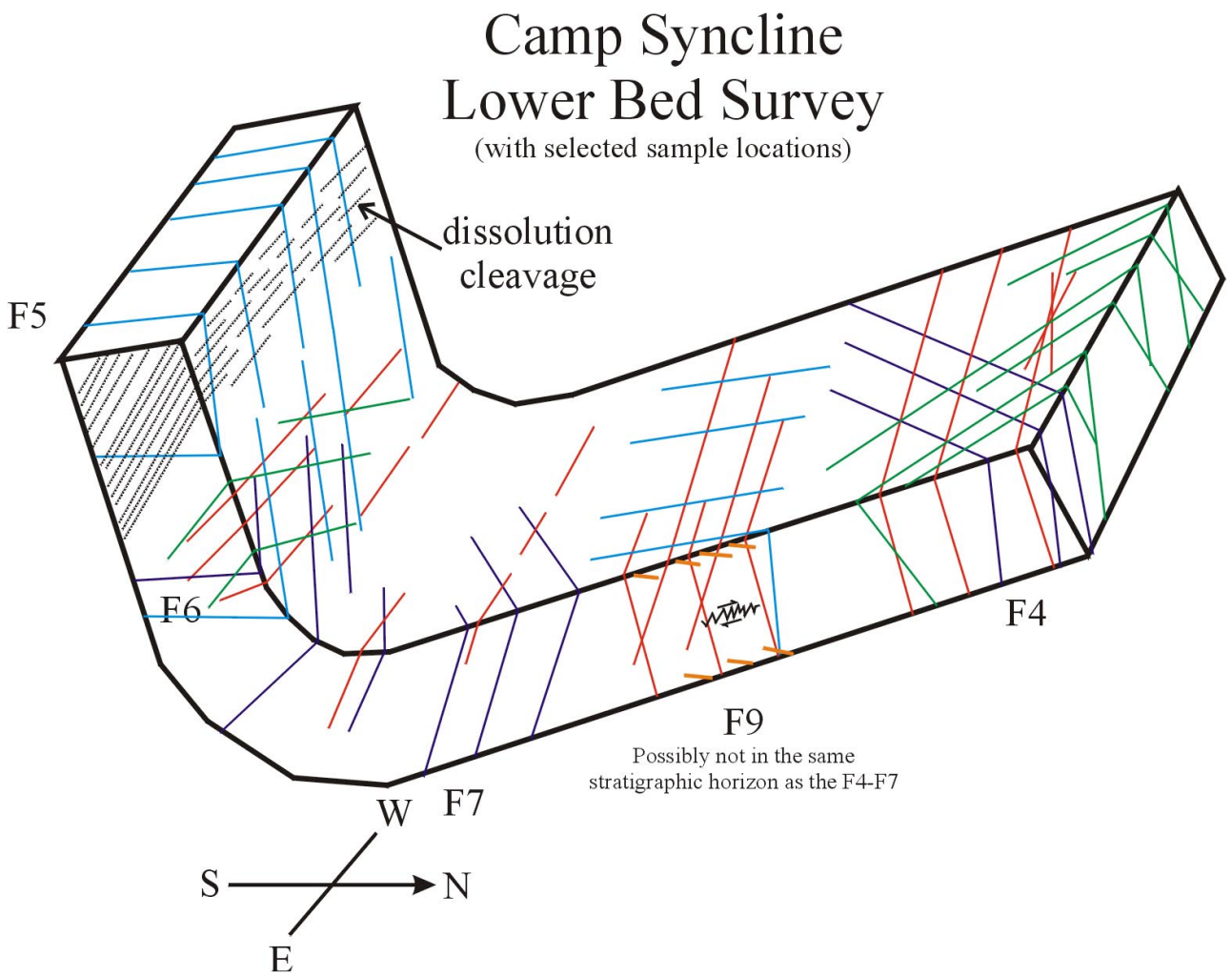

Figure 16: Preliminary interpretive sketch of selected fracture sets recorded in the lower portion of Camp Syncline. This sketch is not representative of the spacing of fractures throughout the fold, but shows the general fracture orientations.

Appendix
Fracture Data

Contents:

Appendix A: Background Fractures
Appendix B: Open Folds
Appendix C: East Camp Syncline
Appendix D: West Camp Syncline: Lower Transect
Appendix E: West Camp Syncline: Upper Transect

Key to Symbols

Terminations:

AB=against a bedding surface
AC=against a chert nodule
ABS=against a chert bed surface
AF=against a fracture
TI=terminates internally within a bed, not at a bedding contact
TG=terminates gradationally
U or blank entry=unknown
TL=terminates laterally (often against other fractures)

Orientation

where orientation shows: RANDOM, followed by a series of orientations, those orientations do not correspond to a given spacing interval, but are simply a "random" sampling of the fractures of a given set.

Aperture

note that aperture values less than or equal to 1 mm are considered to be the largest possible aperture, since measurement of apertures less than 1 mm is ambiguous at best.

Fill

C=calcite
Q=quartz
N=no fill
U or blank entry=unknown

"Background" Fractures

Location within fold: "undeformed" section
Sample Location: **BF1**
Outrcrop Type: x-sec w/ pavements
Stratigraphic Location: Middle "Lower Lisburne"
Rock Type(Field Call): rugose floatstone
Bed Thickness: 5m
Bed Orientation: 040,10SE
Nature of contacts: sharp, gently undulating
Thin Section:
Rock Type(Thin Section):
Hand Samples: BF1-A N-S vein
BF1-B N-S vein w/ parasitic veins
Photos: C-9-N-S fracs in floatstone
C-8-N-S fracs in pavement (location of sample BF-1B)

Prominent Fracture Sets:
N-S: well developed, lots of swarming, up to 5 cm thick calcite fill
shear features, sidestepping, subhorizontal slicks on calcite filled frax
see also sketch
E-W: vertical slicks, lots of normal fault related features
095,85SE, vertical slicks, down to SE
095,60NW, vertical slicks, down to NW
also some horizonntal slicks on E-W frax
large spacings between E-W frax

late shallow dipping conjugate set: 180-190,55-65SE
late shallow dipping conjugate set: 165-175,55-65SW
(this set terminates against N-S vertical set)

BF1	BF1	BF1	BF1	BF1	BF1	BF1	BF1	BF1	BF1	BF1	BF1	BF1	BF1
Fracture Set Orientation	N-S			Transect Orientation:			orthogonal to N-S vertical frax, not shallowly dipping conjugates						
Number	Spacing (m)	Aperture (mm)	Fill	Mode	Height (m)	Width (m)	Upper	Lower	Orientation	Notes			
1	0	2	C		5	1.5	CB		175,75SW				
2	0.45	1			2	0.8	AB		175,80SW				
3	0.8	1			1	1	AF	AF					
4	1	1			0.3	0.3	TI	AF	185,50SE	shallow dipping conjugate, lower term			
5	1.15	0.5			0.1	0.1	TI	AF	175,80NE	lower term = sp 1.20m		N-S vert frac	
6	1.2	20	C		0.4	0.3	TI	TI	175,70SW	part of ech set, down to E, set is at			
7	1.55	10	C		5	1	CB		175,80SW		least 5m high		
8	1.6	1			0.4	0.4	AF	AF	185,55SE	shallow dipping conjugate,			
9	1.7	1	C		0.2	0.1	AF	AF	180,90		term against sp= 1.55		
10	1.75	1			0.4	0.4	AF	AF	190,65SE	shallow dipping conjugate			
11	1.8	0.5			1	1	AF	AF	170,80SW		upper also against sp = 1.55m,		
12	1.9	1			0.05	0.05	TI	TI	175,85SW	ech set	lower vs N-S vert		
13	2.06	0.5			0.5	0.5	TI	TI	175,90	steps down to E			
14	2.15	2	C		5	2	CB			ech set, steps down to E			
15	2.25	1			0.5	0.3	TI	AB	175,90	sinuous			
16	2.35	0.5			0.7	0.3	TI	AF	175,90				
17	2.4	2	C		0.4	0.4	AF	AF	175,90				
18	2.6	1			0.8	0.3	AF	AF	190,65SE	shallow dipping conjugate			
19	2.65	1			0.2	0.1	AF	AF	175,90				
20	2.7	3	C		1	1	CB		180,90	within a shattered interval 10 cm wide			
21	2.95				0.2	0.2	AF	AF	165,60SW	shallow dipping conjugate			
22	3.04				0.5	0.2	TI	TI	175,80SW				
23	3.1	0.5			0.5	0.2	TI	TI	180,75E	shallow dipping conjugate, part of ech set			
24	3.2	1			0.1	0.1	AF	AF	180,90		steps down to E, 4 m high		
25	3.22	1			0.1	0.1	AF	AF	180,90				
26	3.4	1			0.2	0.2	TI	AF	180,55E	shallow dipping conjugate, term			
27	3.5	15	C		4	1	CB		180,85W		against sp = 3.50		
28	3.65	1			0.2	0.3	AB	TI	180,85W				
29	3.8	1			5	1	CB	TI	175,90				
30	4.05	10	C		4	1	AB		175,90				

BF1	BF1	BF1	BF1	BF1	BF1	BF1	BF1	BF1	BF1	BF1
Fracture Set Orientatio		E-W			Transect orientation:					
Number	Spacing (m)	Aperture (mm	Fill	Mode	Height (m)	Width (m)	Upper	Lower	Orientation	Notes
1	0	1	C		6	4	CB		095,80NE	ech set, steps down to S, subhoriz slix
2	1.8		C		5	3	AB		100,90	ech set, steps down to S, subhoriz slix
3	2.3	5	C		3	2	AB	AB	095,85SW	down to S shear, vertical slix
4	6.5	3	C		5	1	AB	AB	095,85SW	down to S shear, vertical slix

c

height of fractures measured is the height of the outcrop, but fractures likely penetrate above and below.
see sketch in notes

Location within fold: "undeformed" section
Sample Location: **BF2**
Outrcrop Type: x-sec
Stratigraphic Location: 59-61m in Michele's Fork's Canyon Section, "Lower Lisburne"
Rock Type(Field Call): dark, fine grained mud-wackestone, not many obvious macrofossils
Bed Thickness: 50-70cm bed thicknesses, with 1-3 cm thick intervals of cm scale bed thicknesses
Bed Orientation: 160,15NE
Nature of contacts: sharp
Thin Section:
Rock Type(Thin Section):
Hand Samples: BF2A-thinly bedded interval
BF2B-from thicker beds
Photos: N-13 N view of outcrop w/ jake staff
N-12 view downsection (death gulley)

Prominent Fracture Sets:
N-S
see detailed for orientation

E-W
see detailed for orientation

lots of small scale echelon features with various senses of shear oriented in various directions
see sketch 155,40SW 165,80NE frac130,45SW
vertical slicks everywhere 105,70NE, slicks rake 90 S

sparse set, N dipping:
105-105,70NE-down to S with vertical slicks

NOTE: no indication of layer parallel slip here,
despite the presence of mechanically weak horizons
such as sample BF2A: thinly bedded shales and mudstones
likely most of layer parallel slip localized in the lower Alapah

BF2	BF2	BF2	BF2	BF2	BF2	BF2	BF2	BF2	BF2	BF2	BF2	BF2	BF2
Fracture Set Orientation		N-S			Transect Orientation:		orthogonal						
Number	Spacing (m)	Aperture (mm)	Fill	Mode	Height (m)	Width (m)	Upper	Lower	Orientation	Notes			
1	0				0.35	1.2	AB	AB	175,90				
2	0.05				0.3	0.2	AB	AB	175,90				
3	0.1	1			0.2	0.1	AB	AB					
4	0.16	1			0.3	0.2	AB	TI	175,90				
5	0.22	2			0.45	0.2	AB	AB					
6	0.3	1			0.15	0.02	AB	TI					
7	0.35	0.5			0.05	0.05	AB	AB					
8	0.38	1			0.05	0.05	AB	AB					
9	0.4				0.25	0.1	AB	AB	175,90				
10	0.45	1			0.15	0.05	AB	AB					
11	0.47	2			0.4	0.2	AB	AB					
12	0.51				0.15	0.03	TI	AB					
13	0.55				0.15	0.03	TI	AB					
14	0.56				0.15	0.03	TI	AB					
15	0.6	1			0.25	0.05	AB	AB					
16	0.66				0.5	0.05	AB	AB					
17	0.9				0.5	0.25	AB	AB	175,80SW				

BF2	BF2	BF2	BF2	BF2	BF2	BF2	BF2	BF2	BF2	BF2
Fracture Set Orientatio		E-W			Transect orientation:		orthogonal			
Number	Spacing (m)	Aperture (mm	Fill	Mode	Height (m)	Width (m)	Upper	Lower	Orientation	Notes
1	0				0.2	0.1	AB	AB	090,75S	
2	0.1				0.1	0.1	AB	AB		
3	0.54				0.2	0.03	AB	AB		
4	0.55	1	C		0.15	0.02	AB	TI	090,90	
5	0.57	1	C		0.15	0.02	AB	TI	090,90	
6	0.7	1	C		0.15	0.02	AB	TI	090,90	frax at sp=.75 and .80: 105, N dipping
7	0.86	1	C		0.15	0.02	AB	TI	090,90	
8	1.2				0.2	0.3	AB	AB	100,85SW	
9	2				0.3	0.03	AB	AB	090,80S	sinuous, term laterally vs N-S frax
10	2.25	1	C		0.15	0.03	AB	AB		
11	2.75				0.25	0.03	AB	AB		
12	3.25				0.4	0.05	AB	AB	065,90	sinuous
13	3.5				0.3	0.1	AB	AB	085,90	
14	3.6				0.25	0.03	TI	AB		
15	3.68				0.15	0.02	AB	AB		
16	3.75				0.1	0.05	AB	AB		
17	3.9				0.25	0.15	AB	AB		

Location within fold: "undeformed" section
Sample Location: **BF3**
Outrcrop Type: x-sec
Stratigraphic Location: 102-104m in Michelle's Fork's Canyon Section, "Lower Lisburne"
Rock Type(Field Call): interbedded grainstones and packstones w/ lenticularly bedded cherts and mudstones
Bed Thickness: 10-20cm
Bed Orientation: 030,5-10SE
Nature of contacts: sharp
Thin Section:
Rock Type(Thin Section):
Hand Samples:

Prominent Fracture Sets:
N-S: 180,85W
180,75W
very swarmy with no recognizable trend
N-S frax w/ 1.5cm aperture and calcite fill every 1.5 m

Photos: N-16: N overview
N-15: closer up on N-15
N-14: E view along E-W

E-W
generally sinuous and terminate against N-S frax

Random spacing data # of fracs measured in 1 meter for N-W, and .7 meter for E-W fracs

Bed Thick(n	N-S set # of fracs	E-W # of fracs	rock type
0.45	13		G/packstone at base
0.4	53	40	P/wackestone/mudstone at top
0.25	35	24	G/packstone-bed that detailed sampling was conducted in
0.5	72	26	packstone
0.06	39	27	70cm thick chert
0.37	41	23	Float/grainstone

BF3	BF3	BF3	BF3	BF3	BF3	BF3	BF3	BF3	BF3	BF3	BF3	BF3	BF3
Fracture Set Orientation		180,75-85W		Transect Orientation:			strike=150						
Number	Spacing (m)	Aperture (mm)	Fill	Mode	Height (m)	Width (m)	Upper	Lower	Orientation	Notes			
1	0.1				0.1	0.1	CB						
2	0.23	1			0.2	0.15	CB						
3	0.27	1			0.1	0.2	CB			bed thickness=25cm			
4	0.29	1			0.1	0.2	AB	TI					
5	0.3	1			0.1	0.2	AB	TI					
6	0.33	0.5			0.05	0.05	CB	TI					
7	0.44	0.5			0.05	0.05	AB	AF					
8	0.45	1			0.2	0.1	AB	AB					
9	0.47	2			0.05	0.05	AB	TI					
10	0.5				0.25	0.2	AB	AB		bed thickness=30cm			
11	0.57	0.5			0.25	0.3	CB	CB					
12	0.59	0.5			0.1	0.15	AB	TI					
13	0.65				0.05	0.05	AB	TI					
14	0.67				0.05	0.05	AB	TI					
15	0.73				0.05	0.05	AB	TI					
16	0.77				0.05	0.05	AB	TI					
17	0.82	0.5			0.25	0.3	CB	CB					
18	0.86				0.1	0.2	AB	CB/TI					
19	0.88				0.1	0.2	AB	CB/TI		bed thickness=20cm			
20	0.93	0.5			0.05	0.05	AB	TI					
21	0.95	0.5			0.05	0.05	AB	TI					
22	0.97				0.25	0.2	AB	CB					
23	1	0.5			0.3	0.25	CB	CB		bed thickness=20cm			
24	1.1				0.2	0.1	AB						
25	1.2	1			0.2	0.1	AB	CB					

BF3	BF3	BF3	BF3	BF3	BF3	BF3	BF3	BF3	BF3	BF3
Fracture Set Orientatio		090,90			Transect orientation:		orthogonal			
Number	Spacing (m)	Aperture (mm	Fill	Mode	Height (m)	Width (m)	Upper	Lower	Bed Thick(m)	Notes
1	0				0.2	0.05	AB		0.2	term against N-S frac laterally
2	0.25				0.25	0.15	AB	AB	0.25	term against N-S frac laterally
3	0.63				0.3	0.2	AB	AB	0.3	
4	0.77	3	C		0.25	0.5	AB	AB	0.25	
5	0.8	3	C		0.05	0.5	AB	TI	0.22	
6	0.9	1	N		0.22	0.1	AB	AB		
7	0.95				0.2	0.05			0.2	term against N-S frac laterally
8	1.01				0.2	0.05			0.2	term against N-S frac laterally
9	1.09				0.2	0.05			0.2	term against N-S frac laterally
10	1.15				0.23	0.05			0.23	
11	1.16				0.05	0.05	TI	AB		
12	1.17				0.05	0.05	TI	AB		
13	1.18				0.05	0.05	TI	AB		
14	1.2				0.25	0.05	AB	AB	0.25	term against N-S frac laterally
15	1.26	0.5	C		0.05	0.05	TI	AB		
16	1.3				0.21	0.05	AB	AB		
17	1.4				0.25	0.2				
18	1.63				0.23	0.03			0.23	term against N-S frac laterally
19	1.65				0.22	0.03			0.22	
20	1.7				0.25	0.03			0.25	term against huge (ap (4cm)) N-S frac laterall
21	2.1	1	N		0.3	0.05			0.3	
22	2.2	1	N		0.3					
23	2.3	1	N		0.3					
24	2.4				0.25	0.05	TI	AB	0.3	
25	2.55				0.35	0.06	AB	AB	0.3	

Location within fold:	"undeformed" section			
Sample Location:	**WBF1** *note:WBF=Wahoo Background Frax="Upper Lisburne" background frax			
Outrcrop Type:	x-sec			
Stratigraphic Location:	10-13m in Michelle's Forks Wahoo, Lower "Upper Lisburne"			
Rock Type(Field Call):	See notes: floatstone, wackestone, grainstone/floatstones			
Bed Thickness:	0.5-1m			
Bed Orientation:	155,15NE	Prominent Fracture Sets:		
Nature of contacts:	gradational		N-S:	large range of strike
Thin Section:				see detailed sample
Rock Type(Thin Section):				
Hand Samples:	WBF1A-see sketch: upper bed (floatstone?) with wavy tan lams		E-W	
	WBF1B-see sketch: middle shattered wackestone			
	WBF1C-see sketch: lower grainstone/floatstone bed			
	WBF1D-see sketch:chert nodule from shattered wackestone		165,75-80NE	sparse, roughly every meter or so
Photos:	E-21 Overview, Mac's head at 10m, hammer at 11m, 12m just above contact between shatter zone and wavy laminated bed		see notes for sketches of major ech frac sets, sub-parallel to 165,75NE set	
	E-20 close up of shattered bed, hammer at 11m-note chert nodules and grad contact between shattered and unshattered			

WBF1	WBF1	WBF1	WBF	WBF	WBF1	WBF1	WBF1	WBF1	WBF1	WBF1	WBF1	WBF1	WBF1
Fracture Set Orientation		N-S			Transect Orientation:		strike=55		sampled in upper floatstone				
Number	Spacing (m)	Aperture (mm)	Fill	Mode	Height (m)	Width (m)	Upper	Lower	Orientation	Notes			
1	0.1				0.1	0.05	AF	AB	160,80NE				
2	0.23	1	N		0.1	0.05	AF	AB	160,80NE				
3	0.35				0.15	0.1	ABS	AB	180,90				
4	0.49				0.1	0.1	ABS	AB	180,90				
5	0.7				0.05	0.05	ABS	AB	180,90				
6	0.75				0.2	0.1		AB	185,90	first frac in large swarm			
7	0.8	5	C		0.4	0.15	AB	TI	185,90				
8	0.83	1	C		0.2	0.1	AB	AB	185,90				
9	0.91		N		0.4	0.05	ABS	AB/CB	185,90				
10	1.1	1			0.4	0.05	ABS	AB	185,90				
11	1.25				0.2	0.05	AF	AF	140,80NE	term against N-S fracs			
12	1.3	25	C		0.45	0.1		AB	150,85NE	part of ech set, down to SW all w/			
13	1.4				0.1	0.1		AB	145,90	calcite fill			
14	1.5				0.2	0.15	AB	AB	135,80NE				
15	1.55	0.5	N		0.1	0.1		AB	155,75NE	lower end crosses through a shatter zone			
16	1.66	0.5			0.05	0.05	TI	AB	155,75NE				
17	1.7				0.2	0.15	TI	AB	145,75NE				
18	1.74	5	C		0.4	0.2	AB	AB	155,80NE	last frac in large swarm			
19	1.94				0.05	0.05	TI	TI	180,75E				
20	2.24				0.5	0.05	AB	AB	170,80SW				

WBF1	WBF1	WBF1	WBF	WBI	WBF1	WBF1	WBF1	WBF1	WBF1	WBF1	WBF1	WBF1	WBF1
Fracture Set Orientatio	N-S set				Transect orientation:		strike=55		measured within the shatter zone				
Number	Spacing (m)	Aperture (mm	Fill	Mode	Height (m)	Width (m)	Upper	Lower	Orientation	Notes			
1	0.1	2	C		0.3	0.05	AB	TI	185,90				
2	0.12	0.5	C		0.5	0.05	AB	TI					
3	0.13	3	C		0.4	0.1	AB						
4	0.17				0.2	0.05	TI						
5	0.2	1	C		0.3	0.2	AF	AB					
6	0.22	1	C		0.2	0.2							
7	0.25	0.5	N		0.3	0.05	AB	AB					
8	0.27	1	C		0.3	0.1							
9	0.3	0.5	N		0.1	0.05	ABS	ABS					
10	0.31	0.5	N		0.1	0.05	ABS	ABS					
11	0.34	1.5	C		0.3	0.05							
12	0.35	0.5	N		0.1	0.05							
13	0.39				0.2	0.05							
14	0.4	0.5	C		0.6	0.1	AB	TI					
15	0.43	1	C		0.2	0.05							
16	0.44	4	C		0.2	0.05							
17	0.46	5	C		0.5	0.05							
18	0.48	2	C		0.2	0.05							
19	0.5	5	C		0.7	0.1	AB	TI					
20	0.51				0.1	0.05							
21	0.53				0.1	0.1	TI	TI					
22	0.55												
23	0.56	1	C		0.2	0.05							
24	0.57	1	C		0.1	0.05	AB	AB					
25	0.61	0.5	N		0.1	0.05	AB	AB					
26	0.65	1	N		0.3	0.05	AB	TI					
27	0.66				0.1	0.05	AB	TI					

WBF1	WBF1	WBF1	WBF	WBF	WBF1	WBF1	WBF1	WBF1	WBF1	WBF1
Fracture Set Orientation		E-W set			Transect orientation:		orthogonal		measured within the shatter zone	
Number	Spacing (m)	Aperture (mm)	Fill	Mode	Height (m)	Width (m)	Upper	Lower	Orientation	Notes
1	0.02				0.15	0.05	AB	AB	bed thickness=15cm	
2	0.07	1	N		0.15	0.05	AB	AB		
3	0.11	0.5	N		0.15	0.05	AB	AB		
4	0.15	1	C		0.15	0.05	AB	AB		
5	0.2				0.15	0.05	AB	AB		
6	0.22	0.5	N		0.15	0.05	AB	AB		
7	0.3	1	N		0.15	0.05	AB	AB		
8	0.35				0.15	0.05	AB	AB		
9	0.37				0.15	0.05	AB	AB		
10	0.4				0.15	0.2	AB	AB		
11	0.46	5			0.22	0.15	AB	AB	bed thickness=22cm, also transect location	
12	0.53	1	C		0.22	0.15	AB	AB		jumps laterally, possibly to a new bed of
13	0.59	1	N		0.22	0.15	AB	AB		similar lithology
14	0.64	1	N		0.22	0.15	AB	AB		width roughly parallel to spacing
15	0.69	2	N		0.22	0.15	AB	AB		of N-S fracs since all E-W fracs term
16	0.73	1	C		0.22	0.15	AB	AB		against N-S
17	0.78									

Location within fold: "undeformed" section
Sample Location: **WBF2** *note:WBF=Wahoo Background Frax="Upper Lisburne" background frax
Outrcrop Type: x-sec
Stratigraphic Location: between 29-32m in Forks Wahoo
Rock Type(Field Call): massively bedded floatstones
Bed Thickness: .5m
Bed Orientation: 155,15NE
Nature of contacts: faint, gradational
Thin Section:
Rock Type(Thin Section):
Hand Samples: WBF2

note: floatstones from 29-41m all appear to be mechanically homogenous--check strat section

Prominent Fracture Sets:
see detailed notes

Photos:
E-19 overview of E-W face along which 150 set was measured
E-18 echelon E-W extension veins
E-17 echelon E-W extension veins
E-16 echelon E-W extension veins: close up
E-15 overview of E-W fracs

Location within fold: "undeformed" section
Sample Location: **WBF3** *note:WBF=Wahoo Background Frax="Upper Lisburne" background frax
Outrcrop Type: x-sec
Stratigraphic Location: between 59-61m in Forks Wahoo
Rock Type(Field Call): wackestones/mudstones/packstones
Bed Thickness: .5m, with minor 20-30cm bed surfaces, see sketch
Bed Orientation: 155,20NE
Nature of contacts: sharp
Thin Section:
Rock Type(Thin Section):
Hand Samples: see measured section samples

note: no detailed sampling due to bad outcrop
see notes for detailed sketch with generalities about fracture character

Prominent Fracture Sets:
110,90 and 095,85SW

Photos:

WBF2	WBF2	WBF2	WBF	WBF	WBF2	WBF2	WBF2	WBF2	WBF2	WBF2	WBF2	WBF2	WBF2
Fracture Set Orientation		N-S			Transect Orientation:		orthogonal						
Number	Spacing (m)	Aperture (mm)	Fill	Mode	Height (m)	Width (m)	Upper	Lower	Orientation	Notes			
1	0.05				0.8	0.4		AB					
2	0.3	1	C		1.5	0.4		AB	165,80SW				
3	0.55	1	N		0.2	0.05	TI	ABS	140,80SW				
4	0.57	1	N		0.3	0.05	TI	TI/CB	140,80SW				
5	0.85				0.35	0.1	CB	CB	150,85SW				
6	0.92	1	N		0.2	0.1	AB	CB	150,85SW				
7	0.95				1.5	0.1	AB		145,80SW	CB above/below			
8	1.2	1	C		1.5	0.3	TI	TI	165,85SW	CB above/below			
9	1.4	1	C		0.5	0.1	AB	TI	160,75SW	CB above			
10	1.5				0.5	0.2	TI	AB	160,75SW				
11	1.55	1	N		0.1	0.1	AB	AB	160,75SW				
12	1.6				0.1	0.1	AB	AB	150,85SW				
13	1.65				0.2	0.1	AB	AB	150,85SW				
14	1.7	1	N		0.1	0.1	AB	TI	150,85SW				
15	1.71	1	N		0.3	0.1	AB	AB	150,85SW				
16	1.75				0.1	0.1	AB	AB	150,85SW				
17	1.79				0.1	0.1	AB	AB	150,85SW				
18	1.85	1	N		1.4	0.2	AB	AB	150,85SW	CB above/below			
19	2.35	2	N		0.7	0.05	TI		150,90	CB above			
20	2.45				0.1	0.1	AB		150,85SW				
21	2.46	1	N		0.1	0.1	AB	TI	180,90				
22	2.6	0.5	N		0.4	0.05	TI		150,90	CB above			

WBF2	WBF2	WBF2	WBF	WBI	WBF2	WBF2	WBF2	WBF2	WBF2	WBF2
Fracture Set Orientatio		80-90,85SE			Transect orientation:		orthogonal			
Number	Spacing (m)	Aperture (mm	Fill	Mode	Height (m)	Width (m)	Upper	Lower	Orientation	Notes
1	0	3	C		0.5	0.3	AB			
2	0.04	2	C		0.25	0.05	AB	AB		
3	0.08	1	C		0.2	0.05	AB	TI		
4	0.11	1	C		0.2	0.05	AB	AB		
5	0.18				0.2	0.05	AB	AB		
6	0.2				0.2	0.25	AB	AB		
7	0.22	3	C		0.2	0.05	AB	AB		
8	0.24	4	C		0.2	0.05	AB	AF		CB below
9	0.27				0.2	0.1	AB	AB		
10	0.29				0.2	0.05	AB	AB		
11	0.34	3	C		1	0.4	TI			CB below
12	0.37	2	C		0.15	0.05	TI	TI		
13	0.4	2	C		0.4	0.05				
14	0.47	2	C		0.5	0.1	AB	TI		
15	0.51	2	C		0.2	0.1	TI			
16	0.57				0.15	0.1				
17	0.6	2	C		0.25	0.15	AB	AB		
18	0.67				0.25	0.1	AB	AB		
19	0.72	2	C		1	0.4	AB	TI		
20	0.77	1	C		0.2	0.05	AB	AB		
21	0.82	2	C		0.2	0.05	AB	AB		
22	0.85				0.2	0.05	AB	AB		
23	0.86				0.2	0.05	AB	AB		
24	0.92				0.25	0.1	AB	AB		
25	0.97				0.25	0.05	AB	AB		

Location within fold: "undeformed" section
Sample Location: **WBF4** *note:WBF=Wahoo Background Frax="Upper Lisburne" background frax
Outrcrop Type: x-sec
Stratigraphic Location: 68-70m in Forks Wahoo
Rock Type(Field Call): massive floatstone interval 13m thick
Bed Thickness: 1-4m
Bed Orientation: 135,20NE
Nature of contacts: relatively sharp
Thin Section:
Rock Type(Thin Section):
Hand Samples:

Prominent Fracture Sets:
see detail

Dissolution Cleavages
065-55SE
065,65SE
070,40SE
065,55SE
070,60SE

Photos: J-9 W facing view, Mac pointing to 69m w frac swarm to her left
J-8 W facing view, Mac pointing to 69m w frac swarm to her left
J-7 Close up of 120, NE+SE fracs in the swarm
J-6 Close up of 120, NE+SE fracs in the swarm

WBF4	WBF4	WBF4	WBF	WBF	WBF4	WBF4	WBF4	WBF4	WBF4	WBF4	WBF4	WBF4	WBF4	WBF4
Fracture Set Orientation		N-S, shallow dip			Transect Orientation:		orthogonal							
Number	Spacing (m)	Aperture (mm)	Fill	Mode	Height (m)	Width (m)	Upper	Lower	Orientation	Notes				
1	0.05		C		0.2	0.2	AB	AB						
2	0.15		C		0.2	0.2	AB	AB						
3	0.43				0.4	0.2		AB	180,80W					
4	0.6				0.4	0.2	TI	ABS	180,80W					
5	0.65	0.5	C		0.1	0.1	TI		180,80W					
6	0.75	1	C		0.3	0.05	TI	AB		en ech set, steps down to W, shear				
7	0.8				0.5	0.05	AB	AB	180,70W	CB	down to E			
8	0.85	1	C		0.1	0.05	AB	AB						
9	0.95	1	N		0.6	0.05	AB	AB	185,70NW	CB	*longer frax CB before			
10	1.1				0.2	0.05	AB	AB	190,70NW		terminating against bedding			
11	1.2				0.2	0.05	AB	AB						
12	1.5	5	C		1	0.3			170,70SW	CB				
13	1.65	5	C		0.5	0.1	AF		160,85SW	CB				
14	1.8				0.2	0.1	AB		175,75SW					

WBF4	WBF4	WBF4	WBF	WBI	WBF4	WBF4	WBF4	WBF4	WBF4	WBF4	WBF4	WBF4	WBF4
Fracture Set Orientatio		110 set			Transect orientation:		orthogonal						
Number	Spacing (m)	Aperture (mm	Fill	Mode	Height (m)	Width (m)	Upper	Lower	Orientation	Notes			
1	0.15				1	2	AF		105,80NE				
2	0.64	1			1	1			110,70NE				
3	0.85				0.5	0.6			110,70NE				
4	0.972				1	1			110,85NE	eh set, 3-4m lateral existence			
5	1.03				0.5	0.5				eh set, 3-4m lateral existence			
6	1.75				0.3	0.3			120,75NE	eh set, 3-4m lateral existence			
7	1.8				0.15	0.15			120,75NE				
8	2.2				0.1	0.1			105,85NE	term AF laterally			

Fracture Set Orientatio		150 set			Transect orientation:		orthogonal						
Number	Spacing (m)	Aperture (mm	Fill	Mode	Height (m)	Width (m)	Upper	Lower	Orientation	Notes			
1	0	1	N		0.2	0.05	AB	TI	135,80NE				
2	0.22	1	C		1	0.5			135,90	CB			
3	1.3	1	N		0.2	0.05	AF	TI	150,80SW				
4	1.42				0.5	0.1	AF		150,85SW				
5	1.64				0.5	0.2	AF	AF	135,80NE	concave to NE			
6	1.67	1	N		0.2	0.2	AF	AF	150,90				
7	1.74				0.2	0.2	AF	AF	150,85NE				
8	2.07	4	C		1	0.2	AB		145,90	ech set 4m high: steps down to NE,			
9	2.33	2	C		0.3	0.1	AF	AF	130,80NE	shear down to SW			
10	2.36	2	C		0.3	0.1	AF	AF	130,80NE				

WBF4	WBF4	WBF4	WBF	WBF	WBF4	WBF4	WBF4	WBF4
Dissolution	Cleavage	065-075,50-65SE						
spacing					measured along	strike=135-150 (frac set)		
1	0.04	throughgoing, pervasive DC, between almost all frax,						
2	0.06				tends to be very small aperture, can't see any fill			
3	0.07							
4	0.1							
5	0.13							
6	0.17							
7	0.2							
8	0.3							
9	0.31							
10	0.34							
11	0.36							
12	0.41							
13	0.43							
14	0.45							
15	0.47							
16	0.49							
17	0.59							
18	0.61							
19	0.63							
20	0.73							
21	0.76							
22	0.77							
23	0.79							
24	0.8							
25	0.82							

Location within fold:	"undeformed" section
Sample Location:	**WBF5** *note:WBF=Wahoo Background Frax="Upper Lisburne" background frax
Outrcrop Type:	x-sec
Stratigraphic Location:	between 73-75m in Forks Wahoo
Rock Type(Field Call):	dark floatstones interlayered with packstones?, with mudstone on top (above 75)
Bed Thickness:	2-3 meter mechanical packages, 1-5cm compositional layers
Bed Orientation:	160,25NE Prominent Fracture Sets:
Nature of contacts:	relatively gradational between compositional layering
Thin Section:	
Rock Type(Thin Section):	
Hand Samples:	WBF5A-between 74-75m (floatstone?) WBF5B-just below 74m WBF5C-chert bearing dark laminated wackestones and muds above 75m
Photos:	M-20 NW view of echelon veins at WBF5, hammer points N M-19 NW view of echelon veins at WBF5, hammer points N

WBF5	WBF5	WBF5	WBF	WBF	WBF5	WBF5	WBF5	WBF5	WBF5	WBF5	WBF5	WBF5	WBF5
Fracture Set Orientation		N-S set			Transect Orientation:		orthogonal						
Number	Spacing (m)	Aperture (mm)	Fill	Mode	Height (m)	Width (m)	Upper	Lower	Orientation	Notes			
1	0	5	C		0.2	0.03	TI	AB	180,70W	shear down to SW			
2	0.05	1	C		0.6	0.03	AF	AF		CB			
3	0.09	3	C		0.2	0.05	TI	AB		CB			
4	0.19	1	C		0.15	0.03	TI	AB	185,75NW	CB			
5	0.31	1	C		0.12	0.1	AB	AB					
6	0.41	1	C		0.12	0.12	AB	AB	185,75NW				
7	0.44	0.5	C		0.5	0.3	AB	TI		CB			
8	0.54	1	C		0.2	0.25	TI	AB					
9	0.59	1	C		0.15	0.15	AB	AB					
10	0.62				0.2	0.3	AB	TI	175,85SW				
11	0.74	0.5	C		0.1	0.1	AB	TI					
12	0.76	1	C		0.25	0.2	AB	TI					
13	0.84	0.5	C		0.2	0.1	TI	TI	180,80W	CB			
14	0.9	1.5	C		0.15	0.1	AB	TI		steps down to W, shear down to E			
15	1.03	0.5	C		0.05	0.05	AB	TI	180,75W				
16	1.04	1	C		0.25	0.05	AB	TI					
17	1.1	0.5	C		0.2	0.05	AB	TI					
18	1.19	0.5	C		0.2	0.05	AB	TI					
19	1.26	2	C		0.2	0.05	AB	TI					
20	1.36	1	C		0.18	0.03	AB	AB					
21	1.51	1	C		0.21	0.05	AB	TI	190,75NW				
22	1.66	1	C		0.1	0.1	AB	AB					
23	1.72	0.5	C		0.15	0.15	AB	TI	185,75NW	CB			
24	1.94	1	C		0.15	0.1	AB	AB					
25	2.04	1	C		0.2	0.05	AB	AB					

WBF5	WBF5	WBF5	WBF	WBI	WBF5	WBF5	WBF5	WBF5	WBF5	WBF5	WBF5	WBF5	WBF5
Fracture Set Orientatio		145 SW dip			Transect orientation:		orthogonal						
Number	Spacing (m)	Aperture (mm	Fill	Mode	Height (m)	Width (m)	Upper	Lower	Orientation	Notes			
1	0	1	N		0.15	0.03	TI	AB					
2	0.07	0.5	N		0.1	0.03	AB	TI					
3	0.3	0.5	C		0.2	0.05	TI	AB	140,75SW				
4	0.47	0.5	N		0.15	0.05	TI	TI	150,75SW	CB			
5	0.8	1	C		0.4	0.1	AF	TI	145,85SW	CB, steps down to N, shear to SW			
6	0.81	0.5	N		0.12	0.04	AB	TI					
7	0.84	1	C		0.12	0.03	AB	TI					
8	0.85	1	C		0.07	0.01	AB	TI					
9	0.95	1	C		0.05	0.02	AB	TI					
10	1.08	0.5	C		0.05	0.02	TI	TI		CB			
11	1.18	1	N		0.15	0.04	AF	AF	145,80SW	CB			
12	1.23	1	N		0.3	0.05	TI	AF		CB			
13	1.3	1	C		0.15	0.03	AB	TI	145,85SW				
14	1.36	0.5	C		0.1	0.05	AB	TI					
15	1.45				0.2	0.03	TI	TI		CB			
16	1.46	0.5	C		0.2	0.03	TI	TI	145,70SW	CB			
17	1.51	0.5	C		0.15	0.03	TI	AB		CB			
18	1.54	2	C		0.2	0.05	AF	AB					
19	1.56	2	C		0.2	0.05	AF	AB					

WBF5	WBF5	WBF5	WBF	WBF	WBF5	WBF5	WBF5	WBF5	WBF5	WBF5
Fracture Set Orientation		095-110? set, E dip			Transect Orientation:		orthagonal			
Number	Spacing (m)	Aperture (mm)	Fill	Mode	Height (m)	Width (m)	Upper	Lower	Orientation	Notes
1	0				0.2	0.1	AF	TI	095,85NE	
2	0.65	1	C		0.5	0.1	TI	AB		steps down to S, shear down to N
3	0.79	0.5	C		0.25	0.02	TI	AB		
4	0.97	0.5	N		0.4	0.02	TI	AF		CB
5	1.12	0.5	N		0.05	0.02	AF	AF		
6	1.14	2	C		0.5	0.02	AF	TI		
7	1.17	0.5	C		0.1	0.03	TI	AF		
8	1.34	1	C		0.35	0.03	TI	AF		
9	1.38	0.5	N		0.12	0.03	AF	AF		
10	1.43	0.5	N		0.08	0.03	AF	AF		

Open Anticline/Syncline

calculated beta axes: open anticline 14,083 Open syncline 11,053

note:these sample locations are in order along the same stratigraphic interval from NW to SE, starting in the forelimb of open anticline and ending in the backlimb of open syncline

Fold Name:	Open Anticline
Location within fold:	overturned forelimb
Sample Location:	**OA3**
Outrcrop Type:	x-sec
Stratigraphic Location:	mid-upper "Upper Lisburne"
Rock Type(Field Call):	float/grainstone
Bed Thickness:	1m?
Bed Orientation:	080,85SE overturned
Nature of contacts:	sharp, lots of bed parallel slip
Thin Section:	
Rock Type(Thin Section):	
Hand Samples:	OA3A-120,78NEoverturned (lithology)
Photos:	P-3,2: overview, see also polaroid P-1, Q-36,35: echelon features

Notes:
see sketches for details on shear features
DC:
060,20SE-better developed
080,50SE

Prominent Fracture Sets:

Fold Name:	Open Anticline
Location within fold:	forelimb
Sample Location:	**OA2**
Outrcrop Type:	x-sec
Stratigraphic Location:	mid-upper "Upper Lisburne"
Rock Type(Field Call):	float/grainstone
Bed Thickness:	1m
Bed Orientation:	100,50NE
Nature of contacts:	sharp, lots of slip at bed contacts
Thin Section:	
Rock Type(Thin Section):	
Hand Samples:	OA2A-006,88NW (both orientations are DC) OA2B-190,85SW
Photos:	P-5 minor 040-055, SE dipping frac set P-4 N view of swarm valley that OA2 was in

Notes:
location characterized by lots of different DC, little fracturing!!
055,55SE 080,40SE
080,70SE
bizarre: N-S set present, similar spacing and characteristics to OA1, but difficult to measure due to location
no major frac sets

Prominent Fracture Sets:

N-S:	180,90	
175,88NW	180,85W	
190,85NW	185,90	
E-W: 1 minor swarm:		
1 frac/.5cm, for only 15cm		
2cm high x 1-2 mm wide		

single fracs measured:

110,70NE	late normal flt
090,70S	
040,55SE	
055,75SE	
050,70SE	

OA3	OA3	OA3	OA3	OA3	OA3	OA3	OA3	OA3	OA3	OA3	OA3	OA3	OA3
Fracture Set Orientation		180,shallow SE dip		Transect Orientation:			orthogonal						
Number	Spacing (m)	Aperture (mm)	Fill	Mode	Height (m)	Width (m)	Upper	Lower	Orientation	Notes			
1	0	5	C		2	0.3	TI		190,25SE				
2	0.12	2	C		0.4	0.2	TI	TI	180,30E				
3	0.37	5	C		1	0.2	AF	AF	165,20NE				
4	0.55	5	C		1	0.2	TI	AF	160,20NE	**AF against 120,85NE frac????**			
5	0.55	5	C		0.7	0.2	TI		220,25SE	possibly folded or measured near cutoffs			
6	0.62	2	C		0.3	0.3			165,20NE				
7	0.84	5	C		2	0.3							
8	1.1	5	C		1.5	0.3			200,25SE	possibly folded or measured near cutoffs			
9	1.27	3	C		0.15	0.02	AF	AF	160,20NE	offset down to N on lower end by 120,80NE			
10	1.33	5	C		1	0.2	AF	AF	170,25NE				

*most of these are EARLY frax x-cut by everything!
most are cut by 090-120 N+S dipping microfracs

OA3	OA3	OA3	OA3	OA3	OA3	OA3	OA3	OA3	OA3	OA3
Fracture Set Orientatio	E-W, N dip			Transect orientation:		orthogonal				
Number	Spacing (m)	Aperture (mm	Fill	Mode	Height (m)	Width (m)	Upper	Lower	Orientation	Notes
1	0.07	2	C		0.3	0.05	TI	TI	125,75NE	
2	0.09	2	C		0.15	0.02	TI	TI	125,75NE	
3	0.11	0.5			0.03	0.03	TI	TI		
4	0.115	microfrax	icrofr	crofr	microfrax	microfrax	nicrofra	microfrax	microfrax	microfrax:not measured b/c they're tiny!
5	0.13	0.5			,1	0.02	TI	TI	130,75NE	
6	0.145	1	C		0.1	0.03	AF	AF	110,80SW	
7	0.17	0.5	C		0.25	0.1	TI	TI	115,70NE	
8	0.19				0.03	0.03	TI	TI	115,70NE	
9	0.205	1	C		0.1	0.05	AF	AF	150,40NE	
10	0.25	0.5	N		0.05	0.05	TI	TI		
11	0.28	2	C		0.1	0.05	TI	TI	125,75NE	
12	0.29	1	C		0.15	0.1	TI	TI	115,75NE	
13	0.32	0.5	C		0.05	0.15	TI	TI	125,70NE	
14	0.33	2	C		0.1	0.1	TI	TI	135,75NE	
15	0.34	2	C		0.05	0.05	TI	AF	140,55NE	
16	0.365	3	C		0.15	0.15	TI	TI	150,50NE	
17	0.385	2	C		0.1	0.1	TI	TI	140,65NE	
18	0.425	3	C		0.15	0.1	TI	TI	135,55NE	
19	0.44	microfrax	icrofr	crofr	microfrax	microfrax	nicrofra	microfrax	microfrax	microfrax
20	0.445	2	C		0.1	0.05	TI	TI	135,65NE	
21	0.47	4	C		0.3	0.2	TI	TI	135,65NE	
22	0.51	1	C		0.1	0.05	TI	TI		
23	0.53	3	C		0.05	0.05	TI	TI	125,65NE	
24	0.535	microfrax	icrofr	crofr	microfrax	microfrax	nicrofra	microfrax	microfrax	microfrax
25	0.56	2	C		0.2	0.1	TI	TI	125,60NE	
26	0.57	0.5	C		0.05	0.05	TI	TI		
27	0.62	0.5	N		0.1	0.02	TI	TI	140,60NE	

*lots of down to S sense of shear on en ech vein sets

Fold Name:	Open Anticline	Notes:
Location within fold:	forelimb/hinge (no distinct hinge)	well developed foliation/DC:
Sample Location:	**OA1**	075,60SE foliation again seems to replace fracturing!!!
Outrcrop Type:	x-sec	080,64SE
Stratigraphic Location:	mid-upper "Upper Lisburne"	minor frac set parallel to this DC
Rock Type(Field Call):	float/grainstone	
Bed Thickness:	2.5m from the white chert to the black chert (see sketch)	
Bed Orientation:	140,30NE 150,35NE 165,30NE	Prominent Fracture Sets:
Nature of contacts:	sharp (fair, taken at	minor E-W frac swarm: see measured set with conjugates:
Thin Section:	detailed sample location)	085,85NW
Rock Type(Thin Section):		080,85NW
Hand Samples:	OA1A-015,85SE overturned (sample for lithology ID)	
	OA1B-075,80SE along DC/foliation	
Photos:	P-10 E view of outcrop	
	P-9 N view along N-S set	
	P-8,7-W view of down to S echelon set between OA1 and OA2	

OA1	OA1	OA1	OA1	OA1	OA1	OA1	OA1	OA1	OA1	OA1	OA1	OA1	OA1
Fracture Set Orientation	N-S set			Transect Orientation:			orthogonal						
Number	Spacing (m)	Aperture (mm)	Fill	Mode	Height (m)	Width (m)	Upper	Lower	Orientation	Notes			
1	0				2	0.3	AB		190,90				
2	0.33				0.65	0.15	TI	TI	155,80NE				
3	0.48				0.15	0.02	TI	AF	155,80NE				
4	0.52				0.15	0.02	TI	AF	155,80NE				
5	0.59				0.2	0.05	TI	TI	160,80NE				
6	0.93				0.7	0.02	TI	TI	160,80NE				
7	1.25				0.5	0.05	TI	TI	175,90				
8	1.95				0.25	0.05	TI	TI	175,90				
9	2.21				1	0.1	TI		160,80NE				
10	2.23				0.1	0.05	TI	TI	160,80NE				
11	2.3				0.05	0.05	TI	TI	160,80NE				
12	2.31				0.05	0.05	TI	TI	160,80NE				
13	2.4				0.7	0.1	TI	TI	160,80NE				
14	2.55				0.5	0.2	AF	AF	175,90				
15	2.93				0.9	0.2	AB	TI	185,80SE				
16	2.97				0.7	0.05	TI	TI	185,80SE				
17	3.01				0.3	0.1	TI	TI					
18	3.35				0.7	0.2	AB	TI					

*seems to represent the "background" N-S fracturing

OA1	OA1	OA1	OA1	OA1	OA1	OA1	OA1	OA1	OA1	OA1	OA1
Fracture Set Orientatio		E-W, SE dip			Transect orientation:		orthogonal		*measured in a swarm, see sketch		
Number	Spacing (m)	Aperture (mm	Fill	Mode	Height (m)	Width (m)	Upper	Lower	Orientation	Notes	
1	0.15	1	C		0.3	0.05	TI	TI	085,60SE		
2	0.16				0.15	0.05	TI	TI	080,65SE		
3	0.21				0.5	0.1	TI	TI	080,65SE		
4	0.23				0.4	0.05	TI	TI	080,65SE		
5	0.25	1	C		0.25	0.05	TI	TI	080,65SE		
6	0.26				0.1	0.1	TI	TI	080,65SE		
7	0.28				0.15	0.1	TI	TI	070,65SE		
8	0.31				0.1	0.05	TI	TI	075,60SE		
9	0.34				0.05	0.05	TI	TI	060,55SE		
10	0.39				0.5	0.05	AB	AB	060,55SE		
11	0.4				0.1	0.03	AB	TI	060,55SE		
12	0.42				0.05	0.05	TI	TI	075,65SE		
13	0.47				0.5	0.03	AB	TI	075,55SE		
14	0.49				0.15	0.03	TI	TI			
15	0.54				0.3	0.1	AB	TI	085,60SE		
16	0.56				0.45	0.1	AB	TI	080,60SE		
17	0.58				0.2	0.03	AB		080,60SE		
18	0.62				0.3	0.01	AB				
19	0.68				0.4	0.1	AB		085,55SE		
20	0.78				0.45	0.1	AB	AB	055,60SE		
21	0.84				0.15	0.1	AB	TI	080,60SE		
22	0.9				0.2	0.05	AB	TI	070,65SE		
23	0.95				0.1	0.02	AB	TI	070,65SE		
24	1.01				0.2	0.05	AB	TI	075,75SE		
25	1.04				0.2	0.05	AB	AB	075,75SE		

Fold Name:	Open Syncline	Notes:
Location within fold:	forelimb	E-W frax terminate against N-S frax
Sample Location:	**OS1**	frac density looks fairly uniform
Outrcrop Type:	x-sec	sampled 2-3m west of the swarm in photo K-7,6
Stratigraphic Location:	mid-upper "Upper Lisburne"	
Rock Type(Field Call):	crinoid floatsones/grainstones	see sketches for detailed bed thickness info
Bed Thickness:	1m	
Bed Orientation:	160,20NE	Prominent Fracture Sets:
Nature of contacts:	sharp	see detailed (N-S and E-W)
Thin Section:		
Rock Type(Thin Section):		
Hand Samples:	OS1A,B,C-see sketch for sample locations, OS1 B from lithology where frax were measured	
Photos:	K-7,6 large scale view of frac swarm (not actually at this location) K-4,5 N view of swarm in N-S fracs K-2 S view of sampled horizon	

OS1	OS1	OS1	OS1	OS1	OS1	OS1	OS1	OS1	OS1	OS1	OS1	OS1	OS1
Fracture Set Orientation	N-S set			Transect Orientation:			orthogonal						
Number	Spacing (m)	Aperture (mm)	Fill	Mode	Height (m)	Width (m)	Upper	Lower	Orientation	Notes			
1	0	1	C		0.4	0.03	TI	TI	170,87SW				
2	0.03	2	C		0.45	0.05	AB	TI					
3	0.06	2	C		0.5	0.05	AB	TI	175,90				
4	0.07	1	C		0.1	0.05	TI	TI					
5	0.1	1	C		0.2	0.05	TI	TI					
6	0.12	2	C		0.8	0.05	AB	AB	180,87E	80cm bed thickness			
7	0.17	1	N		0.4	0.05	AB	TI					
8	0.19	3	C		0.8	0.05	AB	ABS					
9	0.23				0.1	0.1	TI	TI					
10	0.25	2	C		0.8	0.1	AB	AB					
11	0.3	2	C		0.6	0.1	ABS	ABS	180,87W				
12	0.32				0.5	0.1	ABS	ABS					
13	0.37				0.3	0.05	TI	AB	180,85E				
14	0.44				0.7	0.1	AB	AB	180,90				
15	0.53				0.3	0.05	AB	AB					
16	0.62				0.3	0.05	AB						
17	0.65				0.8	0.1	AB	AB					
18	0.67				0.2	0.1	AF	AF					
19	0.77				0.2	0.1	AB	AB	180,85E				
20	0.78				0.8	0.1	AB	AB	185,90				
21	0.87				0.5	0.2	AB	AB	180,90				
22	0.89				0.05	0.05	TI	TI					
23	0.95				0.5	0.2	AB	AB					
24	0.97				0.4	0.2	TI	AB					
25	1.03				0.6	0.2	AB	AB	180,90				

OS1	OS1	OS1	OS1	OS1	OS1	OS1	OS1	OS1	OS1	OS1
Fracture Set Orientatio		E-W variable dip			Transect orientation:		orthogonal			
Number	Spacing (m)	Aperture (mm	Fill	Mode	Height (m)	Width (m)	Upper	Lower	Orientation	Notes
1	0				0.3	0.2	AB	AB	090,75S	*almost all of these are very sinuous,
2	0.05				0.15	0.01	TI	AB		terminate against N-S fracs
3	0.25	2	C		0.3	0.2	AB	AB		and their width should
4	0.31				0.2	0.05	AB	AB		be the spacing of the N-S fracs
5	0.39				0.2	0.03	AB	AB		*orientations are variable due to
6	0.4				1		AB	AB	085,75SE	sinuousity!
7	0.43				0.2	0.03	TI	AB		
8	0.45				0.2	0.03	TI	AB		
9	0.46				0.1	0.03	AB			
10	0.47				0.2	0.04	AB	AB		
11	0.55				0.2	0.05	AB	AB	095,80SW	
12	0.61				0.2	0.05	AB	AB	095,80SW	
13	0.66				0.2	0.06	AB	AB		
14	0.72				0.1	0.05	AB	AB		
15	0.83				0.05	0.05	AB	AB		
16	0.86	2	C		0.2	0.06	AB	AB		
17	0.9				0.15	0.09	AB	AB		
18	0.94				0.1	0.04	AB	AB		
19	1	0.5	N		0.05	0.05	TI	TI		
20	1.09	1	N		0.1		AB	AB		
21	1.17				0.05	0.05	AB	AB		
22	1.19				0.05	0.05	TI	TI		
23	1.27				0.2	0.03	AB	AB		
24	1.31				0.2	0.03	AB	AB		
25	1.34				0.05	0.05	TI	TI		
26	1.38				0.1	0.03	TI	AB		
27	1.43				0.2	0.03	AB	AB		

Fold Name: Open Syncline
Sample Location: **OS2**
Outrcrop Type: x-sec
Stratigraphic Location: mid-upper "Upper Lisburne"
Rock Type(Field Call): crinoid floatstones/grainstones
Bed Thickness: 2m
Bed Orientation: 160,15NE
Nature of contacts: sharp, but not as well defined as in OS1
Thin Section:
Rock Type(Thin Section):
Hand Samples: OS2A-lower part of bed
OS2B-upper part of beds (wackestone?)
Photos: K-2,1 N view of outcrop, jake staff=1.5m

DC: prevalent, but not forming any obvious "cleavage" planes
090,65S
090,60S

Prominent Fracture Sets:

Fold Name: Open Syncline
Location within fold: forelimb
Sample Location: **OS3**
Outrcrop Type: x-sec
Stratigraphic Location: mid-upper "Upper Lisburne"
Rock Type(Field Call): crinoid floatstones/grainstones
Bed Thickness:
Bed Orientation: 135,5NE
Nature of contacts: sharp
Thin Section:
Rock Type(Thin Section):
Hand Samples:

Photos: L-33 N view of outcrop
L-32 W view of outcrop showing OS2 to the right

Notes:
no spacings due to close proximity to a NW oriented fault with 1-3m offset
see sketches for stratigraphy

Prominent Fracture Sets:
conjugate sets:

110,80SW	095,55NE
085,75SE	090,70N
105,80SW	080,60NW
105,75SW	085,65NW

other sets
165,75NE-160,70NE
180,80E-175,90

OS2	OS2	OS2	OS2	OS2	OS2	OS2	OS2	OS2	OS2	OS2	OS2	OS2	OS2
Fracture Set Orientation		N-S/NW, E/NE dip		Transect Orientation:			strike=120, and 110 after spacing 2.63m						
Number	Spacing (m)	Aperture (mm)	Fill	Mode	Height (m)	Width (m)	Upper	Lower	Orientation	Notes			
1	0.1				0.4	0.15	TI	AB	175,85NE	*transect starts at the edge of a swarm			
2	0.21				0.25	0.05	TI	AF	175,85NE	and works its way into the swarm			
3	0.25				0.35	0.05	AB	AB		*not terribly representative of			
4	0.33				0.2	0.05	TI	TI	170,85NE	E-W fracs as a whole at			
5	0.47				0.05	0.05	AB		155,85NE	this particular outcrop			
6	0.7				0.1	0.02	AB		145,65NE	*taken through a generally less fractured			
7	1				0.3	0.1	AF	TI	155,75NE	area			
8	1.04				0.4	0.1	AF	TI	165,75NE				
9	1.3				0.5	0.3	AF	AB	160,85NE				
10	1.8				0.4	0.2	AF	TI	160,80NE				
11	2				0.2	0.05	AB	TI	160,80NE				
12	2.15				0.5	0.2			145,80NE				
13	2.5				0.5	0.2			150,90				
14	2.6				0.2	0.05	TI	TI	150,90				
15	2.63				0.05	0.05	AB	AB	150,90				
strike=110	strike=110	strike=110	strike	strike	strike=110	strike=110	strike=1:	strike=1	strike=110	strike=110			
16	2.73	1	C		0.05	0.03	AB	TI	150,90				
17	2.81				0.05	0.05	TI	TI	150,90				
18	2.85				0.2	0.05	TI	AB	165,85NE				
19	2.93				0.05	0.05	AB	AB	165,85NE				
20	2.98				0.1	0.05	TI	TI	170,85NE				
21	3.16				0.1	0.1	TI	TI					
22	3.27	2	C		0.3	0.05	TI	TI	175,90				
23	3.33				0.5	0.05	TI	TI	175,90				
24	3.5				1	0.5	AB		155,85NE				
25	3.73				0.5	0.05	TI	TI	155,85NE				

OS2	OS2	OS2	OS2	OS2	OS2	OS2	OS2	OS2	OS2	OS2	OS2	OS2	OS2
Fracture Set Orientatio		E-W, NE dip			Transect orientation:		orthogonal						
Number	Spacing (m)	Aperture (mm	Fill	Mode	Height (m)	Width (m)	Upper	Lower	Orientation	Notes			
1	0		C		0.2	0.05	TI	TI	110,80NE	*some frax term against N-S			
2	0.01	2	C		0.05	0.05	TI	TI	110,80NE				
3	0.55				0.5	0.1	AB	AB	105,80NE				
4	0.57				0.1	0.1	AB	AF	105,80NE				
5	0.7				0.5	0.5	AB	TI	100,70NE				
6	0.8	1	C		0.5	0.2	AB	AB	105,80NE				
7	0.81	2	C		0.5	0.2	AB	TI	100,75NE				
8	0.82	1	C		0.5	0.2	AB	TI	100,75NE				
9	0.83	2	C		0.5	0.2	AB	TI	100,75NE				
10	0.84	1	C		0.5	0.2	AB	TI	100,75NE				
11	0.85	2	C		0.5	0.2	AB	TI	100,75NE				
12	0.9	1	C		0.5	0.2	AB		100,75NE				
13	0.93	2	C		0.5	0.2	AB	TI	100,75NE				
14	1				0.7	0.3	TI	AB	095,70NE	CB above			
15	1.04	1	C		0.1	0.03	TI	TI	100,70NE				
16	1.15				0.4	0.3	TI	AF	100,70NE				
17	1.2				0.05	0.05	TI	TI	100,70NE				

OS2	OS2	OS2	OS2	OS2	OS2	OS2	OS2	OS2	OS2	OS2	OS2	OS2
Fracture Set Orientatio		E-W, SW dip			Transect orientation:		orthogonal					
Number	Spacing (m)	Aperture (mm	Fill	Mode	Height (m)	Width (m)	Upper	Lower	Orientation	Notes		
1	0.16				0.1	0.05			105,80SW	*L-35,34 E view of this set		
2	0.2				0.5	0.1		AB	105,80SW			
3	0.29	1	N		0.3	0.05	TI	AB	095,75SW			
4	0.33	1	C		0.3	0.05	AB	TI	095,80SW			
5	0.36				0.2	0.05	AB	AB	095,80SW			
6	0.39				0.3	0.05	AB	AB	095,80SW			
7	0.43				0.3	0.05	TI	AB				
8	0.46				0.2	0.05	TI	AB				
9	0.47				0.2	0.05	TI	AB				
10	0.5				0.3	0.05	AB	AB	090,85SW			
11	0.52								070,60SE	ODDBALL!!!!		
12	0.75								060,60SE	ODDBALL!!!!		
13	0.89				0.1	0.1	AB	TI	110,75SW			
14	0.91				0.3	0.1	AF	AB	110,75SW	term against oddball frac		
15	0.92				0.1	0.1	TI	AB	110,75SW			
16	0.94				0.1	0.1	TI	AB	110,75SW			
17	0.97				0.5	0.2	TI	TI	110,75SW	CB		
18	1.1				0.7	0.1	AB	AB	095,85SW			

Fold Name:	Open Syncline
Location within fold:	hinge
Sample Location:	**OS4**
Outrcrop Type:	x-sec
Stratigraphic Location:	mid-upper "Upper Lisburne"
Rock Type(Field Call):	dark colored floatstones/grainstones
Bed Thickness:	1m
Bed Orientation:	095,25NE
Nature of contacts:	sharp
Thin Section:	
Rock Type(Thin Section):	
Hand Samples:	OS4A,B lower bed on sketch
	OS4C-from lithology where frax were sampled in detail
Photos:	L-31 0verview of OS4
	L-30,29 N view of fault between 0S3 and OS4
	OS3 flagged to the left

Notes:
lots of sketches and detailed notes in fieldbook!!!!

DC:
075,25SE

Prominent Fracture Sets:

OS4	OS4	OS4	OS4	OS4	OS4	OS4	OS4	OS4	OS4	OS4	OS4	OS4	OS4
Fracture Set Orientation		N-S/NW, variable dip			Transect Orientation:		strike= 125						
Number	Spacing (m)	Aperture (mm)	Fill	Mode	Height (m)	Width (m)	Upper	Lower	Orientation	Notes			
1	0.54				0.7	0.3	TI		170,70NE	*all AF terminations are against			
2	0.56				0.1	0.1	TI	TI	160,65NE		W dipping conjugate frax		
3	0.59				0.35	0.1	TI	TI	165,75NE				
4	0.63	0.5	N		0.1	0.05	TI	TI	165,75NE				
5	0.65				0.05	0.05	TI	TI	165,75NE				
6	0.67	0.5	N		0.4	0.15	TI	AF	155,70NE	oddball?			
7	0.95				0.2	0.05	AB	TI	155,90				
8	0.89				0.6	0.25	TI	TI	175,80NE				
9	0.99				0.1	0.1	AB	TI	170,80NE				
10	1				0.35	0.1	AF	AF	170,75NE	concave SE			
11	1.1				0.9	0.2	TI	TI	170,70NE				
12	1.19				0.05	0.05	AB	TI	165,85SW	conj to NE dipping frax			
13	1.21				0.25	0.05	AB	AF	180,75W	conj to NE dipping frax			
14	1.36				0.1	0.1	AF	AF	155,75NE				
15	1.38				0.05	0.05	AF	AF	190,70SE				
16	1.39				0.2	0.05	AF	AF	170,75SW				
17	1.5				0.1	0.1	AB	AF	155,65NE				
18	1.6				0.5	0.1	AB	TI	165,65NE	CB			
19	1.65				0.1	0.05	TI	AF	170,75NE				
20	1.67				0.35	0.1	AF	AF	170,65NE	CB			
21	1.7				0.2	0.05	AF	AF	185,80NW				
22	1.71				0.6	0.1	AB	AF	180,55E				
23	1.8				0.4	0.1	TI	TI	185,80NW	CF			
24	1.82				0.35	0.15	AB	AF	170,55NE				
25	1.91				0.15	0.05	AF	TI	165,65NE				
26	2	2	C		0.1	0.1	AF	TI	160,75NE				
27	2.1				1.5	0.3	TI		185,65NW				
28	2.05				1.5	0.3	TI	TI	160,75NE				
29	2.25				0.5	0.5	AF	TI	165,60NE				

OS4	OS4	OS4	OS4	OS4	OS4	OS4	OS4	OS4	OS4	OS4
Fracture Set Orientatio	E-W, variable dip			Transect orientation:			orthogonal			
Number	Spacing (m)	Aperture (mm	Fill	Mode	Height (m)	Width (m)	Upper	Lower	Orientation	Notes
1	0				0.4	0.05	TI	TI	085,80NW	*measured through small swarm
2	0.09				0.1	0.02	TI	TI	085,80NW	see sketch
3	0.15				0.2	0.02	TI	TI		
4	0.22				0.1	0.1		TI	070,80NW	
5	0.47	2	C		0.6	0.1	TI	TI	075,80NW	CB ech set down to S shear
6	0.5	0.5	N		0.2	0.03	TI	TI	080,75NW	ech set down to S shear
7	0.64	1	C		0.1	0.05	AB	TI		?maybe diff frac set?!!?
8	0.73	,5	N		0.15	0.03			070,80NW	
9	0.84	2	C		0.15	0.05		TI	080,85SE	en ech set, vertical extent 15cm
10	0.85	2	C		0.1	0.03		TI	080,85SE	
11	0.86	2	C		0.1	0.03		TI	080,85SE	
12	0.92	0.5	C		0.05	0.05	TI	TI	095,80NE	
13	0.93	0.5	C		0.1	0.1	TI	TI	095,80NE	
14	0.95	0.5	C		0.2	0.03	AF	TI	075,65NW	
15	0.96	0.5	C		0.1	0.03	AF	TI	075,75NW	
16	0.98	0.5	C		0.1	0.03	AF	TI	075,75NW	
17	1.01	0.5	C		0.15	0.03	TI	TI	080,75NW	
18	1.02	0.5	C		0.05	0.05	TI	TI	080,75NW	
19	1.05	1	C		0.05	0.05	TI	TI	080,75NW	
20	1.1	0.5	C		0.15	0.01	TI	TI	080,75NW	
21	1.12	0.5	C		0.15	0.01	TI	TI	080,85NW	
22	1.16	1	C		0.03	0.03	TI	TI	080,85NW	
23	1.17	1	C		0.1	0.03	TI	TI		ech set down to S shear
24	1.19	0.5	C		0.2	0.05	TI	TI	080,85NW	
25	1.25	0.5	N		0.25	0.05	TI	TI	085,75NW	ech set down to S shear

*many have down to S sense of shear,
as opposed to 100-110 set which seem
to have down to N sense of shear (bed parallel?)

Fold Name:	Open Syncline
Location within fold:	backlimb
Sample Location:	**OS6**
Outrcrop Type:	x-sec
Stratigraphic Location:	mid-upper "Upper Lisburne"
Rock Type(Field Call):	dark colored floatstones/grainstones
Bed Thickness:	1-2m?
Bed Orientation:	055,50NW
Nature of contacts:	sharp
Thin Section:	
Rock Type(Thin Section):	
Hand Samples:	OS6D-056,63NWoverturned (lithology) many others, not in sampled horizon

Photos:

Notes:
major bed parallel slip surface near OS6
VERY detailed notes and sketches in fieldbook!!!
*curiously not very fractured

Prominent Fracture Sets:

OS6	OS6	OS6	OS6	OS6	OS6	OS6	OS6	OS6	OS6	OS6	OS6	OS6	OS6
Fracture Set Orientation		N-S variable dip		Transect Orientation:			orthogonal						
Number	Spacing (m)	Aperture (mm)	Fill	Mode	Height (m)	Width (m)	Upper	Lower	Orientation	Notes			
1	0.09	1	C		0.1	0.05	AF	AF	185,80SE				
2	0.43				0.15	0.05	TI	TI	165,75SW				
3	0.54				0.25	0.1	AF	TI	175,80NE				
4	0.62				0.15	0.05	TI	AF	175,70NE				
5	0.65				0.15	0.05	TI	TI	165,80NE				
6	0.66				0.3	0.05	TI		185,80SE				
7	0.76				0.4	0.05	TI	TI	170,80NE				
8	0.8				0.35	0.05	AF	TI	185,75SE	en ech set, steps down to E, shear to W			
9	0.83				0.3	0.1	TI	TI	185,75SE	en ech set, steps down to E, shear to W			
10	0.85				0.3	0.1	TI	TI	185,75SE	en ech set, steps down to E, shear to W			
11	0.87				0.05	0.05	TI	TI	185,75SE	en ech set, steps down to E, shear to W			
12	1.05				0.1	0.1	TI	TI	180,85W				
13	1.2				0.15	0.05	TI	TI	170,80NE				
14	1.3				0.1	0.1	AF	TI	165,70NE				
15	1.45				0.05	0.05	AF	TI	165,70NE	en ech set, steps down to E, shear to W			
16	1.5				0.15	0.05	TI	TI	165,70NE				
17	1.74				0.4	0.2	TI						
18	1.86				0.1	0.1	TI	TI					
19	1.9				1	0.5							

Camp Syncline East

Fold Name:	Camp Syncline, East Side				Notes:
Location within fold:	forelimb				DC-060,45SE, probably axis II, syncline axis 070, 45SE
Sample Location:	**F1**				Sheared stylolites, bed II, top to north
Outrcrop Type:	x-sec				
Stratigraphic Location:	Mid-Upper "Upper Lisburne"				
Rock Type(Field Call):	crinoid grainstone/packstone with 5cm thick chert beds				
Bed Thickness:	1 meter				
Bed Orientation:	030,20SE	050,15SE	050,20SE	060,16SE	Prominent Fracture Sets:
Nature of contacts:	sharp contacts with chert				055-060,80-90NW
Thin Section:					170,90
Rock Type(Thin Section):					030,90
Hand Samples:	F1A-sheared crinoids + rock type				
	F1B-DC				
Photos:	Roll? Exp 33,32-050 set				

F1	F1	F1	F1	F1	F1	F1	F1	F1	F1	F1	F1	F1	F1
Fracture Set Orientatio		050,80NW-90		Transect orientatio		orthogona	N=	23					
Number	Spacing (m)	Aperture(mm)	Fill	Mode	Height (m)	Width (m)	Upper	Lower	Notes				
1	0	2	C	U	1.5	0.2	TI	AB	lower term against chert layer				
2	0.03	1	C	U	0.11	0.5	TI	TI					
3	0.11	<1	N	U	0.21	0.02	AB	TI					
4	0.25	4	C	U	1	0.13	AB	AB					
5	0.36	<.5	N	U	0.45		TI	TI					
6	0.44	1	C	U	0.7		TI	TI					
7	0.55	2.5	C	U	1	0.2	AB	AB					
8	1	1	C	U	0.4		TI	TI					
9	1.94	0.5	C	U	0.3	0.12	AB	TI					
10	2.55	<.5	C	U	0.45	0.09	AB	TI					
11	2.56	1	C	U	1	0.05	AB	TI					
12	2.63	<.5	N	U	0.45		AB	TI					
13	2.66	1	C	U	0.14		TI	TI	steps down to N				
14	2.7	<.5	N	U	0.35	0.05	TI	TI					
15	3.17	<.5	N	U	0.25		TI	TI					
16	3.23	<1	N	U	0.19		TI	TI					
17	3.87			U	0.4		AB	TI					
18	4.35	5	C	U	0.36		AB	TI	dip=40				
19	4.48			U	0.2		TI	TI					
20	4.65	2		U	0.2		TI	TI					
21	4.8		C	U	0.45		TI	U					
22	4.86	<.5	N	U	0.3		TI	U					
23	4.95			U	1	0.15	TI	U					

F1	F1	F1	F1	F1	F1	F1	F1	F1	F1
Fracture Set Orientatio		170,90		Transect orientatio		orthogona	N=	28	
Number	Spacing (m)	Aperture (mm	Fill	Mode	Height (m)	Width (m)	Upper	Lower	Notes
1	0	U	U	U	1.9	U	TI	U	
2	0.35	U	U	U	0.4	1	TG	TG	
3	1.35	3	C	U	5	1.5	TG	TG	WHAT THE HELL IS TG????
4	1.37	1.5	C	U	0.7	0.2	TI	AF	
5	1.42	3	C	U	0.78	0.3	TI	AF	lower termination into frac: 030,90
6	1.74	1.5	U	U	2	0.5	U	AB	
7	1.94	0.5	N	U	0.2	0.2	U	TI	
8	1.96	1.5	C	U	1.8	U	TI	TI	
9	1.98	1.5	C	U	1.5	U	AB	AB	
10	2.03	1	C	U	2.5	1.6	TG	AB	
11	2.19	U	C	U	3	0.4	TG	AB	
12	2.22	1.5	C	U	0.3	0.2	TI	AF	
13	2.24	1.5	C	U	3	2	U	AF	
14	2.35	U	C	U	0.7	2	TI	U	
15	2.43	2	N	U	0.4	2	U	U	
16	2.48	2	C	U	U	0.6	U	U	
17	2.6	0.5	N	U	U	0.6	TI	U	
18	2.7	0.5	Q	U	0.7	0.4	TI	U	
19	2.77	1	C	U	0.3	U	AB	AF	
20	3	1	C	U	0.35	U	AB	AB	steps down to E
21	3.06	U	C	U	3	0.5	U	AB	
22	3.3	1	C	U	0.9	0.7	TI	AB	
23	3.44	0.5	C	U	0.25	0.1	TI	AB	
24	3.52	1	C	U	0.4	0.4	Upper	AB	steps down to S
25	3.68	1	C	U	2.5	U	TI	TG	
26	3.85	1	C	U	3	U	TI	AB	steps down to W
27	3.95	0.5	C	U	3	0.15	TI	U	
28	4.05	2	N	U	2	0.3	TG	AB	

Fold Name:	Camp Syncline, East side
Location within fold:	forelimb, well N of F1
Sample Location:	**F2**
Outrcrop Type:	x-sec
Stratigraphic Location:	Mid-Upper "Upper Lisburne"
Rock Type(Field Call):	crinoid grainstones w/ round chert nodules (up to 1m diam)
Bed Thickness:	1-3m (but difficult to define)
Bed Orientation:	025,10SE
Nature of contacts:	sharp contacts defined by chert nodules+"normal" contacts
Thin Section:	
Rock Type(Thin Section):	
Hand Samples:	?

Photos: Roll ?, Exp 31-overview outcrop
Exp 30-intense veining/shattering, see sketch

Notes: round chert, not as elongate/bedded as in F1
N dipping fracs + veins, top to N offset
Echelon Fracs zone-155,90, down to N sense,
veins in set described above-160,70SW
DC-050,55SE
DC-070,40SE

Prominent Fracture Sets:
075-080,80-90SE
150-160,45NE
150,90
120,70NE

F2	F2	F2	F2	F2	F2	F2	F2	F2	F2	F2	F2	F2	F2
							N=	29					
Fracture Set Orientatio	075-080,90			Transect orientatio	strike 040 until frac spacing 1.65m, then orthogonal								
Number	Spacing (m)	Aperture (mm	Fill	Mode	Height (m)	Width (m)	Upper	Lower	Notes				
1	0	1	C	U	0.35	0.05	AB	U					
2	0.04	2	U	U	0.8	0.4	U	AF					
3	0.2	1.5	N	U	1.3	0.4	U	TI					
4	0.35	1.5	N	U	1.3	0.2	TI	U					
5	0.5	3	C	U	1.2	0.2	AB	U	hert nodule: 080,85SE				
6	0.74	1	N	U	0.2	0.15	TI	TI	ntation 075,85SE				
7	0.79	1	C	U	0.3	0.15	TI	TI					
8	0.81	2	C	U	0.8	0.4	TI	AB					
9	1.1	4	C	U	1.4	0.35	AB	AB					
10	1.15	4	C	U	1	0.1	AB	TI					
11	1.25	1	C	U	0.4	U	TI	TI					
12	1.43	3	U	U	0.13	0.2	AB	AF					
13	1.49	2	C	U	1.1	0.3	AB	AF	ientation 080,90				
14	1.57	5	C	U	0.9	0.15	AB	AF					
15	1.65	3	C	U	0.6	0.2	TI	TI	SE, shear zone extends 1m				
	ORTHOGONAL												
16	0.1	5	C	U	1.3	0.5	TI	U					
17	0.2	2	C	U	0.65	0.3	TI	AB					
18	0.23	2	C	U	0.3	0.2	AB	AB					
19	0.25	3	C	U	0.25	0.2	AB	AB					
20	0.31	2	U	U	0.3	0.2	AB	AB					
21	0.33	3	U	U	0.3	0.15	AC	TI	AC = against chert				
22	0.36	1	N	U	0.08	0.08	AC	TI	steps down to SE, shear zone extends .4m				
23	0.4	1	C	U	0.4	0.15	AC	TI	F orientation 080,80SE				
24	0.49	0.5	N	U	0.4	0.2	AC	AB					
25	0.5	1	N	U	0.3	0.1	AC	AC					
26	0.51	4	C	U	1	0.15	AC	U	ntation 080,80SE				
27	0.64	1	C	U	1.3	0.2	AB	AC	down to NW				
28	0.7	1	U	U	1	0.2	AB	AF					
29	0.8	4	U	U	2	0.5	AF	U					

F2	F2	F2	F2	F2	F2	F2	F2	F2	F2	F2	F2	F2	F2
Fracture Set Orientatio	N-S set			Transect orientatio	40								
Number	Spacing (m)	Aperture (mm	Fill	Mode	Height (m)	Width (m)	Upper	Lower	Orientation	Notes			
1	0	0.5	N		0.7	0.4	AF		155,85SW	upper=shallow 170frac			
2	0.15	1	C		0.8	0.3	TI		160,75SW				
3	0.43	0.5			0.6	0.2		TI	150,85SW				
4	0.57				1	0.2	TI		135,80SW				
5	0.57	10	C		0.5	0.2	TI	TI	170,80SW	part of ech set, shear down to NE			
6	0.65	3	C		1	0.1	TI		170,80SW				
7	1	3	C		0.7	0.1	TI	TI	150,90				
8	1.15	1	C		1.3	0.2	AF		155,85SW				
9	1.2				0.4	0.1	TI		165,90				
10	1.38	1	C		0.65	0.05	TI	TI	150,90				
11	1.5	1	C		0.7	0.1	TI	AF	155,90				
12	1.55	0.5	N		0.2		TI	AF					
13	1.6	2	C		0.76	0.1	AB	TI	130,90				
14	1.61	1.5	C		0.53	0.05	AF	AC		upper terminates against a frac that is part			
15	1.65	1.5	C		0.8	0.1	TI	AF	145,90	lower terminates against a frac that is part			
16	1.66	1.5	C		0.6	0.1	AF	AF	150,90	both terminations against a fracs that are p			
17	1.72				0.2	0.15	TI	TI	145,90	shear down to NE			
18	1.89				0.85	0.1	AB	AB	160,85SW	sinuous			
19	2.24	1	C		0.8	0.05	AB	TI	140,80SW				
20	3.55				0.4	0.1	AB	AB	130,75SW				
21	3.71				0.5	0.05	AF	AB	140,70SW				

West Camp Syncline, Lower Transect

Fold Name:	Camp Syncline, West side		Notes:	N-S set well developed
Location within fold:	backlimb	top of transect bed		
Sample Location:	**F4**			
Outrcrop Type:	x-sec			
Stratigraphic Location:	Mid "Upper Lisburne"			
Rock Type(Field Call):	mudstone/wackestone			
Bed Thickness:	20-30cm small scale, 2m thick larger scale			
Bed Orientation:	070,20SE	080,10SE	Prominent Fracture Sets:	
Nature of contacts:	difficult to see		040,90	axis II conjugates??
Thin Section:			085,75NW	
Rock Type(Thin Section):			130,85NE	115-120strike, mostly 124-140
Hand Samples:	F4-rock type		130,85SW	120-130strike

Photos:

F4	F4	F4	F4	F4	F4	F4	F4	F4	F4	F4	F4	F4
Fracture Set Orientation		040,90			Transect Orientat	strike = 13(	N=	27				
Number	Spacing (m)	Aperture (mm)	Fill	Mode	Height (m)	Width (m)	Upper	Lower	Notes			
1	0				0.3	0.5	U	AB	040,90			
2	0.05	2.5	N		0.4	0.2	U	AB				
3	0.2				0.1	0.2	AB	AB				
4	0.35				0.45	0.3	AB	AB				
5	0.45				0.15	0.2	TI	AB	044,90			
6	0.65				1	2	U	AB				
7	0.9				0.1	0.2	TI	AB	steps down to S			
8	1				0.25	0.25	AB	AB				
9	1.15				0.25	0.25	AB	AB				
10	1.35	0.5	N		0.25	0.1	AB	AB				
11	1.45				0.15	0.2	AB	AB	040,90			
12	1.48				0.15	0.13	AB	AB				
13	1.53				0.15	0.5	AB	AB				
14	1.55				0.25	0.7	AB	AB				
15	1.6				0.1	0.1	AB	AB				
16	1.67	0.5			0.15	0.2	AB	AB				
17	1.73				0.3	0.4	AB	AB				
18	1.75				0.1	0.15	AB	AB				
19	1.85				0.15	0.15	AB	AB				
20	1.91				0.2	0.35	AB	AB				
21	1.94				0.2	0.5	AB	AB	050,80NW			
22	2	1	N		0.25	0.1	AB	AB	steps down to S			
23	2.03	1	N		0.15		TI	AB	steps down to N			
24	2.1				0.15		AB	AB	050,80NW			
25	2.15				0.2	0.15	AB	AB				
26	2.35				0.5	0.2	AB	AB				
27	2.4	1			0.4	0.1	AB	AB				

F4	F4	F4	F4	F4	F4	F4	F4	F4	F4	F4
Fracture Set Orientation:		130,NE a		Transect orientation:		strike =	N=	18		
Number	Spacing (m)	ture (	Fill	Mode	Height (m)	Width (m	Upper	Lower	Orientation	Notes
1	0	4			2	1	U	U	130,60NE	
2	0.36	1	N		0.1	0.05	TI	TI	150,75NE	
3	1.07				0.15	0.1	AB	AB	135,90	
4	1.15				0.4	0.2	AB	AB	135,90	
5	1.25				0.45	0.25	AB	AB	140,80NE	
6	1.5				1.6	1	AB	U	140,90	
7	1.77				0.2	0.2	TI	TI	135,90	
8	1.9				2	1	U	U	130,85SW	
9	2				0.1	0.05	AB	AB	145,80SW	
10	2.2				0.1	0.05	AF	AF	135,50NE	Terminates against
11	2.3	1	C		0.6	0.2	AF	AF	110,50SW	previous fracture
12	2.65	1	N		1.3	0.5	AB	AB	115,70NE	
13	2.91				0.1	0.1	TI	AB	115,75NE	
14	3.25	1	N		0.1	0.05	TI	AB	125,85SW	
15	3.7				2	1	U	U	120,80NE	
16	4.05				0.1	0.1	AB	AB	125,80NE	
17	4.15				0.3	0.4	AB	AB	125,85NE	
18	4.25				0.5	0.55	AB	AB	145,70NE	

Fold Name:	Camp Syncline, West Side
Location within fold:	middle backlimb
Sample Location:	**F5**
Outrcrop Type:	x-sec w/ underside pavement
Stratigraphic Location:	Mid "Upper Lisburne"
Rock Type(Field Call):	massively bedded mudstone/wackestone
Bed Thickness:	2 m
Bed Orientation:	095,55NE
Nature of contacts:	planar sharp
Thin Section:	
Rock Type(Thin Section):	
Hand Samples:	?

Photos:

Notes: shattered cherty bed above
transect bed w/ thinner bed at base

See sketches!

Well developed DC-085,60SE

timing-DC post N-S set!?!?

A few N-S fracs terminate against DC-contradicts previous note!

Prominent Fracture Sets:

170, 90	well developed, down to E and W sense on steps
035,60NW	minor set, swarms at lower bedding contact
150,60NE	minor set, swarms at lower bedding contact both with height/width no greater than .3m

F5	F5	F5	F5	F5	F5	F5	F5	F5	F5	F5	F5	F5
Fracture Set Orientation	170,90			Transect Orientat	orthogonal	N=	26					
Number	Spacing (m)	Aperture (mm)	Fill	Mode	Height (m)	Width (m)	Upper	Lower	Notes			
1	0	1	C		0.5	0.1	TI	AB				
2	0.1				0.5	0.2	TI	AB	**All fractures of this set**			
3	0.18				0.5	0.5	TI	AB	**are members of echelon**			
4	0.23				0.5	0.3	TI	AB	**sets that step down to the W**			
5	0.3				0.3	0.2	TI	AB	**and cover the thickness of the bed**			
6	0.33				0.1	0.2	TI	AB				
7	0.37				0.1	0.2	TI	AB				
8	0.4				0.1	0.2	TI	AB				
9	0.47				0.4	0.5	TI	AB				
10	0.53				0.4	0.5	TI	AB				
11	0.57				0.2	0.3	TI	AB				
12	0.67				0.3	0.3	TI	AB				
13	0.74				1	1	TI	AB				
14	0.79				1	1	TI	AB				
15	0.84				1	1	TI	AB				
16	0.99				0.5	0.5	TI	TI				
17	1.09				0.5	0.5	TI	TI				
18	1.24				1.3	0.5	TI	TI				
19	1.39				0.4	0.2	TI	AF	terminates against DC			
20	1.44				0.1	0.1	TI	AF	terminates against DC			
21	1.49				2	0.4	AB	TI				
22	1.64				0.8	0.2	TI	AB				
23	1.74				0.3	0.05	TI	TI				
24	1.87				0.3	0.3	TI	TI				
25	1.97				0.4	0.2	TI	TI				
26	2.14	3	C		0.8	0.3	U	TI				

Fold Name: Camp Syncline, West Side
Location within fold: backlimb
Sample Location: **F6**
Outrcrop Type: x-sec
Stratigraphic Location: Mid "Upper Lisburne"
Rock Type(Field Call): massively bedded mud-wackestone
Bed Thickness: 1.5 m
Bed Orientation: 095,65NE
Nature of contacts: planar sharp
Thin Section:
Rock Type(Thin Section):
Hand Samples:

Photos:

Notes:

Prominent Fracture Sets:
138,63SW
175-210,80SE-90
085,55NE

Fold Name: Camp Syncline, West side
Location within fold: backlimb near hinge
Sample Location: **F6A**
Outrcrop Type: pavement
Stratigraphic Location: Mid "Upper Lisburne"
Rock Type(Field Call): ?
Bed Thickness: ?
Bed Orientation: 090,60N 095,65NE
Nature of contacts: ?
Thin Section:
Rock Type(Thin Section):
Hand Samples:

Photos:

Notes: compare to F10 and F6
N-S, W dipping related to normal faulting or folding or plunge?

Prominent Fracture Sets:

200,85NE	very well developed before 175,45SW set
175,45SW	very well developed
090,35S	local?
070,30SE	local?

F6	F6	F6	F6	F6	F6	F6	F6	F6	F6	F6	F6	F6
Fracture Set Orientation		138,63SW		Transect Orientat		strike = 60	N=	13				
Number	Spacing (m)	Aperture (mm)	Fill	Mode	Height (m)	Width (m)	Upper	Lower	Notes			
1	0				0.1	0.1	AF	AF				
2	0.3				0.5	0.3	AF	AB				
3	0.75				0.5	0.25	U	AB				
4	0.85				0.7	0.3	AF	AB				
5	0.9				0.3	0.2	AF	U				
6	1.1				0.3	0.2	AF	U				
7	1.15				0.3	0.15	AF	U				
8	1.25				0.5	0.3	U	U				
9	1.35	1	C		0.12	0.05	AF	AF				
10	2	2	N		1.75	1	AB	AB	135,70SW			
11	2.25	2	N		0.65	0.5	AB	TI	part of echelon set, steps down to NE			
12	2.78	1	N		0.8	0.2	AB	TI	part of echelon set, steps down to NE			
13	2.95	0.5	N		0.8	0.1	AF	TI	part of echelon set, steps down to NE			

F6	F6	F6	F6	F6	F6	F6	F6	F6	F6	F6
Fracture Set Orientation:		N-S-210	Transect orientation:			strike=1	N=	13		
Number	Spacing (m)	ture (	Fill	Mode	Height (m)	Width (m	Upper	Lower	Orientation	
1	0				0.7	0.15	AB	AF	205,90	
2	0.2				0.8	0.1	AF	AF	210,80SE	
3	0.67				0.5	0.1	AB	AF	180,85SE	
4	0.7				0.1	0.2	AF	AF	195,90	
5	0.8				0.2	0.1	TI	AF	185,85SE	
6	1.1				1.5	0.5	AB	U	210,85SE	
7	1.15				0.6	0.2	AB	U	210,80SE	
8	1.23				0.6	0.2	AB	U	210,80SE	
9	1.27				0.4	0.2	AB	U	210,80SE	
10	2	1	N		1	1	U	U	175,85NE	
11	2.4				0.4	0.2	AB	AF	180,80E	
12	3.1				3	0.3	AB	AB	210,80SE	
13	3.6				0.5	0.2	AF	AB	210,70SE	

F6

Fracture Set Orientation:		085,55SE	Transect orientation:			strike=2	N=	7	
Number	Spacing (m)	ture (	Fill	Mode	Height (m)	Width (m	Upper	Lower	Notes
1	0.25				0.6	0.6	U	AF	
2	0.45				0.1	0.1	TI	TI	
3	0.55				0.1	0.1	U	AF	
4	0.73				0.1	0.1	TI	AF	
5	0.8				0.3	0.1	TI	AF	
6	1.1	1			0.4	0.2	TI	AF	
7	1.2	1			0.4	0.2	AF	AF	

Fold Name:	Camp Syncline, West Side				Notes:	2-3m north of the hinge
Location within fold:	hinge/forelimb				see sketch for timing relationships: early N-S followed by later E-W set	
Sample Location:	**F7**					
Outrcrop Type:	x-sec					
Stratigraphic Location:	Mid "Upper Lisburne"				some evidence for strike II conjugates, compare to F8?	
Rock Type(Field Call):	massively bedded mudstone					
Bed Thickness:	2m					
Bed Orientation:	090,20SW	105,20SW	095,20SW	093,35S	Prominent Fracture Sets:	
Nature of contacts:	sharp				220,70SE	
Thin Section:					075,75SE	
Rock Type(Thin Section):					090,70S	
Hand Samples:						

Photos:

Fold Name:	Camp Syncline, West Side	Notes:	see field notes, conjugates of conjugates etc.
Location within fold:	backlimb		
Sample Location:	**F8**		
Outrcrop Type:	x-sec		
Stratigraphic Location:	Mid "Upper Lisburne", stratigraphically ABOVE the detailed frax sample locations		
Rock Type(Field Call):	dolomitized?/silicified? mudstone? Very hard		
Bed Thickness:	20-30cm		
Bed Orientation:	095,60NE	Prominent Fracture Sets:	
Nature of contacts:	undulating sharp contacts	095,40SW	
Thin Section:		235-210,65-50SE	
Rock Type(Thin Section):		130-110,40-55SW	
Hand Samples:		195-180,75-85SE	
		185-175,60-85W	

Photos:

F7	F7	F7	F7	F7	F7	F7	F7	F7	F7	F7	F7	F7
Fracture Set Orientation		220,80SE		Transect Orientat		orthogonal	N=	20				
Number	Spacing (m)	Aperture (mm)	Fill	Mode	Height (m)	Width (m)	Upper	Lower	Orientation	Notes		
1	0.1				0.7	0.3	AF	AF	225,75SE			
2	0.55				0.4	0.1	AF	AF		en echelon, steps down to NW		
3	0.7				0.3	0.1	AF	AF	215,85SE			
4	0.85				0.1	0.1	AF	AF	200,80SE			
5	1.35				0.8	0.2	AB	AF	205,80SE			
6	1.5	1	N		0.1	0.1	AF	AF	215,70SE			
7	1.8				0.05	0.05	AF	AF	200,35SE			
8	1.9	1	N		1	0.1	TI	AF	235,80SE			
9	2.05	0.5	C		0.4	0.1	TI	TI	210,75SE	en echelon, steps down to NW		
10	2.07	0.5	C		0.4	0.05	AF	TI	225,75SE	en echelon, steps down to NW		
11	2.13	0.5	C		0.4	0.05	TI	TI	220,70SE	en echelon, steps down to NW		
12	2.2	0.5	C		0.4	0.1	TI	AF	225,70SE	en echelon, steps down to NW		
13	2.25	0.5	C		0.2	0.1	TI	TI	215,85SE	en echelon, steps down to SE		
14	2.4	0.5	C		0.2	0.1	TI	AF	215,75SE	en echelon, steps down to NW		
15	2.45				0.2	0.1	TI	TI	220,70SE	en echelon, steps down to NW		
16	2.46				0.1	0.1	TI	TI	220,70SE	en echelon, steps down to NW		
17	2.55				0.1	0.1	TI	TI	220,70SE	en echelon, steps down to SE		
18	2.6				0.2	0.1	TI	AF	230,75SE	en echelon, steps down to SE		
19	2.7				0.1	0.1	U	U	210,75SE			
20	2.8				0.05	0.1	U	U	220,75SE			

F7	F7	F7	F7	F7	F7	F7	F7	F7	F7	F7
Fracture Set Orientation:		090,70S		Transect orientation:		orthogo	N=	14		
Number	Spacing (m)	ture (	Fill	Mode	Height (m)	Width (m	Upper		Lower	Notes
1	0				0.7	0.3	U		U	**mostly .5mm aperture w/**
2	0.2				0.3	0.3	AF		AF	**calcite or no fill**
3	0.35				0.4	0.65	AB		AB	(Sorry,this location was on the edge
4	0.5				0.8	0.5	AF		AF	of a cliff and couldn't really measure
5	0.6				0.3	0.2	AB		TI	apertures or see fill very well)
6	0.66				0.15	0.1	AB		TI	**biased to larger sizes because of outcrop**
7	0.72				0.8	0.6	AB		AF	
8	0.95				0.4	0.3	AB		AF	
9	1.14				0.4	0.3			AF	
10	1.17				0.5	0.3			AF	
11	1.27	0.5	N		0.55	0.2	AB		TI	
12	1.36				0.5	0.3	TI		TI	
13	1.44				0.6	0.4	AB		AF	
14	1.59				0.7	0.3	AB		AB	

Fold Name:	Camp Syncline, West Side
Location within fold:	Forelimb
Sample Location:	**F9**
Outrcrop Type:	x-sec
Stratigraphic Location:	Mid "Upper Lisburne", probably just ABOVE the trans
Rock Type(Field Call):	massively bedded wacke-packstone interbeds
Bed Thickness:	1.3-1.5m
Bed Orientation:	095-105,15SW
Nature of contacts:	gradational with bedded white chert at the base, sharp at the top
Thin Section:	
Rock Type(Thin Section):	
Hand Samples:	F9A-Slicks: N85W,80SW, rake 60E, 170,85NE? Overturned? F9B-170,80SW F9C-DC
Photos:	Roll L: Exp 5,4, W view of sheared stylolites, pencil points N Exp 3, W view of outcrop Exp 2, N view of outcrop Roll M: Exp37,36, bed II shear veins Exp 35,34, more bed II shear veins Exp 33, W view at E-W set Exp32, 31, close up of shear veins near bedded white chert

Notes: overall, the N dipping E-W fracs are very thin and curve
some large N dipping E-W fracs show slicks with down to N sense
the S dipping E-W fracs are similar, but are much less dense
larger, thru going S dipping E-W fracs have good slicks with down to the south sense

Slicks on E-W Fracs
Frac:085,50NW, rake 90, down to N
Frac:275,80SW, rake 60E, down to S
E-W fracs appear to post date bed II set, but unclear

N-S fracs post date bed II set
spacing of bed II set concentrated near bed surfaces

Prominent Fracture Sets:
See fracture data below

F9	F9	F9	F9	F9	F9	F9	F9	F9	F9	F9	F9	F9
Fracture Set Orientation		E-W, NE dipping		Transect Orientat		strike = 19(	N=	25				
Number	Spacing (m)	Aperture (mm)	Fill	Mode	Height (m)	Width (m)	Upper	Lower	Orientation	Notes		
1	0	1	N		0.4	0.03		AST	105,55NE	AST=against stylolite		
2	0.04	1	C		0.2	0.03	AB	TI	115,60NE			
3	0.09	1	C		0.05	0.05	TI	TI	045,65NW	CB		
4	0.11	1	C		0.15	0.05	TI	TI	045,65NW	CB		
5	0.12	1	C		0.05		TI	TI	045,65NW			
6	0.15		C		0.15	0.05	AB	AF	105,80NE			
7	0.18	0.5	C		0.1	0.03	AF	TI	095,70NE			
8	0.19	1	N		0.3	0.03	AF		100,75NE			
9	0.23	1	C		0.35	0.05	AF	AF	095,70NE			
10	0.48		N		0.35		ABS	TI	080,75NE	ABS=against chert bedding surfac		
11	0.51	1	N		0.15		AB	TI	080,75NE	orientation rotates to SW at the		
12	0.72				0.05		ABS	AF	105,85NE	lower frac termination, ie:		
13	0.85				0.1		AB	TI		concave SW		
14	0.9				0.1		AB	AB	105,85NE	see previous note		
15	0.95	1	C		0.35	0.03	AF	TI	105,80NE			
16	1.06	0.5	N		0.35	0.03	AB	TI	105,80NE			
17	1.08	1	N		0.3	0.03	AF	AB	105,85NE			
18	1.18	1	N		0.45	0.02	AF	AB	100,80NE	CB		
19	1.22	1	N		0.65	0.05	AB	TI	105,85NE	steps down to S		
20	1.27	2	C		0.7	0.3		TI	100,90			
21	1.33	1	C		0.35	0.05	ABS	TI	105,85NE			
22	1.34	1	N		0.3	0.05	TI	AB	110,90			
23	1.43				0.3	0.05	AF	AF	110,90			
24	1.6	1	C		0.2	0.05	TI	AB	110,85NE			
25	1.64	1	C		0.3	0.05	AB	AF	110,85NE			

F9	F9	F9	F9	F9	F9	F9	F9	F9	F9	F9
Fracture Set Orientation:		N-S set		Transect orientation:		orthogo	N=	11		
Number	Spacing (m)	ture (	Fill	Mode	Height (m)	Width (m	Upper	Lower	Orientation	Notes
1	0				0.15	0.15	AB		175,85NE	
2	0.15				0.3	0.15	AB		175,85NE	
3	0.25				0.25	0.1	AB		200,90	
4	0.31				0.2	0.15	AB	AB	190,90	
5	0.45				0.5	0.1	AB	AB	195,90	
6	0.8	1	C		0.1	0.1	AB	AB	195,85SE	
7	0.9				0.15	0.1	AB	TI	195,85SE	
8	1.03				0.5	0.2	AB	AB	185,90	curving frac
9	1.35				0.2	0.1	AB	AB	175,85NE	curving frac
10	1.49				0.5	0.1	AB	AB	190,85SE	
11	1.8				0.7	0.1	AB	AB		

F9	F9	F9	F9	F9	F9	F9	F9	F9	F9	F9
Fracture Set Orientation:		095,20SV		Transect Orientation:		orthogo	N=	15		
Number	Spacing (m)	ture (	Fill	Mode	Height (m)	Width (m	Upper	Lower	Notes	
1	0	5	C		0.3	1			Sinuous, follows bedding	
2	0.02	2	C		0.05	0.2	TI	TI		
3	0.05	1	C		0.05	0.2	TI	TI		
4	0.06	1	C		0.05	0.7	AF	AF	fold, top to NW shear	
5	0.07	2	C		0.05	0.05	TI	TI		
6	0.08	1	C		0.05	0.1	TI	TI		
7	0.15		C		0.2	1	TI			
8	0.26	2	C		0.1	1				
9	0.32	2	C		0.05	0.5	TI	TI		
10	0.33	0.5	C		0.1	0.5	TI	TI		
11	0.36	1	C		0.1	0.5	TI	TI		
12	0.41	0.5	C		0.05	0.5	TI	TI		
13	0.42	2	C		0.05	0.5	TI	TI		
14	0.44	1	C		0.05	0.3	TI	TI		
15	0.6				0.05	1				

Fold Name:	Camp Syncline, West Side
Location within fold:	backlimb
Sample Location:	**F10**
Outrcrop Type:	x-sec with pavement
Stratigraphic Location:	Mid "Upper Lisburne", between 118m-121m on MS-1
Rock Type(Field Call):	massive mud/wackestone with wispy chert laminations
Bed Thickness:	3.2m
Bed Orientation:	090,60N
Nature of contacts:	relatively sharp
Thin Section:	
Rock Type(Thin Section):	
Hand Samples:	F10-taken from the top of the bed
Photos:	Roll C:Exp 26,25, overview
	Exp 24, x-sec view, W facing, note chert lams

Notes:
N-S terminate against E-W,
but also some E-W terminate against N-S

Prominent Fracture Sets:
175-190,90-85SE
185,85NW
065-085,40-60SE

Minor sets: 150,60SW
035,25SE, 030,85NW
145,15NE, 175,20NE

F10	F10	F10	F10	F10	F10	F10	F10	F10	F10	F10	F10	F10
Fracture Set Orientation		N-S			Transect Orientat	strike=090	N=	21				
Number	Spacing (m)	Aperture (mm)	Fill	Mode	Height (m)	Width (m)	Upper	Lower	Orientation	Notes		
1	0				1.5	3	AB	AF	RANDOM			
2	0.22				0.1	0.02	AB		NOT			
3	1.5				0.95	0.1	AB		CONSISTENT	steps down to E in vertical plane		
4	1.55					1.8	AB		WITH SPACING	very sinuous		
5	1.7					0.7	AB		185,85NW	steps down to W, also in vertical p		
6	1.74				0.1	0.5	AB		190,85SE	same echelon set as prev frac		
7	2.2				0.1	0.5	AB		175,90	echelon set, down to W step in ve		
8	2.34				0.05	0.25	AB		195,85SE			
9	2.59				0.1	1.15	AB		195,85SE			
10	2.95				0.2	3	AB		190,85SE	echelon set, down to E step in ver		
11	3.15					0.35			195,85SE			
12	3.2	0.5	C		0.1	0.9			190,90	echelon set down to E step in vert		
13	3.25				0.03	0.4			195,90	echelon set down to E step in vert		
14	3.47				0.1	0.4						
15	4.15	1	N		0.1	0.75						
16	4.6				0.05	0.3						
17	4.9				0.7	1.5						
18	5.1				0.3	0.4						
19	5.2				0.1	0.7				part of .3m wide echelon set		
20	5.4				0.05	0.2						
21	5.6				0.4	0.4						

F10	F10	F10	F10	F10	F10	F10	F10	F10	F10	F10
Fracture Set Orientation:		E-W, SE		Transect orientation:		orthogo	N=	18		
Number	Spacing (m)	ture (	Fill	Mode	Height (m)	Width (m	Upper	Lower	Orientation	Notes
1	0.6				3	1	AB	AB		
2	0.9				3	0.5	AB	AB		
3	2.3				0.1	2	AB		085,55SE	
4	2.5	1			0.1	0.7	AB		065,30SE	
5	2.66				0.15	0.4	AB		070,15NW	
6	2.75				0.15	0.4			080,20SE	
7	2.9				0.05	0.3			065,55SE	terminate laterally against N-S fracs
8	2.91				0.05	0.4			090,60S	
9	3.1				0.1	0.3			060,45SE	
10	3.11				0.1	0.1			120,50SW	
11	3.29				0.1	0.3			080,60SE	
12	3.39				0.1	0.4			080,30SE	
13	3.66				0.1	0.1			070,50SE	
14	3.83				0.2	0.4			065,20SE	
15	3.9				0.2	0.2			170,45SW	
16	4.1				0.1	0.1			085,30SE	
17	4.12				0.15	0.3			075,35SE	
18	4.25				0.05	0.2			155,25SW	

Fold Name:	Camp Syncline, West Side	Notes:	relativelyshattered bed for it's thickness	
Location within fold:	backlimb		is this due to lithology????	
Sample Location:	**F11**			
Outrcrop Type:	x-sec with pavement			
Stratigraphic Location:	Mid "Upper Lisburne", between 111.5m-113m on MS-1			
Rock Type(Field Call):	massive, packstone/grainstone with chert layers and irreglarly shaped nodules			
Bed Thickness:	?			
Bed Orientation:	095,75NE	Prominent Fracture Sets:		
Nature of contacts:	sharp	195-210,60-80SE	well developed	
Thin Section:		185-190,20-30NW	well developed	
Rock Type(Thin Section):		055-060, 35-55SE	well developed	
Hand Samples:	F11A, F11B See sketch for exact location within bed	170-175,70SW	faint early set between other three sets	
Photos:	Roll C:Exp 23 S view of pavement Exp 22, x-sec view W facing Exp 21,20 F10 and F11, jake staff II to 210 set			

F11	F11	F11	F11	F11	F11	F11	F11	F11	F11	F11	F11	F11
Fracture Set Orientation		210,70SE			Transect Orientat	orthogonal	N=	25				
Number	Spacing (m)	Aperture (mm)	Fill	Mode	Height (m)	Width (m)	Upper	Lower	Orientation	Notes		
1	0				0.5	1.5	AB		190,70SE			
2	0.14	2	N		0.3	0.1	AB			terminates laterally (TL) against 6		
3	0.2				0.2	0.1	AB		210,60SE	TL against fracs: 060,35SE & 190		
4	0.24				0.05	0.05	AB			TL against fracs: 060,35SE & 190		
5	0.3				0.2	0.1	AB			TL against 190,20NW		
6	0.4				0.05	0.05	AB		210,80SE			
7	0.64				0.4	0.7	AB		210,70SE			
8	0.74				0.4	1.1	AB					
9	0.85				0.3	2	AB		195,55SE			
10	1.05				0.1	0.3	AB					
11	1.07	3	C		0.1	0.3	AB		205,70SE	good aperture reading		
12	1.24				0.1	0.1	AB					
13	1.26				0.1	0.2	AB					
14	1.28				0.1	0.4	AB		220,80SE			
15	1.29				0.1	0.1	AB					
16	1.31				0.1	0.3	AB					
17	1.33				0.1	0.4	AB		225,90			
18	1.36				0.1	0.3	AB		220,75SE			
19	1.41	2	C		0.1	0.3	AB		230,80SE			
20	1.47				0.05	0.05	AB					
21	1.48				0.05	0.05	AB		220,70SE			
22	1.49	1	C		0.05	0.6	AB					
23	1.55				0.05	0.05	AB					
24	1.7				0.1	0.1	AB		210,55SE			
25	1.9	1	N		0.2	3	AB		210,70SE			

F11	F11	F11	F11	F11	F11	F11	F11	F11	F11	F11
Fracture Set Orientation:		080,40SE	Transect orientation:			orthogo	N=	9		
Number	Spacing (m)	ture (	Fill	Mode	Height (m)	Width (m	Upper	Lower	Orientation	Notes
1	0				0.1	0.1				
2	0.15				0.1	0.1	AB			terminates laterally against 210 set fracs o
3	0.22				0.2	0.2	AB			terminates laterally against 210 set fracs o
4	0.45				0.1	0.5	AB		070,35SE	terminates laterally against 210 set fracs o
5	0.68				0.2	0.4	AB		075,40SE	terminates laterally against 210 set fracs o
6	0.78				0.2	0.5	AB		070,40SE	
7	0.9				0.15	0.7	AB		085,40SE	
8	1.3				0.2	0.6	AB			
9	1.7				0.05	0.05	AB		090,30S	

F11

Fracture Set Orientation:		190,25NW	Transect Orientation:			orthogo	N=	10		
Number	Spacing (m)	ture (	Fill	Mode	Height (m)	Width (m	Upper	Lower	Orientation	Notes
1	0	2	N		0.1	1.5	AB			RANDOM
2	0.04				0.2	0.7	AB			190,20NW
3	0.26				0.1	0.7	AB			185,25NW
4	0.3				0.1	0.7	AB			185,30NW
5	0.36				0.1	0.8	AB			
6	0.46				0.1	1	AB			swarms of conjugate fractures every 80cm
7	1.17				0.1	1.5	AB		180,25W	
8	1.23				0.1	1.2	AB			
9	1.3				0.1	0.6	AB		195,20NW	
10	1.4				0.2	0.4	AB			

Fold Name:	Camp Syncline, West Side	Notes:	Two senses of shear:
Location within fold:	backlimb		1) bed II veins show top to north shear
Sample Location:	**F12**		2)slicks and echelon veins near the fault,
Outrcrop Type:	pavement and cross section		as well as minor structures show down to S
Stratigraphic Location:	Mid "Upper Lisburne", between 94m-96.5m on MS-1		sense probably related to ?folding?
Rock Type(Field Call):	dark crinoid wacke/packstone		3)bedding contact undulates to some degree
Bed Thickness:	2-5m		Two senses of shear? Thin section analysis of fault breccia?
Bed Orientation:	085,75NW 080,60NW		slicks on bedding: B:085,75NW slicks rake 55E down to S
Nature of contacts:	sharp		Frac 080,75SW slicks rake 75E, down to S
Thin Section:			DC 040,10S
Rock Type(Thin Section):			

Hand Samples:
F12A veins in bed below slicked surface: N75E,45NW, N20E,90
F12B hanging wall fault breccia
F12C sheared chert 065,85NW overturned
F12D hanging wall sheared veins/crinoids 215,85SE
F12E hanging wall dense bed II veins N35W,75SW

Prominent Fracture Sets:
155-180,70-85NE
160-180,75SW-90
see field notes for bed II shear vein sets

Photos:
Roll M: Exp 28,27 sheared? Bed II veins
Exp 26,25 bed II echelon set
Exp 24,23 flattened crinoids, W view
Exp 22, 21N-NW facing Jake staff II to fracs

West Camp Syncline, Upper Transect

Fold Name: Camp Syncline, West side
Location within fold: backlimb
Sample Location: **UCS1**
Outrcrop Type: x-sec
Stratigraphic Location: Upper "Upper Lisburne"
Rock Type(Field Call): wackestone-packstone-grainstone interlayers
Bed Thickness: 1.5-3m
Bed Orientation: 105,60NE 095,70NE
Nature of contacts: sharp
Thin Section:
Rock Type(Thin Section):
Hand Samples: UCS1A-(DC) 185,75W overturned
240,50?SE
UCS1B Chert nodule 010,80SE
Photos:

Notes:
slicks on bedding: B 095,70NE, slicks rake 70W, down to S
LOTS of penetrative deformation, less fracs except N-S
well developed DC, coarser in grainstone: 070,50SE
DC with slicks: 080,50SE slicks rake 50-60W, down to S
Slicks on bed + foliation consistent with folding origin except:
Bed?Frac? 110,80NE, slicks rake 85E down to N
Prominent Fracture Sets:
160-200,70W-90
very prominent DC, see above

fracs at the base of transect bed, see sketches
205-215,80-85NW
165-175,85NE-90
195,70-85SE

Fold Name: Camp Syncline, West Side
Location within fold: backlimb
Sample Location: **UCS2**
Outrcrop Type: x-sec
Stratigraphic Location: Upper "Upper Lisburne"
Rock Type(Field Call): grainstones/packstones w/ chert
Bed Thickness: 3-5m
Bed Orientation: 095,75NE
Nature of contacts: sharp
Thin Section:
Rock Type(Thin Section):
Hand Samples:

Photos:

Notes: 50m from UCS1, very similar,
probably should be grouped into one sample location

Prominent Fracture Sets:
characterized by:
1) 160-175, 70NE-90
2) DC: 080,65SE, 075,55SE

N-S set exhibits down to E sense of shear

UCS1	UCS1	UCS1	UCS1	UCS1	UCS1	UCS1	UCS1	UCS1	UCS1	UCS1	UCS1
Fracture Set Orientatio		N-S		Transect Orienta		orthogonal	N=	9			
Number	Spacing (m)	Orientation	Notes								
1	0.36	RANDOM									
2	0.55	195,75NW	overall lots of penetrative deformation, not					many fractures			
3	0.67	200,70NW									
4	0.71	160,90									
5	0.75	170,80SW									
6	0.76	175,85SW									
7	0.83	170,85SW									
8	1										
9	1.2										

UCS2	UCS2	UCS2	UCS2	UCS2	UCS2	UCS2	UCS2	UCS2	UCS2	UCS2
Fracture Set Orientatio		N-S set		Transect Orienta		strike=090	N=	16		
Number	Spacing (m)	Aperture (mm	Fill	Mode	Height (m)	Width (m)	Upper	Lower	Orientation	Notes
1	0.35	0.5			0.1	0.4	TI	TI		
2	0.4	0.5			0.03	0.15	TI	TI		
3	0.64	0.5			0.05	0.5	TI	TI	160,75NE	
4	0.66	0.5			0.05	0.3	TI	TI	160,80NE	n set, steps down to W
5	0.79	0.5			0.05	0.2	TI	TI	165,80NE	
6	0.95	0.5			0.05	0.2	TI	TI		**swarm between spacing= .95 and 1.1,**
7	0.97	0.5			0.03	0.2	TI	TI		**but not measured, genearally height an**
8	1	0.5			0.1	0.1	TI	TI	175,70NE	**width= .05mx.05m, spacing=1-2cm**
9	1.1	0.5			0.05	0.2	TI	TI		**orientation of swarm=150-170,85NE**
10	1.17	0.5			0.03	0.3	TI	TI	175,90	
11	1.27	2			0.05	0.5	TI	AB		
12	1.35	1			0.05	0.5		AB		
13	1.47	0.5			0.03	0.6	TI	AB	165,85NE	
14	1.55	0.5			0.03	0.5	TI	TI		
15	1.85	0.5			0.03	0.2	TI	TI		
16	2.6									

Fold Name:	Camp Syncline, West Side
Location within fold:	backlimb
Sample Location:	**UCS3**
Outrcrop Type:	x-sec
Stratigraphic Location:	Upper "Upper Lisburne"
Rock Type(Field Call):	grainstone/packstone interbeds
Bed Thickness:	3-5m
Bed Orientation:	095,60NE
Nature of contacts:	sharp
Thin Section:	
Rock Type(Thin Section):	
Hand Samples:	UCS3
Photos:	O-35:N view of the oblique pavement at UCS3
	O-34:N view of the oblique pavement at UCS3

Notes:
down to E sense on N-S, SW dipping set,

N-S, NE dipping conjgates of N-S, SW dipping set?
appear to be late fractures.

Prominent Fracture Sets:
N-S sets, NE and SW dipping (see below)
very swarmy N-S sets, should show up in the spacing
105-115,40NE: near bed II
155,55SW-160,45SW
130, 85E-155,85E

080,5NW	minor sets
050,15NW	minor sets

UCS3	UCS3	UCS3	UCS3	UCS3	UCS3	UCS3	UCS3	UCS3	UCS3	UCS3	UCS3	UCS3
Fracture Set Orientatio		N-S,NE dip		Transect Orienta		orthogonal	N=	26				
Number	Spacing (m)	Aperture (mm	Fill	Mode	Height (m)	Width (m)	Lateral terminatio		Orientation	Notes		
1	0.25	2	C		0.05	0.2	ALL		155,75NE	**All fracs of this set**		
2	0.3	2	C		0.05	0.05	TERMINATE		155,75NE	**W stepping echelon set**		
3	0.47	0.5	C		0.05	0.15	INTERNALLY		165,70NE			
4	0.51	1	C		0.05	0.15	EXCEPT N=16		165,70NE			
5	0.54	1	C		0.05	0.15	WHICH IS		165,70NE			
6	0.56	1	C		0.05	0.15	AF ON		165,70NE			
7	0.6	5	C		0.1	0.2	BOTH ENDS		155,70NE			
8	0.62	1	C		0.1	0.1			155,70NE			
9	0.63	2	C		0.05	0.05			155,70NE			
10	0.7				0.05	0.25			165,75NE			
11	0.72	1	C		0.05	0.1			165,75NE			
12	0.79	1	N		0.05	0.05			175,85NE			
13	0.8	1	N		0.05	0.1			175,85NE			
14	0.86				0.05	0.15			155,75NE			
15	0.9	1	C		0.1	0.1			155,75NE			
16	0.91				0.02	0.02			170,85NE			
17	0.94	1	C		0.03	0.2			160,80NE			
18	1.03				0.05	0.15			160,85NE			
19	1.05	4	C		0.1	0.3			165,85NE			
20	1.07	3	C		0.1	0.1			165,85NE			
21	1.17	1	N		0.5	0.3			155,85NE			
22	1.2	2	C		0.5	0.3			160,85NE			
23	1.29	1	N		0.5	0.4			160,85NE			
24	1.31	1	C		0.5	0.2			160,85NE			
25	1.34	1	C		0.1	0.7						
26	1.45	15	C		0.2	1.3			160,85NE	yes, this really is a 15cm aperture		

UCS3	UCS3	UCS3	UCS3	UCS3	JCS3	UCS3	UCS3	UCS3	UCS3	UCS3
Fracture Set Orientat		N-S,SW dip			Transect c	orthogonal	N=	22		
Number	Spacing (m	Aperture (mm	Fill	Modeight (	Width (m)	eral termination			Orientatior	Notes
1	0.11	2	C	0.1	0.15	TI on both ends			175,55SW	
2	0.14	0.5	N	0.1	0.1					
3	0.18	1	C	0.1	0.2				160,60SW	
4	0.21	1	N	0.1	0.15					
5	0.27			0.1	0.05				160,60SW	
6	0.31	2	C	0.1	0.1				155,70SW	part of echelon set, steps down to E
7	0.39	0.5	C	0.1	0.1				155,70SW	
8	0.45			0.1	0.05				155,70SW	
9	0.51	0.5	C	0.1	0.05	AF on both ends				
10	0.52	1	C	0.1	0.05	AF on both ends			150,50SW	
11	0.56	0.5	C	0	0.3				150,50SW	
12	0.6	1	C	0.1	0.4				150,65SW	
13	0.69	0.5	C	0.1	0.15	AF on both ends			145,60SW	
14	0.73	1	C	0.1	0.25				145,60SW	
15	0.77	0.5	N	0.1	0.1				145,60SW	
16	1.22	0.5	N	0	0.15	AF on both ends			145,65SW	
17	1.3	0.5	N	0	0.2	AF on one end, TI or			145,65SW	part of echelon set, steps down to E
18	1.43	0.5	N	0	0.2				145,65SW	
19	1.68	0.5	N	0.1	0.1	AFone end, TI other			145,55SW	
20	1.76	0.5	N	0	0.1	AFone end, TI other			145,55SW	
21	1.8	0.5	N	0.1	0.05	AFone end, TI other			145,55SW	
22	1.86	1	C	0.1	0.1	AF on both ends			150,45SW	

Fold Name:	Camp Syncline, West Side	Notes:	very penetratively deformed
Location within fold:	backlimb		highly fractured
Sample Location:	**UCS4**		echelon fracs160,80SW, down to E, see 0-29
Outrcrop Type:	x-sec		bed sub II set: 120,55NE top to N shear see O-30
Stratigraphic Location:	Upper "Upper Lisburne"		see sketch in book
Rock Type(Field Call):	wackestone/packstone interbeds w/ lenticular to nodular chert	Prominent Fracture Sets:	
Bed Thickness:	3-5m	see following detailed sets	
Bed Orientation:	095,55NE		
Nature of contacts:			
Thin Section:			
Rock Type(Thin Section):			
Hand Samples:	UCS4A-085,70SE, 095,60NE overturned UCS4B-075,55SE chert UCS4C-040,55SE overturned, from lower bed UCS4D-flattened crinoids at the base of upper bed UCS4E-075,75NW overturned, chert nodule from upper/lower bed contact		

Photos:

O-33: N view of UCS4
O-32:W view of UCS4 along DC parallel fractures and DC
O-31:N view of down to E echelon fracs at UCS4-UCS5
O-30:NW view of bed parallel shear fractures at UCS4-UCS5
O-29:N view of other down to E echelon fracs at UCS4-UCS5

UCS4	UCS4	UCS4	UCS4	UCS4	UCS4	UCS4	UCS4	UCS4	UCS4	UCS4	UCS4	UCS4
Fracture Set Orientatio		E-W,shallow SE di		Transect Orienta		strike=040	N=	25				
Number	Spacing (m)	Aperture (mm	Fill	Mode	Height (m)	Width (m)	Upper	Lower	Orientation	Notes		
1	0.15	1	C		0.15	0.02	AB	AB	070,55SE	**this set measured between**		
2	0.23	0.5	N		0.1	0.02	TI	TI		**two chert nodules (above and below) o**		
3	0.25	0.5	C		0.2	0.05	AB	AB	085,55SE	**area terminate against bed**		
4	0.26	0.5	N		0.15	0.04	AB	AB		**surfaces similar to chert nodules**		
5	0.28	0.5	C		0.05	0.05	AB	TI	070,45SE			
6	0.3	0.5	C		0.1	0.02	AB	AB	070,45SE			
7	0.32	0.5	C		0.1	0.01	TI	TI				
8	0.35	0.5	C		0.1	0.03	AB	TI	070,50SE			
9	0.36	0.5	C		0.1	0.03	AB	TI	070,50SE			
10	0.37	1	N		0.05	0.05	TI	AB				
11	0.4	0.5	C		0.2	0.05	AB	AB	080,45SE			
12	0.41	0.5	C		0.1	0.05	AB	AB	080,45SE			
13	0.42	0.5	C		0.05	0.05	AB	AB	075,40SE	part of echelon set, steps to N		
14	0.43	0.5	C		0.15	0.03	AB	AB	080,50SE			
15	0.45	1	N		0.1	0.05	AB	AB	080,35SE			
16	0.46				0.1	0.05	AB	AB	080,35SE			
17	0.465	0.5	C		0.1	0.02	AB	AB				
18	0.47	0.5	C		0.1	0.03	AB	AB				
19	0.49	1	C		0.05	0.05	AB	AB				
20	0.52	0.5	N		0.1	0.1	AB	AB				
21	0.53	0.5	C		0.1	0.1	AB	AB				
22	0.54	0.5	C		0.05	0.05	AB	AB	075,60SE			
23	0.57	0.5	C		0.05	0.03	AB	AB	085,55SE			
24	0.59				0.05	0.05	AB	AB	085,55SE			
25	0.6	0.5	N		0.05	0.05	AB	AB	075,55SE			

UCS4	UCS4	UCS4	UCS4	UCS4	JCS4	UCS4	UCS4	UCS4	UCS4	UCS4
Fracture Set Orientat	N-S,SE dip			Transect (	strike=075	N=	14			
Number	Spacing (m	Aperture (mm	Fill	Modeight (	Width (m)	Upper	Lower	Orientatior	Notes	
1	0.25			0.3	0.1	AB	AB	195,85SE	**all fracs in this set**	
2	0.33	0.5	N	0.1	0.05	TI	TI		**were in chert except**	
3	0.35	0.5	N	0.1	0.05	TI	TI		**for the last three fracs**	
4	0.37	0.5	N	0.1	0.05	TI	TI	185,80SE		
5	0.38	0.5	N	0.2	0.05	TI	AB	185,75SE		
6	0.4	4	C	0.3	0.05	AB	AB	180,75E		
7	0.44	0.5	N	0.1	0.05	TI	TI	185,80SE		
8	0.53	0.5	C	0.2	0.03	AB	TI	195,75SE		
9	0.61	0.5	N	0.1	0.05	TI	TI			
10	0.67	0.5	C	0.1	0.05	AF	TI	190,80SE		
11	0.77	0.5	N	0.1	0.05	AB	AB	180,85E		
12	0.79			0.1	0.05	TI	TI	185,80SE		
13	0.84	0.5	C	0.2	0.05	TI	TI		CB	
14	0.87	0.5	C	0.5	0.05	TI	TI	170,70NE	CB, echelon set	

UCS4	UCS4	UCS4	UCS4	UCS4	JCS4	UCS4	UCS4	UCS4	UCS4	UCS4
Fracture Set Orientat	095,55NE:bed sub-parallel			Transect (	orthogonal	N=	16			
Number	Spacing (m	Aperture (mm	Fill	Mode	width	-S width (m	West	East	Orientatior	Notes
1	0	2	C	0.5	0.1	TI	TI		115,50NE	top to NE sense of shear
2	0.06	1	N	0.5	0.05	TI	AB			bedding=chert
3	0.07	1	C	0.7	0.1	AB	TI			
4	0.1	0.5	C	0.2	0.05	AB	AB			**this density of fracs only**
5	0.11	0.5	C	0.3	0.05	TI	AB		125,35NE	**found near the bed surface**
6	0.15	1	C	0.2	0.03	TI	AB			**also very sigmoidal/sinuous**
7	0.2			0.4	0.05	TI	TI			in shape
8	0.23			0.2	0.05	AF	AF			
9	0.26	0.5	C	0.1	0.05	TI	TI			
10	0.262			1	0.05	TI	AB			
11	0.32	1	N	0.8	0.05	TI	TI		100,45NE	
12	0.35	1	C	0.3	0.05	AF	AB			terminates against spacing=.32 upper
13	0.36	0.5	N	0.4	0.05	AF	AF			terminates against spacing=.36 lower
14	0.38	0.5	N	0.1	0.03	AF	TI			
15	0.4			0.3	0.05	AF	AF			
16	0.44	0.5	C	5	2				100,40NE	forms the bed surface, cuts along chert nodule

Fold Name:	Camp Syncline, West Side	Notes: NOT within transect layer itself
Location within fold:	hinge	stratigraphically one bed below the transect bed
Sample Location:	**UCS5**	
Outrcrop Type:	x-sec	
Stratigraphic Location:	Upper "Upper Lisburne"	DC: 070,55SE
Rock Type(Field Call):	?	DC: 090,65SE
Bed Thickness:		
Bed Orientation:	115,25NE	
Nature of contacts:	?	
Thin Section:		
Rock Type(Thin Section):		
Hand Samples:	UCS5A-190,90 lower bed	
	UCS5B-075,75SE upper (transect bed)	Prominent Fracture Sets:
	UCS5C-020,85SE	
	UCS5D-085,90 good DC and strained crinoids	SEE BOOK and FINISH THIS STATION

Photos:
O-28:W facing overview of UCS5
O-27:W facing overview of UCS6
O-26:W view of folded veins near the hinge at UCS5
O-25:W view of folded veins near the hinge at UCS6
O-24:W view of folded veins near the hinge at UCS7
O-23:W view of folded veins near the hinge at UCS8
O-22:W view of folded veins near the hinge at UCS9

UCS5	UCS5	UCS5	UCS5	UCS	UCS5	UCS5	UCS5	UCS5	UCS5	UCS5	UCS5	UCS5
Fracture Set Orientatio		E-W,SE dip			Transect Orienta	strike=035, 195 SEE		N=	30			
Number	Spacing (m)	Aperture (mm	Fill	Mode	Height (m)	Width (m)	Upper	Lower	Orientation	Notes		
1	0	1	N		0.25	0.05	AF	AF	070,84SE			
2	0.03				0.2	0.03	AB	AB	070,84SE			
3	0.07	1	C		0.1	0.03	AB	TI	070,84SE			
4	0.09	1	C		0.3	0.05	TI	TI				
5	0.11	1	N		0.4	0.1	TI	TI	070,75SE			
6	0.21				0.6	0.1	AF	TI	075,85SE			
7	0.24				0.1	0.05	AB	AF				
8	0.26				0.25	0.05	AF	AF	070,90	concave to SE		
9	0.41	1	N		0.2	0.03	AB	AB		sinuous		
10	0.42	1	N		0.4	0.05	AB	TI	065,85SE			
11	0.45	1	N		0.4	0.1	AB	TI	075,80SE	CB		
12	0.47				0.2	0.03	ABS	ABS	070,75SE	concave to NE		
13	0.52	0.5	N		0.1	0.03	AB	TI				
14	0.55	0.5	N		0.1	0.03	AB	TI				
15	0.6				0.4	0.1	AB		075,75SE	very sinuous		
16	0.67				0.3	0.05	AB	TI	065,75SE	very sinuous		
17	0.672				0.3	0.05	AB	AB	070,75SE			
18	0.74	10	C		0.1	0.05	AF	TI	085,45SE			
19	0.77				0.15	0.02	AF	TI	075,65SE			
20	0.81				0.15	0.05	AB	TI	080,55SE			
21	0.85				0.55	0.2	AB		075,70SE			
22	0.89	1	C		0.1	0.05	AF	TI	080,60SE			
23	1				0.1	0.1	AB	TI	095,50SW	DC?		
CHANGE	TRANSECT	ORIENTATIOI	TO	RIKE=195								
24	1.1	1	C		0.2	0.1	AB	AF	075,60SE			
25	1.29	1	C		0.2	0.1	AB	TI	080,55SE	slicks rake 75 from W,		
26	1.35				0.4	0.1	AB	TI	080,60SE	shear down to SE		
27	1.39	1	C		0.1	0.03	AF	AB	065,75SE			
28	1.44				0.2	0.05	AF	AB	065,75SE	terminates against spacing=1.35 above		
29	1.45	0.5	C		0.1	0.03	AB	TI	065,75SE	terminates against spacing=1.35 above		
30	1.48				0.15	0.1	AB	TI	060,65SE			

UCS5	UCS5	UCS5	UCS5	UCS5	UCS5	UCS5	UCS5	UCS5	UCS5	UCS5	UCS5	UCS5	UCS5
Fracture Set Orientat		125-140+N-S, variable dip		Transect (	strike=035, 195, 170 s			N=	26				
Number	Spacing (m	Aperture (mm	Fill	Modeight (	Width (m)	Upper	Lower	Orientatio	Notes				
1	0			0.4	0.1	AF		175,80W					
2	0.15			0.3	0.1	AF	TI	200,80NW					
3	0.19			0.5	0.03	AB	TI	155,70SW					
4	0.23	1	N	0.3	0.05	TI	AB	155,70SW					
5	0.42			0.3	0.05	AB	AB	175,75SW					
6	0.55	10	C	0.5	0.1	TI	AB	155,65SW					
7	0.6			0.3	0.05	AB	TI	150,60SW					
8	0.65	1	C	0.1	0.05	AB	TI	150,60SW					
9	0.72	5	C	1	0.1	TI		140,65SW					
10	0.79			0.1	0.1	TI	AB	180,80W					
11	0.8			0.2	0.15	AB	AB	190,85NW					
12	1	4	C	0.6	0.1	AB	TI	125,65SW					
CHANGE	TRANSEC	ORIENTATIO	TO	RIKE=195									
13	1.1	1	N	0.2	0.3	AF	AF	160,80SW					
14	1.2	2	C	0.8	0.2	TI		165,75SW	CB				
15	1.3	1	N	0.2	0.05	TI	AF	130,75SW	concave N				
16	1.33	3	C	0.5	0.3	AB		160,70SW					
17	1.41	1	C	0.2	0.05	AF	AF	135,70SW					
18	1.49			0.5	0.3	TI	AB	160,75SW	CB				
19	1.59	1	C	0.2	0.05	TI		170,80SW					
20	1.6			0.1	0.05	AF	AF	145,70SW					
21	1.63			0.1	0.05	TI		170,80SW					
22	1.69			0.2	0.05	AF	TI	130,70SW					
CHANGE	TRANSEC	ORIENTATIO	TO	RIKE=170									
23	1.75	0.5	C	0.2	0.05	AF	TI	125,70SW					
24	1.77	0.5	C	0.2	0.03	TI	TI	125,70SW					
25	1.81	0.5	N	0.1	0.03	TI	TI	120,70SW					
26	1.85	0.5	N	0.1	0.05	TI	TI	140,70SW					

UCS5	**UCS5**	**UCS5**	**UCS5**	**UCS5**	**UCS5**	**UCS5**	**UCS5**	**UCS5**
Fracture Set Orientatic		080,80NW		Transect Orientation:		orthogonal	N=	25
Number	Spacing (m	Orientation	Notes					
1	0.45	080,75NW	**between spacing=.45-.50, microfrax**					
2	0.46	080,75NW	**every .5cm**					
3	0.47							
4	0.52	070,80NW						
5	0.54							
6	0.55	080,85NW						
7	0.57	080,80NW						
8	0.6	080,85NW						
9	0.605	080,85NW						
10	0.61	080,85NW						
11	0.71	080,80NW	concave S					
12	0.73	080,80NW	concave S					
13	0.75	080,80NW	concave S					
14	0.79							
15	0.8							
16	0.805							
17	0.81							
18	0.815							
19	0.835							
20	0.84							
21	0.855							
22	0.87							
23	0.88							
24	0.9							
25	0.92							

Fold Name:	Camp Syncline, West Side
Location within fold:	forelimb
Sample Location:	**UCS6**
Outrcrop Type:	x-sec
Stratigraphic Location:	Upper "Upper Lisburne"
Rock Type(Field Call):	wackestone/packstone
Bed Thickness:	?
Bed Orientation:	070,10SE
Nature of contacts:	sharp
Thin Section:	
Rock Type(Thin Section):	
Hand Samples:	UCS6A-090,55N
	UCS6B-040,85NW
Photos:	O-20:Hinge at UCS6, Ryan for scale
	O-19:Hinge at UCS6, Ryan for scale
	O-17:Hinge at UCS6, Ryan for scale

Notes: highly penetratively deformed
highly fractured and veined

Prominent Fracture Sets:

095,60NE, 095,80SW
050,30NW slicks rake 50E, top to N
095,45,75SW
125,60SW, 130,50SW
200,85NW, 210,80NW, 220,75NW

UCS6	UCS6	UCS6	UCS6	UCS6	UCS6	UCS6	UCS6	UCS6	UCS6	UCS6	UCS6	UCS6
Fracture Set Orientatio		E-W, NE dip			Transect Orienta	strike=220, N=		15				
Number	Spacing (m)	Aperture (mm	Fill	Mode	Height (m)	Width (m)	Upper	Lower	Orientation	Notes		
1	0				0.1	0.05	AF	AB				
2	0.05				0.2	0.05	AF	AB				
3	0.13	1	C		0.2	0.1	AF	AB	090,60N			
4	0.17	1	C		0.2	0.1	TI	AB	095,60NE			
5	0.19	0.5	N		0.07	0.03	AF	TI				
6	0.22	2	C		0.4	0.3	TI					
7	0.23	0.5	N		0.1	0.03	AB	AF				
8	0.235	2	C		1	1						
9	0.24	1	N		0.2	0.05	AF	AF	090,55N			
10	0.27	0.5	C		0.1	0.05	TI	TI				
11	0.32	2	C		0.4	0.3			095,60NE			
12	0.322	1	C		0.2	0.1	AF	TI				
13	0.38				0.5	0.3						
14	0.4				0.7	0.3		AF				
15	0.45				0.3	0.2	TI	AB				

UCS6	UCS6	UCS6	UCS6	UCS6	JCS(	UCS6	UCS6	UCS6
Fracture Set Orientat		E-W, NW dip Veins		Transect (	orthogonal	N=	22	
Number	Spacing (m)		Orientation	Notes				
1	0		RANDOM	most fracs=10cm high, 1-3mm aperture				
2	0.01		085,40NW	calcite fill, TI on both ends				
3	0.02		075,35NW					
4	0.04		080,45NW					
5	0.05		065,40NW					
6	0.06							
7	0.07							
8	0.08							
9	0.09							
10	0.11							
11	0.135							
12	0.145							
13	0.15							
14	0.155							
15	0.165							
16	0.17							
17	0.175							
18	0.18							
19	0.185							
20	0.195							
21	0.2							
22	0.205							

TIMING AND CHARACTER OF MESOSCOPIC STRUCTURES IN DETACHMENT FOLDS AND IMPLICATIONS FOR FOLD DEVELOPMENT-- AN EXAMPLE FROM THE NORTHEASTERN BROOKS RANGE, ALASKA

C.L. Hanks[1] , W.K. Wallace[1], J. C. Lorenz[2] , P.K. Atkinson[1], J. Brinton[1] and J.R. Shackleton[1]

Abstract

In detachment-folded Lisburne Group carbonates of the northeastern Brooks Range, different mesoscopic structures formed at different times in the evolution of individual detachment folds, providing clues to the mechanism of folding and the conditions under which the fold formed. Rocks in advance of the visible thrust front experienced low magnitude differential stresses of the same orientation as experienced in the fold-and-thrust belt, resulting in orogen-perpendicular extension fractures in undeformed rocks of the foredeep basin. These rocks were later incorporated into the thrust belt, where they were thrust-faulted and folded. The distribution of fractures and other mesoscopic structures in individual folds suggests that folding occurred by both flexural slip and homogeneous flattening. Flexural slip and associated fracturing occurred early in the development of the fold and/or in the outer arc of the fold. These early fractures may be overprinted and/or destroyed by ductile strain as later homogeneous flattening accommodated additional shortening. The penetrative strain is in turn overprinted by late extension fractures, which probably formed during the waning phases of folding and/or unroofing of the orogenic wedge.

Introduction

A close relationship between folds and thrust faults has long been recognized. Recent research has focussed on categorizing the different types of folds based on fold geometry and the genetic relationship of the fold to the fault. Most of this work has been based on seismic reflection data and conceptual and theoretical modeling, and has resulted in recognition of three main types of fault-related folds: fault-bend, fault propagation and detachment folds (figure 1). Much of the current modeling focuses on identifying the geometry and kinematic history of each fold type, using both idealized folds and naturally occurring folds. One approach to identifying the processes active during folding is to look at the distribution and relative timing of fractures and penetrative strain in naturally occurring folds. These structures and when they form during folding should provide a partial record of the processes that were active during fold development, as well as clues to the conditions prior to, during and after folding.

This study focusses on the distribution and relative timing of fractures and penetrative strain in a particular type of thrust-related fold, the detachment fold, in the northeastern Brooks Range of Alaska (figure 2). A single stratigraphic unit, the Lisburne Limestone, is exposed throughout the northeastern Brooks Range fold-and-thrust belt and has been shortened primarily by detachment folding. In addition, a well-defined transition to an older, thrust-dominated deformation front in the hinterland of the fold-and-thrust belt allows comparison of fractures in detachment-folded Lisburne

[1] Geophysical Institute and Department of Geology and Geophysics, University of Alaska Fairbanks
[2] Sandia National Laboratories, Albuquerque, New Mexico

with folded and thrust faulted Lisburne. Thus, the character and distribution of fractures can be compared in Lisburne Group rocks folded in a variety of local and regional structural positions, representing different stages in the development of detachment folds.

Previous Work

Detachment folds

A detachment fold is a fold that develops in a competent layer above a bedding-parallel thrust fault in an underlying incompetent layer (figure 1 C). Several conceptual models for the evolution of detachment folds have been proposed, all of which have implications as to the process by which folding takes place (e.g., figure 3 A -C). While one model may be more 'correct' than another, the manner in which an individual natural fold developed (and thus which model best describes the fold) may be strongly dependent upon the mechanical stratigraphy of the rocks being folded and the conditions under which folding took place.

Geometrically, the detachment folds of the northeastern Brooks Range appear to be most accurately described by a combination of models proposed by Homza and Wallace (1997) and Epard and Groshong (1995) models (figure 3 A & B). The Homza and Wallace (1997) model (figure 3 A) assumes a sharp competency contrast between the competent layer and the underlying incompetent layer, fixed hinges, constant bed length and bed thickness within the competent layer throughout folding, and variable detachment depth. In contrast, the Epard and Groshong (1995) model (figure 3 B) does not recognize differences in the mechanical strength of different layers in the fold. It assumes that constant area is maintained strictly through layer-parallel shortening in all units. Bed thickness and line length are not conserved, detachment level remains constant, and hinges may or may not migrate.

Neither the Homza and Wallace model nor the Epard and Groshong model adequately describe the geometry of detachment folds in the northeastern Brooks Range. A 'hybrid' model (Atkinson, 2001, figure 3 C) incorporates aspects of both of these models while accommodating the observed features of the northeastern Brooks Range detachment folds. These observations include: a strong competency contrast between the competent layer (Lisburne Limestone) and the underlying incompetent detachment layer (Kayak Shale); a detachment layer that is thick relative to the competent layer (~100-200m vs. 500m); fixed hinges; changes of bed thickness and length in both layers during folding; and changes in detachment depth. Two important aspects of the hybrid model that distinguishes it from previous models is that it assumes that both detachment depth in the incompetent layer and bed length and thickness within the competent layer may vary during folding. Thus, this model is consistent with a fold that forms by a combination of flexural slip and homogeneous flattening in the competent unit. Depending upon the interlimb angle, the competent unit may thicken in both the anticline and syncline hinge zones, while material from the underlying less-competent unit can move into or out of the anticline core.

Modeling of observed detachment fold geometries using the 'hybrid' model suggests that the degree to which shortening in the competent unit is by flexural slip vs. homogeneous flattening is a function of the original relative thicknesses and competency contrasts between the units. In addition, a lack of sufficient ductile material to maintain constant area in the fold core may favor thickening of the competent unit. However, the relative timing of flexural slip vs. homogeneous flattening in fold formation is not constrained by the model.

Fold mechanisms: Flexural Flow, Flexural Slip and Homogeneous Flattening

Three different fold mechanisms may be active at various times and at various scales during the formation of detachment folds in the Lisburne Group carbonates.

Both flexural slip and flexural flow are important mechanisms in the formation of parallel folds in layered rocks (Ramsay and Huber, 1987; Tanner, 1989). In both mechanisms, folding is accommodated by displacement parallel to bedding and there is no change in bed thickness. *Flexural slip folding* occurs where such displacement occurs at discrete and discontinuous intervals, commonly at a lithologic discontinuity, such as a bedding surface. Evidence of slip on such surfaces includes quartz-fiber veins or sheets, slickenlines, and/or displaced markers (such as root structures, burrows and crosscutting veins). Extension fractures in overlying and underlying beds may widen towards and terminate at the slip surface. In contrast, *flexural flow folding* occurs when layer-parallel displacement is distributed continuously throughout a volume of rock. This results in shear strain being distributed more-or-less evenly throughout the rocks, with no obvious strain gradient perpendicular to bedding. Bed thickness is still maintained.

Folding via flexural slip and flexural flow can only proceed so far before the folds 'lock up' and are unable to accommodate additional shortening (Tanner, 1989; Yang and Gray, 1994; Twiss and Moores, 1992). After this point, additional shortening can be accommodated by homogeneous flattening of the existing fold. During homogeneous flattening, bed thickness is not maintained. Material flows from the limbs into the hinge area, resulting in thinned beds in the limbs and thickened beds in the hinge area. This process allows additional shortening and fold amplification (Twiss and Moores, 1992). Evidence that the fold has undergone homogeneous flattening includes bed thickening in the hinges and thinning in the limbs. Homogeneous flattening is commonly accomplished by penetrative strain.

Regional setting

The Brooks Range is the northernmost part of the Rocky Mountain fold-and-thrust belt (fig. 2). The majority of shortening in the fold-and-thrust belt occurred in Late Jurassic to Early Cretaceous time when a wide, south-facing late Paleozoic to early Mesozoic passive continental margin collapsed in response to the collision of an intraoceanic arc (Mayfield and others, 1988; Moore and others, 1994). Shortly after the main phase of compressional collapse of the continental margin, rifting led to formation of the oceanic Canada basin to the north (present geographic coordinates) in Early Cretaceous time (Grantz and May, 1983; Moore and others, 1994). Post-collisional contraction has occurred episodically throughout the Cenozoic to the present, and has resulted in progradation of fold-and-thrust deformation in the northeastern Brooks Range and northward toward, and locally across, the Cretaceous rifted margin (Grantz and others, 1990; Hanks and others, 1994).

The stratigraphy of the northeastern Brooks Range can be divided into three distinct depositional sequences (Fig. 4; Reiser, 1970; Mull, 1982). Slightly metamorphosed, deformed Proterozoic to Devonian sedimentary and volcanic rocks are depositional basement for the Mississippian to Lower Cretaceous, northerly derived, passive margin sedimentary rocks of the Ellesmerian sequence (Reiser, 1970; Reiser and others, 1980; Lane, 1991; Moore and others, 1994). These sedimentary rocks are in turn overlain by Lower Cretaceous to recent clastic rocks of the Brookian sequence that are derived from the Brooks Range to the south.

The regional and local structural style of the northeastern Brooks Range is strongly influenced by mechanical stratigraphy (Wallace and Hanks, 1990; Wallace, 1993). The largest structures are regional anticlinoria cored by pre-Mississippian metasedimentary and metavolcanic rocks. These regional anticlinoria are interpreted to reflect horses in a regional duplex between a floor thrust at depth and a roof thrust in the Mississippian Kayak Shale (figure 2 C). The overlying Ellesmerian and Brookian sequences are decoupled from the basement and deform as the roof of a passive-roof duplex. The Carboniferous Lisburne Group (figure 4) is the most rigid member of this roof sequence and deforms predominantly into kilometer-scale symmetrical detachment folds that are only rarely cut by thrust faults. These detachment folds are second-order folds above the basement anticlinoria; overlying Permian and Triassic clastic rocks are slightly decoupled from the Lisburne Group, resulting in third-order folds.

In contrast, the Lisburne in the far south portion of the northeastern Brooks Range is characterized by imbricate stacked thrust sheets with asymmetrical hangingwall anticlines and footwall synclines (Wallace, 1993; Wallace and Homza, in press). The "Continental Divide thrust front" marks the boundary between these two structural styles (Figure 2).

Observations

Mesoscopic structures in non-folded Lisburne Group

The Lisburne Group in the Sadlerochit Mountains of the northeastern Brooks Range and in the subsurface of the North Slope has not been deformed by detachment folds (figure 2, B & C). In the Sadlerochit Mountains, the shale underlying the Lisburne Group, the Mississippian Kayak shale, is depositionally absent. Consequently, the Lisburne has remained structurally coupled to the underlying pre-Mississippian rocks and has not been folded by detachment folds (Wallace and Hanks, 1990; Wallace, 1993). The Prudhoe Bay area to the northeast of the Sadlerochit Mountains lies north of the thrust front and thus has not been visibly affected by thrust deformation (Bird and Molenaar 1992; Moore and others, 1994). Lisburne Group carbonates in these two areas provide the best opportunities for recognizing mesoscopic-scale structures that predate thrusting.

Fractures are the dominant mesoscopic-scale structures in both areas (Missman and Jameson, 1991; Hanks and others, 1997). Past detailed structural studies in these areas have not observed penetrative strain features, such as strained crinoids or stylolites (e.g., Missman and Jameson, 1991; Hanks and others, 1997). Both areas have similar fracture patterns. In the Sadlerochit Mountains, early NNW-oriented extension fractures are cross cut by later ENE-striking extension and shear fractures (figures 5 & 6). Hanks and others (1997) interpreted the early set of NNW-striking extension fractures to have formed while the rocks were still flat-lying in the foredeep of the fold-and-thrust belt. High pore pressures promoted extensional fracturing while the rocks were under relatively low differential in situ stresses (Lorenz and others, 1991). This resulted in extension fractures that were ahead of and orthogonal to the northeastern Brooks Range fold-and-thrust belt, parallel to maximum horizontal in situ stress. Because the Kayak Shale is depositionally absent in this area, the Lisburne remained structurally coupled to the basement during the later thrusting and folding that resulted in formation of the Sadlerochit Mountains. Flexural slip during this thrust-related folding is interpreted to have caused the late ENE-striking fractures (Hanks and others, 1997).

A similar set of NNW-striking extension fractures occurs in the Lisburne at Prudhoe Bay (Decker, 1990; Hanks and others, 1997), but here these fractures postdate earlier ENE-striking fractures that

are probably related to faulting along the Cretaceous continental margin. These NNW-striking extension fractures are also interpreted to have formed in response to low differential in situ stresses in advance of the observed northeastern Brooks Range thrust front. These fractures are thought to be open in the subsurface and actively contributing to permeability in the Lisburne reservoir (Hanks and others, 1997).

In both the Sadlerochit Mountains and in the subsurface at Prudhoe Bay, the extension fractures are interpreted by Hanks and others (1997) to represent a brittle response of the Lisburne carbonates to layer-parallel shortening under relatively low temperature, low differential stress, and high pore fluid pressure conditions.

Mesoscopic structures in detachment-folded Lisburne Group

A variety of both brittle and ductile mesoscopic structures are present in detachment-folded Lisburne carbonates (Hanks and others, 1997; Homza and Wallace, 1997; Atkinson, 2001, this study). In general, mesoscopic structures suggestive of penetrative ductile and semi-ductile deformation are overprinted by brittle structures.

Ductile and semi-ductile structures

Two categories of penetrative mesoscopic structures have been observed in the Lisburne carbonates exposed in the northeastern Brooks Range--mesoscopic-scale strain features that are not obviously associated with map-scale structures, and strain features that are localized in the hinges of detachment folds.

Strain not associated with map-scale structures

While not common, mesoscopic strain is observed in the Lisburne carbonates in areas not within a map-scale fold or immediately adjacent to a thrust fault. This is most commonly observed immediately south of the Continental Divide thrust front (figure 2). Here, thrust sheets consist of extensive flat panels with frontal asymmetric anticlines. Sheared stylolites and strained crinoid stems (figure 7) were locally observed in the flat portion of these thrust sheets. These structures are cut by later extension and shear fractures. This relationship suggests that some amount of early layer-parallel shear in the Lisburne was accommodated by semi-ductile processes prior to significant folding. Pre-folding layer parallel shear is difficult to document north of the Continental Divide thrust front, where detachment folding is pervasive.

Strain associated with detachment folds

Penetrative strain during folding is observed in almost all detachment folds in the northeastern Brooks Range. In open folds, this is usually limited to scattered zones of dissolution cleavage in the hinge area and within muddier intervals (figure 8 C). In tighter folds, other strain features are found in the hinge area, including sheared stylolites and more pervasive dissolution cleavage. In very tight to isoclinal folds, ductile deformation in both anticlinal and synclinal hinges is extreme, and includes pervasive dissolution cleavage and/or transposition of layering (figures 8 B & D).

Brittle mesoscopic structures (fractures)

Several generations of fractures are associated with detachment folds. The earliest fractures are

shear fractures. These shear fractures commonly occur as conjugate sets on the fold limbs, with acute bisectors both subparallel and subperpendicular to the fold axes (figure 9). Shear fractures within the conjugate set often occur as en echelon arrays. Most shear fractures are partially to entirely filled with calcite. Shear fractures of all orientations typically terminate at bedding planes. Because these shear fractures occur predominantly on fold limbs, it is difficult to ascertain their relative age with respect to the penetrative strain seen in the fold hinges. These fractures predate all other observed brittle features associated with folding.

Later extension fractures postdate both the penetrative strain in the fold hinges and shear fractures on the fold limbs, and are oriented both parallel and perpendicular to the fold axes. Extension fractures parallel to the fold axes are typically perpendicular to bedding and terminate at bedding surfaces. While the strike of these fractures parallels the strike of the fold axis, the dip varies, dipping towards the axial plane and only parallel to it in the hinge region. Some of these fractures are filled; others remain unfilled.

The latest extension fractures occur in all folds. These fractures are oriented perpendicular to fold axes, are fairly closely spaced and commonly extend vertically across several beds. The fractures are unfilled, with plumose and twist hackle structures occasionally preserved on the fracture surfaces. These fractures form prominent exposure surfaces.

Discussion

Implications of ductile vs. brittle structures for folding mechanism

The observed sequence of ductile and brittle structures and their relationship to the fold geometry suggest that folding was accommodated by both flexural slip and homogeneous flattening. However, flexural slip and homogeneous flattening probably occurred under different deformational conditions, and thus happened sequentially, not concurrently, during fold development.

Homogeneous flattening increased in importance as a folding mechanism as shortening increased. While the penetrative strain that results from homogeneous flattening is relatively rare in open detachment folds, the amount of strained carbonate in the hinges of the observed detachment folds increases as the axial angles of the folds decrease. In the hinges of folds of moderate axial angle (~90-125°), individual beds commonly exhibit dissolution cleavage, strained crinoids and/or strained stylolites. In the hinges of tight folds (axial angles < 90°) the strain is often extreme, with significant transposition of layering and thickening. It should be noted that any preexisting brittle structures that formed prior to or early in the folding process would be destroyed or significantly modified during this period of homogeneous flattening and penetrative strain.

Brittle structures developed both before and after bulk thickening by penetrative strain in the detachment fold hinges. The prefolding, vertically extensive, orogen-perpendicular extension fractures seen in the Sadlerochit Mts. and North Slope subsurface are probably related to in situ horizontal stresses in the foreland of the fold-and-thrust belt (Hanks and others, 1997; Lorenz and others, 1991). However, no demonstrably pre-fold extension fractures of this set were seen in the detachment folds studied. This is not surprising, in that it is not likely that such fractures survived subsequent ductile deformation in the core of the detachment folds, at least not as unfilled planar fractures.

However, several different sets of fractures are visible in the detachment folds that are probably related to or postdate folding. These fractures vary in character from en echelon tension gashes in fold limbs (fig. 7) to extension fractures parallel to the axial plane that terminate at bedding planes to vertically extensive extension fractures that are perpendicular to the fold axes. All appear to have a geometric relationship to the folds. In a few cases, fractures in the fold limbs appear to predate penetrative strain; however, almost all brittle structures in the hinge overprint the penetrative strain.

The systematic overprinting of ductile and semi-ductile structures by fractures of different origins and types suggest that deformational conditions varied systematically, and possibly predictably. In all the observed folds where high amounts of strain were accommodated by ductile processes, penetrative strain in the hinges is overprinted by strike-parallel and/or strike-perpendicular conjugate and extension fractures. The consistency of this timing relationship suggests that folding by homogeneous flattening dominated during the intermediate phase of growth on these high-strain folds, with flexural slip folding dominating during the waning phases of folding. Evidence of early flexural slip is preserved in the limbs of the folds, where early fractures are subsequently deformed by penetrative strain.

Deformation conditions

Whether folding was dominated by penetrative strain or flexural slip at any given point in the growth of the fold probably depended upon a variety of factors. These factors include pressure, temperature, strain rate, amount of total shortening (i.e., fold interlimb angle), the thickness of the competent unit, and the relative thickness of competent vs. incompetent units.

Experimental data indicates that rocks generally deform brittlely at surface or near surface pressure and temperature (Griggs and Handin, 1960; Twiss and Moores, 1992). However, the ductility of the rock increases with increasing temperature and confining pressure and decreasing strain rate. Thus, under geologically reasonable conditions, a rock will deform ductilely in upper parts of the crust if the strain rate is sufficiently low, and/or temperature is sufficiently high and/or confining pressure is sufficiently high. An increase in strain rate and/or decrease in temperature or confining pressure could result in brittle deformation of the same rock.

Using these general concepts, a conceptual model of potential deformation paths as a function of depth (i.e., pressure and temperature) and cumulative shortening explains the various sequence of structures seen in the detachment folds of the northeastern Brooks Range (figure 10). In this model, different folds may exhibit different types and sequences of structures depending upon the depth at which deformation occurred and the amount of cummulative shortening the fold accommodated. Rocks folded at shallow levels and/or at low amounts of shortening would be expected to develop primarily brittle structures (**A**); folds that are formed at greater depths and/or accommodated greater amounts of shortening are more likely to exhibit penetrative structures (**B**).

This conceptual model illustrates how one fold can experience both ductile and brittle deformation as shortening progresses and/or depth varies during folding. If the in situ stress regimes are similar at different times during deformation, the resulting mesoscopic structures may look very similar. This would explain why extension fractures that form late during folding or even after folding can superficially resemble extension fractures that formed prior to or early during folding.

Conclusions

The complex history of deformation and related fracturing in detachment-folded Lisburne Group carbonate rocks suggests that fracturing may occur at multiple times in a continuum with other structures as originally flat-lying rocks are progressively folded. Regional NNW-oriented extension fractures are well-developed in the Lisburne Group of the Sadlerochit Mountains and in the subsurface at Prudhoe Bay. These fractures probably formed parallel to maximum horizontal in situ stress ahead of and orthogonal to the northeastern Brooks Range fold-and-thrust belt (location a, figure 11). These early strike-normal fractures were a brittle response to layer-parallel shortening under relatively low temperature, low differential stress, and high pore fluid pressure conditions.

As the fold-and-thrust belt advanced into the foreland, previously flat-lying Lisburne was buried by the advancing thrust front and eventually incorporated into it (location b, figure 11). In the process, these carbonate rocks experienced increased pressure and temperature as well as higher differential stress. Evidence of early mesoscopic strain (e.g., sheared stylolites, strained crinoid stems, etc.) suggests that layer-parallel shortening or shear prior to significant folding was at least locally accommodated by semi-ductile processes Increased strain rate during subsequent detachment folding of these layered rocks may have been dominated initially by flexural slip, with formation of associated strike-parallel and/or strike-perpendicular shear and extension fractures. However, folding via ductile processes was important as folding progressed, especially in the cores of the folds. Ductile deformation was favored by the increasing temperature and confining pressure and decreasing fold interlimb angle. The resulting penetrative strain in the hinges during folding resulting in the development of dissolution cleavage and local transposition of layering. As shortening progressed and structural thickening increased, the zone of penetrative strain expanded, overprinting and destroying earlier brittle structures. As folding waned and erosional unroofing progressed (location c, figure 11), temperature, confining pressure and differential stress decreased and the rocks once more deformed brittlely, with formation of late, strike-normal NNW-oriented extension fractures.

When evaluating folded and fractured carbonate reservoirs, this general deformational sequence suggests that it is critical to distinguish between the different fracture sets and determine when and under what conditions the different sets formed. Extension fractures that could act as excellent permeability conduits in undeformed rocks may be destroyed if the same rocks have been folded. However, similar extension fractures may form later in the deformational cycle, providing a second opportunity for enhanced permeability. In addition, the amount of folding and the conditions under which detachment folding occurred influences the amount, distribution, type and timing of fracturing related to the actual fold. Fracturing may occur early in the fold's development, thus potentially providing significant enhanced permeability. However, continued folding could lead to significant destruction of this permeability by penetrative strain and reduction in reservoir quality.

REFERENCES

Atkinson, P.K., 2001, A geometric analysis of detachment folds in the northeastern Brooks Range, Alaska, and a conceptual model for their kinematic evolution: Master of Science thesis, University of Alaska, Fairbanks, Alaska, 209 p.

Bird, K.J., and Molenaar, C.M., 1992, The North Slope foreland basin, in Macqueen, R.W., and Leckie, D.A., eds., Foreland basins and foldbelts: American Association of Petroleum Geologists Memoir 55, p. 363-393.

Decker, P.L., 1990, Structural analysis of the fault and fracture systems of the Lisburne field, North Slope, Alaska: unpublished company report, ARCO Alaska, Inc., 23 p., 6 figs.

Epard, J. L., and Groshong, R. H., Jr., 1995, Kinematic model of detachment folding including limb rotation, fixed hinges and layer-parallel strain: Tectonophysics, v. 247, p. 85-103.

Grantz, A., and May, S.D., 1983, Rifting history and structural development of the continental margin north of Alaska, in Watkins, J.S., and Drake, C.L., eds., Studies in continental margin geology: AAPG Memoir 34, p. 77-100.

Grantz, A., May, S.D., and Hart, P.E., 1990, Geology of the Arctic continental margin of Alaska, in Grantz, A., Johnson, L., and Sweeney, J.F., eds, The Arctic Ocean region: Boulder, Colorado, GSA, The Geology of North America, v. L., p. 257-288.

Griggs, D.T., and Handin, J., 1960, Rock Deformation, Geological Society of America Memoir 79, 382 pp.

Hanks, C.L., Wallace, W.K., and O'Sullivan, P., 1994, The Cenozoic structural evolution of the northeastern Brooks Range, Alaska, in Thurston, D., and Fujita, K., eds., 1992 Proceedings International Conference on Arctic Margins, U.S. Minerals Management Service Outer Continental Shelf Study 94-0040, p. 263-268.

Hanks, C.L., Lorenz, J., Teufel, L., and Krumhardt, A.P. 1997, Lithologic and structural controls on natural fracture distribution within the Lisburne Group, northeastern Brooks Range and North Slope subsurface, Alaska: American Association of Petroleum Geologists Bulletin, vol. 81, no. 10, p. 1700-1720.

Homza, T.X., and Wallace, W.K., 1997, Detachment folds with fixed hinges and variable detachment depth, northeastern Brooks Range, Alaska: Journal of Structural Geology, v. 19, nos. 3-4 (special issue on fault-related folding), p. 337-354.

Lane, L.S., 1991, The pre-Mississippian "Neruokpuk Formation," northeastern Alaska and northwestern Yukon: review and new regional correlation: Canadian Journal of Earth Sciences, v. 28, pp. 1521-1533

Lorenz, J. C., Teufel, L. W., and Warpinski, N. R., 1991, Regional fractures 1: A mechanism for the formation of regional fractures at depth in flat-lying reservoirs: American Association of Petroleum Geologists Bulletin, v. 75, no. 11, p. 1714-1737, 16 figs.

Mayfield, C.F., Tailleur, I.L., and Ellersieck, I., 1988, Stratigraphy, structure, and palinspastic synthesis of the western Brooks Range, northwestern Alaska: in Gryc, G. ed., Geology and Exploration of the National Petroleum Reserve in Alaska, 1974 to 1982: U.S. Geological Survey Professional Paper 1399, p. 143-186.

Missman, R.A., and Jameson, J., 1991, An evolving description of a fractured carbonate reservoir: the Lisburne field, Prudhoe Bay, Alaska: in R. Sneider, W. Massell, R. Mathis, D. Loren, and P. Wichmann, editors, The Integration of Geology, Geophysics, Petrophysics and Petroleum Engineering in Reservoir Delineation, Description, and Management, AAPG-SPE-SPWLA Archie Conference, p. 204-224.

Moore, T.E., Wallace, W.K., Bird, K.J., Karl, S.M., Mull, C.G., and Dillon, J.T., 1994, Chapter 3: Geology of northern Alaska, in Plafker, G., and Berg, H.C., eds., The geology of Alaska: The Geology of North America, Geological Society of America, Boulder, Colorado, v. G1, p. 49-140.

Mull, C.G., 1982, Tectonic evolution and structural style of the Brooks Range, Alaska: An illustrated summary, in Powers, R.B., Ed., Geologic studies of the Cordilleran thrust belt: Rocky Mountain Association of Geologists, Denver, Co., v.1, p.1-45.

Ramsay, J.G., and Huber, M.I., , 1987, The techniques of modern structural geology, volume 2: Folds and fractures: Academic Press, 700 p.

Reiser, H.N., 1970, Northeastern Brooks Range--a surface expression of the Prudhoe Bay section, *in* W.L. Adkison and M.M. Brosgé, eds., Proceedings of the geological seminar on the North Slope of Alaska: AAPG Pacific Section, p. K1-K13.

Reiser, H.N., Brosgé, W.P., Dutro, J.T., Jr., and Detterman, R.L., 1980, Geologic map of the Demarcation Point quadrangle, Alaska: U. S. Geological Survey Miscellaneous Investigations Series Map I-1133, scale 1:250,000, 1 sheet.

Tanner, P.W.G, 1989, The flexural-slip mechanism: Journal of Structural Geology, vol. 11, no. 6, pp. 635-655.

Twiss, R.J, and Moores E.M., 1992, Structural Geology, Freeman, New York, 532 pp.

Wallace, W.K., 1993, Detachment folds and a passive-roof duplex: Examples from the northeastern Brooks Range, Alaska, in Solie, D.N., and Tannian, F., eds., Short Notes on Alaskan Geology 1993: Alaska Division of Geological and Geophysical Surveys Geologic Report 113, p. 81-99.

Wallace, W.K., and Hanks, C.L., 1990, Structural provinces of the northeastern Brooks Range, Arctic National Wildlife Refuge, Alaska: American Association of Petroleum Geologists Bulletin, v. 74, no. 7, p. 1100-1118.

Wallace, W.K., and Homza, T.X., in press (2000), Detachment folds vs. fault-propagation folds and their truncation by thrust faults, in McClay, K.R., editor, Thrust tectonics and petroleum systems: American Association of Petroleum Geologists Memoir.

Wallace, W.K., Moore, T.E., and Plafker, G., 1997, Multistory duplexes with forward dipping

roofs, north central Brooks Range, Alaska: Journal of Geophysical Research, v. 102, no. B9 (special section on the USGS Trans-Alaska Crustal Transect), p. 20,773-20,796.

Yang, X. and Gray, D.R., 1994, Strain, cleavage and microstructure variations in sandstone: implications for stiff layer behaviour in chevron folding: Journal of Structural Geology, vol. 16, no. 10, pp. 1353-1365.

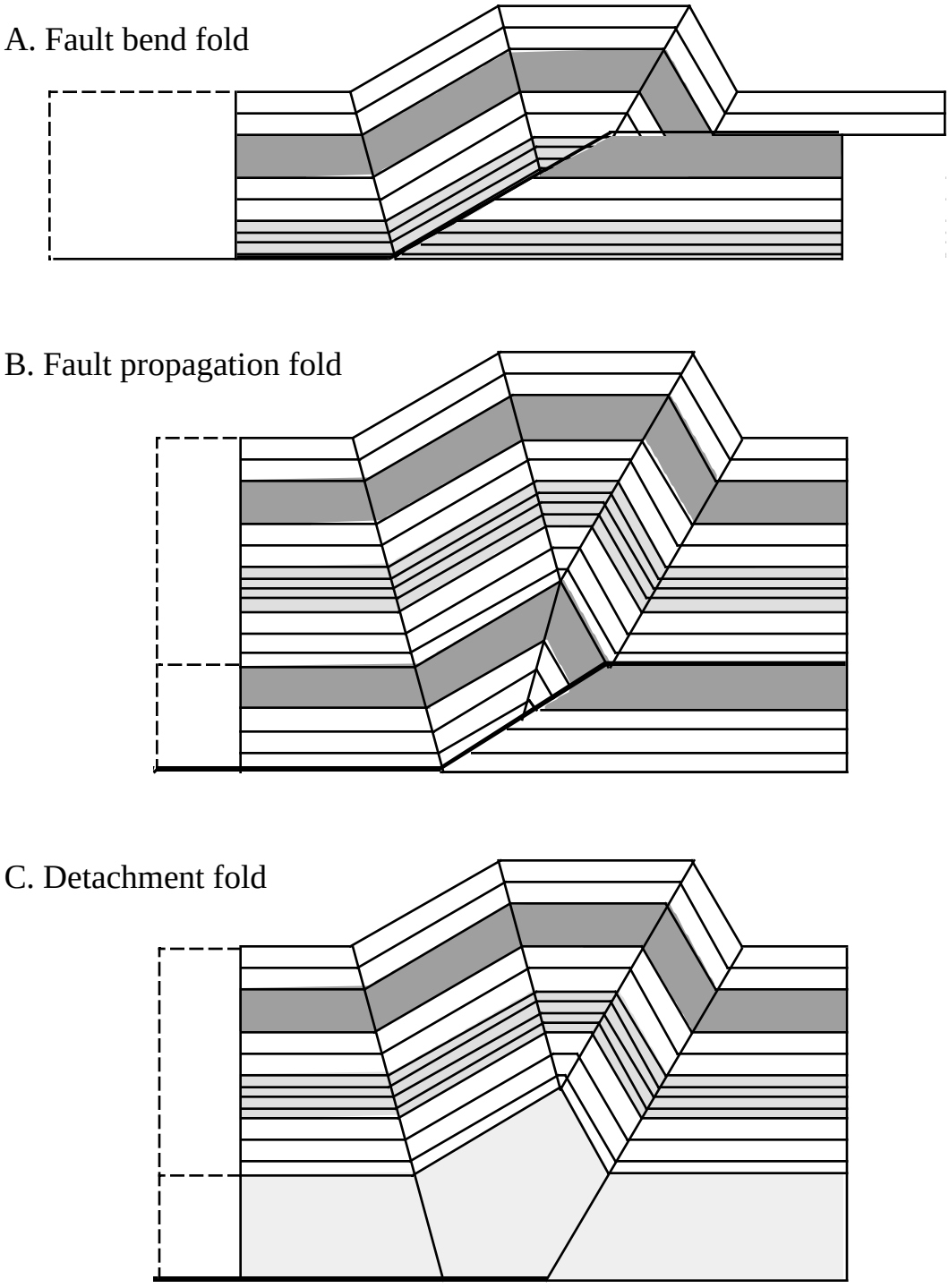

Figure 1. Three types of fault-related folds. A. Fault bend fold; B. Fault propagation fold; C. Detachment fold.

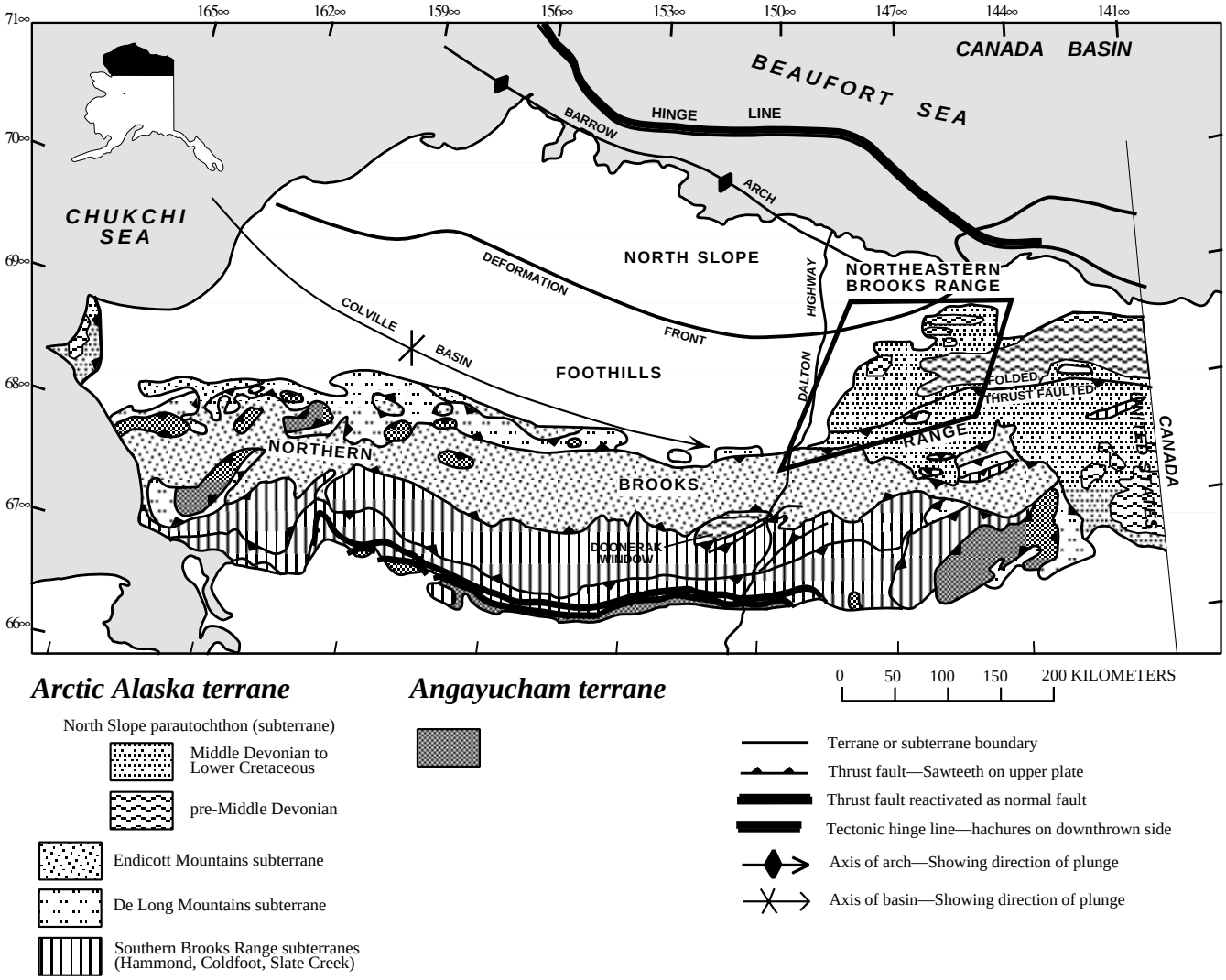

Figure 2 A. Tectonic map of northern Alaska, showing distribution of major structural features. Outlined area shown in figure 3 B. Modified from Wallace and others, 1997.

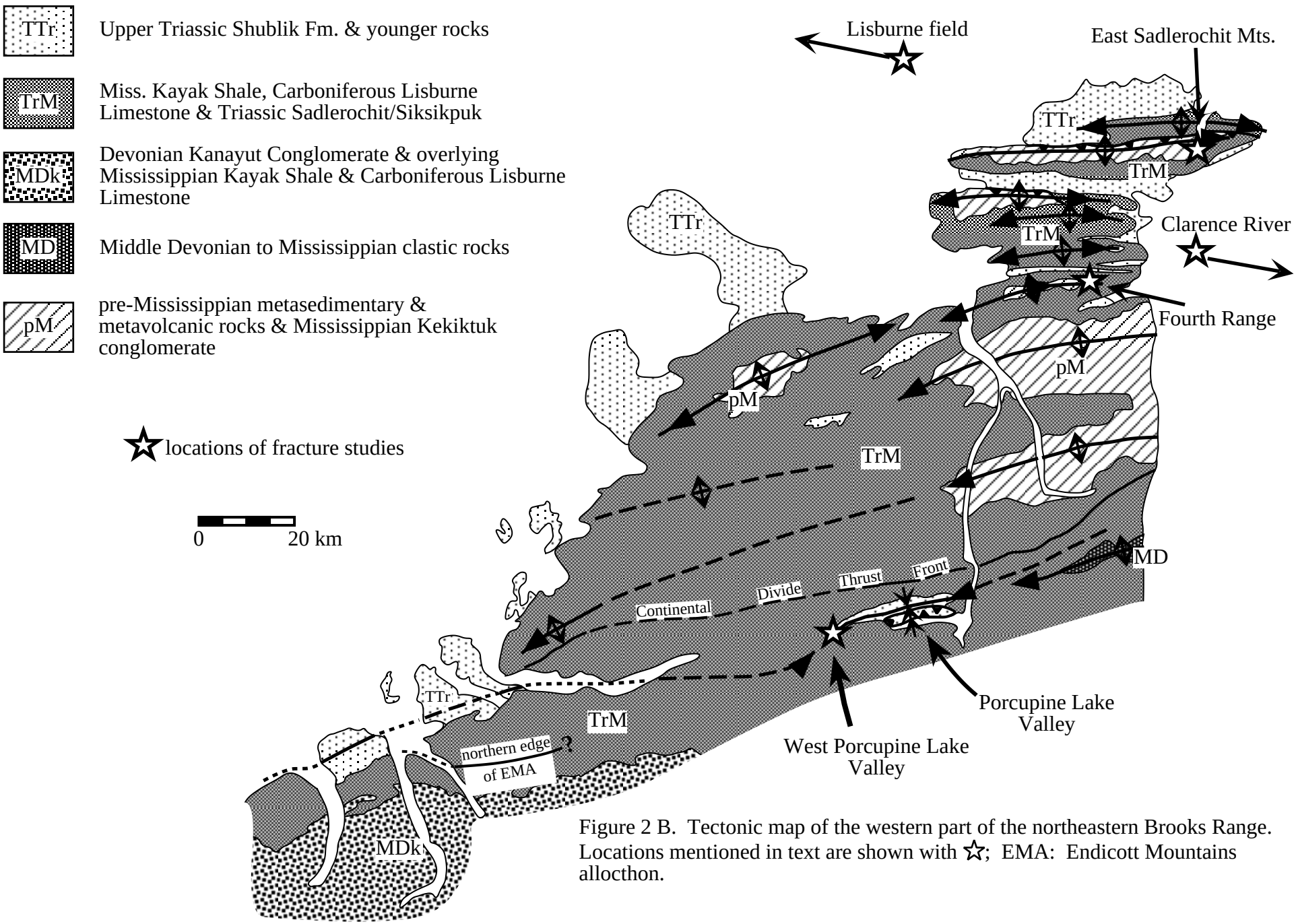

Figure 2 B. Tectonic map of the western part of the northeastern Brooks Range. Locations mentioned in text are shown with ☆; EMA: Endicott Mountains allocthon.

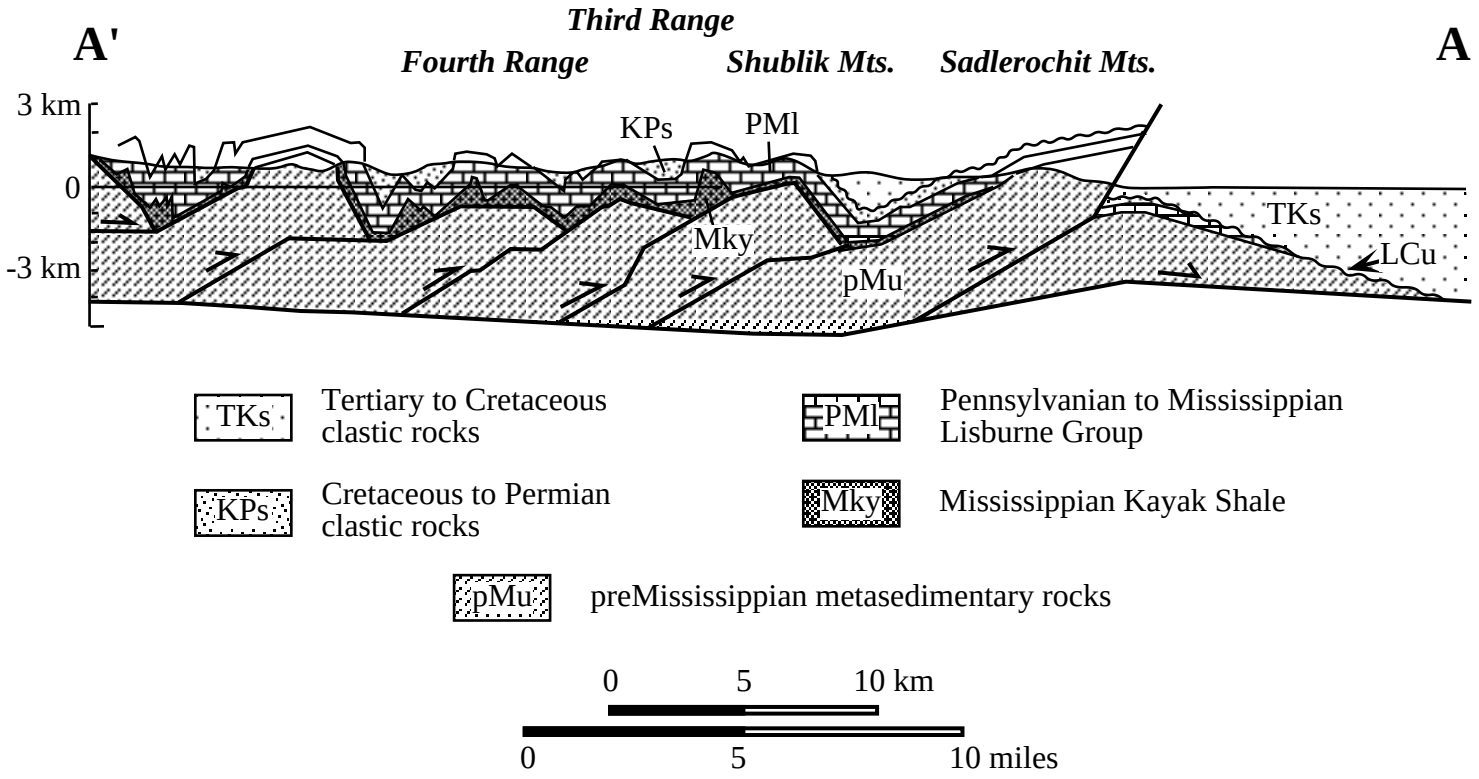

Figure 2 C. Regional balanced cross section across western part of the northeastern Brooks Range. Modified from Wallace, 1993.

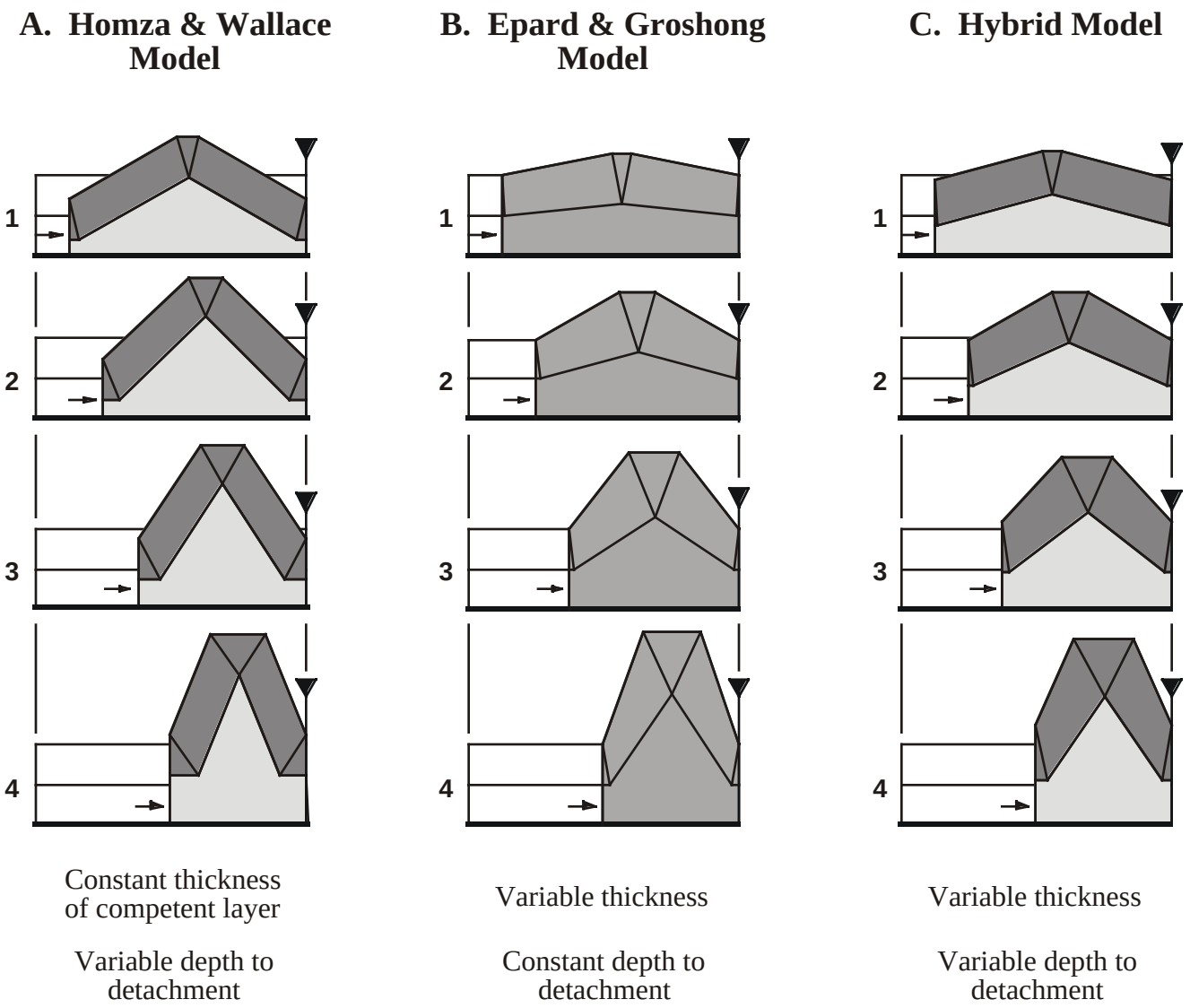

Figure 3. Detachment fold models. A. Homza and Wallace, 1997; B. Epard and Groshong, 1995; C. 'Hybrid' model, Atkinson, 2001.

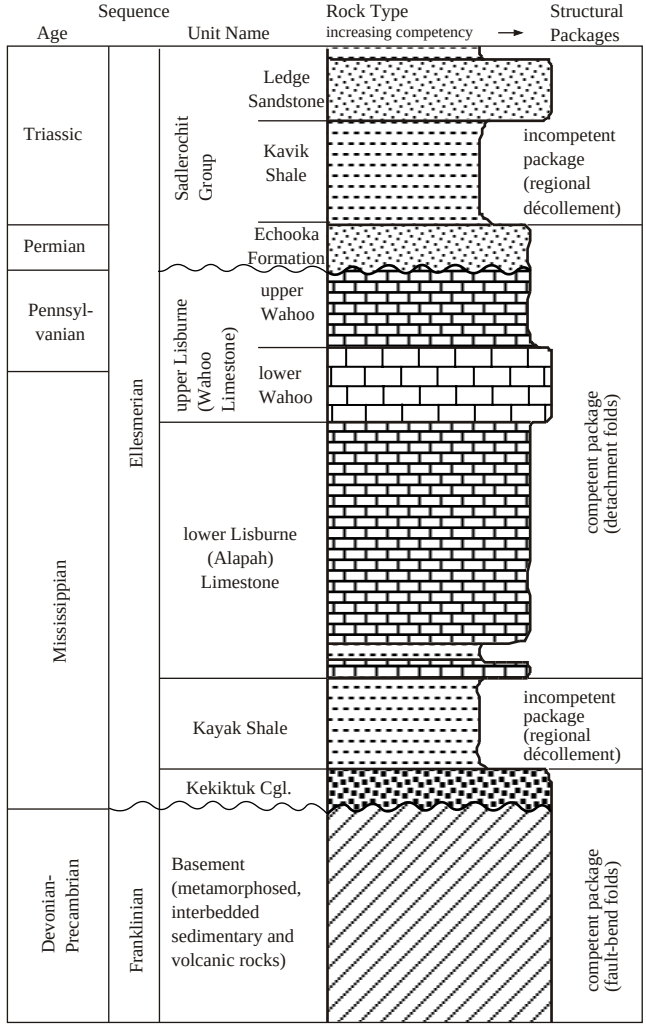

Figure 4. Schematic stratigraphy of Triassic and older rocks of the northeastern Brooks Range, emphasizing the mechanical stratigraphy of structural packages. Stratigraphy is generalized, and relative thicknesses are approximate only.

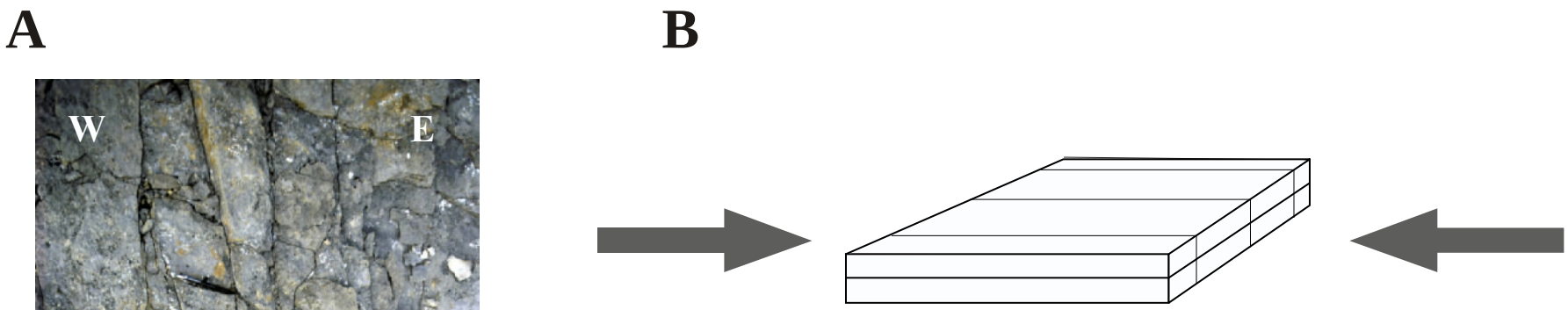

Figure 5. Non-folded, but tilted Lisburne Group carbonates in the eastern Sadlerochit Mountains display the simplest fracture pattern. A. Early NS-striking extension fractures and later EW-striking cross fractures are well-exposed on bedding surfaces in the upper Lisburne. B. The early throughgoing, NS-striking extension fractures are interpreted to represent extension fractures that formed in the foreland basin in front of the advancing thrust belt, parallel to maximum in situ horizontal stresses.

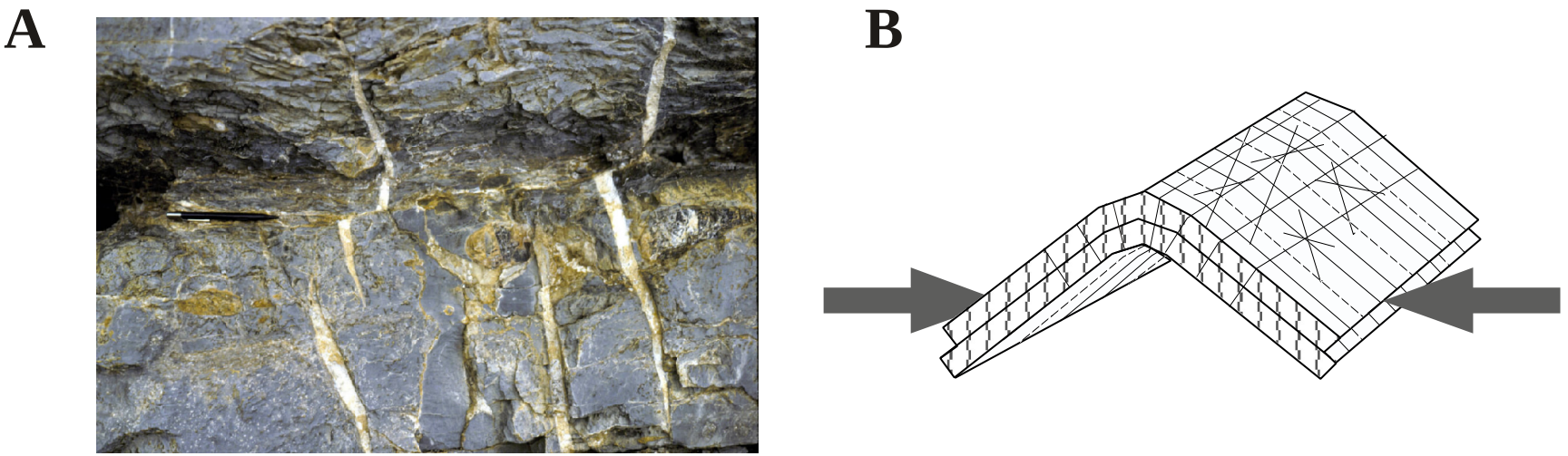

Figure 6. A. En echelon NE-striking extension fractures at grainstone/wackestone interface suggest flexural slip was an important mechanism during folding (B).

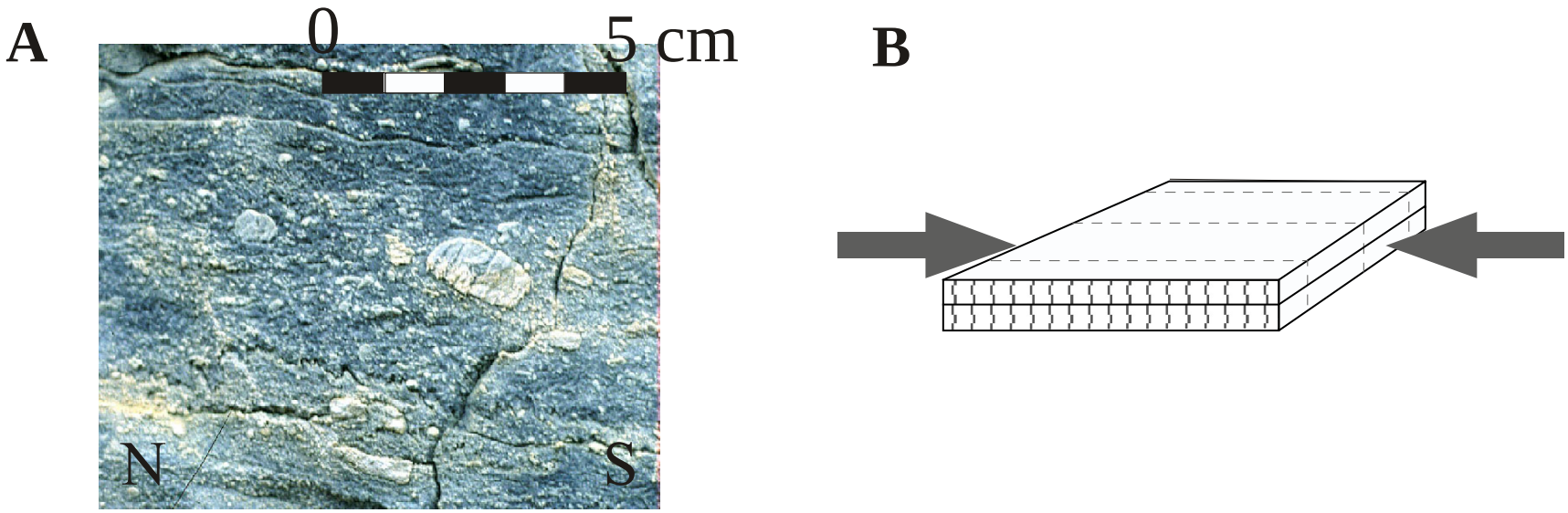

Figure 7. A. Sheared stylolites and crinoid columnals from a flat panel in West Porcupine Lake valley suggest that layer-parallel sheer preceded folding (B). The exposure surface is a NS-striking extension fracture.

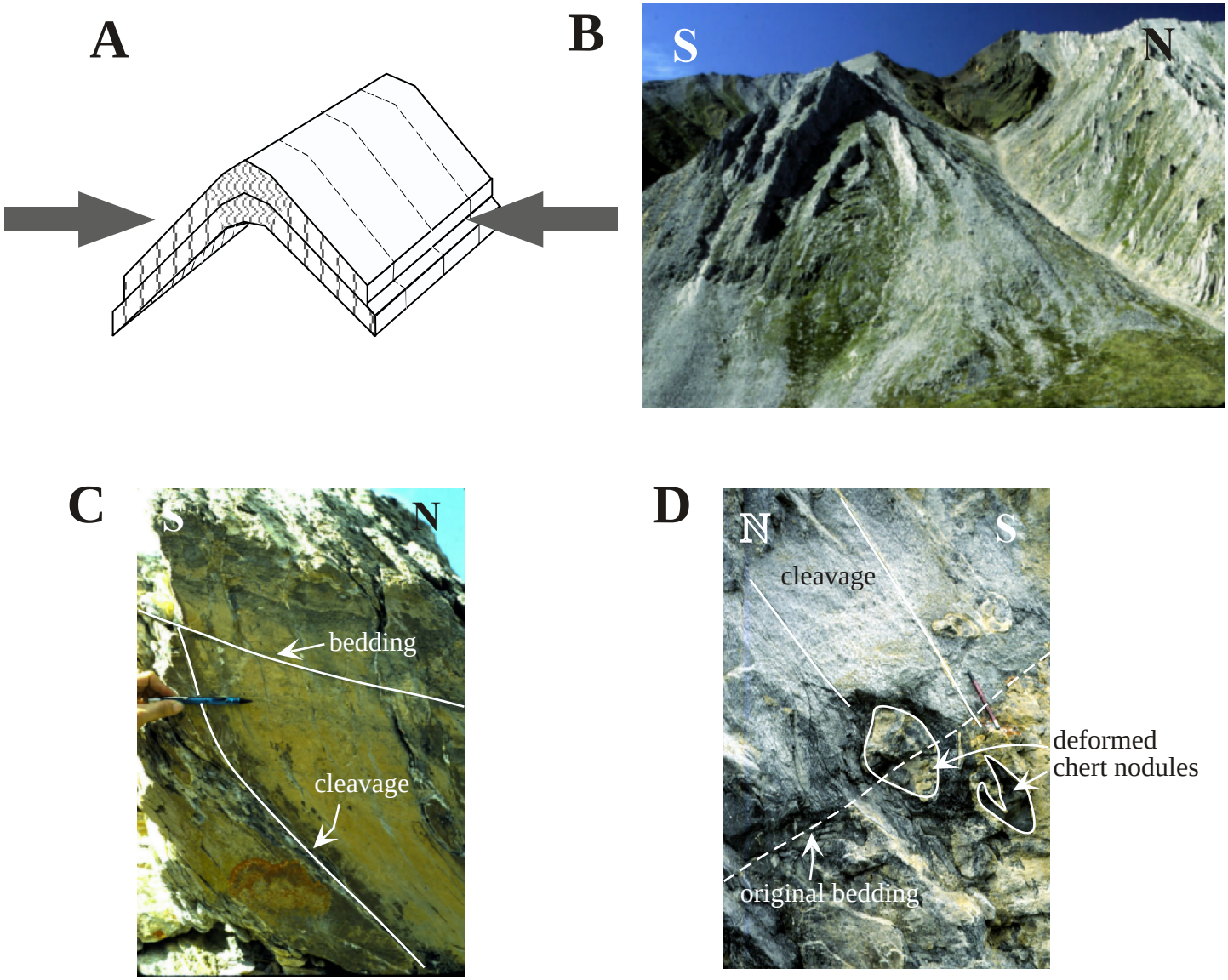

Figure 8. Penetrative strain and flattening resulted in thickening in the hinge areas of the detachment folds (A , B). Thickening was accomplished by dissolution and transport of material into the hinges, as suggested by dissolution cleavage (C) and transposition of layering (D). These penetrative strain features are well-exposed on NS-striking fracture surfaces.

A

B

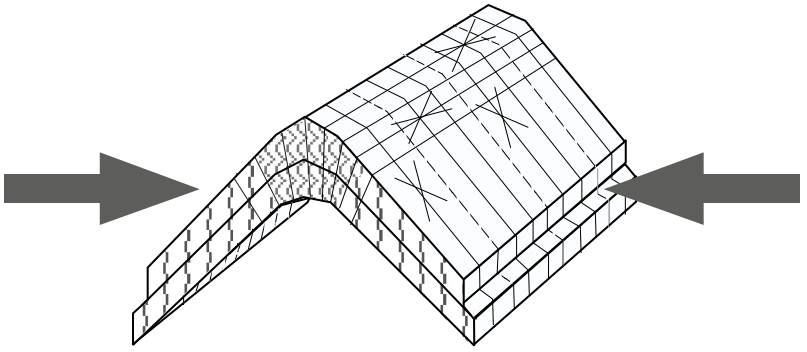

Figure 9. A. A well-developed set of conjugate fractures on a bedding surface in the Lisburne Group exposed in the Fourth Range. These rocks have been folded by a tight, east-west trending detachment fold. B. This fracture pattern is interpreted to be the result of flexural-slip late during folding and postdates penetrative structures preserved in the core and hinge of the anticline.

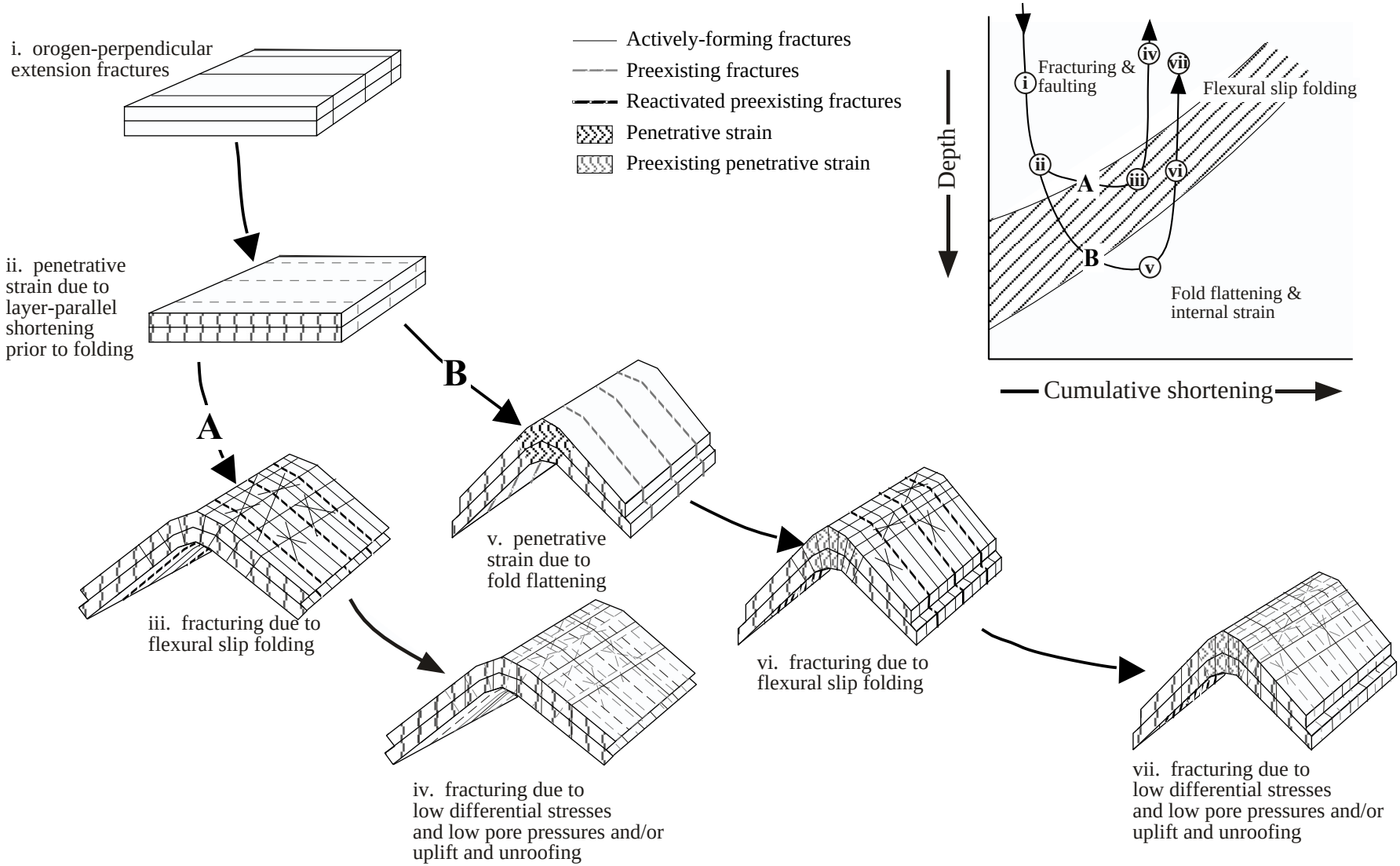

Figure 10. Different folds may exhibit different types and sequences of structures depending upon the depth at which deformation occurred and the overall amount of shortening. Rocks folded at shallow levels and low amounts of shortening would be expected to develop primarily brittle structures (**A**); folds that are formed at greater depths and/or greater amounts of shortening are more likely to exhibit penetrative structures (**B**). Other factors that probably come into play include the thickness of the competent unit, and the relative thickness of competent vs. incompetent units.

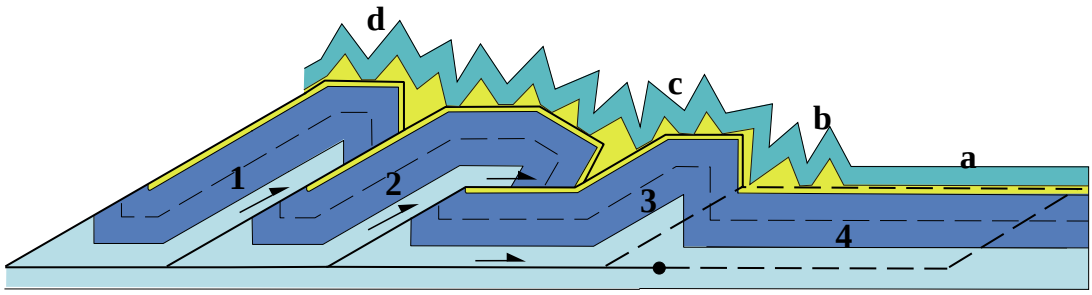

Figure 11. A fold-and-thrust belt generally grows at its leading edge. Thrust sheet 1 is the oldest sheet; thrust sheet 4 is the future thrust sheet. In this example, the thrust belt is a passive roof duplex, like the northeastern Brooks Range. Undeformed cover rocks (a) are initially folded above a roof thrust (b), and subsequently uplifted as during progressive growth of the underlying duplex (c and d). In this model, folds at **d** are the oldest, **b** are the youngest, and rocks at **a** are undeformed.

Lisburne Group Fracture Distribution and Flow Modeling

A.V. Karpov, Thang Bui, J. L. Jensen, Texas A&M University
and C. L. Hanks, University of Alaska Fairbanks

Abstract

Fractures play a key role in the Lisburne Group fluid flow behavior. Field data from grainstone intervals of the Wahoo Limestone in the eastern Sadlerochit Mountains, a relatively undeformed area, have been analyzed to develop fracture distributions and models.

The models covered a range of possible cases. The "base" case assumed vertical fractures with either of two azimuths (to correspond to the two fracture sets observed in the field) and no effect of fracture intersection. Other models allowed more variability in fracture strike and interaction. These models were interrogated for wellbore placement and hydraulic connectivity behavior. The wellbore trajectory analysis showed:

- A positive correlation was observed for the "base" case between number and area of fractures connected to wellbores. This relationship, however, diminished for other cases.
- Optimal horizontal well azimuth orientations for the base case and the case with variable fracture strike and dip are in the range 0^o to 30^o. Wells with such orientation will be connected to the maximum number and area of fractures.
- Variability in strike and dip increases the number and area of fractures connected to the wellbore. However, it does not change the optimal wellbore orientation.
- ENE fracture termination increases the number and decreases the area of fractures connected to the wellbore. It also shifts the optimal wellbore trajectory from the bisector between the two sets (30^o) towards the direction normal to the NNW set (60^o).

The hydraulic connectivity analyses showed:

- The fracture network is weakly anisotropic if uniform fracture transmissivity is assumed.
- The system remains weakly anisotropic when the transmissivity of either set is diminished.
- ENE fractures provide critical connections for flow in any direction, as opposed to the NNW set, whose transmissivity is important only for the NNW flow.
- The fracture system is above the percolation threshold in all the cases.
- The smaller fractures become important if ENE fracture termination and strike and dip variability are included in the model. This case is less interconnected, closer to the percolation threshold, and more sensitive to removal of smaller fractures.

Analysis has also begun of data from five folds exposed in the Forth Range, North Sublik and South Sublik areas. These data are being assessed for fracture geometries and their relationship to position on the fold and fold tightness.

Introduction

The fracture systems of Lisburne Group carbonates have been recognized as being critical to optimal reservoir management (e.g., Missman and Jameson, 1991). A number of problems with the reservoir, including difficulty in establishing an oil-water contact location, highly variable well productivity, disappointing waterflood performance, and uncertain reserves estimates, have been associated with difficulties in the fracture description and characterization.

This study analyzes flow properties and wellbore placements in the naturally fractured Lisburne Carbonate Group, parts of which are exposed in the eastern Sadlerochit Mountains (ESM), Alaska (Hanks et al., 1997). It forms part of a larger study of fracture patterns and

geometries in folded regions of the Lisburne Formation, exposed in the Brooks Range, Alaska. Here, we highlight results obtained from a study (Karpov, 2001) of a relatively undeformed section of the Lisburne Group, which will form a baseline for similar studies in folded regions.

The goal of the wellbore analysis was to find an "optimal" wellbore trajectory in the fracture system. Maximum number of fracture intersections with the wellbore can be the first criterion of optimal wellbore placement in a fracture domain because it may provide the highest well productivity. The second, but not less important, goal is to find a wellbore trajectory where fractures, both directly and indirectly connected to the wellbore, have the maximum total area. In this case, a larger matrix area is exposed to drainage during primary depletion or water imbibition in waterflooding and, therefore, higher sweep efficiency can be achieved.

Fracture Models

The statistical analysis and initial modelling of the ESM fractures was covered in the first annual report. A "base" case and three alternatives (Fig. 1) were formulated to examine the wellbore placement and system connectivity for a range of possible conditions. Based on the geological information, these cases are all viable alternatives and were intended to evaluate fracture system features which could be important to flow.

1. "Base" case. This is the simplest case, allowing no variability in fracture strike and dip and no fracture termination.
2. "Variable strike and dip" case. This case allows strike and dip variability in both sets. Standard deviations of 5^o were assigned to both the strike and dip of the NNW set, 10^o standard deviations were used for the ENE fracture strike and dip. All other parameter values were adopted from the base case.
3. "ENE Terminated" case. For this case 100 % termination of ENE fractures against the NNW set was designated. Since the termination caused a decrease in the ENE fracture size, a fracture intensity (P_{32}) adjustment was necessary.
4. "Realistic" case. This case combines fracture strike and dip variability in both sets and 100 % ENE fracture termination. The "ENE Termination" P_{32} values were used for this case.

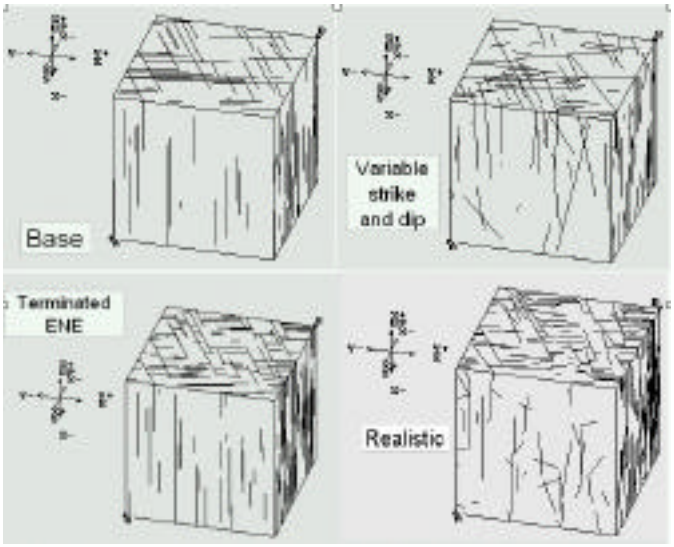

Figure 1¾ Different cases simulated in FracMan software. 20x20x20 m^3 generation region is shown. S – south , E – east.

Wellbore Modelling Results

For the "base" model, wellbores of 0^o and 30^o orientation intersect the largest number of directly-connected fractures and have the largest area of fractures both directly and indirectly connected to the wellbores. Indirectly connected fractures obtain a maximum number in the 30^o and 60^o - oriented wellbores. A weak correlation is observed between the number of fractures and fracture area for both directly and indirectly connected fractures (Fig. 2).

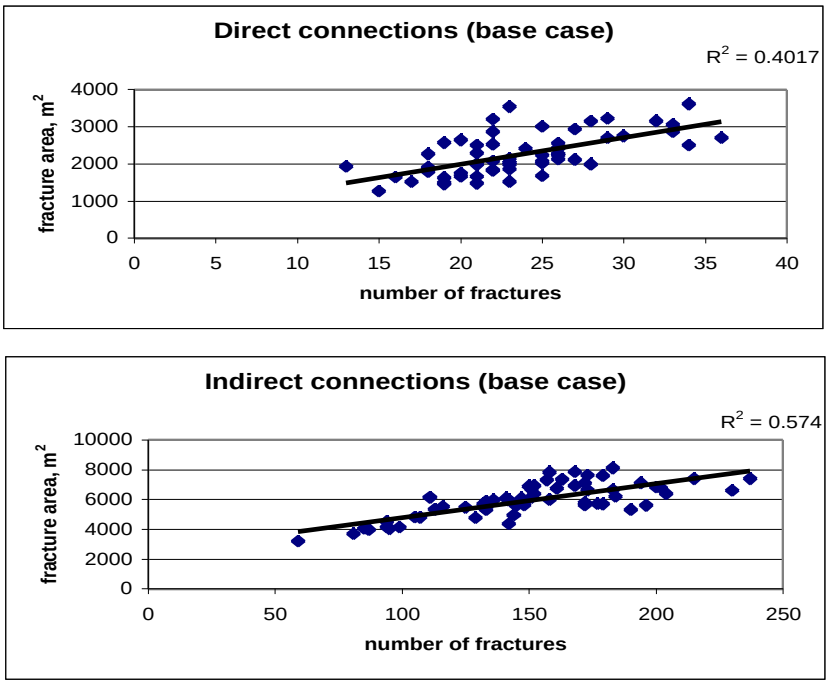

Figure 2¾ Fracture number contacted by the wellbore vs. matrix area accessed for the "base" case model.

When variability in strike and dip is incorporated in the model, the number and area of fractures directly connected to the wellbores do not change. However, the number and area of indirectly connected fractures increase by 10 – 20%. Apparently, variability in fracture orientation allows more fracture intersections. The overall pattern observed in the "variable strike and dip" model is similar to that of the "base" case, showing optimal orientations of 0^o and 30^o.

A different pattern emerges when ENE fracture terminations are incorporated in the model. Directly connected fractures have the maximum number of intersections with a 0^o – oriented wellbore, while the largest area of fractures obtains for a 60^o – oriented wellbore.

There is no correlation between number and area for directly connected fractures. Indirectly-connected fractures show consistent maxima at the 60^o orientation for both number of intersections and fracture area. Number of fractures connected to the wellbores in the "terminated" case is roughly at the same level as in the "base case"; however, the area decreases significantly (more than 2 times). This implies that the effects of fracture termination on the system connectivity is stronger than that of the variability in strike and dip.

The "realistic" case has no azimuth at which there is a pronounced maximum of directly-connected fractures. Wellbores oriented at 60^o still have the maximum number of indirectly-

connected fractures and maximum amount of area for both directly- and indirectly-connected fractures. Compared to the "base" case, the number of indirectly connected fractures is increased in the "realistic" observations. Indirect connections increase their number and area by 30 – 60%.

Wellbore Modelling Comments

Judging from the "base" model wellbore analysis results, no fracture set clearly dominates in the system. The optimal wellbore trajectory is a bisector between the two fracture strikes (330^o and 75^o), in accord with results from other studies (Aguilera et al., Ch. 8, 1991). Variability in dip and strike increases the number and area of fractures connected to the wellbores but does not change the relative influence of the two sets.

The situation changes when 100% ENE fracture termination is incorporated in the model. Although there are 10 times more ENE fractures than NNW fractures in the system, the average area of the latter is 7 times larger. Allowing ENE terminations, we apparently diminish the relative contribution of this set to the system connectivity. The optimal wellbore trajectory shifts to the orientation of 60^o, which is exactly perpendicular to the NNW set strike. Again, strike and dip variability incorporated in the "Realistic" case does not change the pattern observed in the "ENE termination" model since fracture geometry and intensity are the same.

The optimal wellbore trajectory for the "realistic" case is 60^o; the horizontal wellbore of such an orientation has the maximum number and area of fractures connected to it. This result indicates that the wellbore perpendicular to the NNW set strike has the greatest potential of involving matrix into drainage or imbibition and, therefore, increasing oil recovery in a reservoir with characteristics similar to those presented here.

Variability in strike and dip improves connectivity of the system, allowing more fracture intersections and an increasing number of fractures connected to the wellbore. The number of fractures in the "variable strike and dip" is larger than that in the "base" case by approximately 10%. The fracture area also increases, by 30% on average. Even a greater impact of the fracture strike and dip variability is observed when we compare "terminated" and "realistic" cases. Both number and area of fractures connected to the wellbores increase in the "realistic" case by 40 to 50%.

Allowing ENE terminations increases the total number of fractures connected to the wellbores by roughly 30% compared to the "base" model. This happens because there are almost 3 times more fractures in the "terminated" case, than in the "base" case. However, fracture area decreases 2.4 times on average in the "terminated" case, due to the decreased size of the ENE fractures. A similar tendency is observed if we compare "variable strike and dip" and "realistic" cases. Once we incorporate ENE termination in the "variable strike and dip" case, the total number of fractures connected to the wellbores increases by almost 50%, and the corresponding area is halved.

The analysis indicates that fracture termination, unlike dip and strike variability, influences the relative contributions of fracture sets to fluid flow in the modeled fracture system. Having the same initial values of fracture size and spacing and changing termination of the ENE set, we observed a noticeable change in the way the fracture network interconnects and connects with simulated wellbores.

One of the important observations of the wellbore analysis is that the number of fractures connected to a wellbore is not necessarily related to the area of the connected fractures (e.g. number and area of directly connected fractures in the "terminated" case). To assess the potential

area of matrix exposed to the wellbore, one needs to examine both number and area of fractures connected to the wellbore.

Fracture System Conductivity Evaluation

Several models were used to assess the hydraulic properties of the fracture models. All used either the "base" or the "realistic" cases of fracture distributions described above.

System anisotropy was evaluated using the arrangement shown in Fig. 3, assuming equal aperture size for both fracture sets. The first two wells have a 17 m distance and azimuth 60^o, so that the simulated flow direction between them would be parallel to the NNW fracture set strike. In a similar manner, the second pair of wells is located 17 m apart and oriented at 345^o, sampling flow along the ENE fractures.

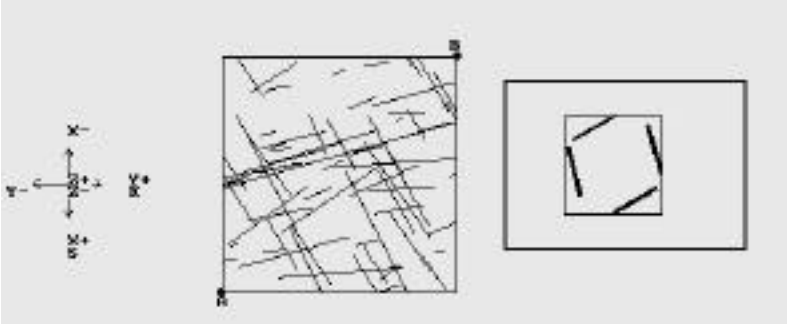

Figure 3¾ FracMan working window showing orientations of four 10 - meter long wellbores used for the anisotropy analysis.

The "base" case system exhibits some anisotropy (Fig. 4); the difference in conductance between wellbore pairs is less than one order of magnitude. Decreasing the transmissivity of either fracture set by one order of magnitude (Cases 1 and 4, Fig. 4) did not affect the well-to-well conductivity in either set of wellbores. Larger decreases (Cases 2, 3, 5, and 6, Fig. 4), however, did affect the system. An ENE set transmissivity decrease of more than 1 order of magnitude substantially affected flow in both directions (Cases 5 and 6, Fig. 4). A NNW set transmissivity decrease significantly affected conductivity only in the NNW direction (Cases 2 and 3, Fig. 4).

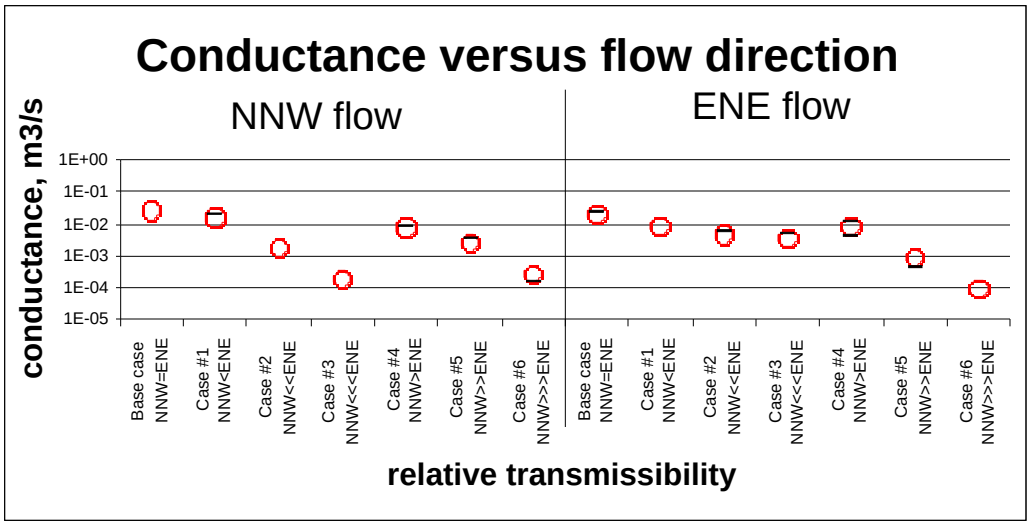

Figure 4¾ Conductance versus flow direction for the "base" case and 6 cases with variable relative transmissibility of the sets. "NNW < ENE", "NNW << ENE", "NNW<<<ENE" denote cases with NNW fracture transmissivity 1, 2, and 3 orders of magnitude lower than ENE fracture transmissivity (similar notation are used for the inverse cases). Circles show average value; bars indicate standard error deviation from the average value.

The "realistic" case yielded slightly different results. The inclusion of strike and dip variation and ENE set termination reduced the system sensitivity to the ENE set transmissivity. However, the system anisotropy increased with reduced ENE set transmissivity.

We assessed the effects of removing certain size fractures on the system conductivity and, therefore, the relative contribution of different size fractures to fluid flow. The simulation was performed in a 20x20x20 m^3 region using two 20 – meter long parallel wells oriented east-west and located 20 meters apart (Fig. 5).

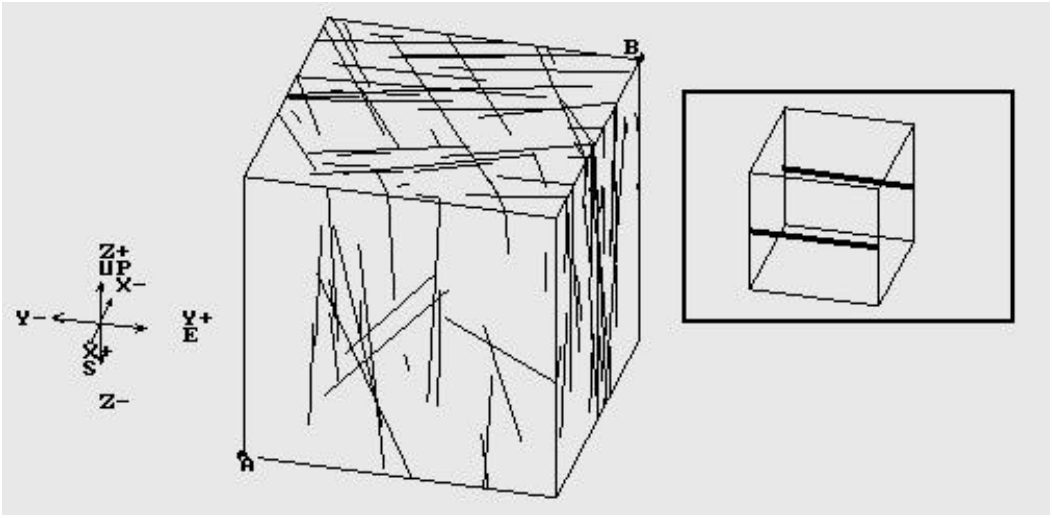

Figure 5¾ FracMan working window showing orientation of 2 wellbores used for the sensitivity study. 20x20x20 m^3 generation region is shown; wellbore length is 20m.

For the "base" case, 88% of the smaller fractures were removed before there was any effect on conductance. 99% of the smaller fractures had to be removed to drop conductance to zero (with radius less than 7 m). On the other hand, a removal of only 2% of the largest fractures significantly decreased conductance and a removal of the largest 12% (radius greater than 4 m) of the fractures makes the fracture network non-conductive.

In the “realistic” case, 97% of the smallest and or 3% of the largest fractures have to be removed to make the system non-conductive. After removal of fractures with radius less than 4 m or more than 3 m, the conductance dropped to zero. Apparently, variability in strike and dip made the system more interconnected and restored some of the connectivity loss caused by the ENE fracture termination.

Similar trends were seen when studying the effect of fracture removal on the network connectivity. The system tolerates removal of the smaller fractures (i.e. <4m "base" and <1m "realistic" cases), which have only a small role in interconnecting the larger fractures. Removal of a few larger fractures, however, substantially reduces connectivity. These results indicate that the system is operating at or above the percolation threshold (Sahimi, 1994).

Conductivity Comments

A few large NNW fractures dominate the system connectivity, with the smaller but more numerous ENE set largely limited to connecting up the NNW fractures. This suggests (e.g., Putra et al., 1999) that viscous-force dominated displacements (e.g., waterfloods with a favorable mobility ratio) would likely benefit from injection - production well placements having positions along an ENE line. In displacements where diffusion is important, system conductivity is not as important as the fracture contact area with the matrix. The ENE set then plays a more important part.

This part of the study assumed no flow through the matrix; all flow was by fractures. Consequently, the sensitivities observed here would be mitigated by the permeable matrix. For example, the loss of very few large fractures reducing the system connectivity to nil may not be observed if flow through the matrix is included. Nonetheless, the trends observed may be important for wellbore placement and injection strategy in producing formations with fracture properties similar to those of the models.

The relative importance of the fracture sets to wellbore connectivity and system connectivity have implications for appropriate sampling of fractures in producing formations. The displacement process, fracture intensity, geometry, and relationships, and matrix conductivity all play a part in defining whether a particular set of fractures is important to flow. Outcrop-based evaluations are particularly difficult in this respect because a variety of displacement processes may be possible. Therefore, which set(s) should be sampled and to what degree has no simple solution. The obvious priority is evaluation of the largest fractures but deciding which fractures are "large" may not become clear until numerous measurements are made.

Conclusions

Fracture systems in the relatively undeformed region of the Wahoo Limestone were modelled. The wellbore trajectory analyses of several cases showed:

- A positive correlation was observed for the base case between number and area of fractures connected to wellbores. This relationship, however, diminished for the other cases.

- Optimal horizontal well azimuth orientations for the base case and the case with variable fracture strike and dip are in the range 0^o to 30^o. Wells with such orientation will be connected to the maximum number and area of fractures.
- Variability in strike and dip increases the number and area of fractures connected to the wellbore. However, it does not change the optimal wellbore orientation.
- ENE fracture termination against the NNW fractures increases the number and decreases the area of fractures connected to the wellbore. It also affects wellbore placement, shifting the optimal wellbore trajectory from the bisector between the two sets (30^o) towards the direction perpendicular to the NNW set (60^o).

The hydraulic connectivity analyses showed:

- The fracture network is weakly anisotropic if uniform fracture transmissivity is assumed.
- The system remains weakly anisotropic when the relative transmissivities of the sets are changed.
- ENE fractures provide critical connections in the fracture network, as opposed to the NNW set, whose transmissivity is important only for the NNW flow.
- The fracture system is above the percolation threshold in all the cases.

The smaller fractures become important if ENE fracture termination and strike and dip variability are included in the model: the "realistic" case is less interconnected, closer to the percolation threshold and more sensitive to removal of smaller fractures.

Future work

Data analysis and modelling of fracture systems in more deformed sections of the Lisburne group will continue. Data from five folds will be analysed and the following issues addressed.

1. The effect of lithology and bed thickness on fracture height and spacing.
2. Comparison of fracture set properties.
3. The effect of position on the fold and degree of folding on fracture properties.

The analysis results will be used for development of fracture models which can be interrogated for wellbore placement and system connectivity, as in the previous study of an undeformed element.

Acknowledgements

We thank Golder and Associates for the use of FracMan software in this project.

References

1. Aguilera, R., et al.: Horizontal Wells, Gulf Pub. Co., Houston, 1991, 401p.
2. Hanks, C.L., Lorenz, J., Teufel, L., Krumhardt, A.P.: "Lithologic and structural controls on natural fracture distribution and behavior within the Lisburne Group, Northeastern Brooks Range and North Slope Subsurface, Alaska", *AAPG Bulletin,* v. 81, No. 10, 1997, p. 1700-1720.
3. Karpov, A.: "Lisburne formation fracture characterization and flow modeling," MS Thesis, Texas A&M University, 2001.

4. Missman, R. A. and Jameson, J.: “An evolving description of a fractured carbonate reservoir: the Lisburne field, Prudhoe Bay, Alaska”, in *R. Sneider, W. Massel, R. Mathis, D. Loren and P. Wichmann (eds.)The integration of geology, geophysics, petrophysics and petroleum engineering in reservoir delineation, description and management, AAPG-SPE-SPWLA Archie Conference,* 1991.
5. Putra, E., Fidra, Y., and Schechter, D. S.: Use of experimental and simulation results for estimating critical and optimum water injection rates in naturally fractured reservoirs," 1999 SPE Annual Conference and Exhibition, SPE Paper 56431.
6. Sahimi, M.: Applications of Percolation Theory: Taylor & Francis Ltd, London, 1994, 258 p.